NASA CR137525

VOLUME I

EVALUATION OF ADVANCED LIFT CONCEPTS AND FUEL CONSERVATIVE SHORT-HAUL AIRCRAFT

FINAL REPORT

JUNE 1974

TO: NATIONAL AERONAUTICS AND SPACE ADMINISTRATION
SYSTEMS STUDIES DIVISION
AMES RESEARCH CENTER

Contract NAS 2-6995

BY: LOCKHEED AIRCRAFT CORPORATION

NASA CR137525

VOLUME I

EVALUATION OF ADVANCED LIFT CONCEPTS AND FUEL CONSERVATIVE SHORT-HAUL AIRCRAFT

FINAL REPORT

JUNE 1974

TO: NATIONAL AERONAUTICS AND SPACE ADMINISTRATION
SYSTEMS STUDIES DIVISION
AMES RESEARCH CENTER

Contract NAS2-6995

BY: LOCKHEED AIRCRAFT CORPORATION

FOREWORD

The evaluation of Advanced Lift Concepts and Fuel-Conservative Short Haul Aircraft was conducted under extensions to NASA Ames Research Center Contract NAS2-6995. Work was initiated in July 1973 and continued to May 1974 as an outgrowth of the studies reported in the basic contract which extended from May 1972 through May 1973; the earlier work was described in CR 114612 and CR 114613, dated June 1973 and was summarized in CR 2355, dated December 1973.

The results of the study are reported in two volumes for ease of handling. Volume I (NASA CR 137525) covers Introductory material, Evaluation of Requirements and Over-the-Wing/Internally Blown Flap Vehicles. Volume II (NASA CR 137526) covers Augmentor Wing and Mechanical Flap Vehicles, other lift concepts, Evaluation of Aircraft Configurations, Economics, and Conclusions and Recommendations.

This study was under the direction of T. P. Higgins, Program Manager, and H. S. Sweet, Deputy Manager. The principal investigators were: J. H. Renshaw, M. K. Bowden, C. W. Narucki, J. A. Bennett, P. R. Smith, R. S. Ferrill, C. C. Randall, J. G. Tibbetts, R. W. Patterson, R. T. Meyer, and L. A. Vaughn.

The work was administered under the direction of T. L. Gallaway, Technical Monitor, R. C. Savin and M. H. Waters, Systems Studies Division, NASA Ames Research Center.

TABLE OF CONTENTS

LIST OF FIGURES

LIST OF FIGURES (Continued)

VOLUME I

LIST OF FIGURES (Continued)

LIST OF FIGURES (Continued)

LIST OF FIGURES (Continued)

LIST OF FIGURES (Continued)

LIST OF FIGURES (Continued)

LIST OF FIGURES (Continued)

LIST OF FIGURES (Continued)

LIST OF FIGURES (Continued)

LIST OF FIGURES (Continued)

LIST OF FIGURES (Continued)

LIST OF FIGURES (Continued)

APPENDICES

LIST OF FIGURES (Continued)

LIST OF TABLES

SYMBOLS AND ABBREVIATIONS

AR	airplane aspect ratio or nozzle aspect ratio, b/h
AW	augmenter wing
b	span
BLC	boundary layer control
BPR	bypass ratio, engine secondary airflow/engine primary airflow
C_D	drag coefficient
C_L	lift coefficient
C_P	pressure coefficient
C_R	roll moment coefficient
C_T	thrust coefficient
C_X	axial force coefficient
C	blowing moment coefficient
c	chord
¢/ASSM	cents/available seat statute mile
CTOL	conventional takeoff and landing
D	diameter
dB	decibel
DOC	direct operating cost
DOC-1	DOC at 11.5¢/gallon of fuel
DOC-2	DOC at 23¢/gallon of fuel
DOC-3	DOC at 46¢/gallon of fuel
DOC-4	DOC at 1.15¢/gallon of fuel
EBF	externally blown flap
EPNdB	equivalent perceived noise decibel
F	engine thrust

f	frequency (Hertz)
FAR	Federal Aviation Requirements
FPR	fan pressure ratio
g	gravitational constant
H	nozzle height
Hz	Hertz, unit of frequency
IBF	internally blown flap
LE	leading edge
M	Mach number or Meter
m	airflow or meter
MF	mechanical flap
NPR	nozzle pressure ratio
OASPL	overall sound pressure level
OPR	overall pressure ratio of engine
OTW	over-the-wing
OTW/IBF	over-the-wing/internally blown flap hybrid
OWE	operating weight empty
PNdB	unit of perceived noise level
PNL	perceived noise level
q	dynamic pressure
R	coanda radius
RGW	ramp gross weight
R_N	Reynolds number
ROI	return on investment
R/STOL	reduced/short takeoff and landing

SFC	specific fuel consumption
SLS	sea level static
SPL	sound pressure level
STOL	short takeoff and landing
T	temperature or airplane net thrust
t	wing thickness
T/O	takeoff power setting
TOFL	takeoff field length
TOGW	takeoff gross weight
T/W	airplane thrust/weight ratio
T/S	airplane thrust/wing area ratio
V	velocity
W	weight or airplane weight
α	angle of attack
γ	flight path angle
Δ	increment of
η	power setting or fraction of wing span
λ	taper ratio

SUMMARY

In 1972 and early 1973, Lockheed conducted for NASA Ames Research Center a "Study of Quiet Turbofan STOL Aircraft for Short Haul Transportation" (Ref. 1,2). This study concluded that quiet, short-field aircraft can be economically viable, provide benefits to short-haul transportation, and also to long-haul transportation through relief of airport congestion. From a comprehensive array of lift concepts, cruise speeds, and field lengths, it was concluded that the most promising concepts were the 910 m. (3,000 ft.) field length Over-the-Wing/Internally Blown Flap Hybrid (OTW/IBF) and the 1220 m. (4,000 ft.) field length Mechanical Flap (MF) concept, both with cruise speeds of 0.8M.

Additional depth of analysis was needed to confirm the potential of these concepts and to evaluate the performance and economics of a twin-engine augmentor wing airplane. The present study covers two phases:

- Investigation of the critical design aspects of the OTW/IBF hybrid, augmentor wing, and mechanical flap aircraft for 910 m. (3,000 ft.) field length with parametric extension to other field lengths.
- Evaluation of the fuel savings achievable by the application of advanced lift concepts to short-haul aircraft and determination of the effect of different field lengths, cruise requirements, and noise levels on fuel consumption and airplane economics at higher fuel prices. This approach to the present study is summarized in Figure 0.1.

All the design comparisons were made with 148 passenger aircraft. The baseline aircraft for design refinement had a single-aisle, 6-abreast fuselage; a 5-abreast fuselage was used in the fuel-conservative configurations because it is slightly lower in weight and wetted area. Engines used in the designs were those defined in the pre-hardware phases of the Quiet Clean STOL Experimental Engine program, with the addition of a near-term bypass 6 engine currently under development. An advanced airfoil was used in all of the

- REFINE DESIGN OF SHORT-HAUL AIRCRAFT -- M 0.8, 9140m. (30,000 FT.)

FIELD LENGTH	610m. (2000 FT.)	910m. (3000 FT.)	1070m. (3500 FT.)	1220m. (4000 FT.)
OVER THE WING/INTERNALLY BLOWN FLAP	o	◎	o—PARAMETRIC DESIGN	
MECHANICAL FLAP		◎	o	◎
AUGMENTOR WING	o	◎←PRELIMINARY DESIGN		

- REOPTIMIZE ABOVE AIRCRAFT (WING AR, CRUISE SPEED AND ALTITUDE) FOR MINIMUM FUEL AND HIGHER FUEL COSTS
  REEXAMINE EXTERNALLY BLOWN FLAP
  ADD DEFLECTED SLIPSTREAM WITH TURBOPROP ENGINES
  EXTEND MECHANICAL FLAP ANALYSES TO COVER 1830m. AND 2440m. (6000 AND 8000 FT.)
  EVALUATE ENGINES WITH FPR 1.25, 1.35, 1.47

- DETERMINE FUEL AND DOC PENALTY FOR POTENTIAL NOISE CRITERIA:
  95 EPNdB AT 150m. (500 FT.) SIDELINE
  PART 36 MINUS 5, 10, 15 EPNdB
  SPERRY BOX LEVEL OF 80 EPNdB
  90 EPNdB FOOTPRINT AREA LIMITED TO 2.59, 1.39, 0.78 km^2 (1.0, 0.5, 0.3 SQ. MI.)
  90 EPNdB FOOTPRINT LENGTH LIMITED TO 6.5, 3.7, 1.9, 1.2 km (3.5, 2.0, 1.0 N. MI., 4000 FT.)

FIGURE 0.1: STUDY APPROACH

148 PASSENGERS

0.8 MACH

910 M (3000 FT) FIELD LENGTH

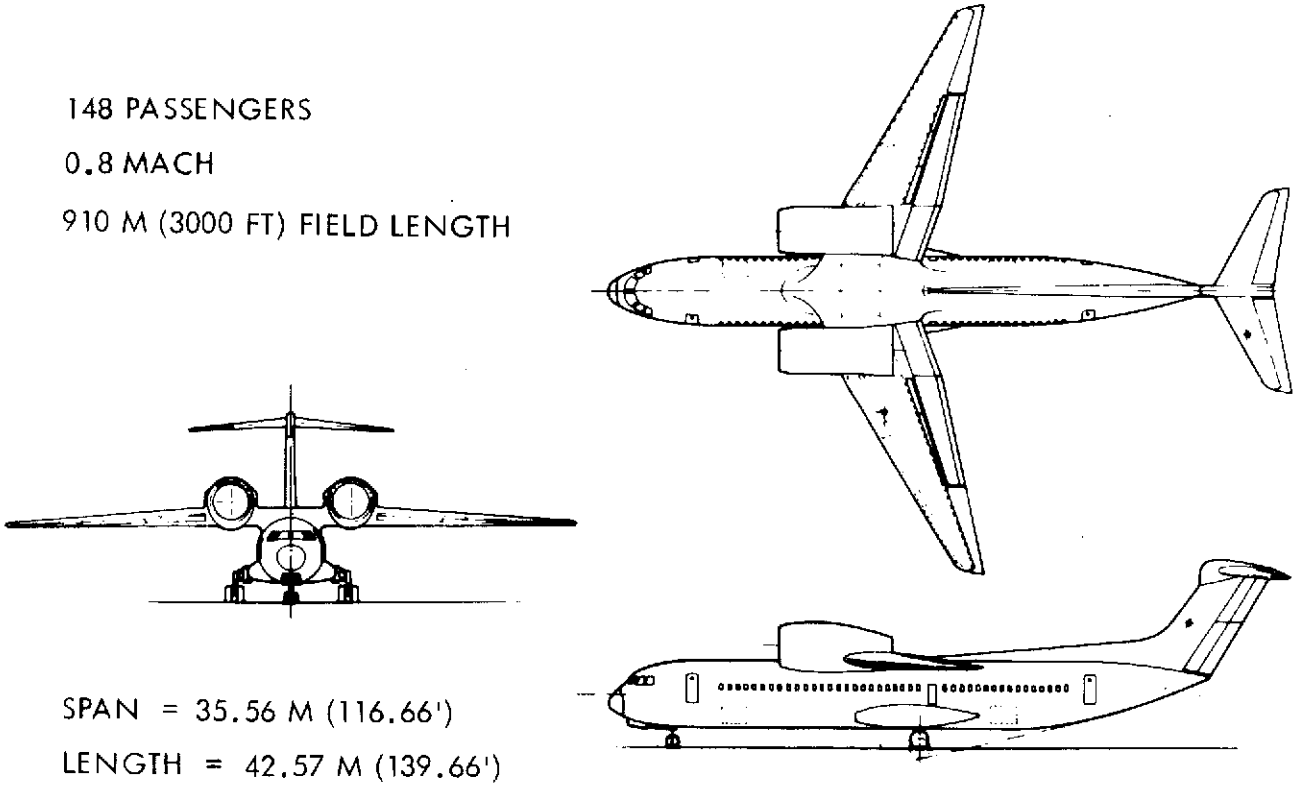

SPAN = 35.56 M (116.66')

LENGTH = 42.57 M (139.66')

HEIGHT = 11.78 M (38.66')

FIGURE 0.2: 910 M (3000 FT) OTW-IBF VEHICLE

configurations, providing a greater wing thickness for a given drag rise, sweep angle, and design cruise speed.

In all cases, emphasis was given to designs meeting noise levels equivalent to 95-100 EPNdB at 153 m. (500 ft.) sideline. The range of fan pressure ratios for engines used in the designs was chosen to cover a range of noise levels from slightly below 95 to considerably higher than 100 EPNdB at this sideline location. Effects of this variation are summarized later. The concepts were compared at approximately the same low noise level by utilizing the engine fan pressure ratios and noise treatment listed in Table 0.1.

The following discussion is organized to cover, first, the design refinement of the hybrid OTW/IBF concept and changes associated with minimizing fuel consumption or minimizing operating cost at higher fuel prices. Next, the augmentor wing and mechanical flap concepts are covered. The other lift concepts are examined more briefly from the standpoint of fuel conservation. The concepts are then compared, noise aspects are summarized, and conclusions and recommendations are listed.

Hybrid OTW/IBF Aircraft

The hybrid OTW/IBF airplane is characterized by location of the engines over the wing and use of Coanda attachment for thrust vectoring, combined with ducting of a small proportion of the fan air to trailing edge flaps for low speed lift augmentation. Cross-ducting of the fan air in the IBF system makes it possible to achieve lift symmetry in a two, three, or four engine configuration. The baseline airplane resulting from design refinement, and optimized for minimum direct operating cost at 1972 fuel prices, is shown in Figure 0.2. Detailed analysis covered the following areas:

- Nacelle inlet, exhaust and thrust reverser design; Coanda jet deflection.
- Mass flow split, ducting, and flap configuration.
- Limits on engine size related to wing area, expressed as thrust/wing area (T/S) limit.
- Aerodynamic performance and comparison of data from Lockheed and other wind tunnel tests.
- Weights of flap, ducting, wing box and other components.

TABLE 0.1 ENGINE SELECTION FOR CONCEPT COMPARISON AT EQUIVALENT NOISE LEVELS

Lift Concept	Engine FPR	Acoustic Treatment
Hybrid OTW/IBF	1.35	Nacelle Wall only
Augmentor Wing	3.0 - 3.2	High Mach Inlet; Exhaust Duct Wall; Flap Cavity
Mechanical Flap	1.35	Nacelle Wall only
Externally Blown Flap	1.25	Nacelle Wall only
Over-the-Wing	1.35	Nacelle Wall only
Boundary Layer Control/ Vectored Thrust	1.3	Nacelle Wall only
Internally Blown Flap/ Vectored Thrust	1.3	Nacelle Wall only
Deflected Slipstream	(Turboprop)	Nacelle Wall and Low Tip-Speed Prop

The engine is positioned so it can be lowered vertically forward of the wing front beam. The nacelle design, coordinated with the available aerodynamic test data, incorporates separate fan and primary exhaust ducts. The length and geometry of the aft fan duct cause significant cruise penalties. This area is considered to have most potential for improvement of the performance potential of the OTW/1BF concept, but requires experimental data which are now lacking.

A subcontract with Detroit Diesel Allison Division of General Motors covered studies of fan-air bleed systems, potential emergency ratings for engine loss conditions, surge margin requirements, and generation of additional noise data.

Characteristics of aircraft resulting from design refinement are shown in Table 0.II for design field lengths of 610, 914, and 1070 meters (2,000, 3,000, and 3,500 ft.). Although these aircraft were optimized for fuel prices of 1972 levels (identified as DOC-1) the table shows the effect of multiples of 2, 4, and 10 times that fuel price (identified as DOC-2, DOC-4, and DOC-10). Direct operating costs are based on 3,000 hours per year utilization of the aircraft with 2780 Km (1,500 n.m.) range capability instead of the 2,500 hours per year utilization which is predicted for aircraft with 926 Km (500 n.m.) range limits.

Modification of design for fuel conservation and for minimum DOC at higher fuel prices involved reexamination of cruise speed and altitude, as well as airplane configuration. Because of the large number of cases to be considered, the aircraft were designed for 926 Km (500 n.m.) range only, with associated utilization of 2,500 hours per year; the comparisons would be valid and could be applied to aircraft with extended range and CTOL takeoff. Figure 0.3 shows mission fuel, DOC-1 and DOC-2 plotted against design cruise Mach number for airplanes optimized for minimum mission fuel and alternately for minimum DOC-1 or DOC-2. The figure shows that the vehicle designed for minimum DOC-1 would have 2 engines and a cruise speed of 0.8 M, as represented in Figure 0.2. Its mission fuel usage would be 5900 Kg (13,000 lb.) and its DOC-1 would be 1.62¢/ASSM. Figure 0.3 also shows that at 0.8 M the alternate 4-engined vehicle incurs an increase in DOC-1 (1.5%), but mission fuel is reduced 16%. When an increase in fuel price is considered, this

TABLE 0.II OTW/IBF BASELINE AIRCRAFT CHARACTERISTICS

148 Passengers — 926 Km Range with Design Field Length

M 0.8 at 9140 m. (30,000 ft.) — 2780 Km Range with CTOL Takeoff

Design Field Length - M (Ft.)		≤ 610 (≤ 2,000)	≤ 914 (≤3,000)	≤ 914 (≤ 3,000)	≤ 1,070 (≤ 3,500)
Engine Fan Pressure Ratio		1.35	1.35	1.47	1.35
No. of Engines		4	2	2	2
Ramp Gross Weight - Kg		73,190	75,987	78,849	73,279
(Lb.)		(161,360)	(167,520)	(173,830)	(161,550)
Operating Weight - Kg		44,489	45,670	46,267	43,768
Lb		(98,080)	(100,680)	(102,000)	(96,490)
Wing Loading - Kg/sq. mi.		467	449	459	471
(T.O. 926 Km Mission) Lb/sq. ft.		95.6	92.0	94.0	96.5
Wing Aspect Ratio		10	7.7	7.7	7.7
Wing Thickness/Chord		0.127	0.131	0.130	0.130
Thrust to Weight Ratio		0.43	0.49	0.47	0.46
Thrust/Engine - KN		74.3	175.5	172.0	160.3
Lb.		16,760	39,450	38,660	36,040
Cruise Thrust Setting		1.0	0.93	0.79	0.98
926 Km (500 n.m.)	DOC-1 - ¢/ASSM	1.74	1.61	1.59	1.59
	DOC-2 - ¢/ASSM	2.02	1.92	1.94	1.89
	DOC-4 - ¢/ASSM	2.58	2.52	2.63	2.47
	DOC-10 - ¢/ASSM	4.25	4.35	4.80	4.24
	Mission Fuel - Kg	6,128	6,687	7,607	6,476
	Lb	13,510	14,742	16,770	14,276
2780 Km (1500 n.m.)	DOC-2	1.51	1.44	1.47	1.40
	Mission Fuel - Kg	13,145	14,554	16,565	13,872
	Lb	28,980	32,086	36,518	30,582
Complete Aircraft Price - $M		9.622	8.831	8.696	8.578
Engine Price - $M		3.128	2.110	1.902	2.045

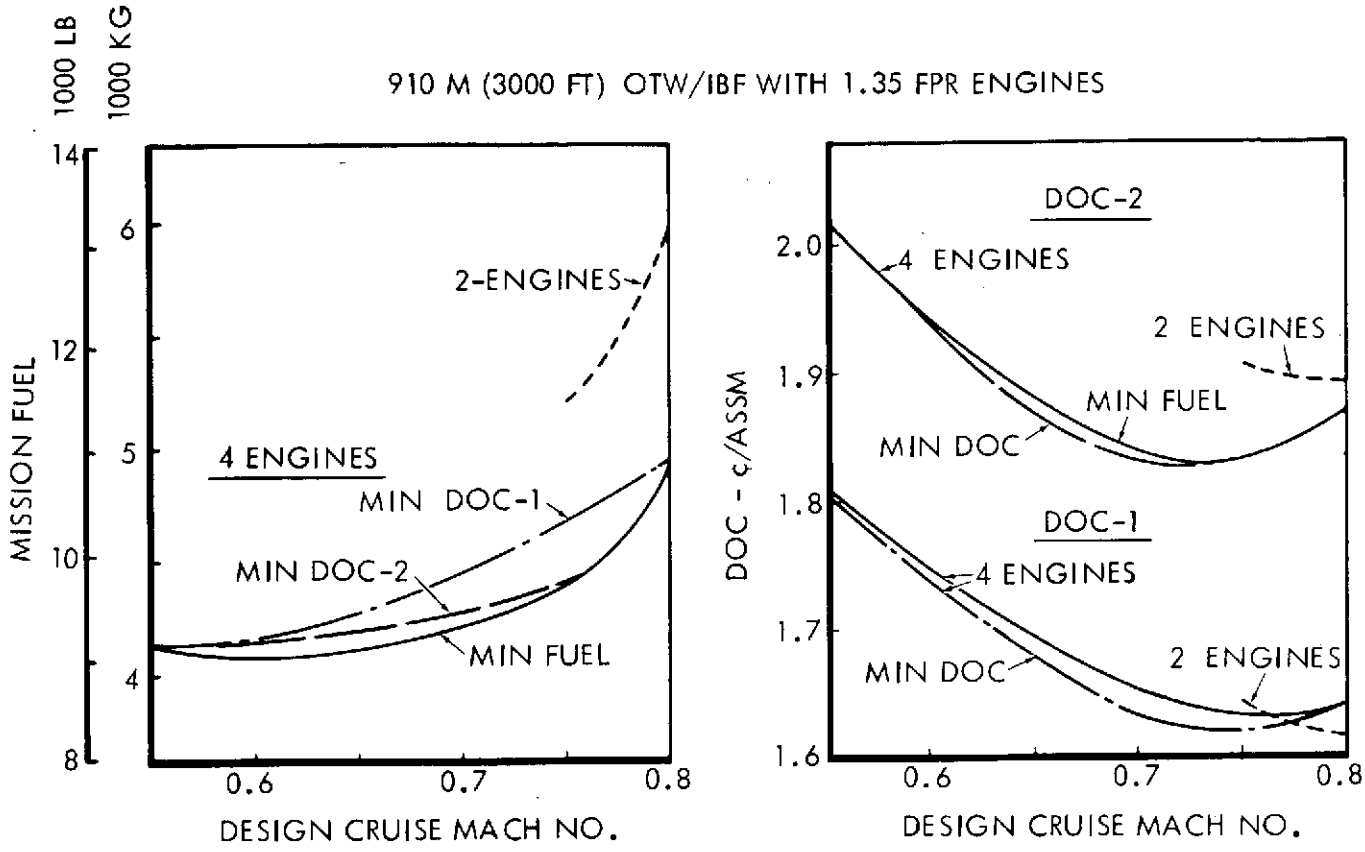

FIGURE 0.3: EFFECT OF DESIGN CRUISE SPEED

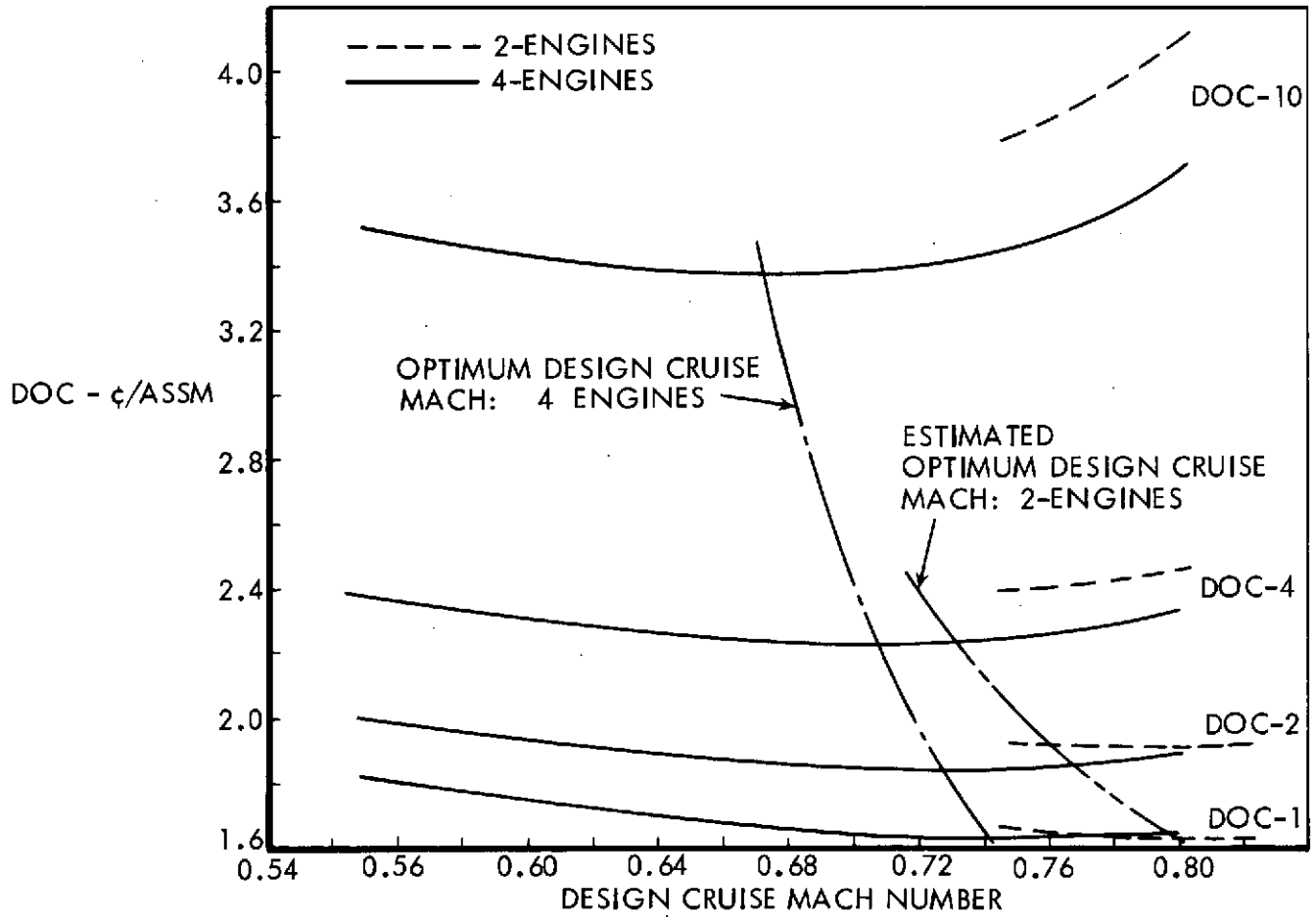

FIGURE 0.4: 1.35 FPR OTW/IBF: EFFECT OF FUEL PRICE ON OPTIMUM DESIGN CRUISE SPEED 910M (3000 FT.) FIELD LENGTH

airplane has a DOC-2 1.3% lower than the 2-engined configuration.

If the airplane had been optimized for minimum mission fuel, the figure shows a 4-engined, 0.6 M design requires only 4080 Kg (9,000 lb.), a saving of 31% relative to the original DOC-1 design. However, this saving is associated with a 8 % increase in DOC-1 to 1.75¢/ASSM, while at DOC-2 the penalty is 2.6%. While this configuration provides an excellent reduction in mission fuel, it is doubtful that it would be accepted because of the increase in DOC and the large reduction in cruise speed.

If the airplane is optimized for DOC at the increased fuel price, a 4-engined, 0.73 M configuration provides a DOC-2, 4% lower than the original optimized design and requires 27% less fuel for the mission. Thus, it can be seen that by optimizing for minimum DOC at the increased fuel price, fuel savings close to the design optimized for minimum fuel can be achieved while still minimizing operating costs.

Figure 0.4 presents DOC at various fuel price levels plotted against design cruise Mach number for 2- and 4-engined designs which use optimum aspect ratios and cruise altitudes. The buckets in the curves determine the design cruise Mach number for minimum DOC at each fuel price, which when connected together form the lines of optimized cruise speed. Note that optimum cruise speed reduces with increase in fuel price as would be expected.

The effect of engine fan pressure ratio on DOC at various fuel price levels is illustrated in Figure 0.5 for airplanes having optimum cruise speed, altitude and aspect ratio. These data were developed for the OTW/IBF, 3,000 ft. concept designed with each of the three engine cycles. It can be seen that DOC-1 is achieved with 1.47 FPR at 0.8 M while minimum DOC-10 is achieved with 1.32 FPR and 0.68 M. An excellent choice for fuel prices ranging from DOC-2 through DOC-10 is 1.35 FPR since it provides DOC's close to minimum in all cases.

The optimum aspect ratio varied for different fuel prices; airplanes optimized for minimum fuel require aspect ratios of the order of 14, while airplanes optimized for DOC-2 require aspect ratios of the order of 10-12, compared to 7-8 for minimum DOC-1.

Table 0.III summarizes the design characteristics of the OTW/IBF configurations

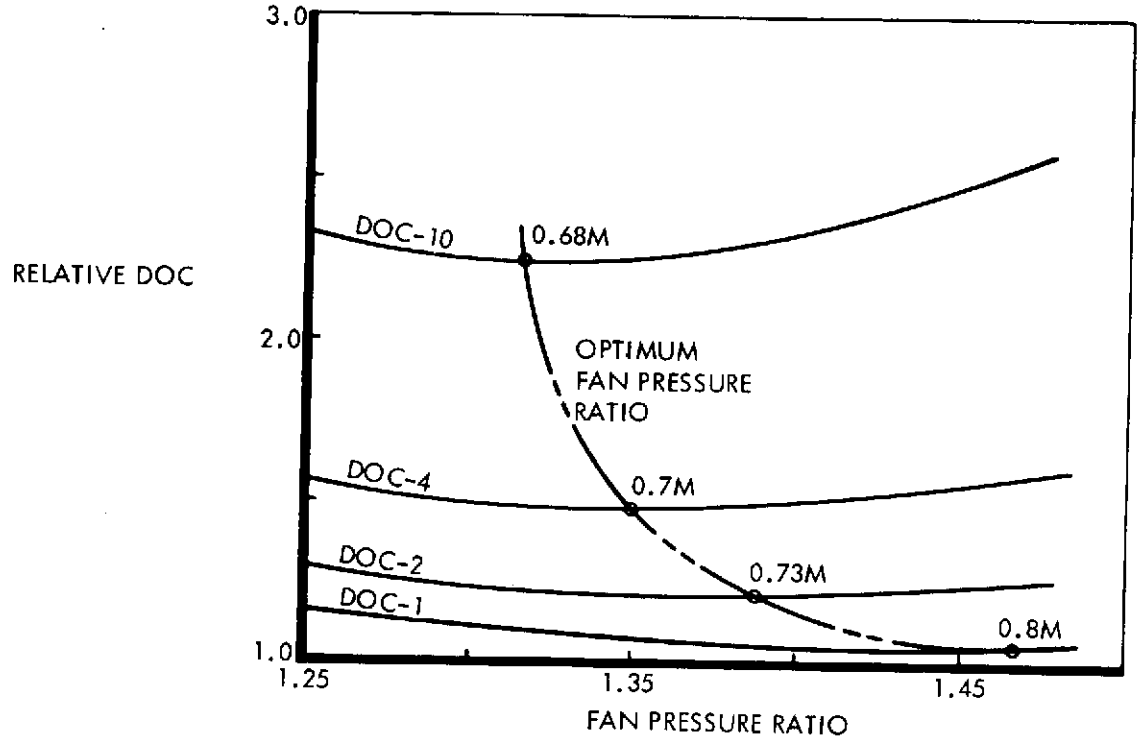

FIGURE 0.5: EFFECT OF FUEL PRICE ON OPTIMUM FAN PRESSURE RATIO - QTW/IBF CONCEPT, 910 M (3000 FT) F.L.

	1.32 FPR V.P. DOC-1 REF. 2	OPTIMIZED FOR DOC-1	DOC-2	DOC-4	DOC-10	MIN. FUEL
MACH NO.	0.8	0.8	0.75	0.70	0.70	0.60
NO. OF ENGINES	2	2	4	4	4	4
OWE - KG	44,570	43,450	36,510	35,290	35,290	34,870
(LB)	(98,250)	(95,790)	(80,490)	(77,800)	(77,800)	(76,880)
GROSS WEIGHT - KG	66,840	65,550	56,450	54,670	54,670	53,910
(LB)	(147,350)	(144,520)	(124,440)	(120,520)	(120,540)	(118,860)
RATED THRUST - KN	163.7	167.5	55.3	48.0	48.0	44.1
(LB)	(36,810)	(37,660)	(12,440)	(10,790)	(10,790)	(9,910)
MISSION FUEL - KG	6,330	6,030	4,400	4,210	4,210	4,070
(LB)	(13,960)	(13,300)	(9,700)	(9,290)	(9,290)	(8,975)
AR	7.0	7.73	12	14	14	14
*DOC-1 -- ¢/ASSM.	1.797	1.616	1.634	1.646	1.646	1.747
DOC-2 -- ¢/ASSM.	-	1.889	1.831	1.837	1.837	1.937
DOC-4 -- ¢/ASSM.	-	2.437	2.246	2.221	2.221	2.307
DOC-10 - ¢/ASSM.	-	4.08	3.441	3.373	3.373	3.422
$W/S_{T.O.}$ - KG/SQ. M.	455	449	554	530	530	457
(LB/SQ.FT)	(93.2)	(92.0)	(113.5)	(108.5)	(108.5)	(93.5)
90 EPNdB T.O. AREA	1.30	1.19	1.53	1.45	1.45	1.40
SQ. KM (SQ. MI)	(0.5)	(0.46)	(0.59)	(0.56)	(0.56)	(0.54)

* ENGINE PRODUCTION QUANTITY: 750 IN REF. 2 IDENTICAL AIRPLANE
1500 IN PRESENT PHASE

TABLE 0.III: FUEL CONSERVATIVE AIRPLANE CHARACTERISTICS 1.35 FPR, OTW/IBF, 910 M (3000 FT) F.L.

designed for 148 passengers, 926 km (500 n.m.) range, 910 m (3,000 ft.) field length and optimized for minimum DOC-1, 2, 4, and 10 and for minimum fuel. For reference, the study airplane reported in NASA CR 1146 12 (Ref. 2) is also tabulated in the first column. The higher DOC-1 for this airplane, compared to the present study airplane shown in column 2, is due primarily to the higher-priced variable-pitch fan (pressure ration 1.32) engine used in the reference 2 design. The data in column 2 reflect the refinement achieved in the present study in the airplane designed for minimum DOC-1. Also shown in this column are the DOC-2, DOC-4, and DOC-10 values for that same airplane. The third column shows that for minimum DOC-2, the design cruise speed is decreased to Mach 0.75, the optimum number of engines increased from 2 to 4, and the gross weight decreased significantly. DOC's at different fuel prices are also shown for this airplane, which is illustrated in Figure 0.6. Aircraft with minimum DOC-4 and DOC-10 were identical in the discrete designs examined; design speed and gross weight were further reduced. The last column shows that the aircraft consuming least fuel has a design speed of Mach 0.60. Because of the lower productivity associated with this speed, and higher crew and amortization costs per mile, the DOC is higher at all fuel prices evaluated -- up to 10 times 1972 fuel prices.

Augmentor Wing (AW) Aircraft

The augmentor wing concept utilizes a jet flap in which air from engines with high fan pressure ratios is ejected from the trailing edge. Excellent lift augmentation for terminal area performance is achieved and thrust is augmented through ejector action. Although the DOC was indicated to be higher than that of the hybrid OTW/IBF or the MF configurations in the reference 2 studies, it was not determined whether a two-engine AW configuration would change this conclusion. Accordingly, comparison of two and four engine configurations was undertaken in the present study, and the effect of higher fuel prices on design optimization was investigated.

Detailed studies were conducted on duct configuration, wing geometry optimization, flow split between leading and trailing edge, and T/S limitations. The resulting characteristics are summaried in Table 0.IV for airplanes optimized for minimum DOC-1, DOC-2, and fuel. Comparison of 2- and 4-engine airplanes is shown under the DOC-1

148 PASSENGERS

0.75 MACH

910 M (3000 FT) FIELD LENGTH

OPTIMIZED FOR DOC-2

SPAN = 34.75 M (114')
LENGTH = 46.3 M (152')
HEIGHT = 11.8 M (38.71')

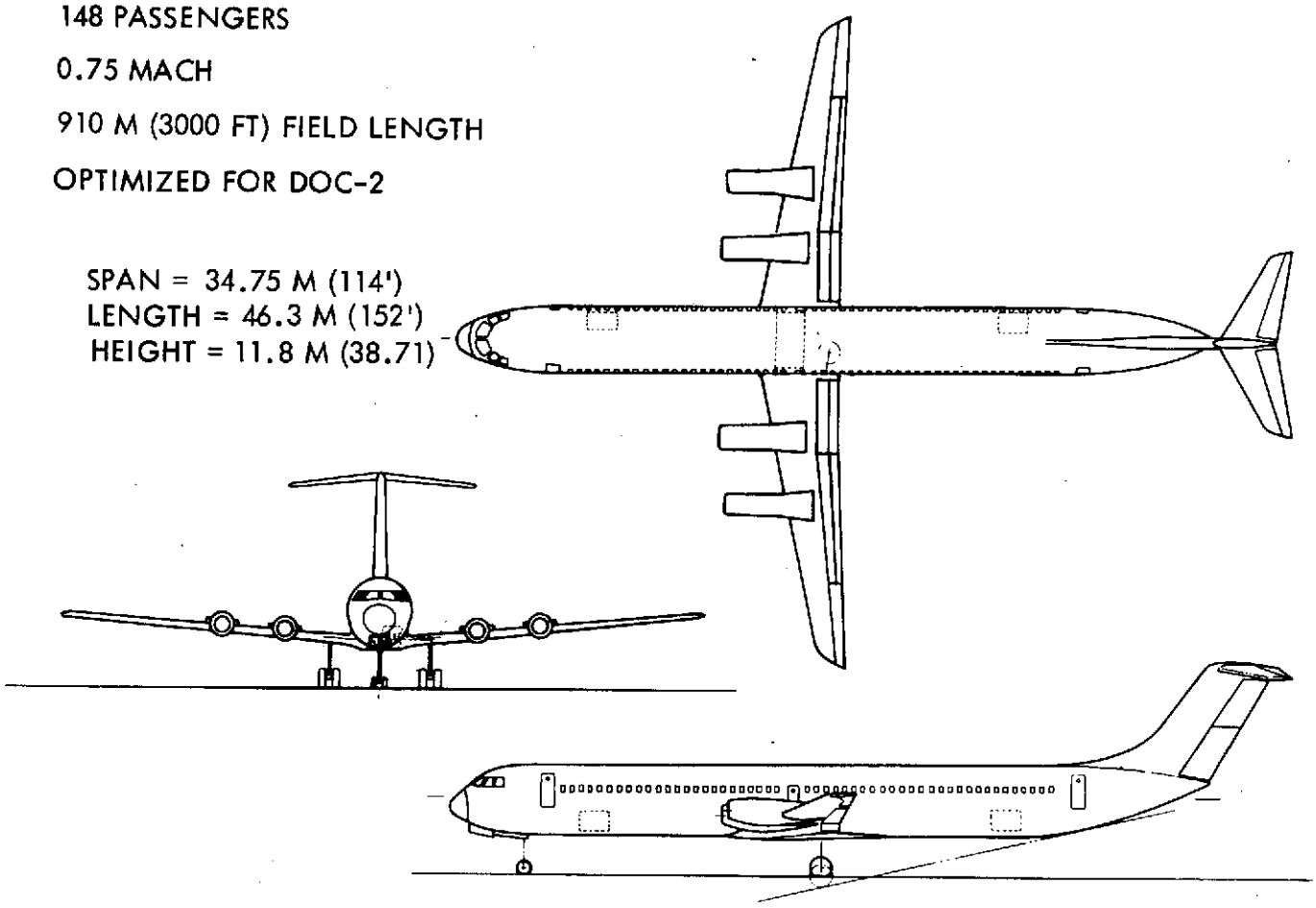

FIGURE 0.6: 910 M (3000 FT) F.L. OTW/IBF VEHICLE OPTIMIZED FOR DOC-2

column; in this concept the 4-engine configuration is superior because of the following factors:

- The wing loading for the 2-engine airplane is restricted to a lower value because duct volume requirements necessitate a larger wing.
- Lower flap deflections associated with second-segment climb provide lower augmentation ratios for the 2-engine airplane defined in Table 0.IV. This factor might be overcome by designing to fully deploy the augmentor at very small flap deflections. The associated reduction in thrust requirement would improve DOC-1 to approximately 1.97¢/ASSM. and the ramp gross weight would be reduced to 82,000 kg (180,000 lb.).
- Engine pricing for the 2-engine configuration was based on a production quantity of 750 engines; if the pricing were based on 1500 engines (300 aircraft plus 25 percent spares in a 4-engine design), the DOC would be reduced further to 1.89¢/ASSM. However, it must be noted that the FPR 3.0 engine cannot be used for other powered lift or CTOL applications; the original engine pricing based on a fixed number of STOL aircraft sets is more realistic.

The 4-engine airplane optimized for DOC-1 is illustrated in Figure 0.7. The configuration features engines placed on the upper surface of the wing in order to maximize available volume for ducts by locating engines as far as possible inboard; the upper surface location permits a more inboard location for the same degree of interference drag. The wing planform has a constant chord section extending to the outboard engine for the purpose of maximizing at a given wing area the chord (and duct volume) at this location.

The columns headed DOC-2 in Table 0.IV reflect the characteristics of aircraft with further design refinement for reducing fuel consumption and minimizing DOC-2. The first airplane uses four engines with 3.2 FPR and improved SFC in a configuration similar to that shown in Figure 0.7. Reduction in mission fuel is significant compared to the

910 M (3000 FT) FIELD LENGTH

OPTIMIZED FOR	REF. 2 DOC-1	DOC-1		DOC-2		MIN. FUEL
NO. OF ENGINES	4	4	2	4	2 + 2	2 + 2
FPR	3.0	3.0	3.0	3.2	1.35 (3.0)	1.35 (3.0)
MACH NO.	0.8	0.8	0.8	0.75	0.75	0.75
CRUISE ALT. - M (FT)	9,140 (30,000)	9,140 (30,000)	9,140 (30,000)	7,620 (30,000)	9,140 (30,000)	9,140 (30,000)
AR	6.5	6.0	5.0	8.5	10.0	14.0
SWEEP - DEG.	30	20	20	10	10	10
$W/S_{T.O.}$ - KG/SQ.M (LB/SQ. FT)	473 (96.9)	512 (105.0)	369 (75.5)	491 (100.5)	547 (112.0)	503 (103.0)
$T/W_{T.O.}$	0.324	.347	.444	.305	.29 (.41)	.28 (.39)
RGW - KG (LB)	72,350 (159,503)	69,900 (154,100)	92,910 (204,830)	63,460 (139,900)	65,030 (143,370	69,070 (152,280)
OWE - KG (LB)	47,530 (104,779)	45,260 (99,790)	63,570 (140,150)	40,890 (90,150)	44,810 (98,790)	49,490 (109,100)
MISSION FUEL - KG (LB)	8,408 (18,537)	8,256 (18,200)	11,706 (25,806)	6,559 (14,460)	7,049 (12,540)	5,583 (12,309)
DOC-1 - ¢/ASSM	1.90	1.88	2.164	-	-	-
DOC-2 - ¢/ASSM	-	-	-	2.11	2.015	2.079
90 EPNdB T.O. AREA - SQ. K (SQ. MI.)	- -	1.30 (0.5)	- -	<1.30 (<0.5)	~ 1.30 (~ 0.5)	- -

TABLE 0.IV AW - AIRPLANE CHARACTERISTICS

148 PAX

0.8 M

910 M (3000 FT) FIELD LENGTH

SPAN = 28.9 M (94.7')

LENGTH = 42.4 M (139')

HEIGHT =11.7 M (38.5')

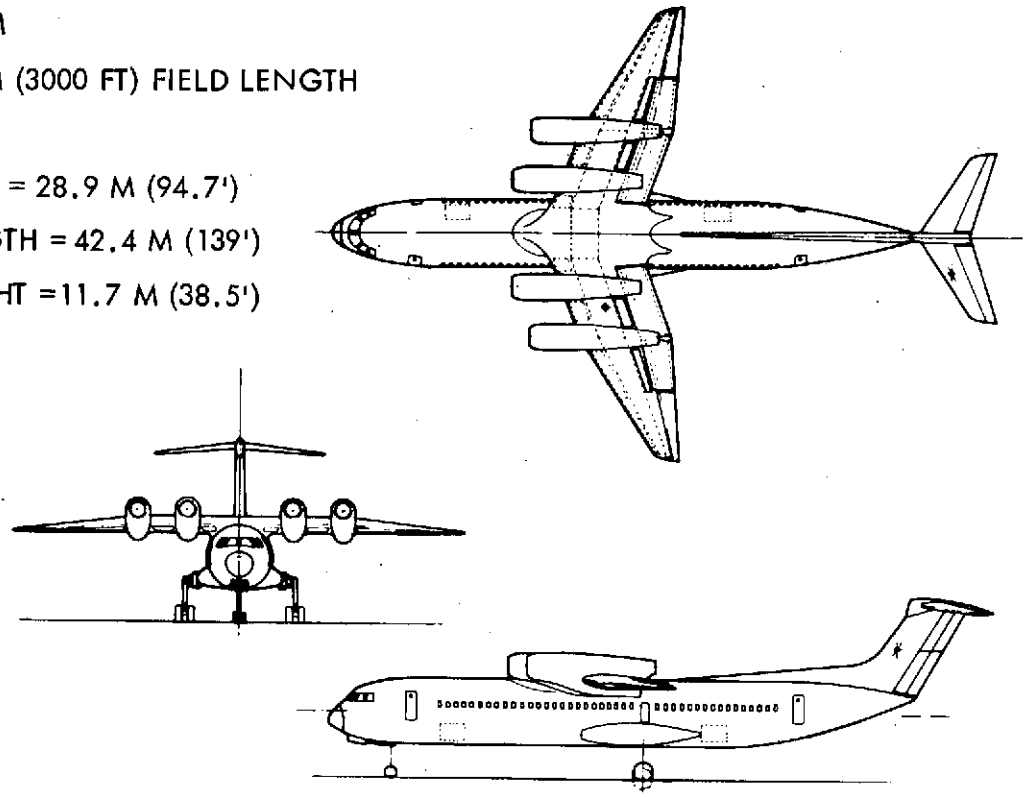

FIGURE 0.7: 910 M (3000 FT) AW VEHICLE - DOC-1

148 PASSENGERS

0.8 MACH

910M (3000 FT) FIELD LENGTH

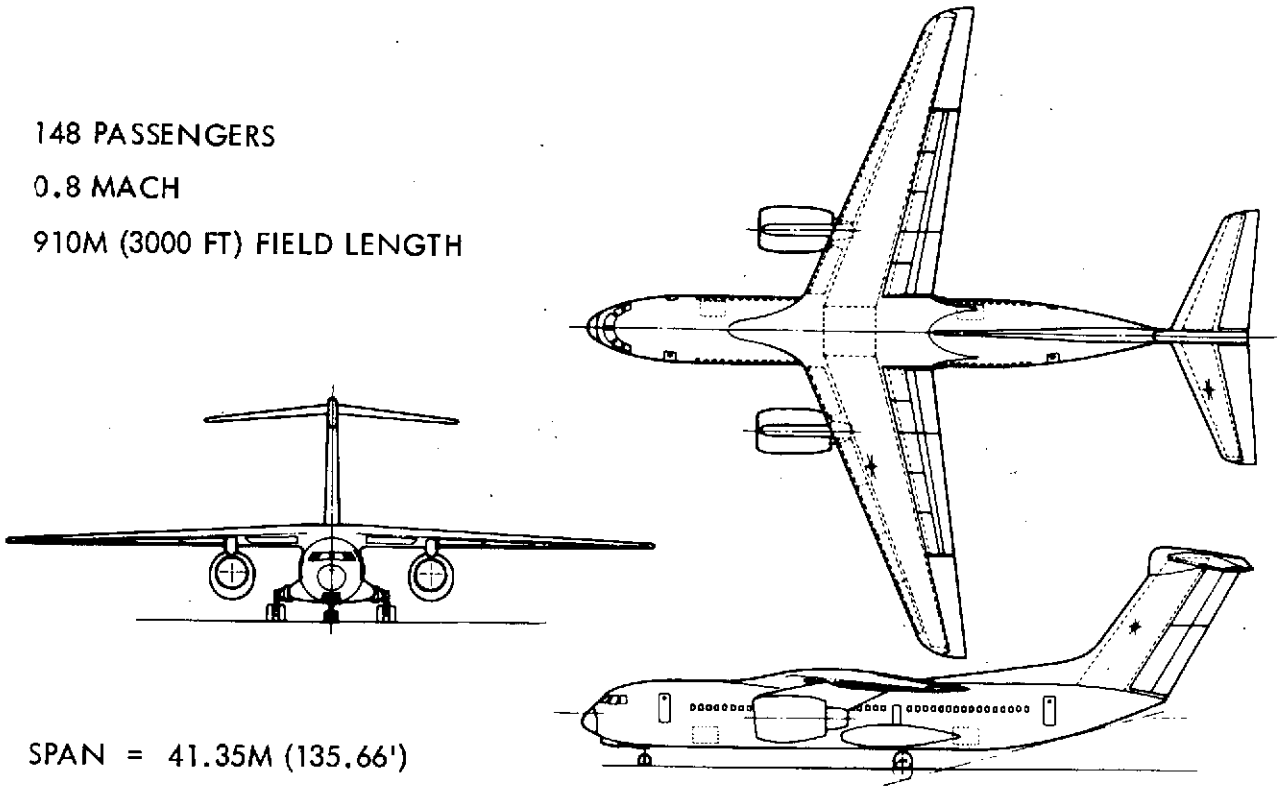

SPAN = 41.35M (135.66')

LENGTH = 43.18M (141.66')

HEIGHT = 14.22M (46.66')

FIGURE 0.8: MF - GENERAL ARRANGEMENT, FPR 1.35

DOC-1 airplane. Further reduction in fuel and DOC is attainable by an arrangement which uses two FPR 1.35 cruise engines combined with two FPR 3.0 load compressors for low speed high-lift operations. This is labeled 2 + 2 in Table 0.IV. It is recognized thar two sets of unlike engines would be regarded with disfavor by airline operators; although this arrangement gives the best fuel performance possible in an augmentor wing concept, it is higher in DOC and fuel consumption than other concepts.

Mechanical Flap Aircraft

Aircraft for 910 m. (3,000 ft.) field performance were defined using a high-performance double-slotted Fowler flap; maximum lift coefficient was 3.3. Landing approach speed of 182.2 Km/hr. (99 kts.) was the critical factor in establishing the wing loading at 287 $Kg/m.^2$ (58.8 psf). The basic arrangement, shown in Figure 0.8, has a 6 abreast fuselage with high wing, tee tail and pylon-mounted nacelles.

Considerable improvement in installed engine performance (compared to previous studies) was achieved in the present study by utilizing nacelles designed for best aerodynamic performance with acoustic treatment installed on wall surfaces only. Preliminary Design weight and analyses with allowances for fatigue, gust loads, and flutter were made, along with control and ride qualities investigations which indicated conceptually that augmentation systems could achieve satisfactory ride qualities.

Characteristics of aircraft resulting from the design refinement are shown in Table 0.V, including the extension of the designs to 1070 m (3500 ft.) and 1220 m (4000 ft.) field lengths. These aircraft were optimized for minimum DOC at 1972 fuel prices; the DOC values shown for different fuel prices are based on taking advantage of the 2780 Km range capability to increase the utilization of the aircraft to 3000 hours per year.

The designs were modified for fuel conservation and for minimum DOC at increased fuel prices by evaluating factors such as cruise speed and altitude, wing aspect ratio and sweep, and number of engines. The effect of cruise speed on mission fuel and DOC-2 is shown in Figure 0.9. (Airplane design range was 926 Km (500 n.m.) and utilization was 2500 hours per year for DOC calculations). The fuel penalty is high for higher cruise speed for the low wing loading airplane with 910 m (3000 ft.) field performance.

148 PASSENGERS MO.8 AT 9140 M (30000 Ft.) ALT. TWO ENGINES, 20 DEG. SWEEP	926 KM (500 N.M.) RANGE WITH DESIGN FIELD LENGTH 2780 KM (1500 N.M.) RANGE WITH CTOL TAKEOFF			
DESIGN FIELD LENGTH - M -(FT)	914 (3,000)	1,070 (3,500)	1,220 (4,000)	1,220 (4,000)
FAN PRESSURE RATIO/TYPE	1.35 F/P	1.35 F/P	1.35 F/P	1.47 F/P
WING ASPECT RATIO	7	8	10	10
RAMP GROSS WT. - KG	77,963	69,289	65,781	68,095
-(LB)	(171,877)	(152,753)	(145,020)	(150,121)
OPERATING WEIGHT - KG - (LB)	47,724 (105,212	41,633 (91,784)	39,529 (87,144)	40,255 (88,745)
WING LOADING T.O. - KG/SQM	287	345	403	403
926 KM MISSION (LB/SQ. FT.)	(58.8)	(70.6)	(82.5)	(82.5)
T/W 926 KM MISSION	0.450	0.416	0.386	0.354
RATED THRUST/ENGINE - KN	168.6	139.7	123.8	114.9
-(LB.)	37,898	31,401	27,826	25,830
CRUISE THRUST SETTING	1.000	1.000	1.000	0.866
T/C	14.16	13.69	13.11	13.07
926 KM DOC-1 - ¢/ASSM	1.62	1.50	1.44	1.40
DOC-2-¢/ASSM	1.93	1.85	1.67	1.65
DOC-4-¢/ASSM	2.53	2.37	2.13	2.17
DOC-10-¢/ASSM	4.33	3.80	3.52	3.72
MISSION FUEL - KG	6593	5625	5088	5676
-(LB.)	(14,536)	(12,400)	(11,218)	(12,514)
2780 KM DOC-2-¢/ASSM	1.43	1.30	1.23	1.25
MISSION FUEL - KG	14,471	12,207	10,964	12, 359
-(LB.)	(31,902)	(26,911)	(24,170)	(27,246)
COMPLETE A/C PRICE - $M	8.629	7.976	7.678	7.573
ENGINE PRICE - $M	2.081	1.948	1.868	1.652

TABLE 0.V: MF - BASELINE AIRPLANE CHARACTERISTICS

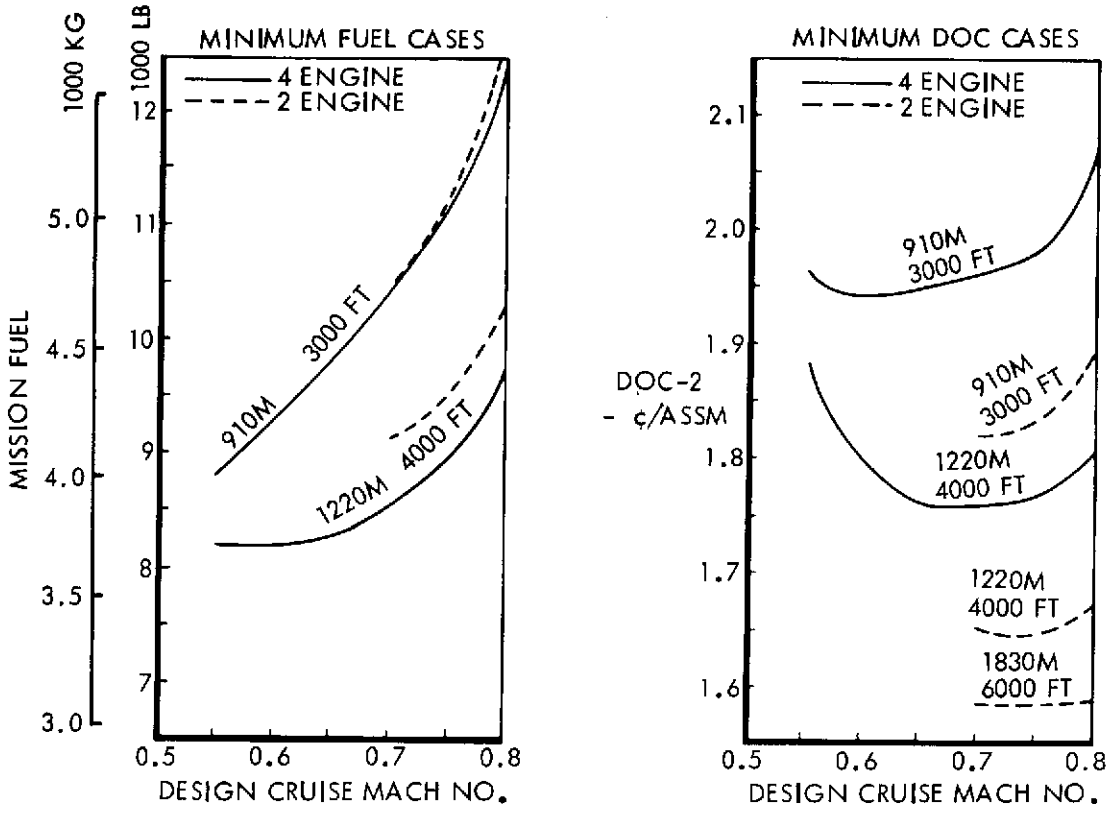

FIGURE 0.9: EFFECT OF DESIGN CRUISE SPEED - MF WITH 1.35 FPR ENGINES

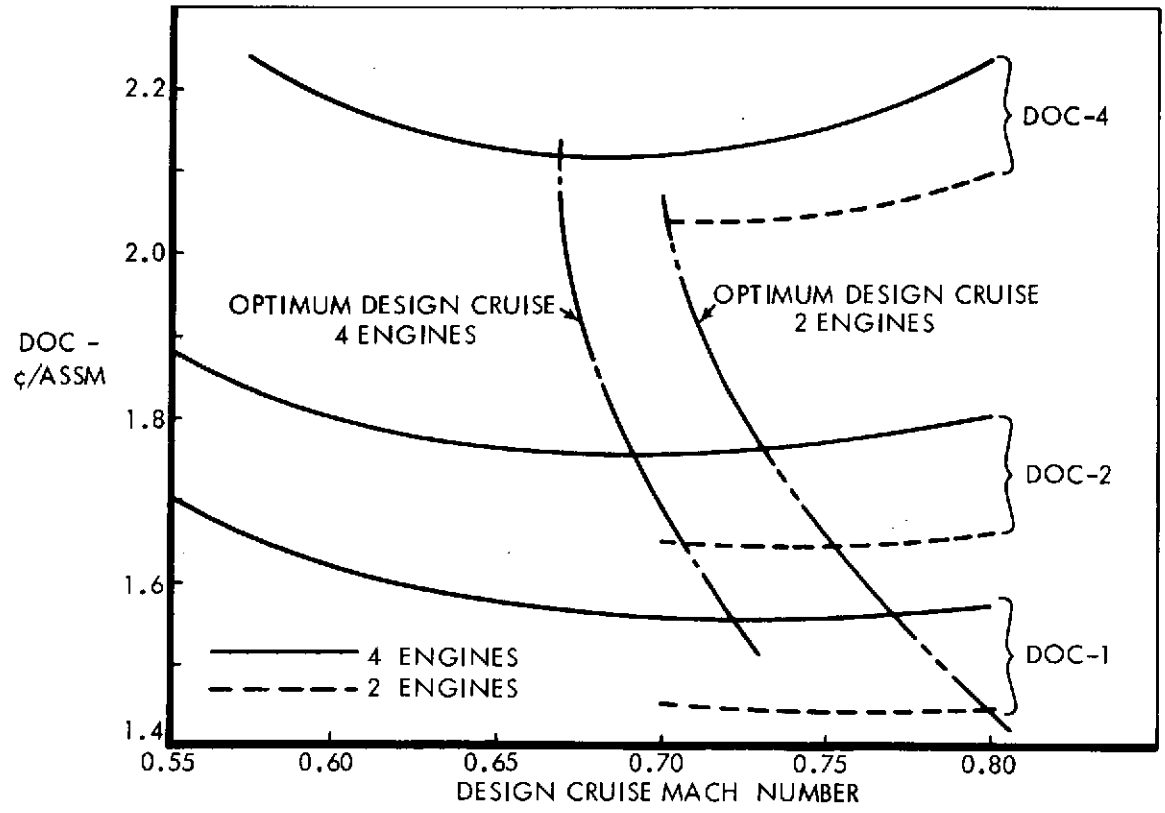

FIGURE 0.10: EFFECT OF FUEL PRICE ON OPTIMUM DESIGN CRUISE SPEED: 1220 M (4000 FT) FIELD LENGTH MF

Effect of other fuel prices on design speed for minimum DOC is reflected in Figure 0.10 for the 1220 m. (4000 ft.) MF airplane. Although the four-engine airplanes require less fuel, the two-engine airplanes provide minimum DOC at fuel prices up to those represented by DOC-4.

Tables 0.VI and 0.VII summarize the characteristics of MF configurations designed for 910 m. (3000 ft.) and 1220 m. (4000 ft.) with 148 passengers and 926 Km (500 n.m.) range. The study airplanes defined in reference 2 are also tabulated. A significant improvement is shown in the present study, primarily due to the improved installed engine performance achieved by elimination of acoustic splitters in the nacelles. The airplane designed for 1220 m. (4000 ft.) field performance and optimized for minimum DOC-2 is shown in Figure 0.11.

Other Concepts Evaluated for Fuel Conservation

The study completed in 1973, "Study of Quiet Turbofan STOL Aircraft for Short Haul Transportation" (reference 2) included evaluation of externally blown flap, over the wing, boundary layer control, and internally blown flap lift concepts. These have been reexamined in the present study in the light of fuel conservation and increased fuel prices.

The externally blown flap airplane with 1.25 FPR engines has a design cruise speed of 0.65 M for minimum DOC-2. It is a four-engine configuration with aspect ratio 10. Fuel consumption and DOC-2 are shown in Figure 0.12, along with other lift concepts. Although its fuel is acceptably low, the DOC-2 is high, principally because of the low cruise speed and low fan pressure ratio engine which is required for comparable noise levels.

The over-the-wing concept is closely comparable to the four-engine hybrid OTW/IBF except, of course, the IBF component is deleted and the flap would be modified for Coanda turning aft of the nacelle, and slotted elsewhere. At higher fuel prices, the economic advantage of two engines in the hybrid OTW/IBF is lost so the four-engine OTW must be regarded as a competitive concept.

Boundary layer control and internally blown flap concepts both require vectoring of the fan air to achieve the required approach glide slopes. Under-wing installations with

	REF. 2 DOC-1	OPTIMIZED FOR DOC-1		DOC-2	DOC-4	DOC-10	MIN FUEL
MACH NO.	0.8	0.8	0.75	0.70	0.70	0.60	0.55
NO. OF ENGINES	2	2	2	2	2	4	4
OWE - KG	52,590	46,870	41,760	40,020	40,020	38,270	35,290
(LB)	(115,940)	(103,330)	(92,060)	(88,230)	(88,230)	(84,380)	(77,800)
GROSS WEIGHT - KG	76,610	69,000	62,690	60,210	60,210	57,700	54,200
(LB)	(168,890)	(152,110)	(138,200)	(132,740)	(132,740)	(127,210)	(119,480)
RATED THRUST - KN	195.5	151.6	125.3	118.4	118.4	43.4	38.5
(LB)	(43,950)	(34,070)	(28,160)	26,610)	(26,610)	(9,760)	(8,660)
MISSION FUEL - KG	7,550	6,110	5,440	4,870	4,870	4,200	3,980
(LB)	(16,640)	(13,460)	(12,000)	(10,730)	(10,730)	(9,250)	(8,770)
AR	7.0	7.0	7.0	7-10	7-10	10	14
*DOC-1 -- ¢/ASSM.	1.931	1.632	1.582	1.597	1.597	1.75	1.828
DOC-2 -- ¢/ASSM.		1.912	1.832	1.818	1.818	1.94	2.010
DOC-4 -- ¢/ASSM.		2.472	2.328	2.262	2.262	2.32	2.376
DOC-10 -- ¢/ASSM.		4.152	3.760	3.589	3.589	3.46	3.472
$W/S_{T.O.}$ - KG/SQ.M.	302	287	287	287	287	287	287
(LB/SQ.FT)	(61.8)	(58.8)	(58.8)	(58.8)	(58.8)	(58.8)	(58.8)
90 EPNdB T.O. AREA SQ. KM (SQ. MI)	1.04 (0.4)	1.48 (0.57)	1.40 (0.54)	1.37 (0.53)	1.37 (0.53)	1.09 (0.42)	1.06 (0.41)

IDENTICAL AIRPLANE

* ENGINE PRODUCTION QUANTITY: 750 IN REF. 2 1500 IN PRESENT PHASE

TABLE 0.VI: AIRPLANE CHARACTERISTICS
1.35 FPR, MF 910 M (3000 FT) F.L.

	REF. 2 DOC-1	OPTIMIZED FOR DOC-1	DOC-2	DOC-4	DOC-10	MIN. FUEL
MACH NO.	0.8	0.8	0.75	0.70	0.65	0.60
NO. OF ENGINES	2	2	2	2	4	4
OWE - KG	40,510	39,140	36,770	35,790	33,800	33,920
(LB)	(89,300)	(86,280)	(81,060)	(78,900)	(74,520)	(74,770)
GROSS WEIGHT - KG	62,120	59,400	56,460	55,340	52,590	52,530
(LB)	(136,950)	(130,950)	(124,480)	(122,000)	(115,950)	(115,800)
RATED THRUST - KN	150.3	114.3	111.0	104.8	40.9	38.0
(LB)	(33,800)	(25,690)	(24,950)	(23,560)	(9,190)	(8,550)
MISSION FUEL - KG	5,865	4,717	4,382	4,218	3,801	3,715
(LB)	(12,930)	(10,400)	(9,660)	(9,300)	(8,380)	(8,190)
AR	7.0	10.0	10.0	10.0	14.0	14
*DOC-1 -- ¢/ASSM.	1.681	1.446	1.45	1.466	1.626	1.70
DOC-2 -- ¢/ASSM.		1.67	1.648	1.659	1.798	1.87
DOC-4 -- ¢/ASSM.		2.10	2.05	2.044	2.142	2.21
DOC-10 -- ¢/ASSM.		3.408	3.25	3.20	3.174	3.23
$W/S_{T.O.}$ - KG/SQ.M.	455	391	393	379	403	361
(LB/SQ.FT)	(93.1)	(80.0)	(80.5)	(77.6)	(82.5)	(74.0)
90 EPNdB T.O. AREA SQ. KM (SQ. MI)	0.97 (0.375)	1.42 (0.55)	1.37 (0.53)	1.32 (0.51)	1.088 (0.42)	N/A

* ENGINE PRODUCTION QUANTITY: 750 IN REF. 2
1500 IN PRESENT PHASE

TABLE 0.VII: AIRPLANE CHARACTERISTICS
1.35 FPR, MF, 1220 M (4000 FT) F.L.

148 PASSENGERS

0.75 MACH

1220 M. (4000 FT) FIELD LENGTH

OPTIMIZED FOR DOC-2

SPAN = 37.8 M (124')
LENGTH = 46.3 M (152')
HEIGHT = 11.8 M (38.7')

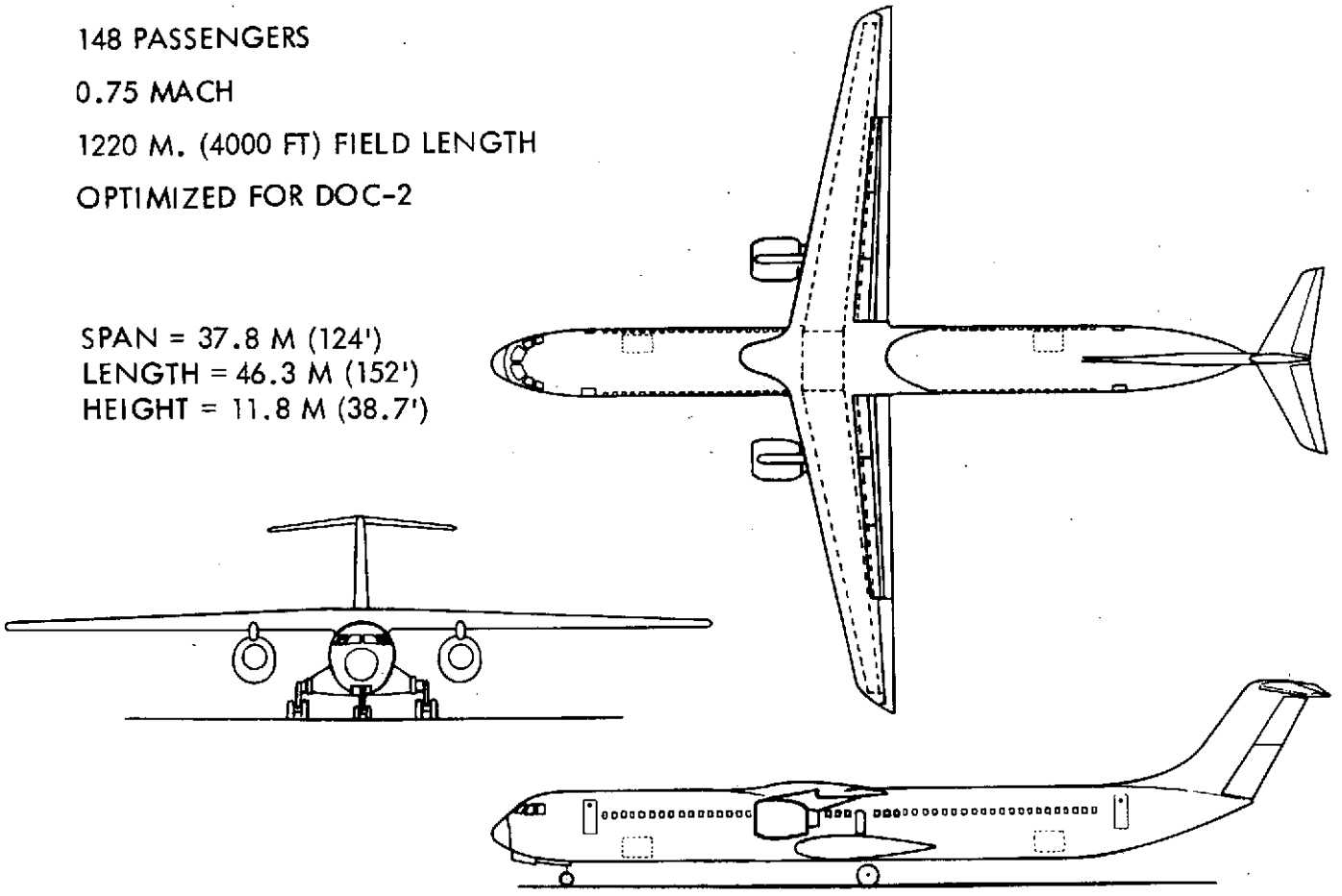

FIGURE 0.11: 1220 M (4000 FT) MF VEHICLE - DOC 2

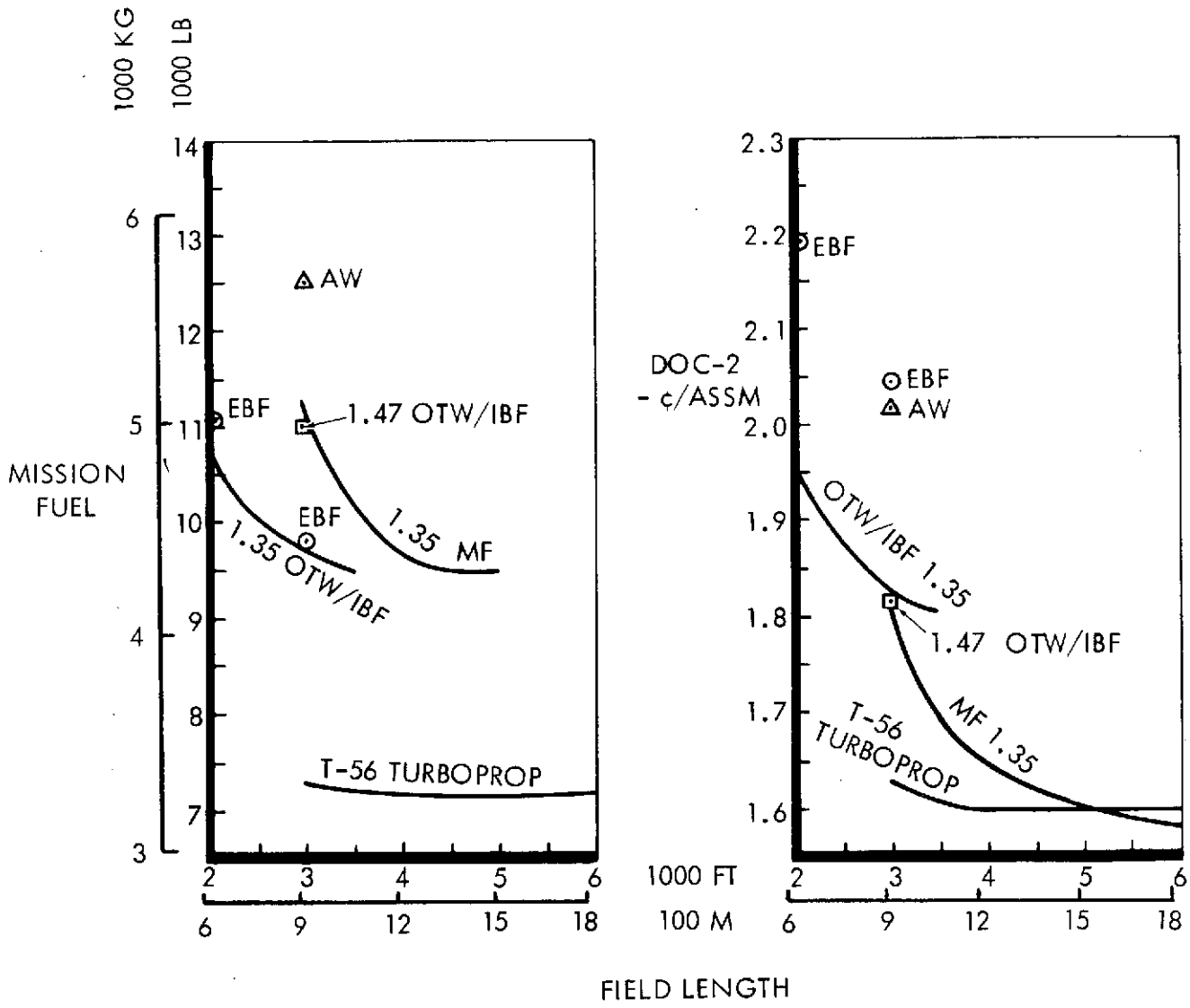

FIGURE 0.12: COMPARISON OF CONCEPTS - MINIMUM DOC-2 CASES

Pegasus-type nozzles showed inferior cruise performance, DOC and fuel consumption compared to other concepts.

Aircraft were designed with rubberized T-56 turboprop engines and with conventional and low-tip-speed propellers. Stall speed margins were based on power-on conditions, providing allowable wing loadings higher than those based on power-off as required by FAR Part 25. The quiet propeller aircraft had better fuel consumption and DOC due to the higher low-speed thrust permitting higher wing loadings for a given field performance. Cruise speeds were Mach 0.5 to Mach 0.6. Fuel and DOC-2 are shown as a function of field length in Figure 0.12. Characteristics of aircraft designed for 910 m. (3000 ft.) field performance with different fuel price levels are shown in Table 0.VIII.

If the T-56 turboprop deflected slipstream concept were acceptable from considerations of passenger appeal and cruise speed, it would be the best choice for field lengths up to 1525 m. (5000 ft.). It is suggested that this application is most suitable in the low to medium density short haul market, particularly at stage lengths below 700 Km (380 n.m.). It is not likely to compete successfully for passengers in competition with higher-speed fan-powered aircraft in high-density routes such as Chicago-New York. Since the present study is primarily concerned with the latter high-density arena, the turboprop deflected slipstream aircraft have been included only as a reference in the comparisons that follow.

Evaluation of Aircraft Configurations

Noise analyses and tradeoffs were conducted to determine the economic penalty associated with the various potential noise requirements, such as FAR 36, less than FAR 36, 95 EPNdB at the 500 ft. sideline, 80 EPNdB at Sperry Box, and footprint area and length for various noise level contours. The analyses were arranged to indicate the effect of concepts, fan pressure ratio, field length and fuel price variations on the various noise level measuring parameters.

Table 0.IX summarizes the effect of noise constraints on airplane configuration, DOC-2, and fuel consumption with no restriction on the performance factors. With cruise speed and block time unrestricted, the two-engine mechanical flap aircraft with 1830 m. (6000 ft.) field length and FPR 1.35 engines satisfies many noise restrictions with no

	OPTIMIZED FOR				
	DOC-1	DOC-2	DOC-4	DOC-10	MIN. FUEL
MACH NO.	0.60	0.55	0.55	0.50	0.50
NO. OF ENGINES	4	4	4	4	4
OWE - KG	35,690	34,805	34,805	34,360	34,360
(LB)	(78,680)	(76,730)	(76,730)	(75,750)	(75,750)
GROSS WEIGHT - KG	54,440	53,170	53,170	52,720	52,720
(LB)	(120,028)	(117,223)	(117,223)	(116,232)	(116,232)
MISSION FUEL - KG	3,656	3,293	3,292	3,148	3,148
(LB)	(8,060)	(7,260)	(7,260)	(6,940)	(6,940)
AR	14	14	14	14	14
DOC-1 -- ¢/ASSM.	1.473	1.477	1.477	1.500	1.500
DOC-2 -- ¢/ASSM.	1.642	1.629	1.629	1.643	1.643
DOC-4 -- ¢/ASSM.	1.977	1.935	1.935	1.935	1.935
DOC-10 -- ¢/ASSM.	2.985	2.851	2.851	2.805	2.805
$W/S_{T.O.}$ - KG/SQ.M.	391	387	387	371	371
(LB/SQ.FT)	(80.0)	(79.2)	(79.2)	(76.0)	(76.0)
INST. THRUST/ENG. - KN	40.1	37.8	37.8	35.6	35.6
(LB)	(9,019)	(8,502)	(8,502)	(7,996)	(7,996)
CRUISE POWER %	90	80	80	70	70
90 EPNdB AREA - SQ. KM	1.30	1.30	1.30	1.30	1.30
(ESTIMATE) (SQ. MI)	(0.5)	(0.5)	(0.5)	(0.5)	(0.5)
		IDENTICAL AIRPLANE		IDENTICAL AIRPLANE	

TABLE 0.VIII: T-56 AND QUIET PROPELLER - 910 M (3000 FT) F.L.

	LIFT CONCEPT	NO. ENG.	FPR	FIELD LENGTH M (FT)	CRUISE SPEED	PAX	DOC-2 ¢/ASSM	FUEL KG (LB)
MIN DOC-2 CASE:								
MIN DOC FOR FAR36-5	MF	2	1.47	1,830 (6,000)	0.75	148	~1.59	–
MIN DOC FOR FAR36-10	MF	2	1.35	1,830 (6,000)	0.75	148	1.599	4,199 (9,258)
MIN DOC FOR FAR36-15	MF	2	1.35	1,830 (6,000)	0.75	148	1.599	4,199 (9,258)
MIN DOC FOR 95 EPNdB @ 152 M (500')	MF	2	1.35	1,220 (4,000)	0.75	148	1.641	4,318 (9,519)
MIN DOC FOR 80 EPNdB @ SPERRY BOX SIDELINE	OTW/IBF	4	1.25	910 (3,000)	0.75	50	3.87	2,223 (4,900)
MIN DOC FOR 80 EPNdB @ SPERRY BOX FLYOVER	OTW/IBF	4	1.25	610 (2,000)	0.75	5-10	7+	
MIN DOC-2 FOR 90 EPNdB FOOTPRINT:								
2.60 SQ. KM (1 SQ.MI.)	MF	2	1.35	1,830 (6,000)	0.75	148	1.599	4,199 (9,258)
1.3 SQ. KM (0.5 SQ.MI.)	MF (0.526)	2	1.35	1,220 (4,000)	0.75	148	1.641	4,318 (9,519)
.83 SQ. KM (0.32 SQ. MI.)	OTW/IBF (WITH SPLITTERS)	4	1.35	910 (3,000)	0.75	148	1.863	4,790 (10,560)
.75 SQ. KM (0.29 SQ. MI.)	MF	4	1.25	1,220 (4,000)	0.65	148	1.887	4,027 (8,877)
MIN DOC-2 FOR 90 EPNdB FOOTPRINT LENGTH:								
6.48 KM (3.5 N.MI.)	MF	2	1.35	1,830 (6,000)	0.75	148	1.599	4,199 (9,258)
3.704 KM (2.0 N.MI.)	MF	2	1.35	1,830 (6,000)	0.75	148	1.599	4,199 (9,258)
1.85 KM (1.0 N.MI.)	OTW/IBF	2	1.35	< 910 (3,000)	0.75	148	1.90	6,350 (14,000)
1220 M (4000 FT)	OTW/IBF	2	1.25	610 (2,000)	0.75	148	2.3	6,804 (15,000)

TABLE 0.IX: DOC AND FUEL PENALTIES - NO PERFORMANCE CONSTRAINTS

penalty indicated for DOC-2 or fuel. For purposes of further comparisons, the 1830 m. (6000 ft.) MF airplane is used as a basis for expressing penalties. If field lengths for short haul aircraft are restricted to 1220 m. (4000 ft.) or less, as suggested throughout the study, the penalties for meeting the different potential requirements are those indicated in Table 0.X. Most of the cases are best satisfied with MF aircraft. Significant increases in DOC and fuel penalties are indicated if 90 EPNdB requirements of less than 1.0 sq. Km. (0.39 sq. mi.) area, or 2.3 Km. (7500 ft.) footprint length are imposed. As noted, the 80 EPNdB STOLport requirement designated 'Sperry box' calls for a very small airplane probably designed for low wing loading and short stage lengths. This requirement does not appear compatible with the high density scenario although it may become feasible for commuter operations.

The penalties for different noise requirements with field length restricted to 910 m. (3000 ft.) are given in Table 0.XI. This comparison was also restricted to designs for Mach 0.75 cruise speed. The low wing loading mechanical flap aircraft designed to cruise at Mach 0.70 would be approximately one percent lower in DOC and nine percent better in fuel consumption. It is concluded that most of the prospective noise requirements can be met with 910 m. (3000 ft.) aircraft at a total penalty of 17 percent compared with a 1830 m. (6000 ft.) airplane. Penalties for mechanical flap and hybrid OTW/IBF are about equal from the standpoint of noise level and direct operating cost at twice 1972 fuel prices; the hybrid is superior in fuel consumption and its DOC would become superior with further increases in fuel price.

It is suggested that attention be given to restricting the 90 EPNdB contour to one sq. Km. (0.39 sq. mi.) in area and 2.3 Km. (7500 ft.) in length. Cost and fuel penalties increase for more stringent requirements. Shorter footprint lengths would require shorter field length requirements and would change the optimum design from four to two engines in the OTW/IBF aircraft.

The effect of field length on direct operating costs and fuel consumption can be summarized for three potential noise requirements as follows (Ref. is the 1830 m. (6000 ft.) aircraft meeting FAR 36-10):

	Lift Concept	No. of Engines	Engine FPR	Field Length m (ft)	Cruise Speed M	DOC 2 Penalty %	Fuel Penalty %
Reference	MF	2	1.35	1830 (6000)	0.75	0	0
FAR 36 - 10 - 15	MF	2	1.35	1220 (4000)	0.75	3.0	4.3
95 EPNdB @ 152m (500 FT.)	MF	2	1.32	1220 (4000)	0.75	4	5
90 EPNdB Footprint							
Area = 2.60 Km^2 (1.00 sq mi)	MF	2	1.40	1220 (4000)	0.75	3	4
1.30 Km^2 (0.50 sq mi)	MF	2	1.33	1220 (4000)	0.75	4	5
0.83 Km^2 (0.32 sq mi)	OTW/IBF	4 Splitler	1.35	910 (3000)	0.75	17	14
0.75 Km^2 (0.29 sq mi)	MF	4	1.25	1220 (4000)	0.65	18	(- 4)
90 EPNdB Footprint							
Length = 1.85 Km (1.0 n.m.)	OTW/IBF	2	1.35	850 (2800)	0.75	20	50
1220m (4000 FT)	OTW/IBF	2	1.25	610 (2000)	0.75	40	60
Sperry Box - 80 EPNdB	Small airplane with low wing loading designed for short stage lengths					400	200 (per passenger)

TABLE 0.X DOC AND FUEL PENALTIES @ FIELD LENGTH 1220 M (4000 FT) OR LESS

NOISE REQUIREMENT	LIFT CONCEPT	NO. OF ENGINES	ENGINE FPR	FIELD LENGTH m. (FT.)	DOC-2 PENALTY PCTG	FUEL PENALTY PCTG
REFERENCE	MF	2	1.35	1830 (6000)	0	0
FAR 36 - 10 OR 15	MF*	2	1.35	910 (3000)	15	27
FAR 36 - 15	OTW/IBF	4 (SPLITTER)	1.35	910 (3000)	17	14
95 EPNdB @ 152 m. (500 FT.)	OTW/IBF	4	1.35	910 (3000)	15	6
90 EPNdB AREA						
2.6 SQ. Km (1 SQ.MI.)	MF*	2	1.40	910 (3000)	14	27
1.3 SQ. Km (0.5 SQ.MI.)	OTW/IBF	4	1.37	910 (3000)	15	6
0.83 SQ. Km (0.32 SQ.MI.)	OTW/IBF	4 (SPLITTER)	1.35	910 (3000)	17	14
90 EPNdB LENGTH						
2.3 Km (7500 FT.)	OTW/IBF	4 (SPLITTER)	1.35	910 (3000)	17	14
1.86 Km (1 N.MI.)	OTW/IBF	2	1.35	850 (2800)	20	50
1.22 Km (4000 FT.)	OTW/IBF	2	1.25	610 (2000)	40	60

* MF AT LOW WING LOADING REQUIRES RIDE QUALITY GUST ALLEVIATION AND DEMONSTRATION FOR PASSENGER ACCEPTABILITY ON LONGER STAGE LENGTHS.

TABLE 0.XI DOC AND FUEL PENALTIES @ FIELD LENGTH 910 m. (3000 FT.) OR LESS -- M 0.75

Field Length		% Penalties for Meeting					
Meters	Feet	FAR 36-15		1 sq. Km 90 EPNdB		90 EPNdB 2.3 Km Long	
		DOC	Fuel	DOC	Fuel	DOC	Fuel
1830	6000	3	4	10	10	17	14
1220	4000	3	4	10	10	17	14
915	3000	17	14	16	10	17	14

To meet FAR 36 minus 15, the landing field length must be reduced below 1830 m. (6000 ft.) because of approach noise. If the requirement is one sq. Km for the 90 EPNdB footprint area, the penalty is 10 percent in DOC and fuel and no additional penalty is incurred for reduction in field length to 1220 m. If the length of the 90 EPNdB footprint is required to be 2.3 Km. the 910 m. (3000 ft.) field length is required and the DOC and fuel penalties are 17% and 14% respectively.

Table 0.XII summarizes the characteristics of aircraft designed for 610 and 910 meter field lengths. As noted previously, the AW and EBF aircraft represented here have about the same noise characteristics as the OTW/IBF aircraft with 1.35 FPR engines. Their direct operating costs are 10 to 11 percent higher. Penalties for meeting noise requirements would be increased to approximately double those listed in the above discussions.

Further comparison of the MF and OTW/IBF aircraft is shown in Figure 0.13 for 0.75 M designs on the basis of fuel and field length. The 4-engined OTW/IBF is clearly superior to the MF at field lengths shorter than 1070 m. (3500 ft.) while the 4 engined MF is superior at field lengths longer than 1220 m. (4000 ft.). However, it should be noted that minimum DOC's are achieved with the 2-engined, rather than the 4-engined MF and therefore the primary comparison should be between the 4-engined OTW/IBF and the 2-engined MF. The direct operating costs of these concepts are presented in Figure 0.14 for 0.75 and 0.8 M and as a function of field length. At 910 m. (3000 ft.) and DOC-1, the OTW/IBF is superior at 0.8M, while the MF is slightly superior at 0.75 M. For DOC-2, the OTW/IBF is superior at 0.8 M, while the concepts are equal at 0.75 M.

FIELD LENGTH	610 M (2000 FT)				910 M (3000 FT)			
CONCEPT	NO. OF ENG. (FPR)	M	FUEL KG (LB)	DOC-2 ¢/ASSM	NO. OF ENG. (FPR)	M	FUEL KG (LB)	DOC-2 ¢/ASSM
OTW/IBF	4 (1.35)	0.75	4,944 (10,900)	1.961	4 (1.35)	0.75	4,400 (9,700)	1.831
	—	—	—	—	4 (1.47)	0.75	5,117 (11,280)	1.820
MF	—	—	—	—	2 (1.35)	0.70	5,089 (11,220)	1.818
AW	—	—	—	—	2 + 2 (1.35/3.0)	0.75	5,688 (12,540)	2.015
EBF	4	0.65	5,003 (11,030)	2.196	4 (1.25)	0.65	4,427 (9,760)	2.046
DEFLECTED SLIPSTREAM	—	—	—	—	4 (T-56)	0.55	3,293 (7,260)	1.629

TABLE 0.XII SUMMARY OF 610 M AND 910 M (2000 AND 3000 FT) AIRCRAFT (MIN. DOC 2)

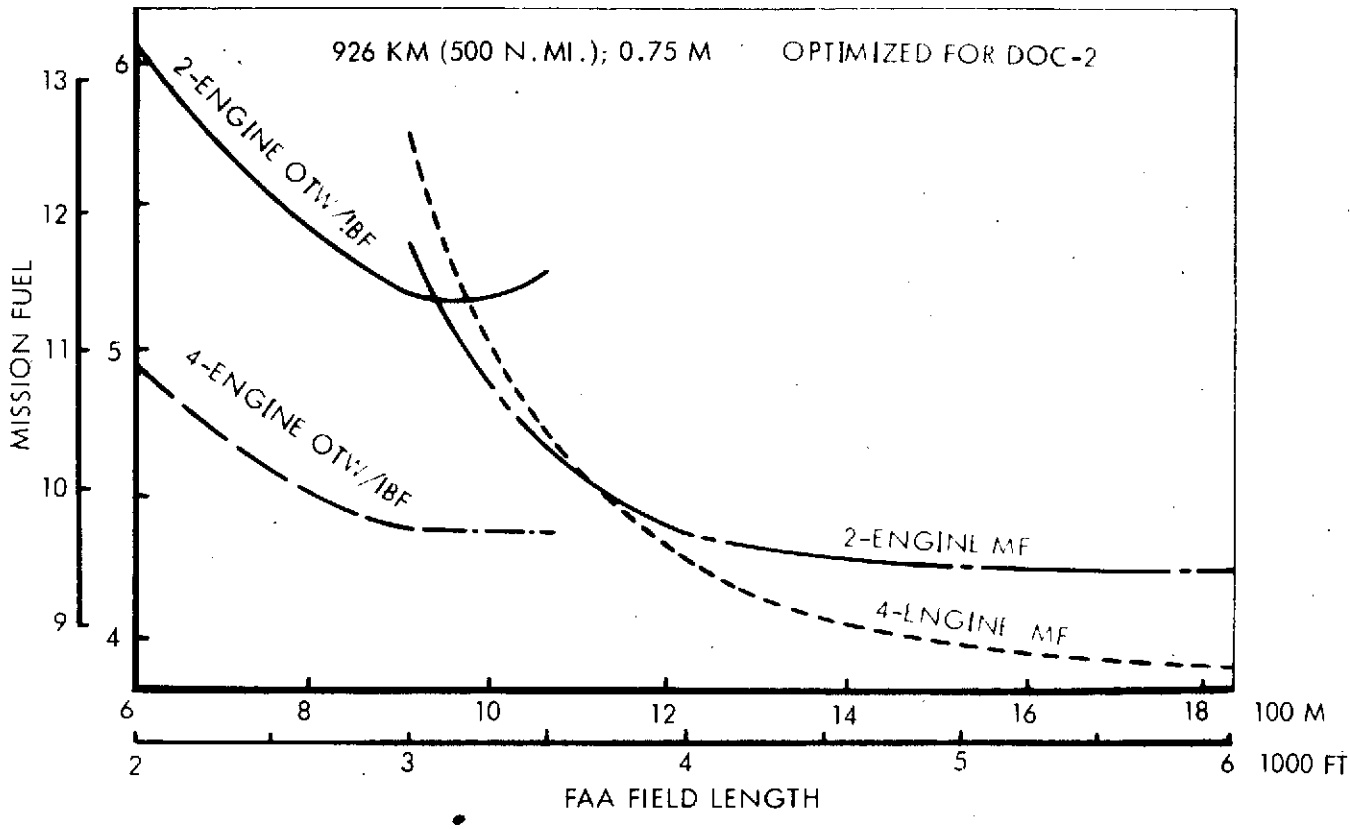

FIGURE 0.13: EFFECT OF FIELD LENGTH ON MISSION FUEL

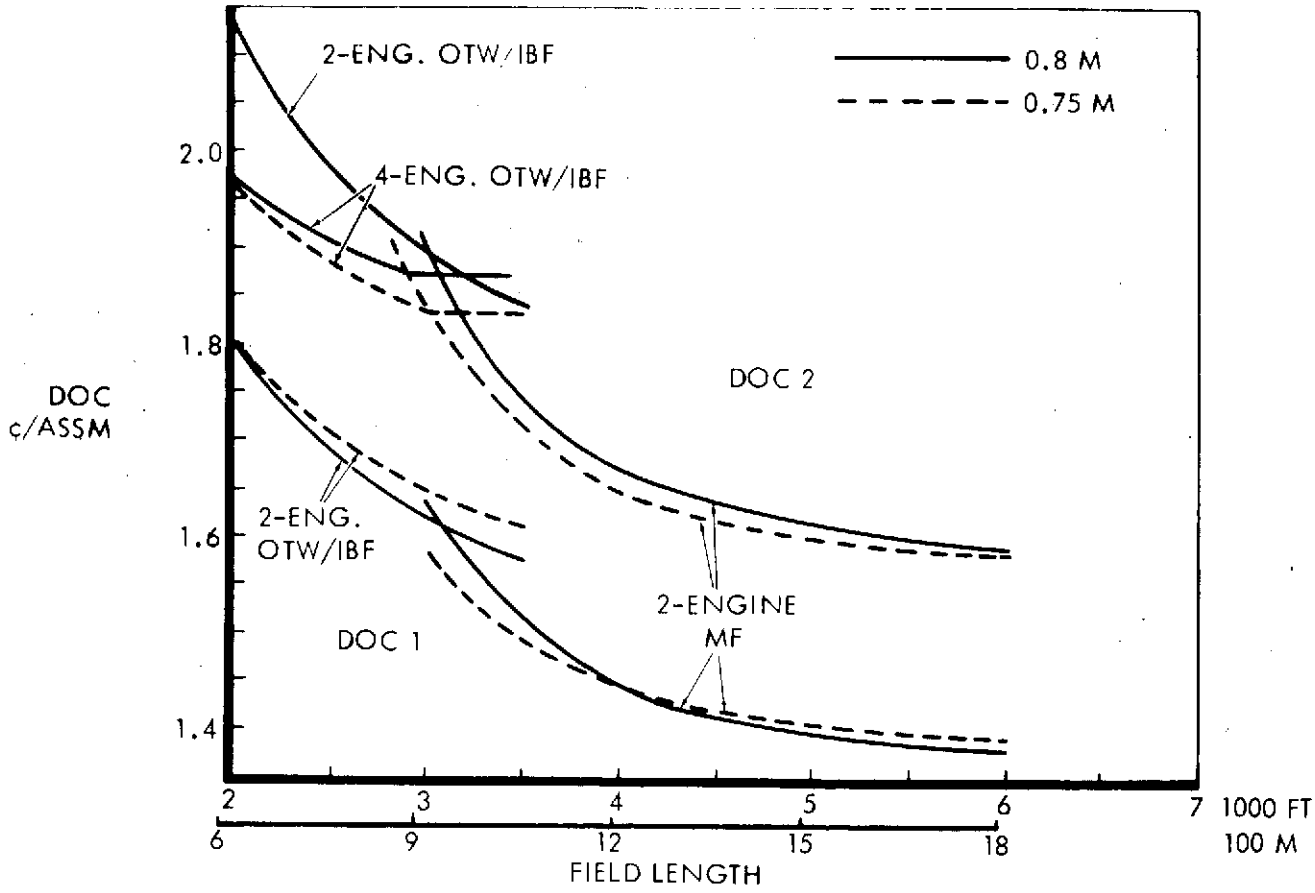

FIGURE 0.14: EFFECT OF FIELD LENGTH ON DOC

The choice of lift concept for 610 m. (2000 ft.) field length is clear cut; the four-engine hybrid OTW/IBF has a DOC-2, 23 percent higher than the 1829 m. (6000 ft.) MF airplane and 7 percent higher than the 910 m. (3000 ft.) hybrid. Previous estimates of the penalty of reduction in field length from 910 m. to 610 m. were 15 percent (Ref.1) and 20 percent (Ref. 3). Whereas the former estimates represented a DOC penalty of 50 percent over CTOL, the current conservative optimization of the hybrid OTW/IBF indicates that 610 meter field performance may well be economically viable. These results would have significant consequences in conserving real estate.

The configuration selection for 910 m. (3000 ft.) is not clear cut; since there is no demand currently for an implementation decision, it is suggested that several years are available in which additional data can be made available, such as the following:

- Clarification of the land-side costs and needs for congestion relief associated with 610 m. to 1220 m. (2000 to 4000 ft.) short haul runways.
- Demonstration of the gust alleviation technology and passenger acceptance of associated ride quality for an airplane with 293 Kg/m^2 (60 psf) wing loading.
- Further development and demonstration of propulsive lift.
- Establishment of rational specific noise criteria for long haul aircraft using existing runways and for short haul aircraft using additional runways not now contributing to community noise.
- Establishment of specific performance certification criteria (modification and implementation of a modified FAR Part XX).
- Experimental verification of the potential for further improvement in the performance attainable in the hybrid OTW/IBF concept.

On the latter point, the long duct nacelle used conservatively in the performance analyses causes high losses in cruise. There is considerable potential for improvement

in this area but experimental data are lacking. An improvement of 15 percent in DOC and 10 percent in fuel consumption was estimated for an engine arrangement which avoids the long exhaust duct. Improvement less than this magnitude, if verified experimentally, would make the OTW concept (possibly combined with IBF) an overwhelmingly superior approach at all field lengths up to 6000 feet.

It is concluded that the hybrid OTW/IBF concept with design cruise speed of Mach 0.75 and FPR 1.35 engines should be considered the best potential solution for 910 m.(3000 ft.) or shorter field performance on the basis of lower fuel consumption and further potential for improvement. The versatility of full-load, longer range performance should be incorporated; using CTOL runways; a 2780 Km (1500 n.mi.) range can be provided with a takeoff field length of 1280 m. (4200 ft.). If 1.35 FPR engines with 57.8 KN (13,000 lb.) thrust were developed, aircraft sized for 90, 120, or 150 passengers could be designed with 2, 3, or 4 engines.

Recommended Compromise Concept

The potential of the hybrid OTW/IBF for both 610 and 910 m. (2000 and 3000 ft.) field lengths and small noise footprints indicates that it should be pursued in research and development programs. Implementation decisions are downstream so that confirmation of the results of current analyses can be obtained and a minimum risk program could be initiated in the 1980's. Decisions and actions which are appropriate are the following:

- Continuation of the Quiet STOL Research Airplane program.
- Implementation of further analytical and experimental development of improved nacelle and engine installation with emphasis on improving cruise performance and determining the optimum combination of high speed and low speed installation approaches.
- Analytical refinement of engine design characteristics through an integrated airframe/engine study in the fan pressure ratio range of 1.3 to 1.4 for noise.
- Initiation of a quiet R/STOL engine development with technology drawn from the QCSEE program and guidance from the integrated airframe/engine study.

Figure 0.15 summarizes the conclusions of the fuel conservation portions of the study by indicating the available fuel savings and the associated DOC and speed penalties at 1830 m. (6000 ft.) and 910 m. (3000 ft.) field lengths. Figure 0.16 summarizes the comparison of OTW/IBF and MF concepts at 910 m. (3000 ft.) field length from which it can be concluded that the OTW/IBF is economically superior in fuel and DOC at field lengths below 910 m. (3000 ft.) while the MF is superior at field lengths greater than 910 m. (3000 ft.). At 910 m. (3000 ft.) the OTW/IBF is considered superior because of its better fuel consumption, better ride quality, and greater potential for improvement. Figure 0.17 summarizes the conclusions regarding aspect ratio effects and the EBF, AW, and deflected slipstream lift concepts.

The recommendations regarding the desirable engine fan pressure ratio and additional Research and Development are summarized in Figures 0.18 and 0.19 while the recommendations regarding noise requirements are summarized in Figure 0.20.

- AT 1830 M (6000 FT) F.L.,
  - 926 KM. MISSION FUEL CAN BE REDUCED BY UP TO 24% AT THE EXPENSE OF A 31% REDUCTION IN SPEED AND A 15% INCREASE IN DOC-2 (20% IN DOC-1).
  - BY OPTIMIZING FOR DOC-2, MISSION FUEL CAN BE REDUCED BY 5% FOR THE SAME DOC-2 AND A 7% REDUCTION IN SPEED
- AT 910 M (3000 FT) F.L.,
  - MISSION FUEL CAN BE REDUCED BY UP TO 20% AT THE EXPENSE OF A 31% REDUCTION IN SPEED AND A 12% INCREASE IN DOC-2 (18% IN DOC-1).
  - BY OPTIMIZING FOR DOC-2, MISSION FUEL CAN BE REDUCED 11% FOR THE SAME DOC-2 AND 7% REDUCTION IN SPEED.
- 0.75 M AND OPTIMIZATION FOR DOC-3 ARE RECOMMENDED FOR FUTURE SHORT HAUL TRANSPORTS

FIGURE 0.15: SUMMARY OF RESULTS -- FUEL CONSERVATION

- AT 910 M (3000 FT) F.L.,
  - OPTIMIZED FOR DOC1 AT 0.8M, THE OTW/IBF HAS 1% BETTER DOC AND 1% BETTER FUEL CONSUMPTION THAN MF.
  - OPTIMIZED FOR DOC2 THE OTW/IBF HAS 1% POORER DOC, 9% BETTER FUEL CONSUMPTION & 7% HIGHER SPEED THAN MF.
  - OPTIMIZED FOR DOC4, THE OTW/IBF HAS 2% BETTER DOC AND 13% BETTER FUEL CONSUMPTION THAN MF.
  - OPTIMIZED FOR MINIMUM FUEL, BOTH CONCEPTS ARE EQUAL.
  - OTW/IBF HAS BETTER RIDE QUALITIES THAN MF.
- AT > 910 M THE MF IS BETTER THAN OTW/IBF IN BOTH FUEL CONSUMPTION AND DOC.
- AT < 910 M THE OTW/IBF IS BETTER THAN MF IN BOTH FUEL CONSUMPTION AND DOC.

FIGURE 0.16: SUMMARY OF RESULTS - COMPARISON OF OTW/IBF AND MF

- TO MINIMIZE FUEL CONSUMPTION ASPECT RATIOS UP TO 14 ARE REQUIRED.
- TO MINIMIZE DOC 2 ASPECT RATIOS OF 10 TO 12 ARE REQUIRED.
- THE AW & EBF CONCEPTS ARE NOT RECOMMENDED.
- THE T-56 TURBOFAN DEFLECTED SLIPSTREAM DESIGN PROVIDES BETTER FUEL AND DOC ECONOMY THAN THE FAN-ENGINED DESIGNS AT LESS THAN 1520 M (5000 FT) FIELD LENGTH
- AN ADVANCED TURBO-PROP HAS NO ADVANTAGE OVER T-56 EXCEPT FLEXIBILITY IN SIZING AIRCRAFT DUE TO DEVELOPMENT COST.

FIGURE 0.17: SUMMARY OF RESULTS - ASPECT RATIO AND OTHER CONCEPTS

- 1.35 FPR IS RECOMMENDED
  - IT PROVIDES GOOD FUEL & DOC ECONOMICS AT PRESENT AND INFLATED FUTURE FUEL PRICE LEVELS.
  - IT CAN MEET THE PROPOSED NOISE REQUIREMENTS.
  - PRELIMINARY ANALYSES INDICATE IT IS AN EXCELLENT ENGINE FOR FUTURE CTOL AIRPLANES OPTIMIZED FOR INCREASED FUEL PRICE.
- ADDITIONAL STUDY AND R AND D IS NEEDED:
  - COMMONALITY OF 1.35 FPR ENGINE FOR BOTH SHORT-HAUL AND LONGER-RANGE MISSIONS.
  - FUEL AND ECONOMICS OF INTERMEDIATE AND LONG-RANGE COMMERCIAL AIRCRAFT RELATED TO FUTURE NOISE CRITERIA.
  - LOW WING LOADING AIRCRAFT FOR LOWER DENSITY SHORT-HAUL ARENA.
  - ENGINE DESIGN INTEGRATED WITH AIRCRAFT OPTIMIZATION FOR REFINEMENTS OF FPR, FAN STAGES, GEARING OR NOT, VARIABLE PITCH OR NOT.

FIGURE 0.18: RECOMMENDATIONS - ENGINE AND AIRCRAFT

- CONTINUE SUPERCRITICAL AIRFOIL TECHNOLOGY AT SPEEDS BELOW M 0.8.
- DEVELOP HIGH ASPECT RATIO TECHNOLOGY (M 0.75)
- CONTINUE PROPULSIVE LIFT RESEARCH -- NOT FOR EARLY APPLICATION TO SPECIFIC STOL DESIGNS, BUT TO REFINE HIGH LIFT TECHNOLOGY FOR STOL, RTOL, AND CTOL.
- INCREASE RESEARCH ON GUST ALLEVIATION/RIDE QUALITY FOR MECHANICAL FLAP AIRPLANES WITH W/S OF ABOUT 40 TO 80.
- ADDITIONAL ANALYSIS OF ADVANCED ENGINE CHARACTERISTICS FOR FUEL CONSERVATION.

FIGURE 0.19: RECOMMENDATIONS - TECHNOLOGY

- PART 36 - 10 dB FOR CTOL, LONG RANGE MISSIONS
- LESS THAN 2.6 SQUARE KILOMETERS (1/4 SQUARE STATUTE MILE), 90 EPNdB FOOTPRINT AREA BEYOND EACH END OF THE RUNWAY.
- LESS THAN 1.6 KILOMETERS (1 STATUTE MILE), 90 EPNdB FOOTPRINT LENGTH BEYOND EACH END OF THE RUNWAY
- SPERRY BOX 80 EPNdB LEVEL IS NOT FEASIBLE OR APPLICABLE IN HIGH-DENSITY SHORT-HAUL
- 500 FT SIDELINE IS NOT RECOMMENDED - NOT PERTINENT FOR RELIEF OF CONGESTION AT HUB AIRPORTS OR USE OF SECONDARY AIRPORTS
- STUDY OF LAND-SIDE ECONOMICS OF PROVIDING TERMINAL FACILITIES COMPATIBLE WITH THESE SUGGESTED NOISE CRITERIA

FIGURE 0.20: RECOMMENDATIONS - NOISE REQUIREMENTS

1.0 INTRODUCTION

1.1 BACKGROUND

Studies of Quiet Turbofan STOL Aircraft for Short Haul Transportation were conducted by Lockheed and McDonnell-Douglas for NASA Ames Research Center in 1972 and early 1973. These were reported in detail in references 1, 2, and 3. Both studies concluded that quiet short field aircraft can be economically viable and benefit both long and short-haul transportation. To be economically viable, field lengths of 3000 to 4000 feet were strongly preferred; operating cost penalties for 2000-foot or shorter field length appeared to be greater than could be balanced by STOL indirect benefits.

In the Lockheed study it was determined that the various powered high lift concepts such as the externally blown flap, the internally blown flap, and the over-the-wing blown flap (upper surface blown flap) produced configurations with approximately equal economic results. However, two particularly promising concepts appeared to be the Over-the-Wing/Internally Blown Flap (OTW/IBF) hybrid at a field length of 910m (3000 ft.) and the Mechanical Flap (MF) at a field length of 1220m (4000 ft.). Unfortunately, the data base upon which the OTW/IBF concepts is based is neither as extensive nor as well substantiated as competing concepts, such as the externally blown flap or augmentor wing.

It was also shown that more economical vehicles could be developed for both these concepts if the 152m (500 ft.) sideline noise level requirement was relaxed somewhat from 95 EPNdB. Additional benefits would accrue from such a choice of noise level since the engines suited for slightly higher noise level have fan pressure ratios (FPR's) on the order of 1.4 to 1.6 which make them suitable for advanced CTOL airplanes meeting FAR 36 minus 10dB noise levels, a level to be expected in the 1980 time period.

It was therefore proposed to investigate and analyze the critical aspects of 910M (3000 ft.) OTW/IBF design to that level which will provide a meaningful configuration for developing test configurations for future R&D programs and to compare the performance

of this concept to the performance of the MF concept at 910m (3000 ft.) field performance. The number of engines has a significant effect upon operating cost as illustrated by the mechanical flap configuration examined in references 1, 2, and 3. Whereas the preference for two engines for unpowered lift systems was clear-cut, more detailed analysis was required to resolve the question in a rigorous manner for powered lift systems. Accordingly, 2, 3 and 4 engine OTW/IBF vehicles were included in the present study and these were complemented with a study of a twin-engine augmentor-wing vehicle. Since the twin engine pure OTW and EBF configurations are virtually excluded by engine-out trim considerations and the other candidate configurations have already been examined, the AW study completed a comprehensive review of this aspect for all powered lift systems. (The twin-engine Boeing AMST is classified here as a hybrid OTW system since it uses leading-edge blowing.)

Work was initiated on this study extension in July 1973. Early in the program it was observed that the fuel consumption of airplanes using the hybrid propulsive-lift concept was lower than for the mechanical flap or augmentor wing concepts for aircraft designed for 3000-foot field performance, low noise level, and cruise at M 0.8. The wing loading and aspect ratio for propulsive lift aircraft can be higher than that possible for a mechanical flap airplane at any given field length; this generally means lower fuel consumption. Increasing prices and scarcity of fuel in late 1973 highlighted the need to examine operating requirements such as cruise speed and altitudes, as well as the effect of different potential noise requirements, on fuel consumption and airplane design for minimum operating costs at higher fuel prices. Accordingly, an additional task was initiated in early January 1974 to cover these aspects.

1.2 OBJECTIVES

This report describes the results of analyses integrated to accomplish the following objectives:

- Detailed definitive design and economic comparison of 910m (3000 ft.) field length MF, AW and OTW/IBF configurations. A primary objective is establishing credibility of performance estimates, including sensitivity to variations in basic data.

- Detailed determination of the economic and noise level effects of using an intermediate bypass engine suitable for an advanced CTOL, as well as use of a low-noise engine.

- Development of the preliminary design of optimized OTW/IBF airplanes to that level which could provide test configurations for future R&D programs.

- Development of additional data for OTW/IBF configurations with 610 and 1070m (2000 and 3500 ft.) field length capability and MF configurations with 1070 and 1220m (3500 and 4000 ft.) field length capability.

- Evaluation of the fuel savings achievable by application of advanced lift concepts to a short-haul aircraft; determination of the effect on fuel consumption of different field lengths, cruise requirements and noise levels.

1.3 APPROACH

Specific configuration design points were selected for different lift concepts and field lengths, as summarized in Figure 1. Emphasis was placed on the points designated "preliminary design" in the figure: 910m (3000-ft.) field lengths for over the wing/internally blown flap, mechanical flap, and augmentor wing; 1220m (4000-ft.) field length for the mechanical flap. The preliminary design data was then extended to other field lengths, as shown. Initially these aircraft were optimized for M 0.8 cruise at 9140m (30,000 ft.) for minimum direct operating cost with 1972 prices for fuel, aircraft and engines, maintenance, and other DOC elements. Optimization would not be affected if these inflated uniformly; for convenience in comparing to previous studies, the 1972 price basis was maintained. However, the rapid price increase for fuel in 1973 indicated that fuel consumption would assume a more dominant position in airline economics and that airplane and engine features which conserved fuel should be evaluated from two standpoints: minimum fuel consumption and minimum direct operating cost optimizations at higher fuel prices.

- REFINE DESIGN OF SHORT-HAUL AIRCRAFT -- M 0.8, 9140m. (30,000 FT.) CRUISE

FIELD LENGTH	610m. (2000 FT.)	910m. (3000 FT.)	1070m. (3500 FT.)	1220m. (4000 FT.)
OVER THE WING/INTERNALLY BLOWN FLAP	o	◉	o—PARAMETRIC DESIGN	
MECHANICAL FLAP		◉	o	◉
AUGMENTOR WING	o	◉—PRELIMINARY DESIGN		

- REOPTIMIZE ABOVE AIRCRAFT (WING AR, CRUISE SPEED AND ALTITUDE) FOR MINIMUM FUEL AND HIGHER FUEL COSTS
- REEXAMINE EXTERNALLY BLOWN FLAP
- ADD DEFLECTED SLIPSTREAM WITH TURBOPROP ENGINES
- EXTEND MECHANICAL FLAP ANALYSES TO COVER 1830m. AND 2440m. (6000 AND 8000 FT.)
- EVALUATE ENGINES WITH FPR 1.25, 1.35, 1.47

- DETERMINE FUEL AND DOC PENALTY FOR POTENTIAL NOISE CRITERIA:
  - 95 EPNdB AT 150m. (500 FT.) SIDELINE
  - PART 36 MINUS 5, 10, 15 EPNdB
  - SPERRY BOX LEVEL* OF 80 EPNdB
  - 90 EPNdB FOOTPRINT AREA LIMITED TO 2.59, 1.39, 0.78 km^2 (1.0, 0.5, 0.3 SQ. MI.)
  - 90 EPNdB FOOTPRINT LENGTH LIMITED TO 6.5, 3.7, 1.9, 1.2 km (3.5, 2.0, 1.0 N. MI., 4000 FT.)

* REF. 4

FIGURE 1: STUDY APPROACH

A range of cruise speeds and altitudes was investigated for each lift concept and engine combination. The wing loading, thrust loading and wing aspect ratio for minimum fuel at each speed and altitude were determined. For each of these cases the direct operating cost at 1, 2, 4 and 10 times the 1972 fuel price was determined, as well as the gross weight and operating weight of the aircraft. As indicated in Figure 1 the externally blown flap and deflected slipstream (turboprop engines) were also included in the evaluation of fuel consumption. Finally, the noise characteristics and footprint areas of representative cases were determined so that the interaction of potential noise criteria with aircraft economics and fuel consumption could be defined.

In the next section, the short haul system elements are re-examined briefly to review qualitatively the effects of the fuel shortage on short haul air transportation and on the need for fuel- and real-estate-conserving quiet aircraft. Section 3 defines the evaluation criteria and design requirements. Sections 4 through 7 show the design features of the candidate aircraft. (Details of analyses are presented in an appendix.) Evaluation of the aircraft configurations from the standpoint of fuel consumption, DOC at different fuel prices, and noise are presented in Section 8; the penalties in fuel and DOC for different potential noise requirements are also defined. The effect of selected aircraft on airline return on investment is described in Section 9 from airline simulations of 1985 and 1990 scenarios. Section 10 then discusses the compromises in the selection of potentially viable systems combining the factors of fuel economy, noise, aircraft versatility and flexibility, and airline economics.

Finally, conclusions are summarized and recommendations are listed for further research and development and institutional development toward an improved short haul air transportation system.

2.0 SOME ASPECTS OF THE SHORT-HAUL SYSTEM SCENARIO

The previous systems studies (References 1-3) highlighted the primary need for STOL short-haul capability for the relief of congestion at the major hub airports. An additional major advantage was cited as the increase in convenience to the public if additional airports could be utilized which were closer to the sources of origin and destination. Current study activity has involved an examination of the effect of recent developments on this scenario. Of major importance is the recognition that a very effective short-haul and long-haul air transportation network is functioning today. It is a complex interacting system in which a major effect on profitability of the long haul system is the short haul collection system which brings people to a hub airport by air in sufficient quantity to achieve profitable load factors on wide-body equipment.

2.1 ENERGY SHORTAGES AND AIRPORT CONGESTION

The effects of the energy crises on airline operations have been discussed with representatives of Delta, Eastern, and Northeast Airlines. These discussions investigated the impact of short fuel supply on passenger travel habits, schedules, load factors, and average delay rates. Fuel allocations and increased fuel costs were also examined to determine the influence on operations and future planning. Anticipated changes in previously projected air passenger traffic growth and airport congestion were analyzed to better determine the benefits of quiet R/STOL aircraft for short haul traffic with short runways added on a non-interfering basis with CTOL operations.

Air passenger travel habits have not changed as drastically as first anticipated. The reduction in low demand flights appears to have an insignificant effect on loss of passengers to other modes of transportation. Passengers appear to reschedule their own activities to accept other available flights. The anticipated passenger traffic has been boosted somewhat by a shift to the airlines from automobile travel, caused by the gasoline shortage. Records show that the 1973 air passenger traffic exceeded expectations and 1974 is expected to exceed predictions made in the initial phases of the fuel crisis.

Schedule cuts have been made at the times of least demand so that peak hour airport operations have not been affected to any extent. Considerable improvements have been experienced in average load factor; however, this has not affected the ability to meet demand.

Fuel allocation cutbacks have led the airlines to examine further the various means of conserving fuel in addition to eliminating low demand flights. Reduced throttle settings result in reduction in fuel consumption with no troublesome reduction in block time. Other methods exercised during peak hours as initiated by Reference 5 include holding a departing flight at the gate until clearance to takeoff is obtained, thereby conserving fuel in ground operations, or holding at the point of origination until clearance is obtained at the point of destination to reduce airborne delays.

The higher fuel prices have increased the break even load factor, even though various cost reduction practices have been implemented. This has been offset somewhat by the improvements in average load factor that are presently being experienced. Continued fuel cost increases and lower fuel allocations are still a major concern with all airlines. This situation tends to favor the more fuel efficient wide body aircraft and, in some cases, airlines are attempting to accelerate the introduction of these aircraft into their route structure.

The consensus of all airlines is more optimistic toward a continued passenger growth rate during the coming years. However, the predicted rate of growth varies somewhat. Airport congestion is not viewed as a significant problem for the next several years. Nevetheless, congestion is being viewed as a future problem that must be recognized in present planning. Atlanta and other cities are continuing to evaluate the anticipated traffic growth in terms of the need for expanding the capabilities of existing facilities and property or the need for acquiring additional property for new airports. Recognizing the extremely long lead times in obtaining necessary land and constructing required facilities, the Atlanta Regional Commission has an active transportation planning program in progress which is studying the feasible ways of meeting the future air traffic needs of the Atlanta area. A second airport

is in serious consideration at the present time to augment the capabilities of the Hartsfield Atlanta International Airport. New York is also looking at the possibility of an additional airport, and Chicago is still studying the problems of a workable system in the Midway/ O'Hare combination. Of course, any steps in developing additional workable airports for congestion relief will have a tendency to postpone the need for, and benefits to be derived from, R/STOL type aircraft operations.

A recent paper by Charles L. Blake (Ref. 6) summarizes the report of the FAA Airport Study Team which highlights the groundside congestion problem assuming considerable ATC improvements in airside capacity. Recognizing the fuel shortage and the uncertainties in predicting future developments, it is noted that "the FAA Airport Study Team predicts a steadily increasing strain on airport capacity." Mr. S. B. Poritzky of the Air Transport Association has commented (Ref. 7) that "quantifiable ATC-based airport capacity improvements... are smaller than expected. The bigger payoff must come from optimized total airport design and enough runways, and in the long run more 'real-estate-stingy' airplanes."

2.2 DEMAND - CAPACITY ANALYSES

The airport capacity and demand analyses in Reference 2 have been reexamined in the light of the energy crisis to determine if the saturation of major airport hub capacities still remains a serious concern inhibiting the growth and prosperity of the national air transportation industry. The changes resulting from the fuel shortage such as the anticipated future growth of air passenger traffic, airline operations, and cost of fuel were assessed in terms of future airport demand versus capacity and cost of delay under various levels of fuel costs. The cost of delay with and without R/STOL capabilities was compared to show the economics of augmenting airport CTOL capacity with R/STOL capabilities. All costs used in these analyses are in 1973 dollars.

The Atlanta Airport was used as an example of a major hub airport in these analyses. Figure 2 shows the presently predicted demand and capacity of the Atlanta Airport. Some changes are shown from that reported previously in the predicted average aircraft seat capacity, average load factor, and the originating and connecting passenger ratio.

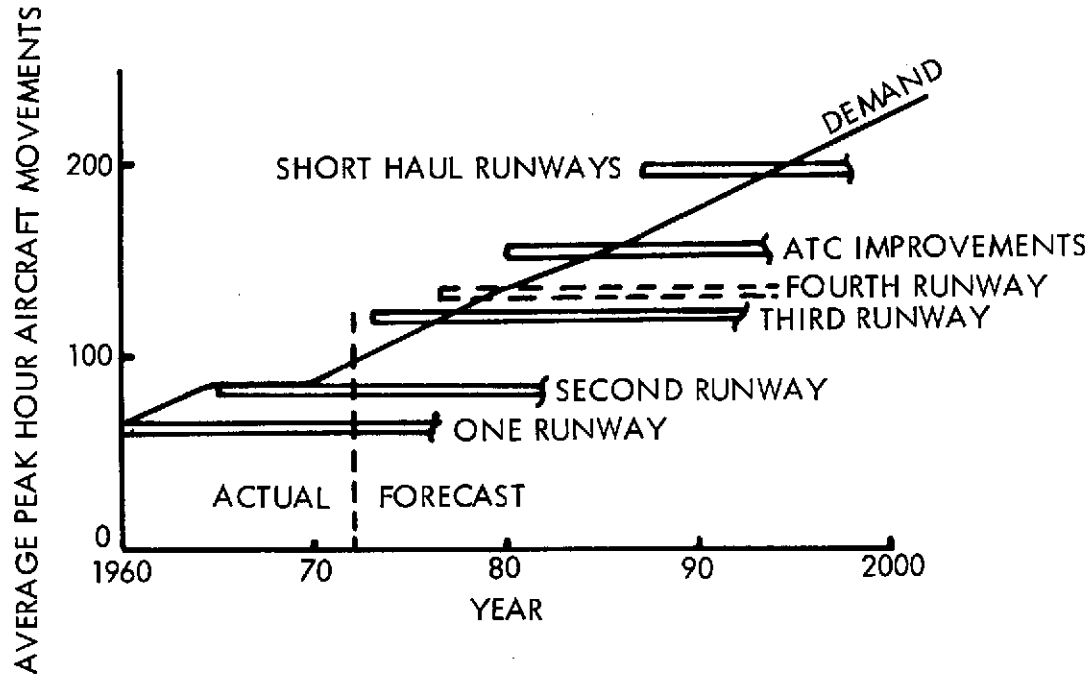

FIGURE 2: ATLANTA AIRPORT TRAFFIC PROJECTION

These corrections were based on a consensus forecast as a result of feedback from various agencies including airlines, ATA, Atlanta Regional Commission, and the Atlanta Airport and are contained in Reference 8. The updated demand estimate takes into consideration the trend that, as passenger traffic grows, the increased demand will justify more direct flights overflying Atlanta which had previously required connections in Atlanta such as Birmingham to New York, Nashville to Miami, etc. This new demand prediction does not reflect the optimistic growth that is anticipated by some, nor does it reflect the predictions coming out of the early days of the fuel shortage which have already been proven overly pessimistic. The capacity of the Atlanta Airport in the figure shows an estimate including a proposed fourth CTOL runway, ATC improvements operational by 1980, and two short haul runways by 1987. These estimates are conservative compared with some of the possible improvements in ATC involving solution of the wake vortex problem (Ref. 6 and 9). Nevertheless, they serve to illustrate the severe limitation resulting without these runways after 1986 or 1987. The demand versus capacity reflected in this figure was used in determing the delays and results of the delays.

Fuel used per hour of delay increases with time because of the larger average capacity aircraft reflected in Reference 8 as follows:

Year	Average Seat Capacity	Fuel per Hour	
		Kg	Lb
1978	131	4700	10,400
1983	160	5400	11,900
1988	188	6000	13,200
1993	217	6500	14,400
2000	257	7200	16,000

An appropriate mix of aircraft to represent the average seat capacity was used in determining the block hour fuel costs from historical ATA records. Assuming that half of the delay time is airborne delay at maximum endurance fuel consumption and half is ground delay at a fuel consumption slightly more than idle, the resulting hourly fuel consumption during delay is approximately 50% of the block hour fuel. Peak hour delays and annual delays are shown in Figures 3 and 4 as derived from the demands and capacities of Figure 2 in accordance with Reference 10. Delays are shown for only four CTOL runways, with and without ATC improvements, and with ATC improvements and R/STOL runways. Since the assumed level of ATC improvements is highly probable, the solid line in both Figures 3 and 4 reflecting the delay associated with four CTOL runways and ATC improvements should be used as the baseline for comparison with the improvement offered by the additional capabilities of the R/STOL runways. The delay effect on fuel consumption is shown in Figure 5 for the three previously described conditions. The annual fuel savings are substantial with incorporation of the R/STOL runway capabilities compared with the capabilities of four CTOL runways with ATC improvements and, as shown, the savings increase with time. Cost of delay at the Atlanta Airport is reflected in Figure 6 at two and four times the 1972 fuel prices for the three conditions, with and without ATC improvement and with R/STOL runways. The annual savings offered by R/STOL at this one airport are approximately 25 to 30 million dollars in 1990 and 50 million dollars in 1995, and justify considerable expenditures in implementing this additional capability. It appears that analysis of O'Hare Airport would give similar results at an earlier time period.

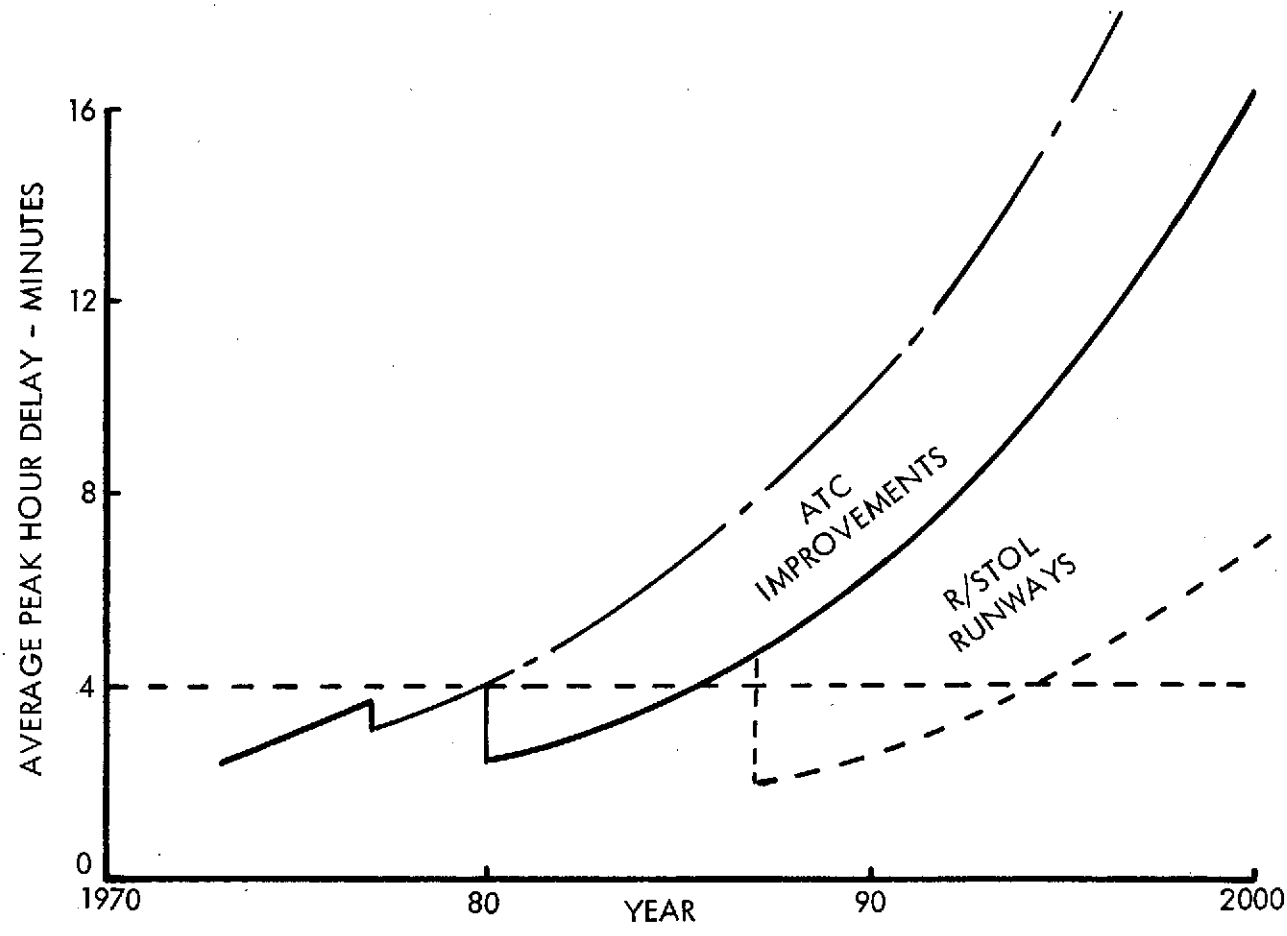

FIGURE 3: PEAK HOUR DELAY ATLANTA AIRPORT

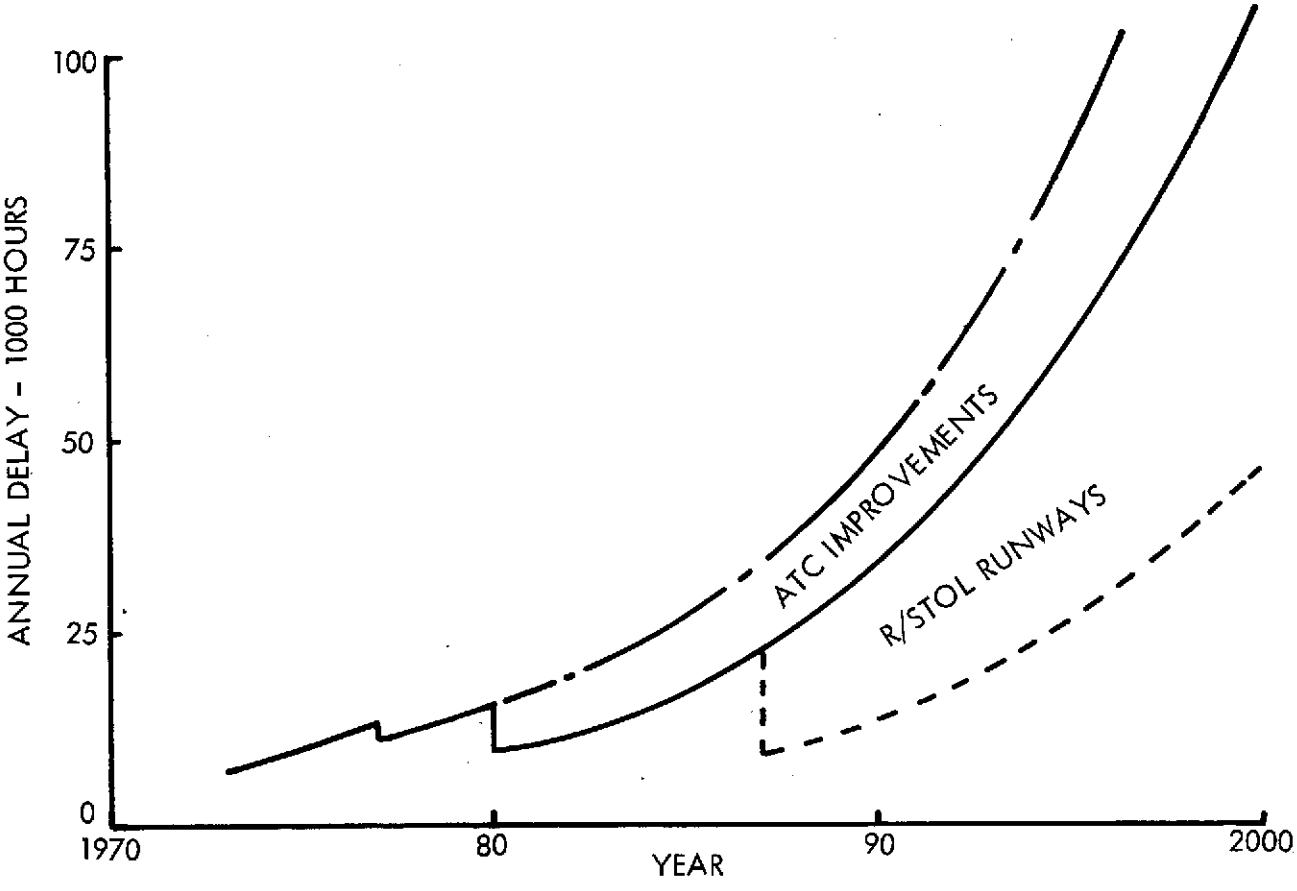

FIGURE 4: ANNUAL DELAY ATLANTA AIRPORT

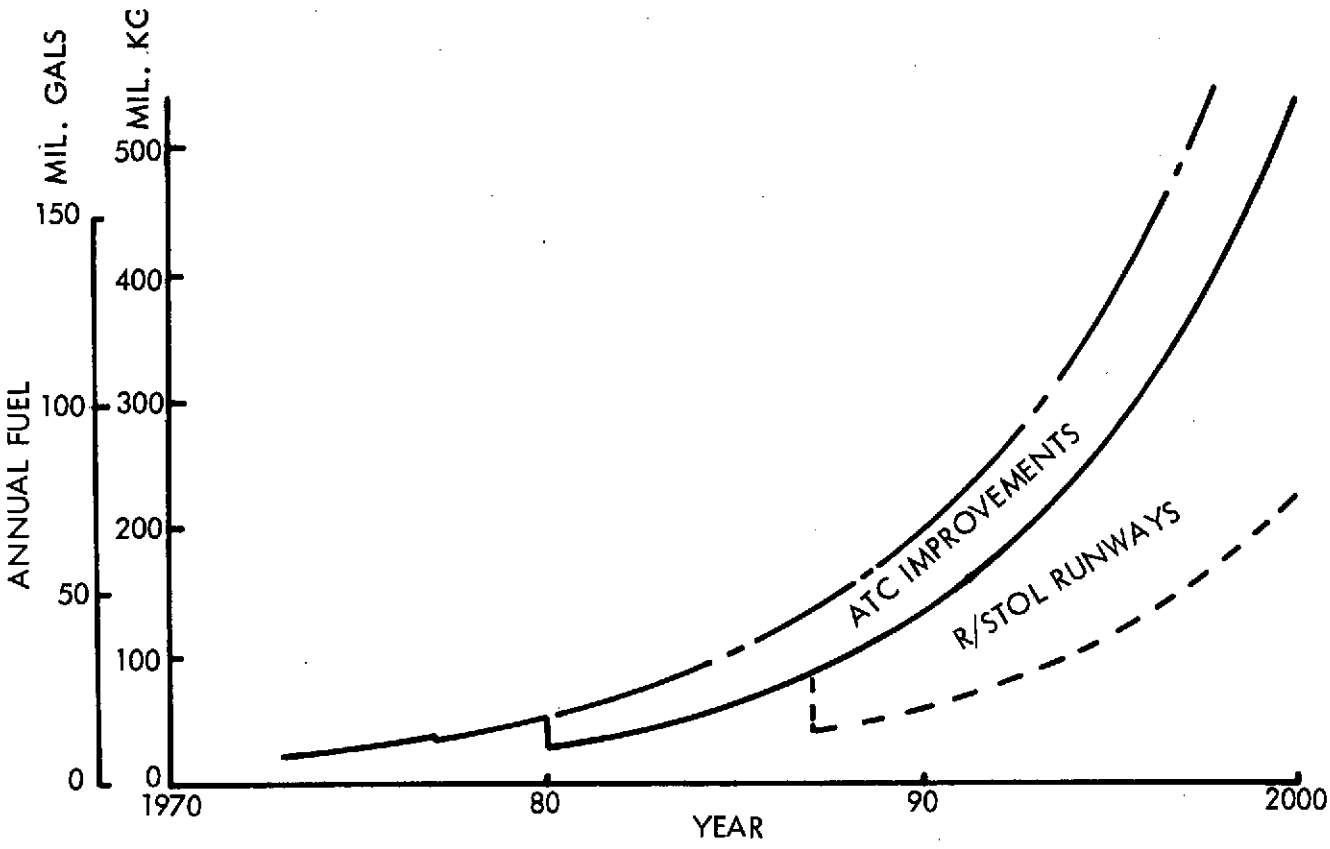

FIGURE 5: DELAY EFFECT ON FUEL CONSUMPTION - ATLANTA AIRPORT

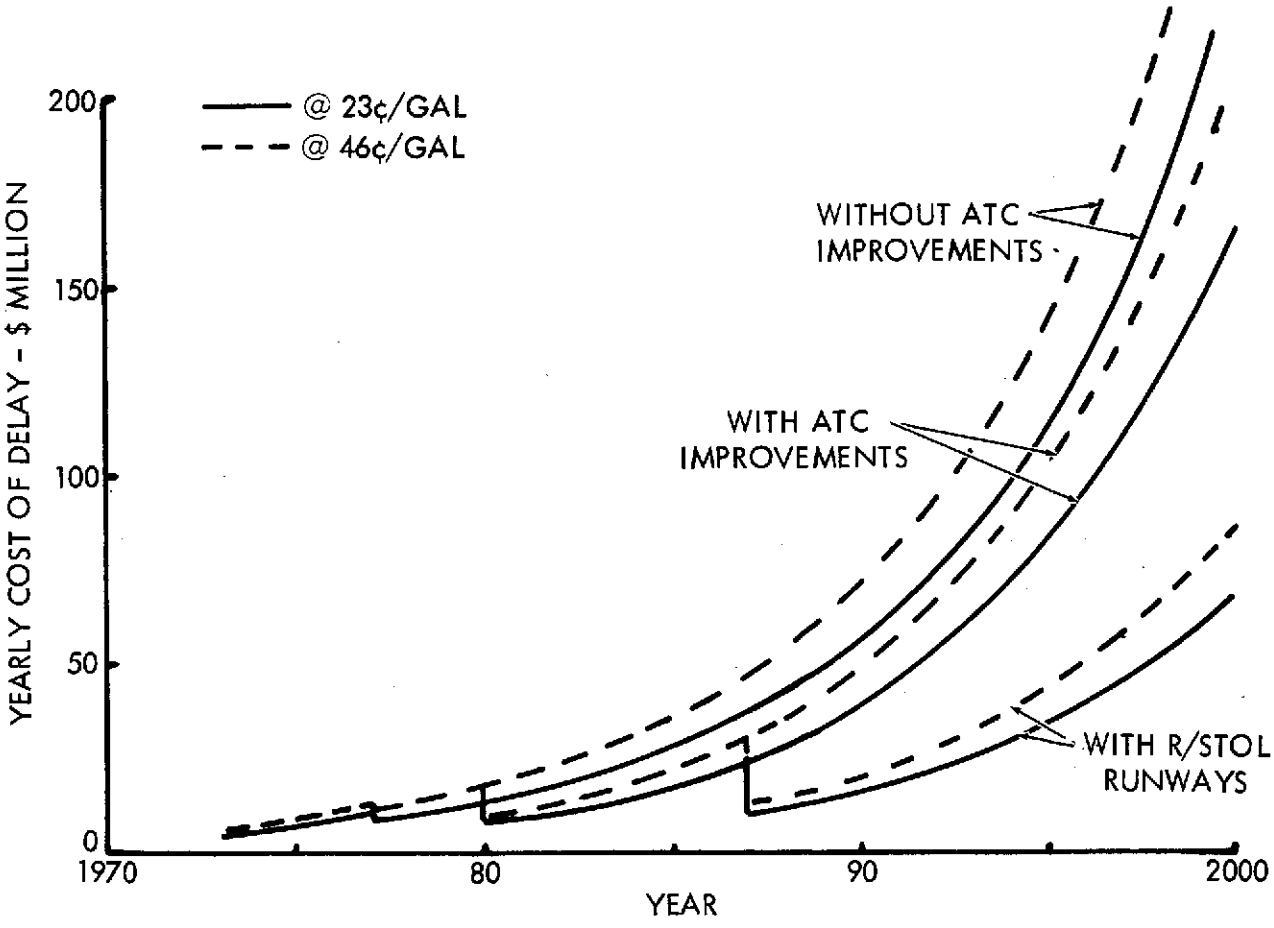

FIGURE 6: ANNUAL COST OF DELAY - ATLANTA AIRPORT

Savings in fuel through relief of congestion would be achieved, also, by construction or use of additional airports. The California corridor represents a significant example of the successful dispersion of air traffic from the hubs to secondary airports; the volume of passengers not interconnecting with long-haul is high enough to support this system with sufficient frequency of flights at the secondary airports. However, the importance of the interconnection problem in other areas must be recognized. Chicago and Atlanta are primary examples of the cases where a short-haul collection system brings passengers to an interchange which offers a tremendous choice of destinations with high frequency of service. Some quotations from a working paper of the Atlanta Regional Commission, Reference 14, serve to illustrate the magnitude of this valuable service to the public:

> "Atlanta now serves 92 cities with nonstop flights...some 597 nonstop flight departures daily... A large number of the Atlanta nonstop flights are on-line continuation flights which provide service to other cities involving one or more stops... (including off-line connections) these scheduled routes provide service to 171 other cities... (providing) convenient access to all domestic airports when the connection potential of the served cities is considered... for every 100 inbound plus outbound passengers at Atlanta only 27 are Atlanta orginations or destinations. Only one in 10 of the inbound plus outbound passengers is a resident of the Atlanta region."
>
> "During the morning busy hour from 10:00 o'clock to noon there are over 200 scheduled flights at the Atlanta airport. Flight connections are those flights departing one-half hour to two hours after a flight arrival. There are 97 flight arrivals from 68 different cities during the time interval from 10:00 o'clock to 11:30 daily each morning. There are 89 flight departures to 72 different cities during the time interval from 10:30 o'clock to noon... a total of 4,093 directional flight connections can be made during the peak involving service between the 116 different cities. Each day Atlanta provides over 14,000 directional flight connections."
>
> "Diversion of connecting passengers may be a natural result of the evolution of a mature domestic route network. The medium hubs surrounding Atlanta will grow and develop more nonstop routes in the future. Cities such as Birmingham, Memphis, Nashville, Charlotte and Jacksonville will provide additional flight connections in the future which will permit passengers to use these airports as alternative connection points having a more direct path than Atlanta between cities connected. In addition, Birmingham/Charlotte nonstop service will become more frequent which provides a diversion by overflying Atlanta. Other examples of overflights would be between the growing medium hubs and other large hubs, such as: Charlotte/Miami and New York/Birmingham... Atlanta scheduled

aircarrier activity might reach a level of operations which was uniform and within the capacity of Hartsfield airport. Such diversion would not contribute to a degradation in frequency of service to the O and D passenger. There would still be more flights than now scheduled..."

"The uniquely high connectivity at Atlanta was a result of the development of high frequency nonstop service to many cities. This was a benefit to the Atlanta O and D passenger and was a factor in the rapid growth of Atlanta. The need for a second aircarrier airport is based on the continuation of a high connectivity at Atlanta, even though passengers connecting at Atlanta would prefer nonstop service between their origination and destination cities."

"The above discussion was presented to illustrate the complexity of the Atlanta regional route structure and its relationship to the total domestic route structure. It is probable that the future Atlanta regional route structure will not change greatly from that existing. Nonstop service may be added to cities such as Omaha, Denver, and Seattle and the frequency of service to other cities will show some increase. However, due to the increase in average aircraft capacity and a higher load factor, the number of peak hour operations experienced today will double by the year 2000 while the forecast of enplaned passengers increased by a factor of six. When all considerations are taken into account, it would not be until the year 2000 that Atlanta as a two aircrarrier airport hub could provide the present level of scheduled service at both airports."

"Atlanta demand will grow and it is upon this growth that the second airport will obtain its demand for service. The second airport could become operational in 1984 at the earliest date. At this time the forecast peak hour operations are predicted to be 136% of the present level. Each airport would have 68% of the present demand for peak hour operations with the forecast demand split evenly between the two. At either airport the peak hour arrivals and departures would be 68% of that now found at Hartsfield and flight connections theoretically would be reduced to 34% of the present 4,000 plus or to approximately 1350 connections. The majority of the cities served have only one arrival or departure flight during the two hour morning peak. The New York hub has 10 flight arrivals (5 non-stop, 5 one-stop) with five to Newark, four to LaGuardia and one to Kennedy. There are only two flights to New York between 10:30 a.m. and noon - a one-stop to Kennedy and a two-stop to Newark. The five non-stop arrivals from the New York hub are a Delta and an Eastern flight from both Newark and LaGuardia and a United flight from LaGuardia. There is no non-stop arrival flight from Kennedy. At 68% of this traffic level, it becomes difficult for an aircarrier to provide an adequate schedule frequency between a two airport Atlanta hub and the three airport New York hub."

"This paper has been prepared to provide a better understanding of the Atlanta scheduled aircarrier route network and how this network is used by the air traveler. The scheduling problems of a two aircarrier airport hub are given a preliminary examination in terms of future levels of demand. Alternative future connecting points and development of nonstop service between cities now using Atlanta as a connecting point may alter the forecast Atlanta demand. These factors should be investigated in more detail to determine the functional impact of a second aircarrier airport on the type of scheduled service that could be provided to Atlanta in the future."

"In addition to the relationship of Hartsfield to a second aircarrier airport for Atlanta, the expansion potential at Hartsfield should be determined for future development of a centrally managed air traffic control system to provide increased runway aircraft acceptance rates. Development of an independent short-haul air system at Hartsfield airport using quiet, reduced take-off and landing aircraft should be studied to determine the probability of such a future technical improvement in operating capacity."

2.3 ASSESSMENT OF THE AIRCRAFT FUEL SHORTAGE

Certain premises are advanced for planning in the areas of short haul transportation and aircraft design, in spite of the numerous uncertainties and hazards in projecting the petroleum fuel situation. Aircraft fuel is such a small fraction of the petroleum used in transportation that its destiny will be determined as a by-product of the situation (or solution) worked out for the major users. It seems inevitable that reason will prevail in the long run and that aviation will be allocated a reasonable share of whatever resources are available, recognizing that air transportation is an indispensable integral part of the national economy.

In very approximate terms, air transport revenue passenger miles grew 10 percent annually from 1967 to 1972 while fuel use grew about 5 percent annually. It is projected that air passenger growth may be maturing such that growth rates of 6 to 8 percent are projected for the future along with fuel demand growth rates of 2 to 4 percent. (The fuel requirements are, of course, lower because of the phasing-in of larger, more 'fuel-efficient' aircraft.) It is concluded that requirements for aircraft fuel are likely to grow more slowly than the most modest estimates of total energy growth rates. Therefore, extreme penalties in airplane design and economics for absolute minimum fuel consumption are unwarranted. Fuel is likely to be available, especially if the recognized current good performance of the airlines in conserving fuel is continued.

Aviation fuel could come from a combination of domestic and imported fuel, in which case air transportation would contribute detrimentally to the balance of payments problem -- to the extent of a billion dollars a year or more in the next few years but still only 5 percent of the balance of payments deficit generated by the other petroleum users. It seems likely that solutions for converting coal and shale will be implemented; something of this kind is essential to avoid the trade deficit and a rational ceiling would be available to avoid arbitrary wild upward swings in fuel prices. Studies at NASA Ames Research Center have indicated that these processes may stabilize aircraft fuel prices at two to three times the 1972 levels. No projections have been observed for fuel prices returning to less than twice 1972 prices. It is concluded that future aircraft design and operational procedures should be predicated on at least double the 1972 fuel price -- and escalated or inflated from that point along with the rest of the economy.

The aircraft design implications of fuel shortages include a slight lowering of design speeds to those which give minimum operating costs at the higher fuel prices. Fuel savings offset the penalty of increased block times. Moderate weight and cost increases for wings with higher aspect ratios are more than balanced by the savings in fuel costs. The lowering in speed also permits an increase in wing aspect ratio with minimum weight penalty. Of particular significance is the increase in aspect ratio without weight penalty which can be afforded by the greater thickness of advanced supercritical airfoils.

2.4 ASSESSMENT OF COMMUNITY NOISE PROJECTIONS

The premise is advanced that the proposed rules for fleet noise levels will be in effect or that modifications will achieve the same effect by 1980 -- all aircraft at or below FAR Part 36. Although the L1011 and DC-10 are quieter than the levels permitted by FAR Part 36, the EPNdB levels of smaller aircraft just meeting Part 36 are roughly the same as the noise level of the heavier wide-body aircraft. Frequency at the major airports is unlikely to increase significantly since passenger growth can be satisfied by substitution of larger aircraft. Thus, frequency and level of noise exposure will not change significantly by 1980.

Airplanes being delivered now or on order will be in service through the 1980's and it seems clear that it would be disastrous to both the airline and the national economy to force more stringent standards on this fleet. Nevertheless, a gradual lowering of average fleet noise levels (and average airport community exposure levels) seems to be in the best interest of all concerned. Design requirements for new aircraft of 10 dB below existing FAR 36 levels are highly probable by the 1980's. It would be logical that a fleet noise averaging process be incorporated in the regulations so that the community noise benefit of the gradual introduction of quieter aircraft could be passed on as an incentive to airline operators.

Further quieting to 90 EPNdB at the airport boundary (18 EPNdB below the FAR 36 level 3.5 N.M. from brake release) for large aircraft was called for as a research goal by the CARD study (Ref. 11). Aircraft below 34,000 Kg (75,000 lb.) gross weight would have a level of 80 EPNdB at the airport boundary (22 dB below the FAR 36 level for approach noise at 1 N.M. from threshold). These goals are indeed ambitious, as the CARD report recognized in stating "... establishment of such ambitious research goals at this time is a controversial issue but the failure to establish a low-level noise goal now could result in the application of scarce resources to R and D activities that may fail to provide the desired solution to the noise problem on a long-term basis."

It is concluded that designers of new aircraft to be operational by 1985 should recognize the high probability of a FAR 36 minus 10 noise requirement (as others have concluded,

Ref. 12 and 13). Further lowering of levels for large long-range CTOL aircraft is likely to be much slower in coming, as the economic penalties are high for this class of aircraft. Aerodynamic noise calculations and measurements on 272,000 Kg (600,000 lb.) aircraft show that FAR 36 minus 8 to 10 EPNdB would be the lowest noise level on approach that a large CTOL aircraft could achieve, regardless of how quiet the engines are. Additional quieting of aerodynamic noise would require a technological breakthrough or a decrease in approach speed (toward R/STOL characteristics). For long-range aircraft the penalties for this performance have not been assessed. For shorter-range aircraft the penalties may not be prohibitive for further lowering of noise level by 1990.

If aircraft capacity is increased by provision of non-interfacing runways for short haul aircraft, new areas of the community are subject to impingement by aircraft noise. The appropriate compromise for establishing an allowable level at the airport boundary has not been established. The CARD research goal shows noise level varying from 80 EPNdB for 34,000 Kg (75,000 lb.) aircraft to 90 EPNdB for 272,000 Kg (600,000 lb.) aircraft. The data needed for a rational answer would be the tradeoff of aircraft operating cost against the cost to move the airport boundary. Data on the aircraft cost portion of this balance are given in subsequent sections of this report. It seems clear that the noise level on the takeoff or approach path will be more pertinent than the sideline noise level.

2.5 POTENTIAL SOLUTIONS

The data and analyses presented in subsequent sections of this report reaffirm the potential of technology advances in airfoil technology, high bypass engine development, ride quality technology, and propulsive lift. It will be shown that fuel conservation and low noise are compatible requirements and that reduced field lengths can be achieved with minimum operating cost penalties for short-range aircraft.

3.0 EVALUATION OF REQUIREMENTS

Requirements and criteria for mission performance, airworthiness and operations originated in the NASA request for proposal on the original systems study. During the course of that study, NASA requested that these be reexamined and that changes be recommended. The following discussion summarizes the bases for performance analysis and economic evaluation that have been applied

3.1 MISSION DEFINITION

3.1.1 Range

A baseline mission range of 926 km. (500 n.m.) has been applied widely as a criterion for short-haul transportation. It is based on analyses which show that approximately 50 percent of revenue passengers travel this distance or less. It was also the range suggested by Eastern Air Lines and American Airlines in their past requests for proposal of STOL aircraft. However, it is slightly inadequate for some significant high density segments between Chicago, New York, Atlanta and Miami. Both Eastern and Delta Air Lines have indicated a preference for additional range, suggesting that the flexibility for scheduling would increase utilization sufficiently to more than compensate for the penalties of flying a heavier airplane on short legs. Their experience in scheduling DC-9 and 727 aircraft leads to this conclusion. It has been suggested that the airplane should be capable of R/STOL performance for stage lengths up to 926 km. (500 n.m.) and able to perform CTOL takeoffs with a full passenger load and fuel for 2780 km. (1500 n.m.). On the other hand, strong cases have been made for uncompromised austere short haul aircraft which would be most economical for the short segments (300 to 800 km.) that form the majority of legs. Passenger amenities that are required for stage lengths of more than 900 km. contribute to increased aircraft size and cost, as well as the structure required for heavier fuel loads.

The issue will be resolved in the long run by negotiation with airline customers when the environment permits implementation of advanced short haul aircraft. This is most likely to be deferred to the 1980's in the case of high-density short-haul. The current task of evaluation of advanced lift concepts and fuel conservation is not significantly affected by this variable, although somewhat higher design cruise speeds would be appropriate for the longer ranges.

3.1.2 Passenger Capacity

Both Lockheed and McDonnell-Douglas have concluded that a passenger capacity of approximately 150 is well-suited for the high-density scenarios which were being examined in systems studies. The Lockheed analysis showed that return on investment for a representative case was essentially the same with aircraft of 100 and 200-passenger capacities. A passenger size of 148 was chosen for the purposes of further evaluation of lift concepts and fuel consumption.

As with the question of ranges, the size of the operational airplane will be resolved considering customer needs and the conditions prevailing in the 1980's; the comparative evaluations in the current study are essentially unaffected by this issue. It is anticipated that R/STOL evolution will progress from the current Twin Otter service through larger propeller-driven aircraft serving the shorter low-density segments; the next step may be fan-powered aircraft in the 60 to 100 passenger size, also with stage lengths limited to less than 900 km. Evolution to the high-density arena with extended range capability and larger aircraft is likely to follow these other steps. In each step, the availability and size of a suitable engine will be a strong factor in determining the matching airplane size.

3.1.3 Field Length

The rapid increase in cost as design field length was reduced below 910 m. (3000 ft.) has led both Lockheed and McDonnell-Douglas to conclude that the best chance for a viable economical R/STOL short-haul system would involve 910 m. (3000 ft.) or

higher in available runway lengths. McDonnell-Douglas emphasized the use of secondary airports for city-pairs with significant local origination and destination traffic. They concluded that 910 m. (3000 ft.) field performance would be desirable and that this capability was available at almost every site examined. Lockheed emphasized the importance of interconnection with other airline flights and suggested that congestion and noise relief would occur if CTOL short haul traffic was offloaded to non-interfering short haul runways of 910 m. (3000 feet) or more at existing hub airports. The need for expanding the airport boundaries would be zero or minimal if the runway lengths were 910 m. (3000 feet) and would increase at some of the major airports if runway lengths of 1220 m. (4000 feet) were required. The Aviation Advisory Committee concluded that 1220 m. (4000 feet) runways were appropriate, and needed for short haul transport. No definitive cost tradeoff has been made that includes the airport expansion cost increment as a function of runway length. It is concluded that the requirement for 910m. (3000 feet) airplane capability is sufficiently probable that it should continue to be pursued. Conditions in the late 1980's and beyond are most likely to lend considerable value to a 'real-estate stingy' airplane.

The design requirement that the airplane be capable of a given field performance on a 95°F day has been associated with a sea level field elevation. It seems reasonable that higher-elevation airports can be assumed to compensate with additional runway length for the elevation effect. Other field requirements have also been included in the current study: 610 m., 1070 m. 1220 m. and 1830 m. (2000, 3500, 4000 and 6000 ft.). The consequent airplane designs and economics give perspective to the effect of this variable.

3.1.4 Cruise Speed and Altitude

Cruise speed of M 0.8 and 9140 m. (30,000 feet) altitude were selected as design requirements for 926 km (500 n.mi.) aircraft in the basic system study, based on the following considerations:

- Initial screening of quiet propulsive lift aircraft indicated that this performance gave the lowest direct operating cost in most cases - at 1972 cost and fuel price levels.

- Air-traffic compatibility with aircraft currently employed in short-haul air transport indicated the desirability for cruise in the neighborhood of M 0.8.

- For stage lengths up to 926 km. (500 n.m.), flexibility in routing and ATC assignments indicated the desirability of 9140 M. (30,000 FT.) altitude capability.

- For 926 km. (500 n.m.) flights it was felt that block times should be approximately equivalent to those available from CTOL aircraft now performing the mission so that this factor would not be detrimental from the standpoint of passenger preference.

With the advent of an aircraft fuel shortage, and increased fuel prices, the aircraft in current use were slowed slightly to conserve fuel. This was beneficial with current aircraft designs such as the DC-9, down to approximately M 0.75. The influence on block time was negligible from the standpoint of the passenger for short-haul segments. Direct operating costs, in real terms, were either unaffected or slightly reduced from the fuel saving, compared with what they would be at faster speeds and lower block times. This amount of slow down did not require rescheduling of the airplane so that it flew as many revenue-miles per year as previously; the annual utilization increased in terms of block hours and the annual productivity was essentially unchanged.

In considering new short-haul aircraft designs it was considered appropriate to reexamine design cruise speed and altitude as they affected fuel consumption and direct operating cost at higher fuel prices. Design cruise speed of M 0.75, and perhaps lower would be competitive with current generation aircraft in the short-haul mission and would be compatible with air traffic in this environment. An evaluation of the effect of cruise speed and altitude, as a function of fuel price, is presented in the following sections of this report. It is suggested that aircraft flying a spectrum of stage lengths up to 900 km, with average stage lengths of 400-500 km., should have the capability of flying M 0.75 at 9140m. (30,000 feet). In the following analyses, the DOC calculations are conservatively high for the slower aircraft because annual utilization has been assumed to be 2500 hr. per year; in practice the slower aircraft would probably have a higher

annual utilization in terms of hours. The annual productivity in short-haul missions would probably be as high as faster aircraft.

3.1.5 Flight Profile and Reserves

The flight profile and definition of fuel reserves were presented in Reference 1/2. No changes from the conditions selected initially have been deemed necessary or desirable. The following summarizes the criteria used:

1. Takeoff and initial climb according to the performance criteria discussed in Section 3.2.

2. Power cut-back at 213 m. (700 feet) for 4-engine aircraft or 305 m. (1000 feet) for 2-engine aircraft to that throttle setting which will maintain a positive climb gradient if an engine fails (Ref. FAR Part 36).

3. Acceleration to 250 KEAS and maximum climb at this speed after reaching a point where ground noise level is below 80 PNdB. It is recognized that the safety of the cutback maneuver has been questioned and that it is generally not applied below 460 meters (1500 ft.) when it is used in current practice. This is discussed later in connection with the noise data.

4. Climb to 3050 m. (10,000 feet) at 460 km./hr. (250 knots) EAS with allowance of 2 minutes for air maneuver.

5. Climb to cruise altitude at best climb speed for minimum block time.

6. Cruise at design cruise speed.

7. Descend at best descent speed for minimum block time, decelerating to 460 km./hr. (250 knots) EAS at 3050 m, (10,000 feet). Cabin pressurization of 61 KN/m^2 (8.8 psi) was established to permit maximum climb and descent rates while restricting change of pressure in the cabin to 91 m. (300 feet) per minute change in cabin altitude.

8. Descend at 860 km./hr. (250 knots) EAS to 305 m. (1000 ft.) decelerating to approach speed defined in Section 3.2. Allowance in block time of 2 minutes is made for air maneuvers.

9. Descend to touchdown at 4.6 m./sec. (900 feet per minute).

Reserves are provided for 370 Km (200 n.m.) at cruise altitude plus 15 minutes at 3050 meters (10,000 ft.) altitude, maximum endurance speed.

3.2 PERFORMANCE CRITERIA

The performance criteria dopted in the current work for the propulsive lift systems are identical to those agreed with NASA for the Phase II analysis of the original studies (Ref. 2). These criteria are based, with minor deviations, on FAR XX tentative airworthiness standards for powered lift aircraft. The mechanical flap designs are based on FAR Part 25 standards as currently applied to CTOL aircraft. The differences in such basic factors as speed margins and climbout requirements between the two sets of airworthiness factors, have a significant influence on some of the comparisons which are made in this report between propulsive lift and mechanical flap designs. Examination of the takeoff and landing speed and load factor criteria indicates that the required speed margin above the stall is higher for the mechanical flap than for the propulsive lift system. As an example, the mechanical flap is required to have a minimum takeoff obstacle speed of 1.20 times the stall speed, while the obstacle speed for the powered lift system is required to be not less than 1.15 times the stall speed with one engine inoperative. In terms of pure speed margin, therefore, the powered lift system derives a definite advantage in performance. Whether this advantage is justified in terms of equivalence of safety with a mechanical flap design is the subject of many arguments on both sides. On one hand, the available load factor margin above the stall at the ostabcle speed for a mechanical flap system is 44 percent. However, due to a reduction in thrust coefficient and hence $C_{L\ MAX}$ in going from the stall speed to the obstacle speed, the comparable load factor margin for the powered lift system is somewhat less than 30 percent with one engine inoperative. On the other hand, the shape of the C_L versus α curve approaching $C_{L\ MAX}$ is more

gradual for the powered lift system, so that the angle of attack margin prior to the stall point is significantly greater for the powered lift system at a given obstacle/stall speed ratio. This type of argument is equally applicable to the landing/approach case.

The question of rational margin selection should be the subject of a research program which would provide a thorough understanding of all relevant factors. Such a program could be provided by the proposed NASA QSRA airplane.

In the computation of field lengths, takeoff and landing speeds are determined as the most critical of the five appropriate requirements:

- Engine out lift-off or approach speed
- All engines lift-off or approach speed
- Engine out minimum load factor speed
- All engines minimum load factor speed
- Minimum control speed. (The tail areas are sized to ensure that V_{MCA} is equal to or less than V_{MIN})

All designs are equipped with thrust reversers on each engine. No credit has been taken, however, for use of reverse thrust during takeoff or landing. These devices are employed to provide additional margins for slick runway conditions, and to reduce brake usage when field length is not a limiting factor. All landing performance data shown throughout the report is computed at the 926 m. (500 n.m.) STOL mission takeoff weight.

The performance criteria used are summarized below. Where differences exist between FAR Parts 25 and XX standards, the criteria are designated by PL and MF to denote powered lift and mechanical flap systems, respectively.

- Takeoff:
  - Sea level field at 35°C (95°F)
  - FAR balanced field - greater of
    - 1.15 times normal takeoff distance to 10.67 m. (35 feet)

- distance to accelerate to V_1 and clear 10.67 m. (35 ft.) with critical engine failure at V_1

- distance to acclerate to V_1, followed by an average deceleration rate of 0.4g to a stop with a 3 second time delay between acclera-tion and deceleration phases.

- Rolling coefficient of friction - 0.015

- Lift-off/stall pseed ratio = 1.15 - 1 engine out (PL)
  = 1.20 - all engines operating (PL)
  = 1.20 (MF)

- Minimum load factor capability = 1.20 - 1 engine out (PL)
  = 1.30 - all engines operating (PL)
  = 1.30 (MF)

- FAR minimum control speed margins.

- FAR 25 and XX second segment climb gradient
  = 2.4 percent for two engine aircraft
  = 2.7 percent for three engine aircraft
  = 3.0 percent for four engine aircraft

- Landing:
  - Sea level field at 35°C (95°F)
  - Minimum approach/stall speed ratio = 1.20 - 1 engine out (PL)
    = 1.25 - all engines operating (PL)
    = 1.30 (MF)

  - Minimum load factor capability = 1.20 - 1 engine out (PL)
    = 1.30 - all engines operating (PL)
    = 1.30 (MF)

  - Approach over 10.67 m. (35 ft.) with sink rate = 4.6m./sec (900 fpm)

- Flare to touchdown at 3 m./sec (10 FPS)
- 1 second delay between touchdown and brake and/or thrust reverser application
- Roll out deceleration rate = 0.35g
- Landing field length = landing distance divided by 0.6.
- FAR 25 and XX approach climb gradients
  = 2.1 percent for two engine aircraft
  = 2.4 percent for three engine aircraft
  = 2.7 percent for four engine aircraft
- FAR 25 and XX landing climb gradient
  = 3.2 percent

3.3 OPERATIONAL QUALITIES

3.3.1 Handling Qualities

The philosophy and reference studies of handling qualities are discussed in Section 2.7 of reference 2; criteria selected are summarized below.

Longitudinal - For STOL aircraft the trim requirement plus maneuver capability for landing approach at the approach speed is most critical and will be used to establish the tail size and type of horizontal tail. To the basic trim requirement is added a maneuver capability of 0.3 rad/sec^2 at the most forward center of gravity. This level of pitch acceleration beyond trim produces a pitch angle in the first second of 4.3 degrees assuming maximum control deflection is achieved in 0.3 seconds with a 0.1 second transport lag and a time constant of 2.0 seconds.

Lateral - The criteria for lateral control power required is based on an acceleration capability of 0.42 rad/sec^2 at the landing approach speed in symmetric flight. A further

requirement is to retain 30 percent of this control power for maneuvering after trimming a critical engine failure in a 46 km/hr (25 knot) crosswind at the approach speed.

Directional - Directional control power requirements are expressed in terms of the ability to trim the most critical engine failure in the presence of a 25 knot (46 Km/hr) crosswind at the approach speed and an initial yaw acceleration capability in trimmed flight of 0.16 rad/sec^2.

3.3.2 Ride Qualities

The criteria for ride qualities were RMS gust levels of 1.7 m/sec (5.7 ft/sec) for cruise, 2.5 m/sec (8.2 ft/sec) for descent, and 3.0 M/sec (9.8 ft/sec) for landings were used. These criteria are sufficient to insure that a design goal is achieved. However, since scale of turbulence is such an important parameter which at times seems as arbitrary as the criteria, it should also be specified. The values used in this analysis for the longitudinal scale of turbulence were 990, 570 and 210 m (3250, 1700 and 700 feet) for the cruise, descent, and landing approach conditions respectively. The velocities considered were M 0.8 and 9100 m (30,000 ft.) for cruise, 463 km/hr (250 knots) at 1500 m (5000 ft) for the descent, and a velocity that varied with configuration (1.25 V_s) at 150 m (500 ft) for the landing approach.

3.4 NOISE CRITERIA

Potential noise criteria of the 1980's were discussed in Section 2.4. It was concluded that aircraft noise requirements equivalent to FAR 36 minus 10 EPNdB should be the basis for a new design of CTOL aircraft; further reduction of approach noise would require a lowering of approach speeds which would introduce the trend toward R/STOL performance. Short-haul runways on hub airports or use of secondary airports will require different criteria such as minimum footprint area and length. Downtown STOLports, now regarded as unlikely to be accepted or be operational in the 1980's, might well require 80 to 90 EPNdB noise levels at the airport boundaries; the Sperry box dimensions would represent a rectangular area 1830 m. (6000 feet) long by 610 m. (2000 feet) wide.

The approach used in the current analyses was based on the previous work which indicated that selection of an engine fan pressure ratio capable of meeting a given noise level without extensive nacelle treatment provided the lowest cost aircraft system. Consequently, the nacelles for all the systems (except augmentor wing) were designed for aerodynamic performance and acoustic treatment was applied to the walls only. In the case of the augmentor wing, the high fan pressure ratio required inlet treatment and acoustic lining of the augmentor flap. Airplanes covering a range of noise levels were designed by the use of different engines, each with acoustic wall treatment in fan inlet and exhaust. The footprint areas and contour shapes were determined for a wide range of aircraft designs and from these the economic and fuel penalties were determined for meeting any chosen level of community noise.

3.5 ECONOMIC EVALUATION CRITERIA

The primary basis for evaluating airplane designs and for selecting optimum airplane characteristics was the direct operating cost based on updating the 1967 ATA "Standard Method of Estimating Direct Operating Costs of Turbine Powered Transport Aircraft." In the initial systems studies the following factors were agreed upon as representative of 1972 costs and prices:

1. Block time minus flight time = 10 min.

2. Block fuel as determined from the flight profile, using 6 minutes ground time and 4 minutes air maneuver time.

3. Reserve fuel as defined in Section 3.1.

4. Crew costs = 3 man crew with 40% increase per man over 1967 ATA.

5. Hull insurance: Retain 2% ATA rate

6. Utilization: 2500 hr. per year.

7. Labor rate: $6/hour

8. Maintenance cost: 75% of 1967 ATA value.

9. Maintenance burden: Retain ATA factor of 1.8.

10. Depreciation: ATA 12 years, 0 residual, 25% engine spares in lieu of 40%.

11. Fuel costs: 11.5¢/gal.

These same factors were retained for convenience of comparison with the initial studies, assuming that price escalation would apply uniformly to all factors except for fuel. In this case additional fuel price cases were considered and defined as follows:

DOC-1	-	11.5¢/gal.
DOC-2	-	23¢/gal.
DOC-4	-	46¢/gal.
DOC-10	-	$1.15/gal.

For return on investment analysis, some minor changes in the DOC factors were applied, based on examination of 1972 operating statistics. These are discussed in Section 9, along with the procedures used for ROI analysis.

Airframe and engine costing was on the same basis as described in Section 2.9 of Reference 2. Cost factors were derived from detailed value engineering analysis of component cost in the Electra and C-141 programs with adjustments for complexity factors. Production quantities of 300 aircraft and 1500 engines formed the basis for pricing, with an allowance of 13 percent profit. These quantities, in general terms, are considered to represent approximately the minimum size program which would be viable and, at the same time, the maximum number of units which would be projected for the purpose of setting a price considering normal practice with respect to risk assessment.

In the case of 2-engine aircraft, the number of engines including spares was 750 and was associated with a 300-aircraft program. Pricing data from the QCSEE studies showed that

the unit price for this quantity would be 25 percent higher than the price for a 1500-unit production. The effect of this is approximately 4 percent increase in aircraft DOC and this effect is shown in the subsequent analyses. However, it was concluded that engines with fan pressure ratios of 1.35 to 1.6 would have sufficient value for CTOL applications that the larger production quantity should be used as the baseline condition for the evaluation of twin-engine aircraft for this category of engines.

4.0 OVER-THE-WING/INTERNALLY BLOWN FLAP (OTW-IBF) VEHICLES

4.1 OTW-IBF CONCEPT

The evaluation of altemate lift concepts in reference 2 showed the hybrid OTW-IBF to be particularly promising for field lengths of 910m (3000 ft) and less, where the augmentor wing (AW) might have been expected to be superior. Moreover it did not appear to be at a great disadvantage to the preferred longer-field concept, i.e., the mechanical flap (MF) for fields approaching 1220m (4000 ft). Since the hybrid concept was necessarily based upon a far less extensive technology data base than either of these competing concepts, a more refined conceptual design of the hybrid vehicle for 910m (3000 ft) has been undertaken in subsequent studies, which are reported here in order to improve the credibility of economic comparisons. Furthermore all vehicles in in reference 2 were constrained to a common 152m (500 ft) sideline noise level of 95 PNdb which generally necessitated the use of acoustic splitters as well as nacelle wall treatment. It now appears that the use of wall treatment alone and an appropriately selected fan pressure ratio are the most economic means of compliance with noise criteria. Accordingly subsequent studies have been based upon nacelle wall treatment alone for each candidate fan pressure ratio (FPR) engine and imply variable noise standards from which trade studies of cost and noise may be developed (as discussed in Section 8.0). The OTW-IBF vehicles derived for the foregoing purposes which are described in Section 4.4 retain the baseline mission requirements established in reference 2 and carry 148 passengers over a capacity payload stage length of 926 km (500 n mi) when operating from a 910m (3000 ft) field. The baseline cruise speed and the initial cruise altitude are Mach 0.8 and 9140m (30, 000 ft) respectively.

A more surprising trend observed in the vehicle data from reference 2 was the indication that powered lift concepts such as the OTW-IBF might offer mission fuel savings relative to MF vehicles. Accordingly fuel-conservative OTW-IBF vehicles have also been derived in the studies reported here and are described in Section 4.5. The scope of the investigation of these aspects has been greatly expanded from that of the baseline mission vehicles in that significant mission parameters (cruise speed, altitude

and field length) have been optimized as well as the main configuration parameters included in both cases. Furthermore attention has been equally devoted to mission fuel consumption per se and operating costs at the elevated fuel prices now in prospect whereas the baseline mission vehicles have been optimized with respect to DOC at 1972 prices (as in reference 2).

The baseline mission vehicles have high-wing arrangements and a landing gear which is mounted on a fuselage seating six-abreast in a single aisle arrangement. Subsequent examination of alternate fuselage configurations has indicated that whereas the additional weight and surface area of a twin aisle six-abreast arrangement would increase mission fuel by 2.6% and DOC by 1%, a single aisle five-abreast arrangement was both lighter and had a lesser surface area. Because of the 1% saving in fuel and 0.3% saving in DOC of this configuration, all fuel conservative vehicles have the longer five-abreast fuselage which implies a longer landing gear and thus a low-wing arrangement for its convenient attachment and retraction. The two classes of vehicle also differ with respect to engine location in that a two-engine arrangement is preferred for the baseline mission with the most inboard possible nacelle location which is best suited to the IBF ducting requirements and incidentally minimizes the asymmetric lift and rolling moment following engine failure. With the substantially higher aspect ratio wings, at which the fuel conservative vehicles are optimized, a four-engine configuration has generally appeared more advantageous.

Independently cross-ducted IBF flows were utilized in the two-engine OTW-IBF in reference 2 in order to exploit asymmetric IBF lift as a counter to the rolling moment induced by the OTW asymmetry in single-engine operation. However it was shown that this arrangement seriously impeded fuel storage provisions and thereby precluded wing loadings exceeding approximately 440 Kg/m^2 (90 lb/sq ft) which was an effective barrier to further DOC reduction. Furthermore the IBF duct losses associated with the unavoidable changes in flow direction effectively restricted the IBF flow to little more than 10% of the total fan flow which was undesirably low. From consideration of all possible duct configurations it has been concluded that the most desirable arrangement which minimizes the intrusion upon fuel storage volume and yet satisfies

the need for cross flow is a spanwise plenum duct aft of the wing rear beam and supplied by chordwise ducts within the nacelle boundaries. At the time of the initial studies, this arrangement, was thought to restrict the IBF mass flow to around 5% in a two-engine vehicle because of stable engine operating problems similar to those of the AW which are in Section 5.1. However an examination of parallel engine operations (in the specific context of a low FPR engine) by Detroit-Diesel Allison (DDA) has subsequently disclosed that up to 20% may be accepted and accordingly all OTW-IBF vehicles have been predicated upon a plenum duct configuration.

A number of OTW-IBF flap concepts have been examined with a view to establishing the best combination of low surface curvature (for efficient Coanda deflection of the OTW stream) and large plenum duct cross section (for minimum IBF system losses). A radical conflict between these qualities was evident as illustrated by the data presented in Figure 7 for the opposite ends of the spectrum of flap concepts, i.e. a constant curvature Coanda flap of generally similar appearance and motion to a Fowler flap and the expanding Jacobs-Hurkamp internally blown flap. In view of the importance attached to the controlled use of the trailing edge nozzles of the latter as a rolling-moment trimming and direct drag control (DDC) device for flight path modulation, the concept selection has concerned the acceptability of the latter for Coanda vectoring. Empirical data derived from limited Coanda tests originally conducted at Lockheed-Georgia has now been correlated with powered wind tunnel tests of a representative hybrid vehicle with this flap and has thus justified its adoption in principle. Detailed drawings of the proposed flap and duct system for the baseline vehicle have been included in Section 4.10.

C2

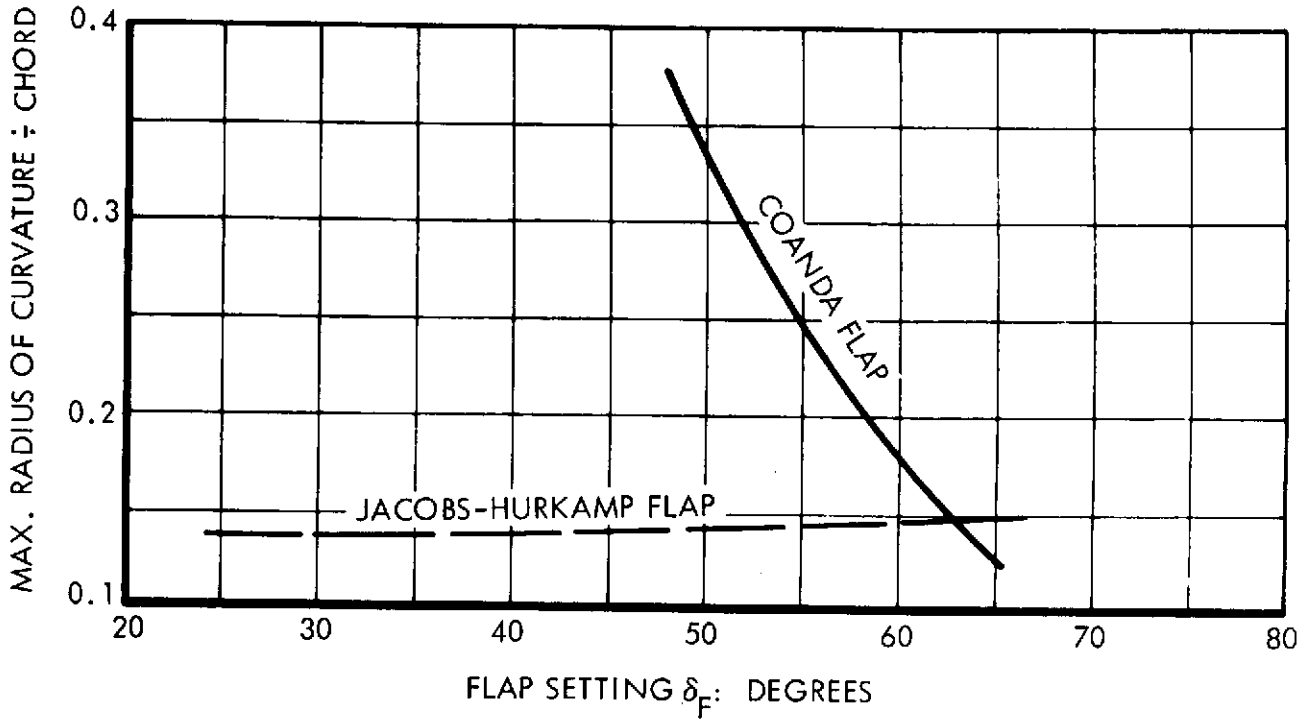

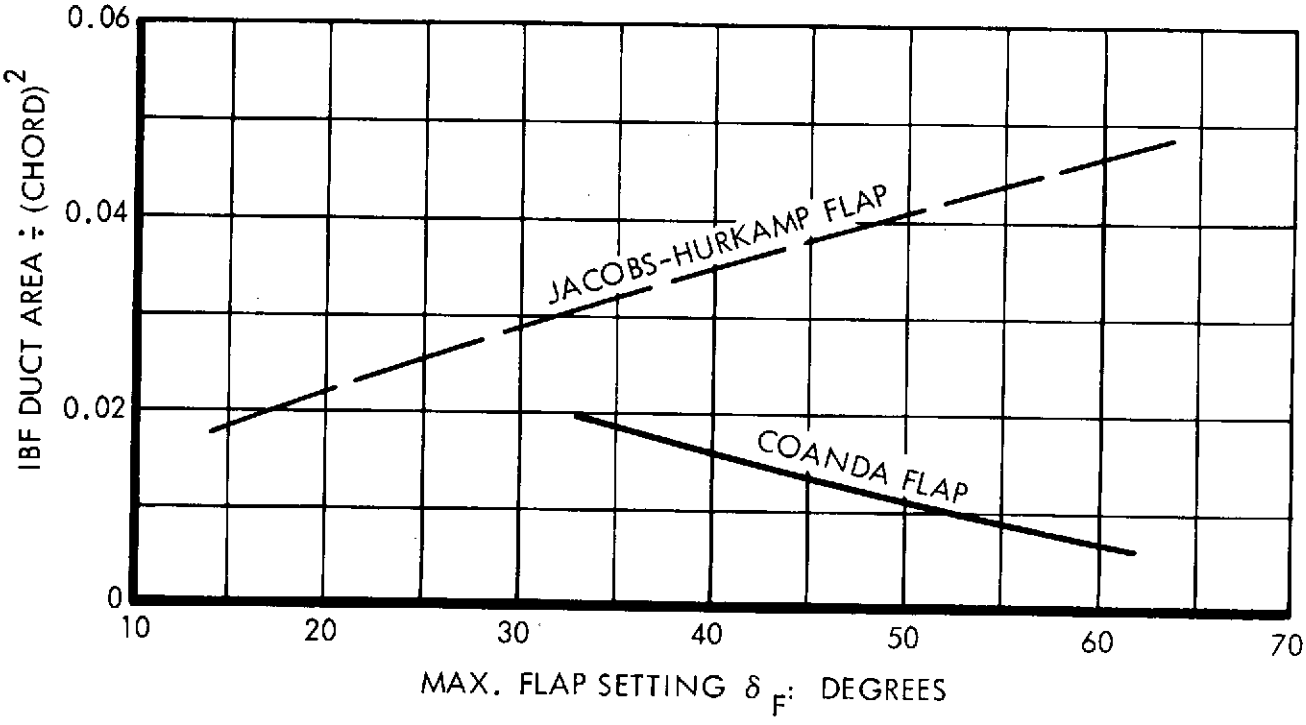

FIGURE 7: COMPARISON OF FLAP CONCEPTS

4.2 OTW/IBF PROPULSION DATA

4.2.1 Candidate Engines

To meet the requirements for fan pressure ratio variations required by the presently contracted study effort, candidate engines have been selected from Phase I and Phase II of the NASA-Lewis Contract NAS3-16727 QCSEE Study. These engines, shown in Table I, provided the most consistent data available for the pressure ratios and technology levels (mid 1980's) desired for the study. An additional set of engine data was derived for a higher fan pressure ratio, representative of the RB211, CF6 and JT9D, with modification factors for technology advances to achieve consistency with the engines of Table I. A 1.47 FPR turbofan which is under active development was subsequently introduced into the study. This is an advanced-technology, low-noise engine in the 100 KN (22,000 lb.) S.L.S.T. class, and is expected to be certified in late 1977. Rubberized parametric data have been generated based on this engine as being representative of an intermediate by-pass engine suitable for an advanced CTOL.

The uninstalled engine performance data for the 1.25 and 1.35 fan pressure ratio engines were generated by UNIVAC 1106 cycle matching computer programs. Uninstalled engine performance for the 1.47 FPR turbofan were gathered from various brochures and publications and were installed by Lockheed to reflect the characteristics and the performance penalties of the OTW/IBF and MF nacelle installations. At the end of the study, an UNIVAC 1106 computer cycle simulation of the engine became available in-house at Lockheed, but the timing of this program set-up precluded any extensive use of this deck. Spot checks of several deck data points show very close comparison with the data used for the study. Scaling factors of weight, dimensions, and costs used for the engines were generated by Lockheed based on the data provided by the manufacturers during Phase I and II of the QCSEE effort.

TABLE I: OTW/IBF ENGINE CANDIDATES

FAN PRESSURE RATIO	FAN TYPE	BASED ON ENGINE	NOISE TREATMENT
1.25	VP	PD287-5	WALL TREATMENT ONLY
1.325	VP	-6	WALL TREATMENT ONLY
1.35	FP	-11	WALL TREATMENT ONLY
1.35	FP	-11	INLET SPLITTER & WALL TREATMENT
1.40	FP	-39	WALL TREATMENT ONLY
1.40	VP	-4	WALL TREATMENT ONLY
1.47	FP		WALL TREATMENT ONLY
1.47	FP		INLET SPLITTER & WALL TREATMENT
1.50	FP	PD287-23	WALL TREATMENT ONLY

4.2.2 Installation Performance Characteristics

The nacelle configuration of one of the candidate OTW/IBF engines is shown on Figure 8. These nacelles represent aerodynamically designed internal and external contours with no compromise for acoustic materials. However, acoustic materials are installed on walls of the inlet and exhaust ducts where this treatment does not interfere with the internal aerodynamic lines. The aft nacelle contains the thrust reverser which consists of an upward movable panel and blocker door arrangement to reverse the OTW portion of the fan exhaust stream; the IBF fan stream and the primary stream will remain unaltered. The lower aft nacelle will contain a "flow collection" device to route fan air flow into the IBF system for terminal area operation and that can then be shut down for cleaned up climb and cruise operation. The nacelle inlet/forebody shapes have been designed by proven Lockheed methods and charts to provide good cruise recovery levels while maintaining reasonable losses for terminal area operation. The inlets have been designed to minimize the flow distortions due to upwash angles that might be experienced by over-the-wing mounted engines.

The internal and external installation aspects of a typical OTW/IBF engine/nacelle combination are listed below for a typical cruise altitude and flight Mach number:

Installation Parameter	Penalty
Inlet $\Delta P/P$	0.005
Fan Duct and Nozzle $\Delta P/P$	0.016
Primary Duct and Nozzle $\Delta P/P$	0.004
Fan and Primary Nozzle Velocity Coeff.	0.980
ECS Airbleed (Total for 150 PAX)	99.5 Kg/min (220 lb/min)
Power Extraction (Total for 150 PAX)	104.2 KW (140 HP)
Nacelle External Drag D_N/F_N	0.18*

* Typical value shown for baseline engine, value is dependent on flight Mach number and engine design cycle, i.e. FPR.

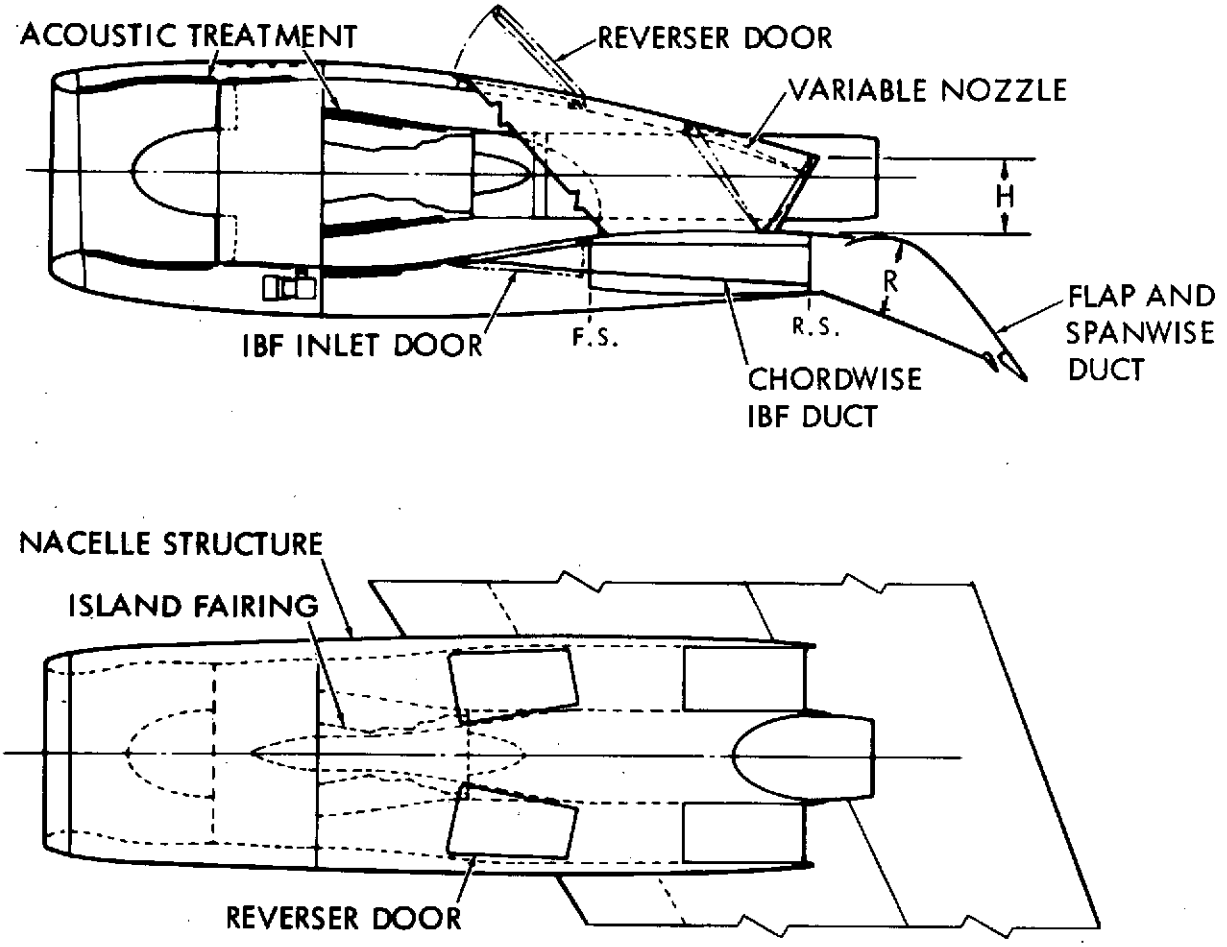

FIGURE 8: OTW-IBF NACELLE INSTALLATION

The environmental airbleed extraction has not been included in the basic engine data used by the airplane sizing program to allow a greater flexibility in the use of the data. Performance penalties that relate the magnitude of mid-stage airbleed and number of engines were applied by the sizing program to properly evaluate the effects of bleed extraction. The ground rules of this study permitted the ECS airbleed to be turned off for terminal area operation; thus, these bleed effects apply only to the climb and cruise data. The installed engine performance of Table II has been presented as "no bleed" performance consistent with the basic input to the airplane sizing program.

The nacelle external drag is computed as a combination of individual friction and pressure drag component forces. These components are the freestream friction drag that acts on that portion of the nacelle exterior which is washed by the ambient airstream, the drag attributed to the boattail and aft-fairing surface pressure forces, and the forebody additional drag defined as the force difference between the momentum drag incurred in the precompression of the inlet stream tube and the cowl thrust recovered on the forebody. The penalty for the total nacelle drag has been included in the installed performance of Table II.

The major nacelle dimensions of the candidate engines for the OTW/IBF airplanes are presented in Figure 9. The dimensions all relate to the base rated thrust as shown, the dimensions of any actual installation are scaled to match the thrust of that specific airplane. The dimensions of two PNL trade study nacelles have not been included in Figure 9 since only an internal splitter was placed in the inlet with only a slight increase of 20-25 cm (8-10 in), in the inlet length, L_1.

4.2.3 OTW/IBF Propulsion Bookkeeping Methods

Distinct airplane/propulsion bookkeeping procedures have been adopted for the OTW/IBF concept in terminal area operations and cruise operations. The terminal area operations on those flight operations in which the aircraft is in the high lift mode and cruise operations are those for which the airplane/wing/nacelle are cleaned-up for climb

TABLE II: OTW/IBF CANDIDATE ENGINE CHARACTERISTICS

(PROPULSION-AERODYNAMIC DESIGNED NACELLE, WALL TREATMENT ONLY)

FAN PRESSURE RATIO	1.25	1.325	1.35	1.35***	1.40	1.40	1.47	1.47***	1.50
FAN TYPE	V/P	V/P	F/P	F/P	V/P	F/P	F/P	F/P	F/P
UNINSTALLED T/W (T.O.)* - N/Kg (LB/LB)	65.2 (6.65)	66.6 (6.79)	67.1 (6.84)	67.1 (6.84)	64.7 (6.60)	66.4 (6.77)	55.7 (5.68)	55.7 (5.68)	62.8 (6.40)
INSTALLED T/W (T.O.)** - N/Kg (LB/LB)	30.8 (3.14)	32.9 (3.35)	33.6 (3.43)	32.6 (3.32)	33.8 (3.45)	34.4 (3.51)	32.1 (3.27)	31.2 (3.18)	33.7 (3.44)
INST. SPEED LAPSE RATE (0.2M)	0.702	0.743	0.746	0.746	.754	0.754	0.780	0.780	0.781
UNINSTALLED $/T (T.O.) - $/N ($/LB)	7.46 (33.20)	7.31 (32.50)	6.36 (28.30)	6.36 (28.30)	7.31 (32.50)	6.36 (28.30)	5.78 (25.70)	5.78 (25.70)	6.36 (28.30)
INSTALLED $/T (T.O.)** - $/N ($/LB)	11.58 (51.50)	11.49 (51.10)	10.30 (45.80)	10.41 (46.30)	11.08 (49.30)	10.05 (44.70)	9.22 (41.00)	9.28 (41.30)	8.90 (39.60
INST. ALTITUDE LAPSE [0.8 M/9130m. (30,000 FT.)]	0.134	0.161	0.173	0.171	0.185	0.182	0.218	0.217	0.197
INST. CRUISE SFC - mg/Ns (LB/HR/LB)	2.52 (.891)	2.31 (0.816)	2.20 (0.777)	2.23 (0.786)	2.25 (0.793)	2.22 (.785)	2.38 (0.839)	2.39 (0.845)	2.28 (0.804)

* RATED THRUST SCALED TO 133.8 KN (30,000 LB) THRUST

** S.L., 35°C (95°F) @ SCALED RATED THRUST

*** NOISE TRADE-OFF STUDY CANDIDATE ENGINE (INLET SPLITTER)

Rated Thrust - KN (Lb.)	122.9 (27,600)	127.0 (28,800)	89.0 (20,000) F.P.	89.0 (20,000) V.P.	89.0 (20,000)	129.8 (29,200)	49.5 (22,000)
Fan Pressure Ratio	1.325	1.350	1.40	1.40	1.50	1.25	1.47
D_1 - m (in.)	2.52 (99.0)	2.53 (99.2)	2.08 (82.0)	2.09 (82.1)	2.06 (81.0)	2.72 (107.0)	2.09 (82.3)
L_1 - m (in.)	1.42 (56.0)	1.39 (54.9)	1.11 (43.6)	1.11 (43.6)	1.00 (39.4)	1.63 (64.2)	1.05 (41.2)
L_2 - m (in.)	1.32 (51.9)	1.56 (61.3)	1.14 (44.8)	1.21 (47.6)	.940 (37.0)	1.64 (64.7)	.813 (32.0)
L_3 - m (in.)	1.72 (67.8)	1.793 (70.6)	1.59 (62.6)	1.43 (56.4)	1.75 (69.0)	1.60 (62.8)	1.51 (59.3)
L_4 - m (in.)	1.04 (40.8)	1.04 (40.8)	.65 (25.6)	.65 (25.6)	.517 (20.4)	1.25 (49.1)	.615 (24.2)
L_5 - m (in.)	1.83 (72.0)	1.86 (73.3)	1.22 (48.0)	1.22 (48.0)	1.07 (42.2)	2.09 (82.3)	1.23 (48.4)
h_1 - m (in.)	.572 (22.5)	.584 (23.0)	.36 (14.2)	.36 (14.2)	.324 (12.8)	61.7 (24.3)	.277 (10.9)
h_2 - m (in.)	.80 (31.5)	.795 (31.3)	.498 (19.6)	.498 (19.6)	.447 (17.6)	.98 (38.6)	.445 (17.5)
W_1 - m (in.)	.817 (32.2)	.894 (35.2)	.632 (24.9)	.632 (24.9)	.775 (30.5)	.75 (29.5)	.597 (23.5)
W_2 - m (in.)	2.81 (110.3)	2.79 (110.0)	1.83 (71.3)	1.83 (71.3)	1.72 (67.5)	3.34 (131.6)	1.67 (65.6)

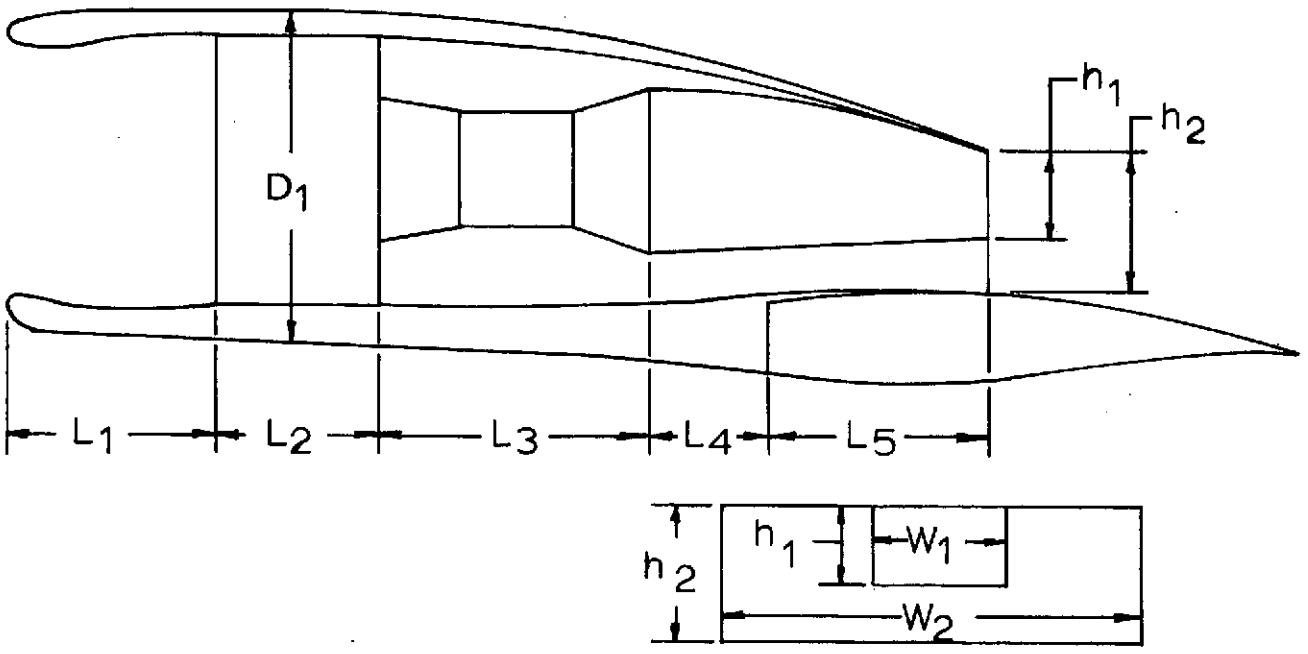

FIGURE 9: ESTIMATED OTW/IBF NACELLE DIMENSIONS

and cruise flight. This high lift system is unique in that, for terminal area operations, a portion of the fan exit flow is routed through the wing and out of the flap trailing edge to aid in the creation of the super-circulation flow field surrounding the wing. The remainder of the fan stream and the primary stream are directed through separate nozzles on the upper surface of the wing. For climb and cruise operation, the total fan exit flow and the primary flow are both exhausted through nozzles on the upper surface and are appropriate to more conventional bookkeeping techniques.

Terminal Area Bookkeeping - The bookkeeping procedures for the OTW/IBF propulsion system with its primary nozzle stream directed over and above the OTW nozzle stream and with a portion of the fan exhaust routed through the wing require special consideration. Since the lift aerodynamics of both segments of this hybrid system are expressed as functions of a gross thrust coefficient, the propulsion forces are divided into three components, i.e. IBF gross thrust, OTW gross thrust, and propulsion system drag. Terminal area installed propulsion performance is represented by the following forces, each of which is corrected for its appropriate installation losses.

- IBF Gross Thrust, OTW Gross Thrust - The IBF thrust and OTW thrust are derived solely from the installed fan gross thrust. The fan gross thrust has been degraded for inlet recovery loss, power extraction, exhaust pressure losses, and nozzle coefficients. The performance bookkeeping assumes that any fan exit flow not ducted through the IBF nozzle will be directed through the OTW nozzles, the IBF duct/flap/nozzle arrangement losses being the difference between the actual sum of the OTW/IBF components and the ideal sum of 100 percent.

- Propulsion System Drag - This item consists of the algebraic sum of the engine ram drag (degraded by the appropriate installation losses), the proper allowances for nacelle forebody, skin friction, afterbody boattail, base, and scrubbing drag, and the installed primary gross thrust. The primary stream acts in the opposite axial direction to the nacelle drag and the ram

drag. Since the primary thrust acts to negate the drag terms, proper accounting of these forces must be exercised to insure correct use of the drag characteristics which apply to this lift concept.

Figure 10 is an example of the terminal area data presentation used for a typical candidate engine installed in an OTW/IBF airplane. The nomenclature of Figure 10 is explained below:

F_S Installed static total thrust. This value is the total uninstalled engine thrust degraded for inlet pressure recovery, fan duct pressure losses, primary duct pressure losses, slot and primary nozzle characteristics, and power extraction.

F_{G_F} Installed fan gross thrust. This value is the uninstalled fan gross thrust degraded by those of the above installation items which affect the fan stream.

D_R Propulsion drag term. This value is the sum of the installed ram drag plus the external aerodynamic drag minus the installed primary gross thrust.

As discussed above, the terminal area operations call for a segment of the flow from the fan being routed through the IBF system. This aspect involves the additional installation penalty of the duct losses between the fan and the IBF slot. In a representative case, the pressure losses in the ducting between the engine fan discharge and the inlet to the IBF slot have been based on the assumption of a design maximum duct Mach number of the order of 0.3 and a design pressurehead loss of $\Delta P/q = 1.67$. Design analysis of the wing planform and duct arrangement selected for this particular OTW/IBF airplane indicated that the critical flow passage would occur in the region of the cross-ship ducting/wing box intersection. Adhering to the duct design parameters resulted in the performance loss characteristics shown on Figure 11. The performance bookkeeping methods used for this lifting system assume that any fan flow not ducted

SEA LEVEL, 35°C (95°F)

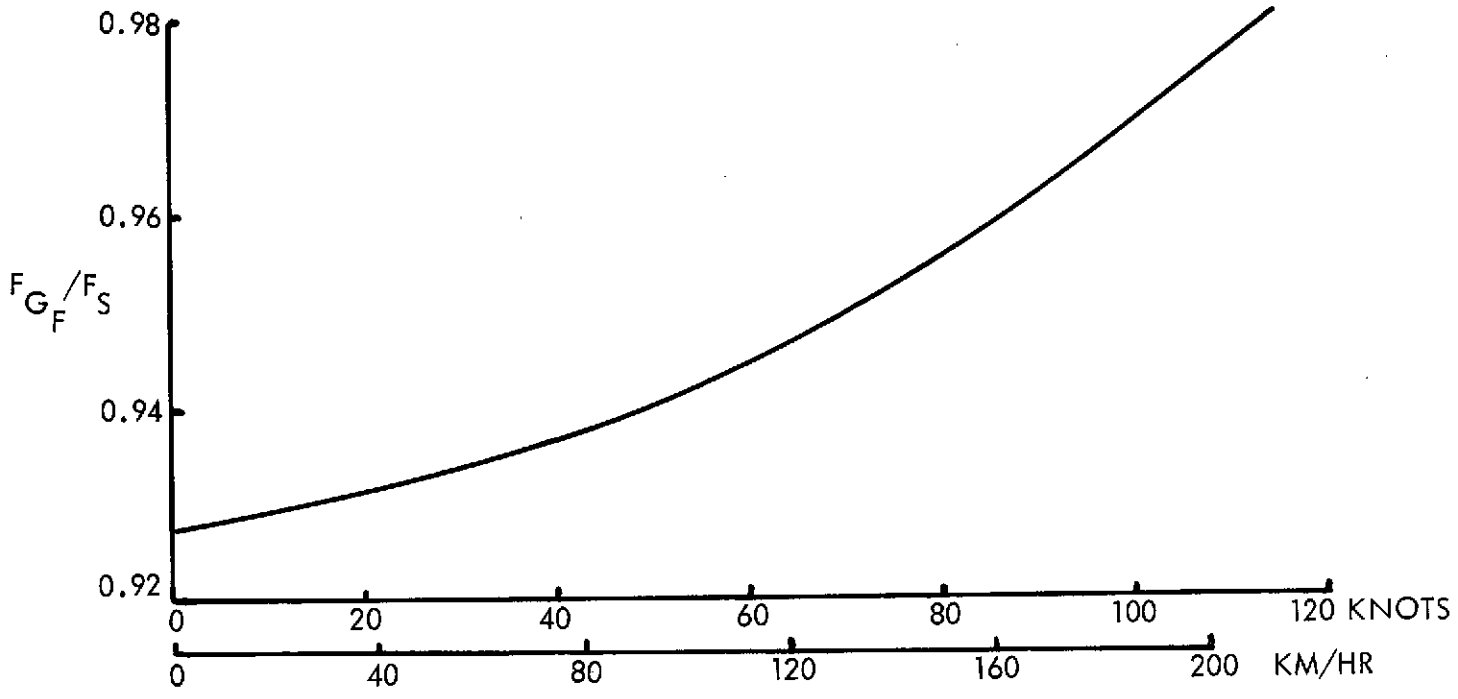

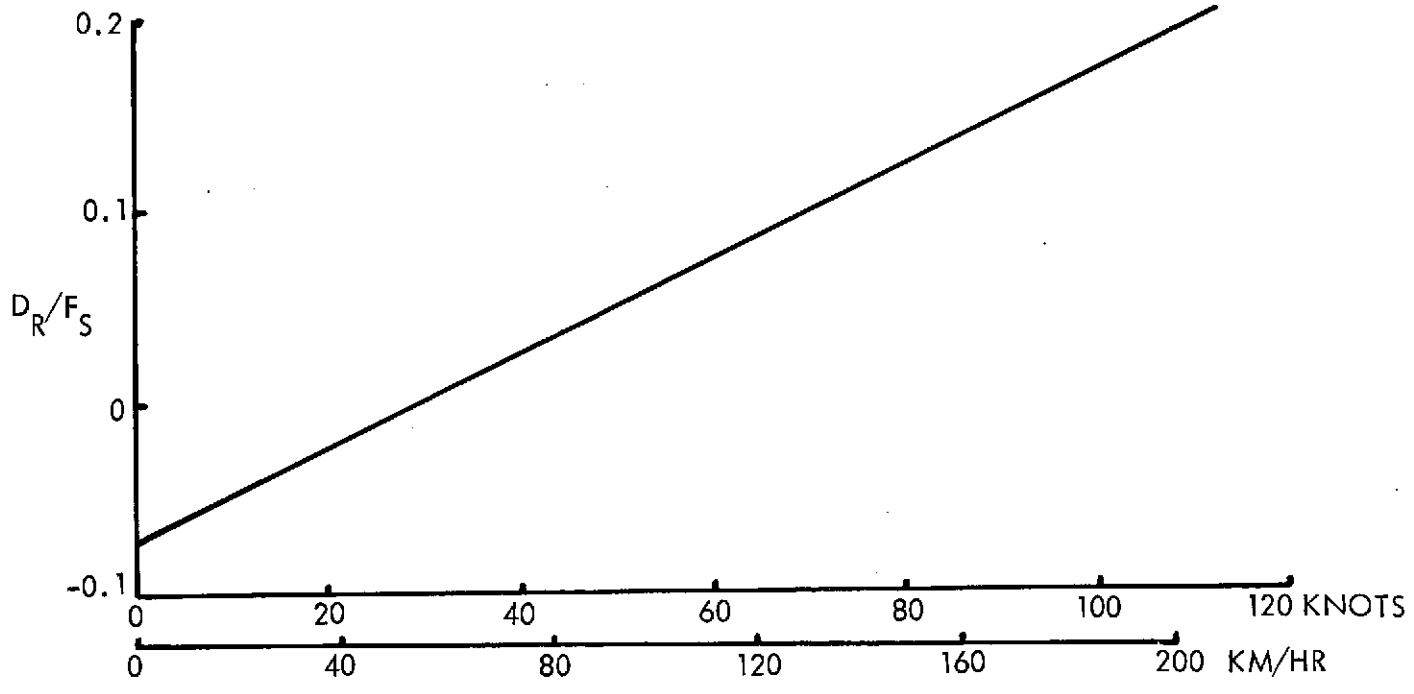

FIGURE 10: OTW/IBF ENGINE TERMINAL AREA DATA

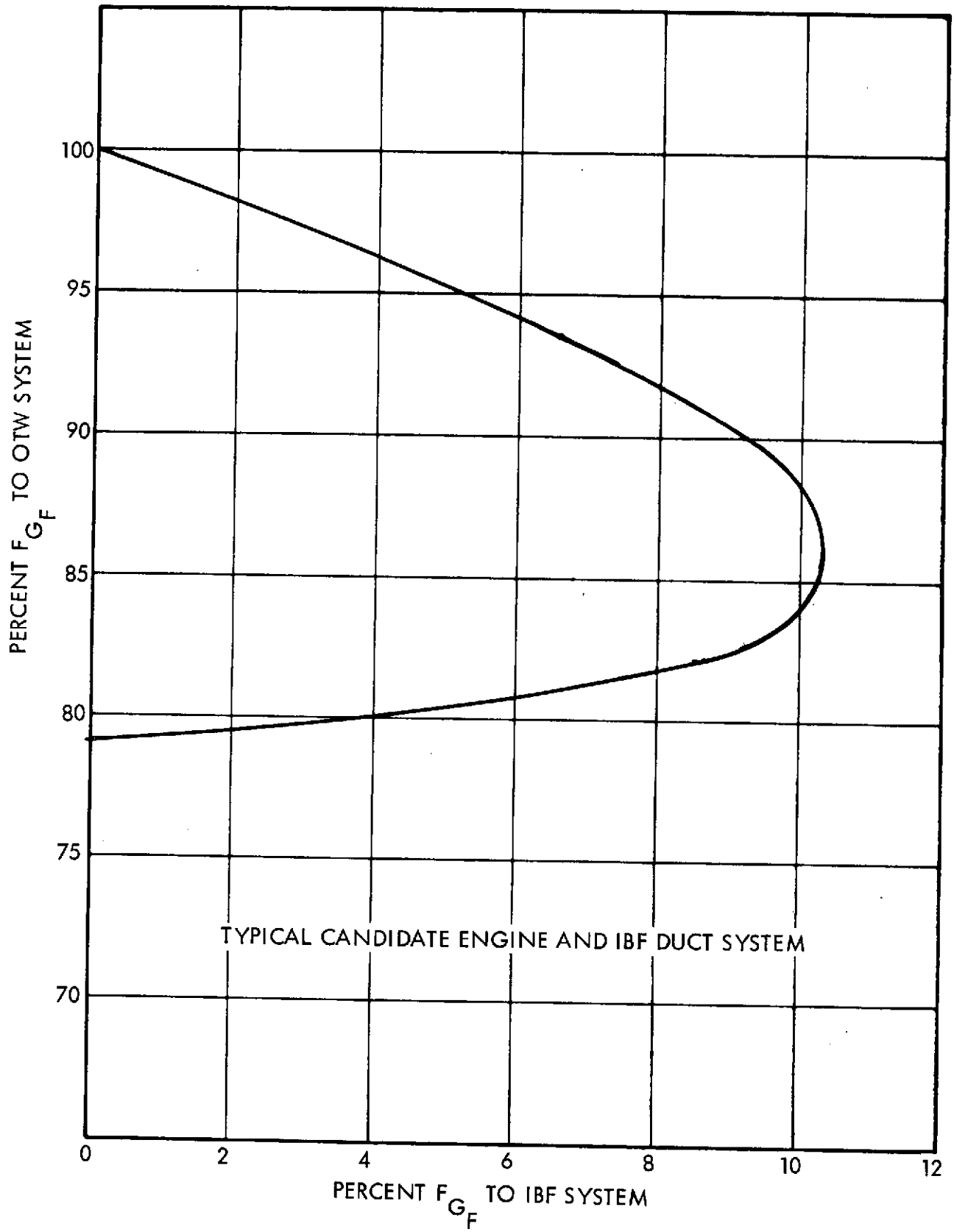

FIGURE 11: OTW/IBF THRUST SPLIT CHARACTERISTICS

through the IBF duct would be directed through the OTW nozzles; the difference between 100 percent and the sum of the IBF thrust and the OTW thrust is the duct system performance loss. More flow to the wing results in higher wing lift performance up to the point at which the wing critical flow area pressure losses begin to exceed the performance gain of additional wing flow. The optimum fan thrust split for the typical engine and airframe combination is shown to be approximately 10 percent to IBF, 88 percent to OTW with a 2 percent fan thrust loss. It must be recognized that the thrust loss characteristics such as are given by Figure 11 are used in conjunction with the terminal area data presented on Figure 10. Note that the F_{G_F} term in Figure 11 (when it is applied to this lift system) is split into an OTW component and an IBF component of which the IBF portion is the energy available to the IBF slot.

Cruise Bookkeeping - Conventional CTOL thrust/drag bookkeeping procedures have been employed for both climb and cruise data presentation in this study. Propulsion system net thrust and fuel flow values are presented on the basis of isolated nacelle forces acting on the top of the wing in the cruise configuration. Exhaust scrubbing drag on the upper surface of the wing and wing/nacelle interference drag terms are included in the airplane cruise aerodynamic drag polar. These nacelle forces include the basic performance of the engine, as determined from the engine manufacturer's data, degraded for inlet recovery losses, power extraction, exhaust duct pressure losses due to friction and acoustical material, and nozzle coefficients. In addition to their internal losses, the engine net thrust is further degraded for external isolated nacelle drag including forebody, afterbody, skin friction, and scrubbing drag to result in the net propulsive forces acting at the intersection of the nacelle and the upper surface of the wing.

4.2.4 Nacelle Inlet Design

The inlet alternatives included a standard length duct with wall treatment for sound suppression, and a blow-in door inlet configuration. External design considerations did not appear to impose any particular constraints on the internal inlet geometry -

preliminary calculations indicated that a 30% contraction internal lip could be employed without compromising the drag characteristics of the external nacelle. With this much contraction, very little performance advantage could be shown for a blow-in door inlet system. Noise levels are increased because available treatment area is reduced and because of the interruptions in the slot flow due to the inlet lip carry-through structure. Also, costs of developing and testing the standard inlet are significantly lower than for the blow-in door configuration. Thus, because of lower development cost and better noise reduction potential, a standard inlet duct was selected for this airplane.

Typical STOL operation necessitates adequate inlet performance at high angles of attack, which usually means a high contraction ratio inlet lip is required. Good cruise performance, however, is achieved with a slender nacelle of minimum frontal area. This requirement reduces the allowable cowl and lip thickness. Thus, the selected inlet must be a carefully chosen compromise between the conflicting low speed and cruise performance constraints. High total pressure recovery during static, low-speed, and high angle of attack operation is achieved for the configuration with a 30% contraction elliptical inlet lip, which has a length to height ratio of 2.0. As discussed in Reference 15 and shown in Figure 12 , the static lip loss coefficient is very low, closely approaching bellmouth performance. The 2:1 length to height ratio is an acceptable compromise between the requirements for low and high speed operation. Figure 13 illustrates how the lip performance improves with slenderness as the speed goes up and the mass flow ratio goes down. An inlet duct L/D of 0.5 would provide a low diffusion angle and allow for dissipation of lip induced turbulence before reaching the fan face. This inlet has been designed with no compromise for acoustic materials. However, acoustic materials are installed on the walls of the inlet when this treatment does not interfere with the internal aerodynamic lines.

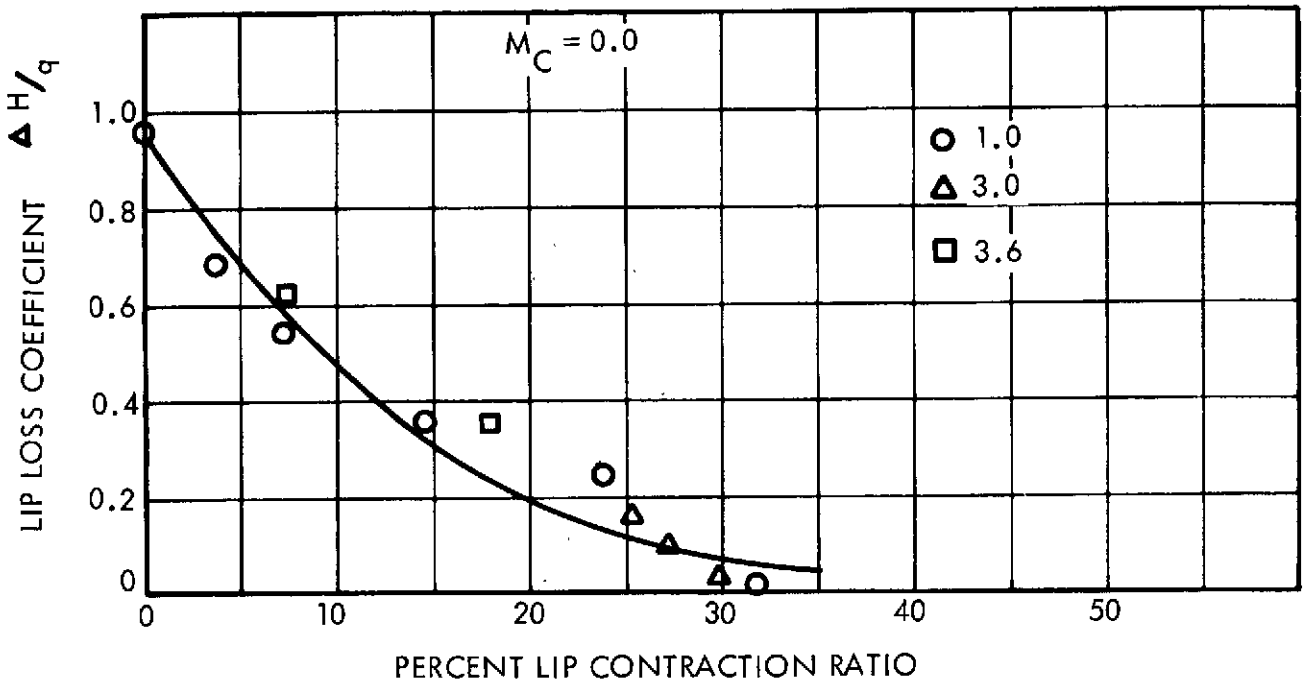

FIGURE 12: INLET LIP LOSS CHARACTERISTICS

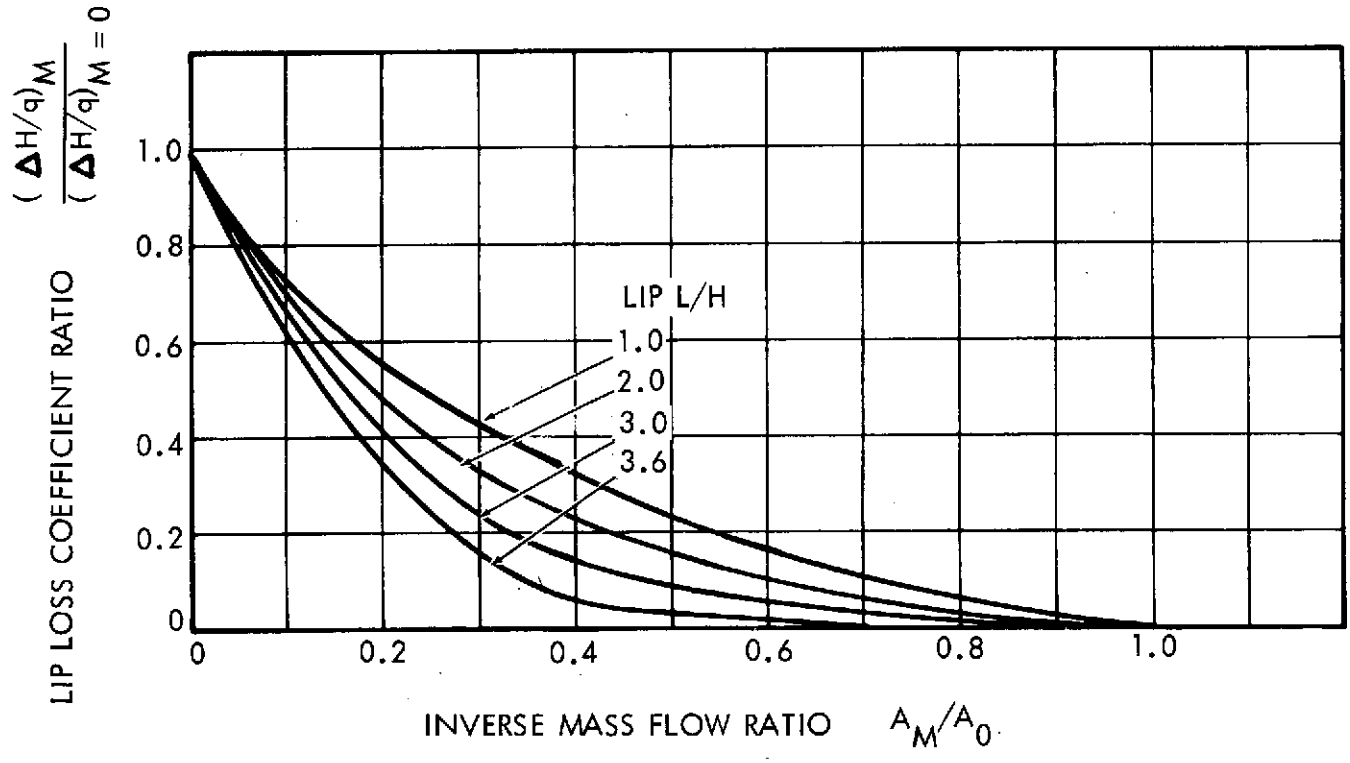

FIGURE 13: LIP LOSS CHARACTERISTICS AS A FUNCTION OF MASS FLOW RATIO

4.2.5 Thrust Reverser Design

As noted in reference 2 and reconfirmed in the course of the studies reported here, the use of reverse thrust to meet the stopping requirements of these airplanes can be avoided. The braking system designed for these aircraft will exceed the maximum allowable deceleration coefficient of 0.35g; thus, detailed reverse thrust performance data have not been required for the airplane sizing program. However, for all airplanes studied the weight penalty and the nacelle interfacing problems of installing a thrust reverser device have been recognized.

The OTW/IBF nacelle has been configured to include the thrust reverser in the aft section of the nacelle. Figure 7 shows a sketch of the reversing device which consists of an upward moveable panel and blocker door arrangement to reverse the OTW portion of the fan exhaust stream; the IBF fan stream and the primary stream are not affected. When used for high bypass engines, this reverser scheme should provide performance equivalent to present-day reversers and the up-flow aspects of the reversed stream should minimize exhaust ingestion and allow a relatively low cut-off velocity to be achieved.

Figure 7 has the upward moveable panel identified as the thrust reverser intake or exit. The 'exit' designation applies to the conventional thrust reverser as described in the above paragraph. The thrust reverse 'intake' is utilized for the variable pitch fan candidate engine nacelles. These engines depend on the reverse pitch of the fan blades and the resulting reversed airflow for the necessary retarding forces. Since the variable pitch fan engine accomplishes thrust reverse by this fan pitch reversal, the exhaust duct must pass the fan flow plus the core inlet airflow. This high flow requires an increase in both duct area and intake entrance at the panel, compared with the fixed pitch engine reversed thrust exit. These differences have been included in the weight penalties and nacelle configurations of the variable pitch engine used for the OTW/IBF airplanes. Again good reversal performance is expected since the entire fan flow of a high bypass engine is reversed with only the relatively small primary streams remaining in the forward direction. Very low reverser cut-off speeds should be achieved for the variable pitch OTW/IBF airplanes.

4.2.6 Coanda Jet Deflection

The principle of Coanda deflection of a jet stream over a curved surface as applied to the OTW-IBF concept is well known and has found practical application for BLC and lift augmentation on several operational aircraft. The mechanics of such systems have been relatively well documented and may be applied in a straightforward manner. These systems have employed relatively small quantities of high pressure ratio source air blowing through narrow, high aspect ratio slots over curved surfaces having large radii compared to the height of the slot. Basic data acquisition has generally been limited to such systems. The current application of the Coanda principle to powered high-lift system involving the deflection of the entire engine exhaust over the flap extends the range of variables well beyond those that have been established for BLC applications.

Two features of the system make it particularly attractive for quiet, short haul, short field length airplanes, but such airplane applications embody particular requirements that complicate the attainment of good Coanda performance. The location of the engine exhaust on top of the wing provides a degree of wing shielding of the jet noise, thus reducing the noise level and noise footprint areas on the ground. The induced supercirculation lift and vectored thrust of the system provide powered lift augmentation that is particularly attractive for short field lengths. These airplane requirements, however, dictate that to achieve the short field lengths, higher airplane thrust to weight ratios are required compared to CTOL applications. As shown elsewhere in this report, relatively low jet velocities, hence low fan pressure ratios, are required to meet the low noise criteria. These two considerations serve to dictate a large volume of flow at low pressure ratio, a combination that is well outside the classic data base for Coanda turning. Aerodynamic and propulsive performance considerations inhibit the spreading of the jet efflux across the flap by means of a very narrow slot nozzle. The high bypass engines involved are large relative to the wing by CTOL standards and appreciable fishtailing of the engine exhaust would obscure a large portion of the wing upper surface. Fishtailing the nozzle is further complicated by the requirement for an increased fan nozzle area at low Mach number conditions. This requirement is typical of the advanced technology engines appropriate for the OTW-IBF airplanes. The thrust coefficients of such a nozzle would

be low and, at the low fan pressure ratios, would result in a prohibitive net thrust and SFC penalty at the airplane cruise condition. The impact of the fishtail nozzle on the wing cruise characteristics would also impose a prohibitive penalty and the scrubbing drag of the engine efflux over the wing surface would be excessive. For these reasons, a nozzle aspect ratio of the order of four to one approximates the upper practical limitation for fishtailing the nozzle. This results in a nacelle of nearly constant width with most or all of the nozzle convergence accomplished by the upper and lower nozzle contours. Recognizing these constraints produces a nozzle exit height (h) in the order of 30 percent to 100 percent of the flap radius (r) of curvature. The classic work by Poisson-Quinton in Reference 16 is limited to h/r values of the order of 10 percent, well below the practical values for the OTW-IBF configuration. Also, the slot pressure ratios of this reference are generally of the order of 2 to 3, which are not representative of the low pressure ratios required for the OTW-IBF engine exhaust because of the noise limitations. Reference 16 is generally typical of the basic Coanda work accomplished prior to 1970. There were a number of OTW tests performed prior to 1970 that serve to demonstrate the potential of this aspect of the hybrid concept but do not observe the geometric limitations imposed by an operational installation. In much of this work, the simulation of propulsive forces has fallen short of the airplane T/W requirements for short field operation or has achieved the T/W by utilizing pressure ratios in excess of the limits imposed by airplane noise considerations.

Much of the work carried out since 1970 has been oriented to more appropriate geometries and thrust parameters but has been highly configuration oriented. It has provided much in the way of trends and variation in concepts but has provided relatively little in the way of basic parametric design data that may be applied directly to configurations at significant variance from those tested.

From the work of reference 16 and others, Coanda turning sensitivity to the ratio of stream height to surface radius (h/r) and to slot pressure ratio may be inferred and extrapolated into the range of current interest. Figure 14 illustrates the relative interaction between these parameters as a basic criterion for attached flow. This

$$\frac{P_T}{P_0} = \frac{1.4}{\left(\frac{h}{r}\right)^{0.333}}$$

STATIC CONDITIONS ($q_\infty = 0$)

O TEST POINTS FOR CYLINDER ONLY. ANGLES NOTED INDICATE SEPARATION.

X TEST POINT FOR CYLINDER FOLLOWED BY FLAT PLATE. FLAT PLATE WAS LIMITED TO 67° WHICH REMAINED ATTACHED FOR ALL CONDITIONS TESTED.

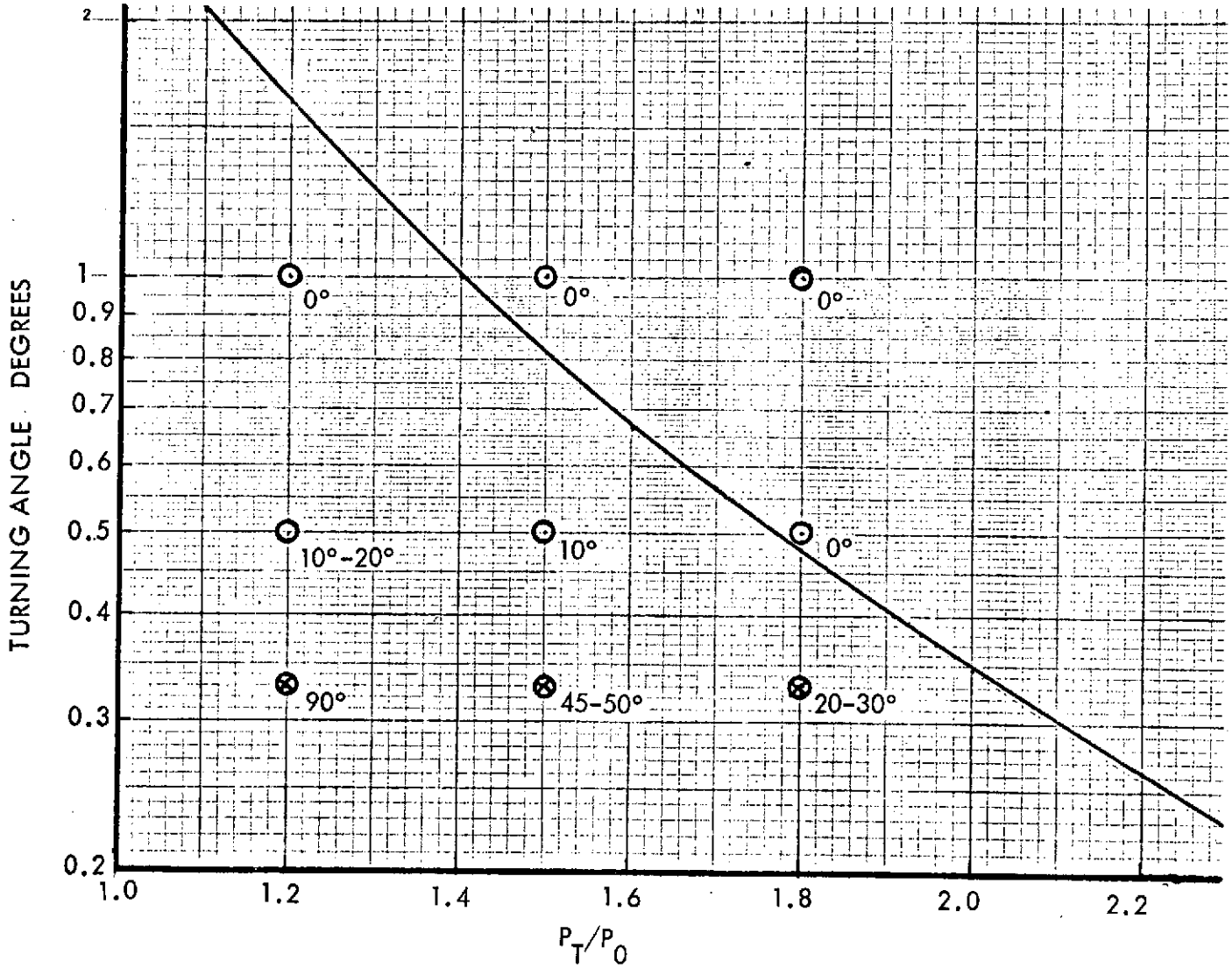

FIGURE 14: POISSON - QUINTON & LOWERY COANDA PERFORMANCE

extrapolation has not been definitively verified in the literature, reflects some geometry constraints and lacks dynamic influences. The importance of attached flow is self evident, and as illustrated in Reference 17 where the vertical component of the Coanda vectored thrust accounts for one-third to one-half of the ΔC_L for the system. It is evident that the ΔC_L resulting from super circulation is also dependent on attached flow over the Coanda surface. Thus, the criterion for achieving and maintaining attached flow is a prime consideration in achieving the desired C_L benefits.

The data reflected in Figure 14 represent an extrapolation of data generated for BLC type applications wherein the Coanda curved surface is followed by a flat or nearly flat surface that is large relative to the dimensions of the Coanda curved surface. If the h/r limitations imposed by Figure 14 are applied to realistic OTW configurations of wing and engine exhaust geometry, it is observed that the combination of desired turning, allowable flap chords and required flap radius leaves little or no opportunity for a flat surface to be incorporated on the flap upper surface. The absence of a flat surface would not provide an opportunity for the attached flow to stabilize prior to the trailing edge and would indicate a low surface pressure at the trailing edge to balance the centrifugal forces created by the continuously turning stream. This condition would invite separation at the trailing edge which would move forward along the flap until equilibrium between the surface pressures, centrifugal forces and entrainment of secondary air in the separated region is achieved. This hypothesis leads to the conclusion that h/r alone is not an adequate criterion if a flat surface is present. This is borne out by Reference 17 which data are presented reflecting the effect of a 60 percent increase in radius combined with elimination of the flat surface. In these data, the smaller radius with the flat surface reflected superior turning capability. This leads to the conclusion that the extrapolation of Figure 14 is likely to be optimistic since it was extrapolated from data acquired with configurations having a large flat surface.

The effect of dynamic flow fields on the Coanda turning stream are not likely to exert a significant influence on the data from which Figure 14 was extrapolated since the slot pressure ratios were generally quite high and the freestream q_∞ of interest is

quite small. It is, however, apparent that as the jet stream pressure ratio is reduced, the freestream q_∞ will exert an increasing influence on the Coanda attachment. Since the freestream represents a very large h/r, albeit at a low q, its influence on limiting attachment will be detrimental although the flap surface incremental pressure (hence ΔC_L and ΔC_D) will be larger in the attached area. This effect is evident in Reference 17 and 18. Again, the characteristics in Figure 14 are likely to be optimistic.

While numerous sources in the literature address these influences, limitations of test facilities or basic configurations have precluded a comprehensive parametric survey of these influences. In 1972, Lockheed completed a two dimensional test program that was oriented towards a parametric definition of some of these influences. The basic test rig permitted variation of h/r over a range from 0.16 to 2.0 at slot pressure ratios from 1.2 to 2.4 with freestream q values from 0 to 967 $N/m.^2$ (20.0 psf_a). Although the capability of the rig extended beyond these limits, they were considered adequate for the particular field of interest. The rig did not permit measurement of the forces acting on the system because of the physical coupling between the freestream nozzle and the slot nozzle. Consequently, the primary measure of the configurations was the pressure at the Coanda surface. This provided pressure coefficients and separation angles for the system. The plane of the slot nozzle was geometrically located on a radius of the curved surface with the discharge tangent to the surface.

Figure 15 presents the separation angle derived from the foregoing test data for the zero freestream case. This curve appears conservative relative to some of the data that have been generated in recent years but two influences tend to produce this effect. In much of the recent testing, the nozzle has been located well forward on the wing chord and vectored downward to the wing in such a manner that the engine exhaust flow can spread and entrain air, thus thinning and reducing the jet dynamic head or effective pressure ratio. In some cases, spreading deflectors have been installed to enhance this effect. In these cases, the true stream heights have not generally been measured so the h/r and effective jet dynamic head at the beginning of the Coanda

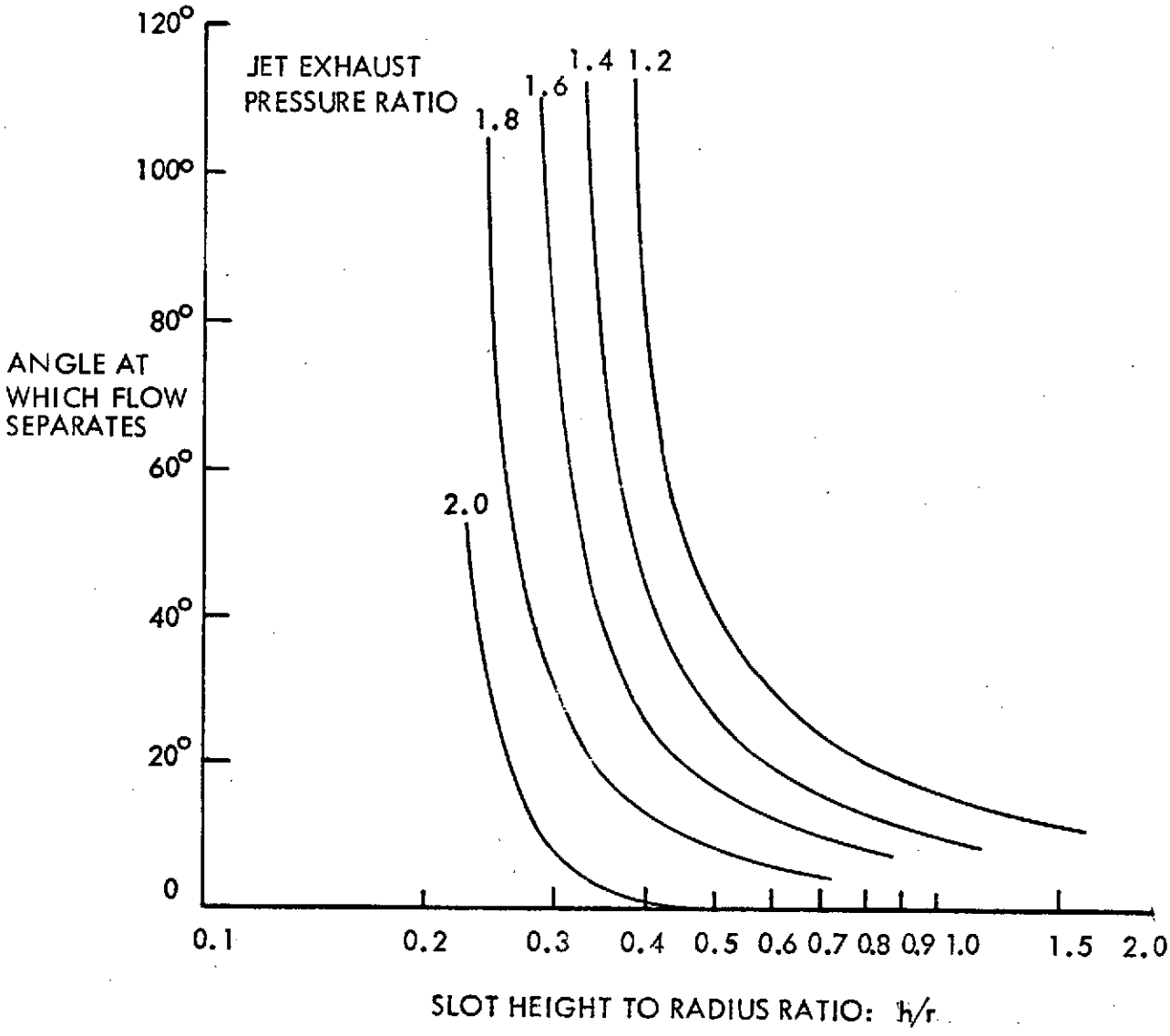

STATIC RESULTS

FIGURE 15: PLAIN COANDA TEST

surface are not known. A general concentration of the higher velocities in the jet stream near the flap, accompanied by a thickening of the lower velocity stream and a significant reduction in the effective jet dynamic head are indicated at the flap trailing edge in Reference 19. The second influence is the absence of a flat surface following the cylindrical turn. The fact that the separation point on the cylinder is free to move continuously without the influence of a fixed flat surface provides a true measure of the Coanda characteristics and is probably representative of what may be expected of a flap configured without a flat surface. The basic characteristics of Figure 15 have been empirically reduced to an equation for the separation angle (θ) that is a relatively simple function of the square of the slot pressure ratio and the natural antilog of a simple h/r function suggesting that these are the basic parameters governing the characteristics. The data available permit further refinement of this conclusion which is currently underway. A significant conclusion to be drawn is that test data acquired at ultra low pressure ratios or jet dynamic pressures are likely to be extremely optimistic.

Similar data were obtained for freestream q_{∞} values of 483 and 967 N/m.^{2} (10 and 20 psf$_a$). These data reflected a significant reduction in the attachment angle as a function of the freestream q_{∞} , the slot pressure ratio, and the h/r of the nozzle. As expected, this effect diminished dramatrically as slot pressure ratio increased. It was found that the data for the three freestream cases tested collapsed to the form shown in Figure 15 as a function of $q^{0.321}$ (freestream). Further reduction of this expression resulted in a natural logarithmic function of jet stream dynamic head (q_j) and a natural anti-log function of h/r, again suggesting that these are the significant parameters. The influence of function $q^{0.321}$ indicates that as the freestream q initially increases from 0, the attachment angle decreases rapidly but as q_{∞} continues to increase it is accompanied by diminishing changes in attachment angle. As expected, the low slot pressure ratios are the most dramatically influenced by the freestream q but is is interesting to note that the higher h/r configurations are influenced to a significantly lesser extent.

A very limited test exploration was undertaken of the installation of a flat plate having a chord of approximately 4 r tangent to the cylindrical surface at 30°, 60° and 67°

angles. The h/r for this test was 0.33. The results from this testing indicated that at static freestream conditions, and at all slot pressure ratios including 1.8, the flow attached for all three flat plate angles. This represented an increase in attachment angle for the 1.8 slot pressure ratio from 22° for the cylinder to at least 67° for the configuration with the flat surface. When the freestream q_∞ was increased to 967 $N/m.^2$ (20 psf_a), the slot flow remained attached to the flap indicating an increase in turning capability for the flat surface from 16° to 67°. The ΔP of the Coanda surface increased by more than 20 percent as a result of this freestream dynamic head. Since the test configuration was not capable of simulating supercirculation effects, this cannot be readily translated into ΔC_L and, ΔC_D effects but the influence is apparent. From a practical airplane geometry standpoint, the chord of the flat surface was much too large but inspection of the surface pressure data indicated that the pressure gradient across the slot efflux stabilized almost immediately at the transition to the flat surface encouraging the possibility that a short flat surface might be adequate. The potential of the combination of a reduced flap radius (increased h/r) followed by a short flat surface under the circumstance of a limited flap chord would indicate significant optimization possibilities. Further testing of these variables is needed.

Using the limited data obtained with the flat plate installed at the q_∞ = 967 $N/m.^2$ (20 psf_a) condition, the upper limit of the 1.8 nozzle pressure ratio condition at h/r = 0.33 was taken as the most adverse condition that remained attached with the 67° flat plate. This reference angle was increased by the amount indicated in Figure 16 for these conditions in order to translate these dyanmic data back to a static case. The empirical expression for the static separation angle discussed earlier was then modified to agree with these data and Figure 17 was derived to represent the static attachment limits for the 4 r flat surface. Turning angles for three values of h/r and for 1.5 nozzle pressure ratio in a Lockheed-Georgia test conducted on a full span, twin engine configuration have been superimposed on this figure. These data were obtained with 0° flap having a 1.75 r flat surface and with the nozzle discharge at approximately 35% chord. The characteristics of the derived curve are seen to be slightly optimistic compared with these points but agreement is relatively good.

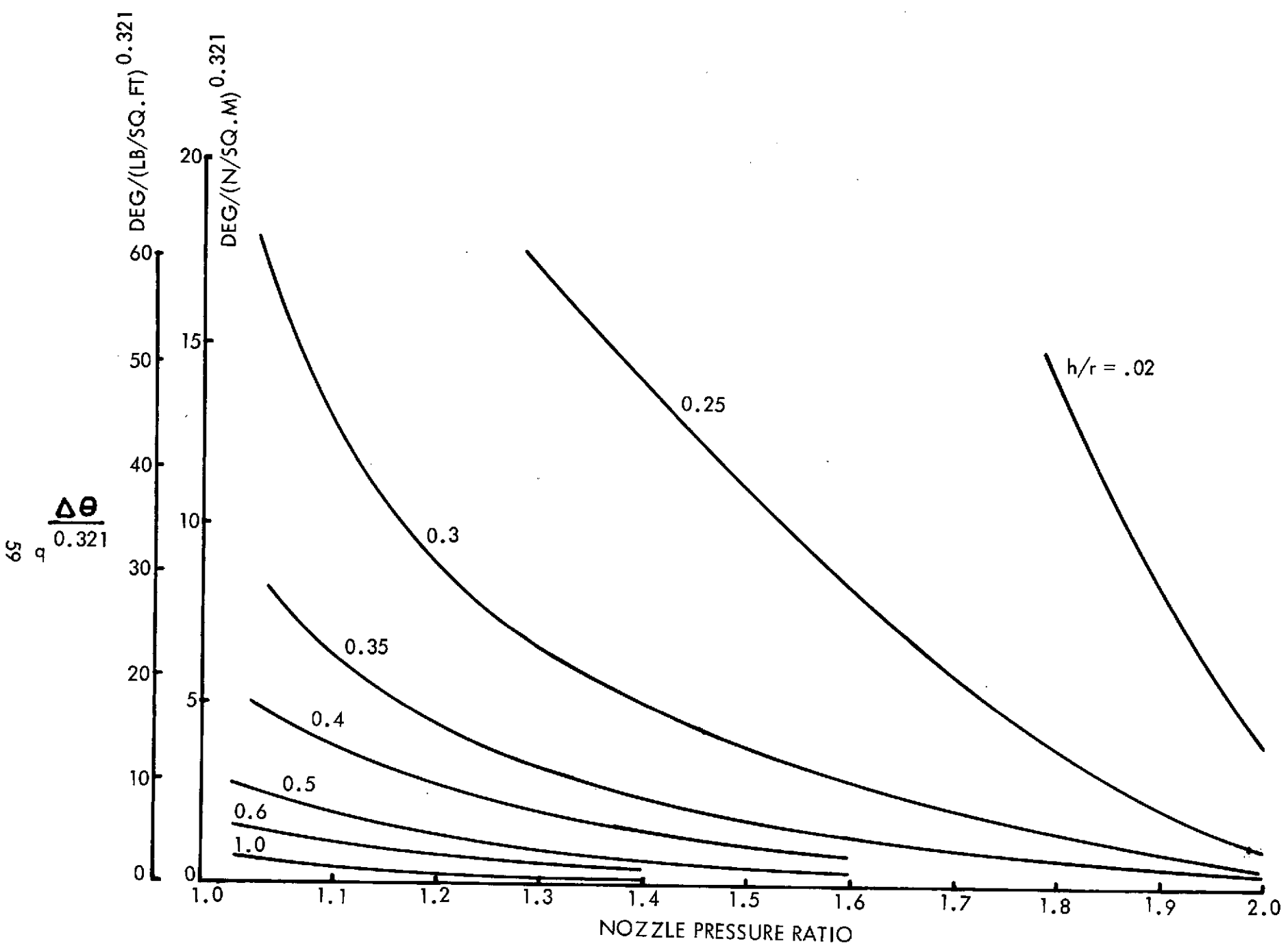

FIGURE 16: FREESTREAM DYNAMIC EFFECTS ON COANDA TURNING

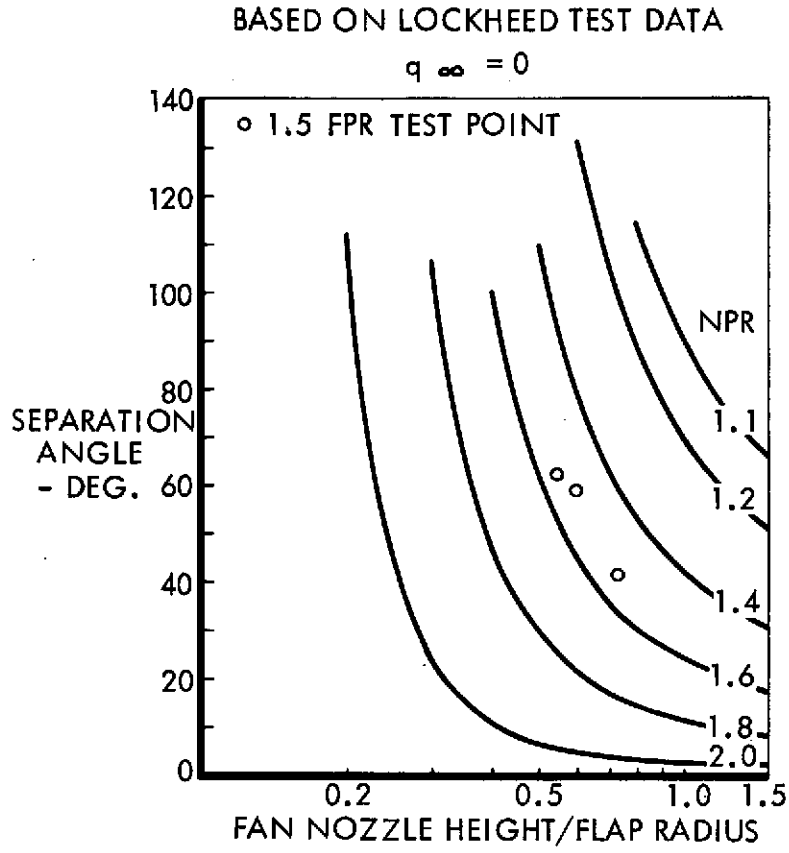

FIGURE 17: STATIC COANDA TURNING (CYLINDER + FLAT PLATE)

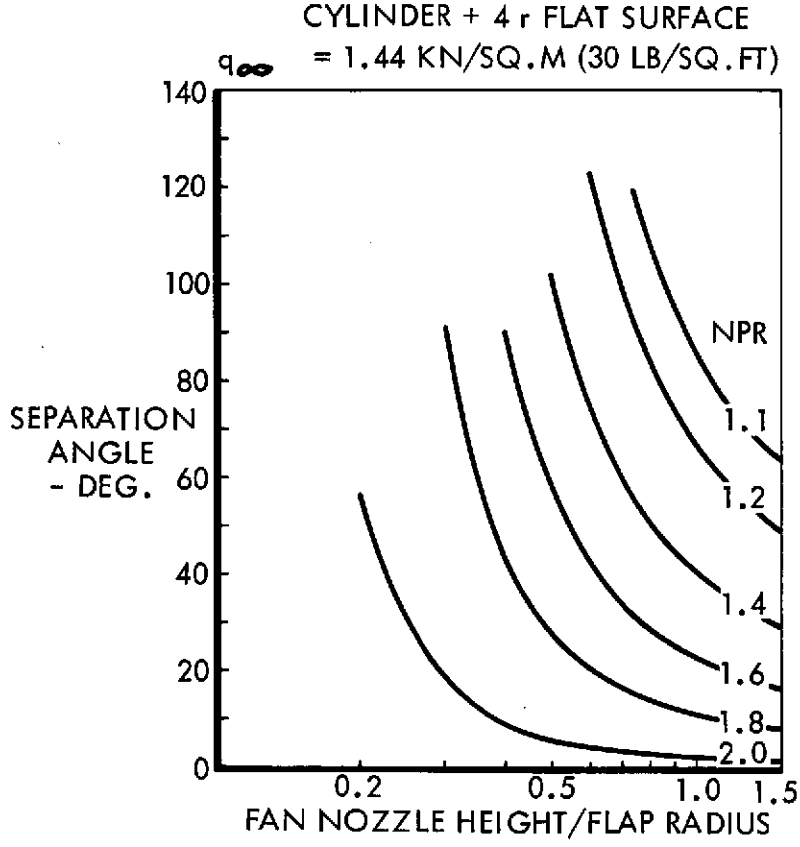

FIGURE 18: DYNAMIC COANDA TURNING (CYLINDER + FLAT PLATE)

The data of Figure 17 were then modified for a dynamic q_∞ of 1450 N/m.^{2} (30 psf_a). This condition represents a typical take-off and landing condition where the high-lift characteristics of the OTW-IBF configuration would be most beneficial. These data are presented in Figure 18. This curve presents a reasonable design criterion for OTW attached flow conditions.

Much of the testing performed in recent years has indicated considerable variation of the attachment characteristics with basically similar test configurations. The foregoing presents a rationale for the basic parametric variables but there are many others which may be introduced by each specific configuration. These are currently difficult (if not impossible) to correlate. Numerous tests have shown that significant improvements of a given configuration may often be achieved by minor changes and Figure 18 intended to represent the characteristics which should ultimately be achievable in practice by development of any given configuration.

A basic concern in the OTW-IBF concept is the effect of a gust on flow attachment to the Coanda surface. In the testing of the cylindrical surface previously described, the separation point was not influenced by a hard geometric limit such as a flat plate and therefore represented a "pure" Coanda turning limitation. As noted, the addition of the flat plate resulted in a marked increase in the turning capabilities of the configuration. However, whereas the turning capability of the cylindrical surface rapidly diminished with increasing q_∞, that of the flat plate and cylinder combination was unchanged over a limited range of q_∞. This suggests that a surface embodying a flat element might have a dramatic hysteresis effect with variation of freestream q With the cylindrical surface, 80 percent of the decrease in attachment angle had been experienced by the time q_∞ reached 483 N/m.^{2} (10 psf_a). Employing the $q_\infty^{0.321}$ normalizing parameter to derive a further increase in q_∞ to 1450 N/m.^{2} (30 psf_a) implies a reduction in attachment angle 10 percent greater than that encountered at 967 N/m.^{2} (20 psf_a). This indicates that if the system were selected to provide but a margin at the design condition it would be adequate to meet gust conditions. This conclusion is only applicable to cylindrical surface flaps, however, in which the point

of separation is free to move to any point on the curved surface. In the cases with the flat plate extension once the flow over the flat element has separated, the point of separation would in all likelihood revert to that associated with the cylindrical surface and as was seen in the test case for slot nozzle pressure ratio of 1.8 this angle could be as much as 30° to 40° less than the original jet deflection.

Once a separation of this magnitude has occurred, it is questionable whether the flow will re-attach to the flat surface. The probability of this occurring with a short chord flat plate is particularly evident since the flap system would be more likely to continue to behave as a cylindrical surface. Unfortunately, this aspect was not explored in Lockheed-Georgia testing of basic Coanda configurations; however, numerous tests with complete airplane configurations have failed to reveal any evidence of hysteresis with flat plates of the order of 1.75 r. The three test points superimposed on Figure 18 specifically tested to determine any hysteresis and none was evident under the most adverse conditions. It is therefore concluded that while hysteresis may exist with extremely short chord flat surfaces, hysteresis will present no problem with moderate length flat surface chords.

4.2.7 Exhaust Nozzle Design

The exhaust system of the OTW-IBF engines is required to provide a number of unique functions while conforming with several equally unique design constraints. Integration of these requirements pose difficult design problems, a number of which are not fully resolved in an optimized fashion and indeed cannot be fully resolved without the aid of specific, configuration-oriented testing. The system designed for this study is considered to be a workable configuration and the performance characteristics and weight of the system are considered achievable although, in practice, some further optimization of the design would be required. The basic constraints of the configuration include:

- Vertical engine removal
- Minimum scrubbing of exhaust on wing surface in cruise
- Minimum afterbody drag in cruise

- o Low interference drag
- o Separate primary nozzle (Required for the PD287-11 engine specifically)
- o Structural feasibility

The specific functions required of the nacelle configuration include:

- o Spread, thinned exhaust flow over the wing/flap upper surface
- o High capacity, high recovery fan bleed extraction capability for the IBF system (approximately 15% of fan flow)
- o Variable effective fan exit area to maintain engine match
- o Reversed thrust capability

While the design constraints largely address the location of the engine relative to the wing and fuselage and relate to the nacelle in general, they do provide guidance to the envelope into which the exhaust system must be configured. The requirement for vertical removal of the engine dictates that as a minimum, the aft-most projection of the engine must be located forward of the front wing spar such that the engine can be lowered past the spar with no structural interference. This defines the aft most location of the entrance to the fan and primary exhaust systems. The requirement for minimum scrubbing of the exhaust efflux on the wing surface in cruise is in conflict with the functional requirement of the high lift system for a relatively thin spread efflux over the wing and flap system. At first consideration of this factor, it might appear that the low fan pressure ratios utilized in the OTW/IBF system would produce low velocities and consequently low scrubbing drag losses. However, the high ram recoveries associated with cruise speed coupled with actual cruise fan pressure ratios produce nozzle pressure ratios sufficient to generate exhaust velocities well into the sonic region. Additional consideration of the reduced static pressure field on the wing upper surface has the effect of further increases to these pressure ratios and consequent velocities. Figure 19 presents a spectrum of exhaust velocities relative to nominal engine fan pressure ratios and flight Mach numbers. This figure includes allowance for the cruise requirements and lapse characteristics of actual engines and also includes the effect of the lower static pressures on the wing upper surface. It will be observed that the fan

FULLY EXPANDED EXHAUST AT CRUISE CONDITIONS

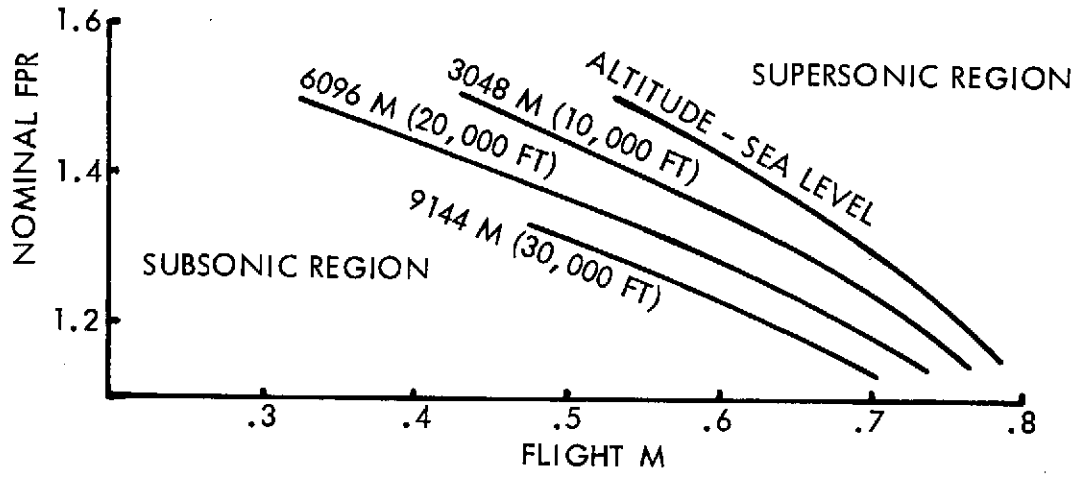

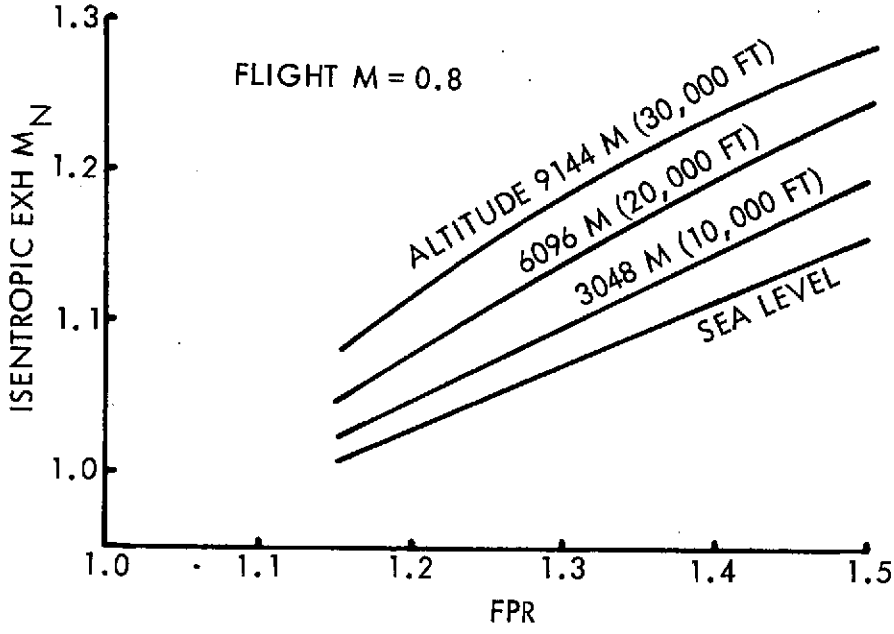

FIGURE 19: OTW ENGINE EXHAUST MACH NO.

exhaust flow in all cases which represent the study airplanes will be in the low supersonic region with attendant high scrubbing drag and shock losses. This condition is not unique to the OTW-IBF configuration since the same condition exists in many conventional under-wing CTOL engine installations having a short fan cowl. In these latter cases, a trade-off is made between the scrubbing drag of the fan exhaust over the core cowl versus the freestream friction drag of a longer fan cowl. In the OTW-IBF configuration, the impetus to achieve good high lift performance must be weighed against the cruise drag. The only degree of freedom available to reduce the scrubbing drag in the OTW-IBF configuration is to reduce the scrubbed area by locating the nozzle well aft or limiting the exhaust spanwise spread. As indicated in Figure 20 which presents the measured effect of various chordwise nozzle locations upon the high lift characteristics of an OTW-IBF vehicle, moving the nozzle aft from 45% to 60% chord only degrades $C_{L\ MAX}$ by 2%. An alternative solution that is perhaps worthy of further consideration is to provide a freestream flow sheet under the fan exhaust at cruise conditions. No useful data for such a configuration are available and the advantages are undefined but it would add to the complexity and structural problems associated with the system.

The large diameter of the engine combined with the thinned fan exhaust leads to a large aft facing surface on the top of the nacelle. Various layouts of the OTW-IBF system have shown that care must be taken to avoid an excessive afterbody angle on this surface. If this surface should separate in cruise, the associated drag would be prohibitive. The problem is aggrevated by lower fan pressure ratio engines and their attendant large diameters. It is apparent that the afterbody is significantly improved by locating the engine as low relative to the wing as is practical from exhaust duct, structural and other considerations. The choice of engine vertical location is thus largely a compromise between the exhaust duct constraints involved in passing the fan flow up and over the forward wing spar and the minimization of the aft facing surface of the top of the nacelle.

EFFECT OF U_{10}^{4} DEFLECTOR AT VARIOUS CHORDWISE LOCATIONS OF NACELLE EXIT ON LIFT AT 60° FLAPS, $C_T = 2.0$

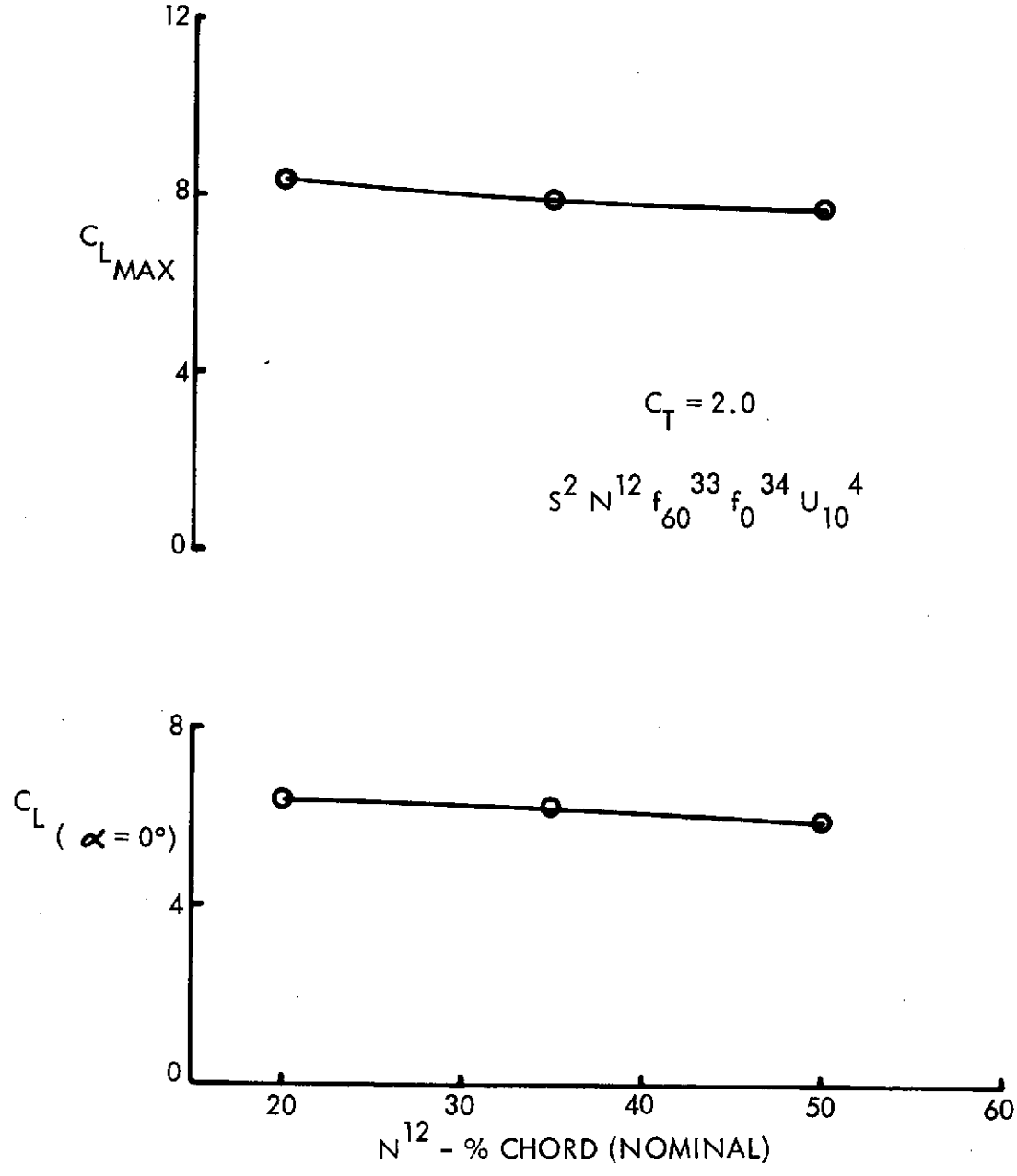

FIGURE 20: EFFECT OF NOZZLE LOCATION ON OTW LIFT

Basic interference drag considerations have little influence on the exhaust system since the primary degree of freedom to alleviate this drag is spanwise location. The benefits accruing to a two-engine airplane to locate the engines as close to the fuselage as possible to minimize engine out problems can present an impact on the exhaust system. If the engines are located too close to the fuselage, the exhaust flow may impinge on the fuselage in the cruise and/or the high lift modes. This is unacceptable and may be relieved by canting the nozzle outward although locating the engine farther from the fuselage appears to be a more desirable solution. Discrete interference problems with the nozzle exhaust flow may be in evidence at cruise but there presently appears to be no systematic design criteria to avoid these interferences. There is evidence that such problems may be resolved by specific tailoring of the exhaust system through on iterative test program.

4.3 OTW-IBF AERODYNAMIC DATA

4.3.1 High Speed Data

The high speed aerodynamic data used for sizing of all configurations and for performance computation have been estimated using proven subsonic and transonic lift and drag estimation techniques. These techniques have been validated by correlation with wind tunnel test data as indicated by Figure 21 taken from a previous systems study in which high speed wind tunnel test data was available for correlation purposes.

The high speed drag calculation method uses the incremental drag build-up method summarized in Figure 22 for both parametric and final performance drag calculations. ΔC_{D_P}, $\Delta C_{D_{COMP}}$, $\Delta C_{D_{INT}}$ and $\Delta C_{D_{TRIM}}$ values from available tests permit build-up of the alternate configurations studied. The steps involved in the standardized configuration build-up method are:

(1) The zero-lift drag of each component, C_{D_O}, is estimated by considering skin friction drag, with appropriate form factors, at the flight Reynolds number. C_{D_O} calculations have been generalized from existing Lockheed and NASA tests on various types of configurations.

(2) A generalized change in wing profile drag, ΔC_{D_P}, is applied which is a function of departure from design values of either Mach number or lift coefficient.

(3) A drag increment at the design C_L level, $\Delta C_D (C_{L_{DES}})$, is applied as a function of design lift coefficient to account for the basic adverse supervelocity effects of camber on parasite drag. This increment is computed from:

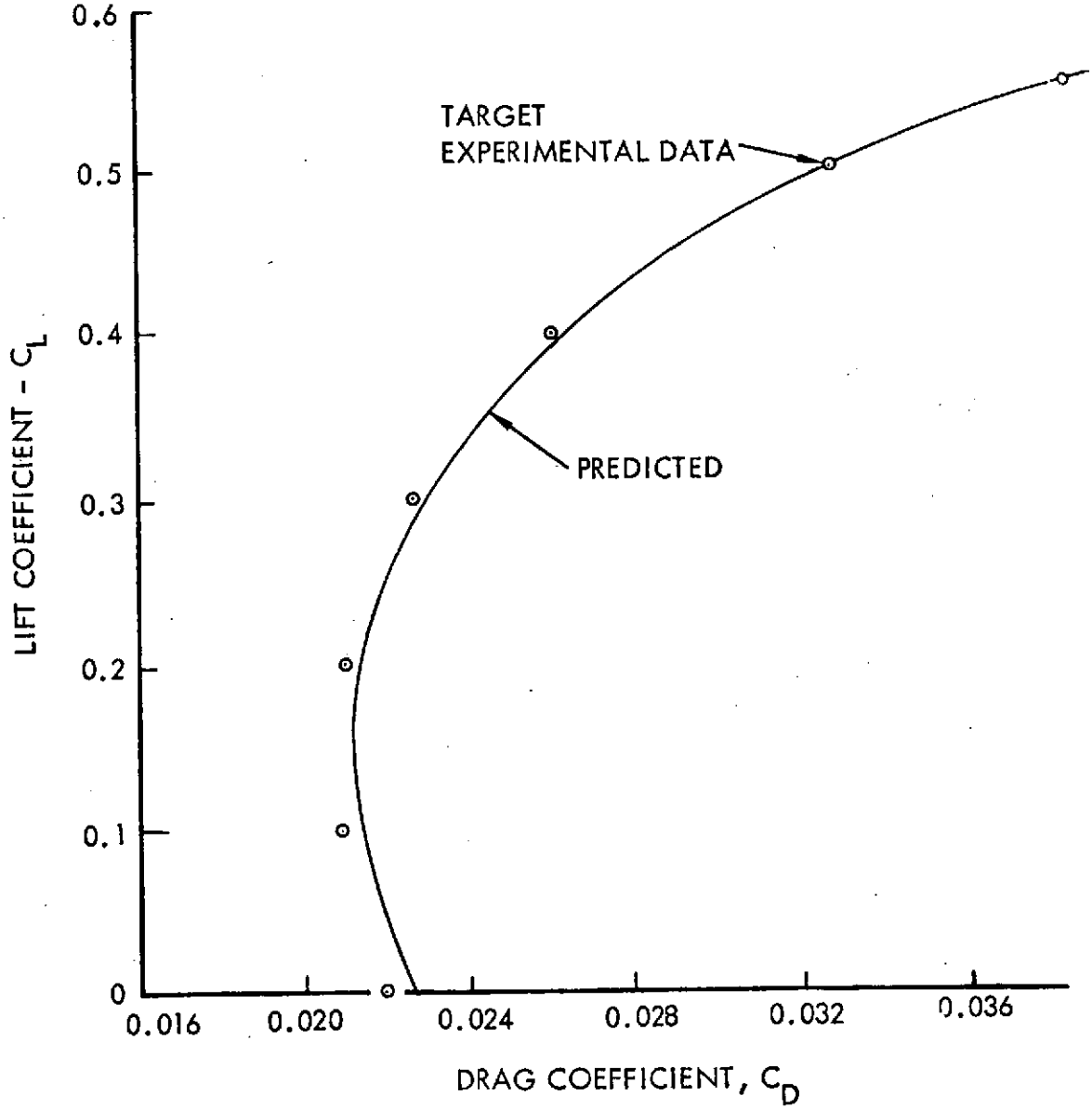

FIGURE 21: TYPICAL DRAG CORRELATION

$$C_D = C_{D_o} + \Delta C_{D_P} + \Delta C_{D_{C_{L\,(DES)}}} + \Delta C_{D_{COMP}} + \Delta C_{D_i} + \Delta C_{D_{INTERF}} + \Delta C_{D_{MISC}} + \Delta C_{D_{ROUGH}} + \Delta C_{D_{TRIM}}$$

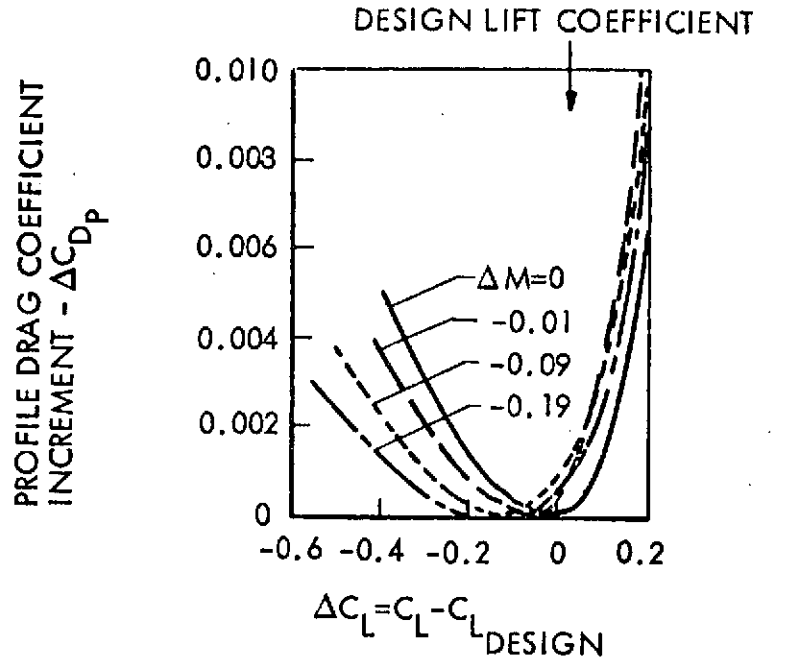

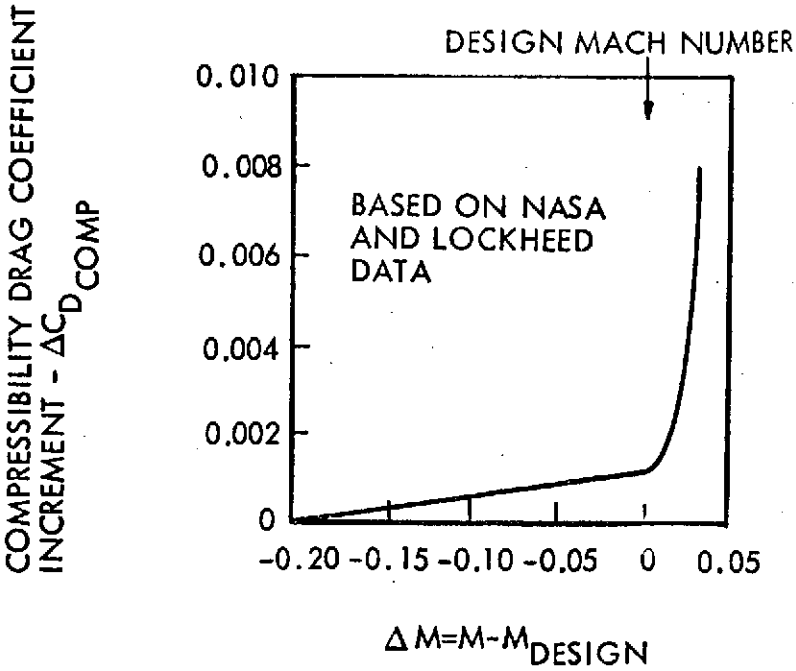

FIGURE 22: DRAG BUILDUP METHOD

$$C_D(C_{L_{DES}}) = 30\ (t/c + C_{L_{DES/5}})^4 + (t/c - C_{L_{DES/5}})^4 - 60\,(t/c)^4$$

where t/c is wing reference thickness/chord ratio

$C_{L_{DES}}$ is wing design lift coefficient

and $t/c > C_{L_{DES/5}}$

if $t/c < C_{L_{DES/5}}$, then the term $(t/c - C_{L_{DES/5}})^4$ is omitted.

(4) A compressibility drag increment, $\Delta C_{D_{COMP}}$, is applied as a function of increment from the design Mach number. Generalized data for this increment are shown in Figure 22 . Generalized stored data for this drag increment may be used or they may be over-ridden manually if more exact data are available.

(5) The drag build-up is completed in a conventional manner by adding components to account for induced drag, CD_i; interference, $\Delta C_{D_{INT}}$; surface roughness, $\Delta C_{D_{ROUGH}}$; trim, $\Delta C_{D_{TRIM}}$; and landing gear pod, $\Delta C_{D_{POD}}$.

(6) A miscellaneous drag increment, $\Delta C_{D_{MISC}}$, is available to account for such items as flap-track fairings when appropriate. $\Delta C_{D_{MISC}}$ has also been used in drag level sensitivity studies.

The validity of the build-up method depends on good detailed aerodynamic design for a basic lift coefficient, aspect ratio, wing thickness, Mach number combination. Inattention to high speed design detail could, for example, result in an undesirable decrease in the Oswald efficiency factor e as defined by $e = \dfrac{dC_D/dC_L^{\,2}}{\pi(AR)}$.

This could be caused by a number of improper design choices such as the selection of too little wing wash-out for a high aspect ratio, high lift coefficient wing. As explained in Reference 37 however, highly efficient, high speed wings can be designed with careful attention to detail and this type of wing is assumed in estimations of high speed drag.

4.3.2 Low Speed Data

The OTW/IBF (Hybrid) low speed aerodynamic data have been updated, from that used in the previous system study based on Lockheed-Georgia Wind Tunnel Test No. 107 results, Ref. 23. A general arrangement of the test model is shown in Figure 23. The revised data has been used in the optimization studies of thrust splits between OTW and IBF, aspect ratio, number of engines and baseline definitions. The development of the data base from the uncorrected wind tunnel test results is described below.

Corrections to Lockheed Wind Tunnel Test 107 Data - Tare and skin friction corrections have been applied to all data; based on a power off, flaps up, C_L and C_X comparison with expected full-scale drag, an increment ΔC_X of + 0.058 has been added to basic wind tunnel C_X values for all values of flap angle, angle of attack and C_T. This correction is based on comparison of flaps-up power-off wind tunnel model drag data with predicted full-scale drag characteristics. A flaps-up power-off C_D of 0.036 at $C_L = 0$ results from this correction. At present, no C_{L_α} correction has been applied to the linear C_{L_α} range of α since the slight favorable Reynolds No. effect is approximately offset by the higher sweep of the baseline OTW/IBF configuration. For other study aircraft, the effects of C_{L_α} on basic performance results should be well enough approximated for a parametric type of study. A more eleborate treatment of C_{L_α} is beyond the basic scope and intent of this study. For the $C_{L\ MAX}$ correction, flaps up, a $\Delta C_{L\ MAX}$ of + 0.6 has been applied to all power off data to account for favorable Reynolds Number effects and further configuration optimization. A varying $\Delta C_{L\ MAX}$ as a function of flap angle and C_T has been applied to hybrid data as indicated in Figure 24. Corrections of the same order of magnitude have

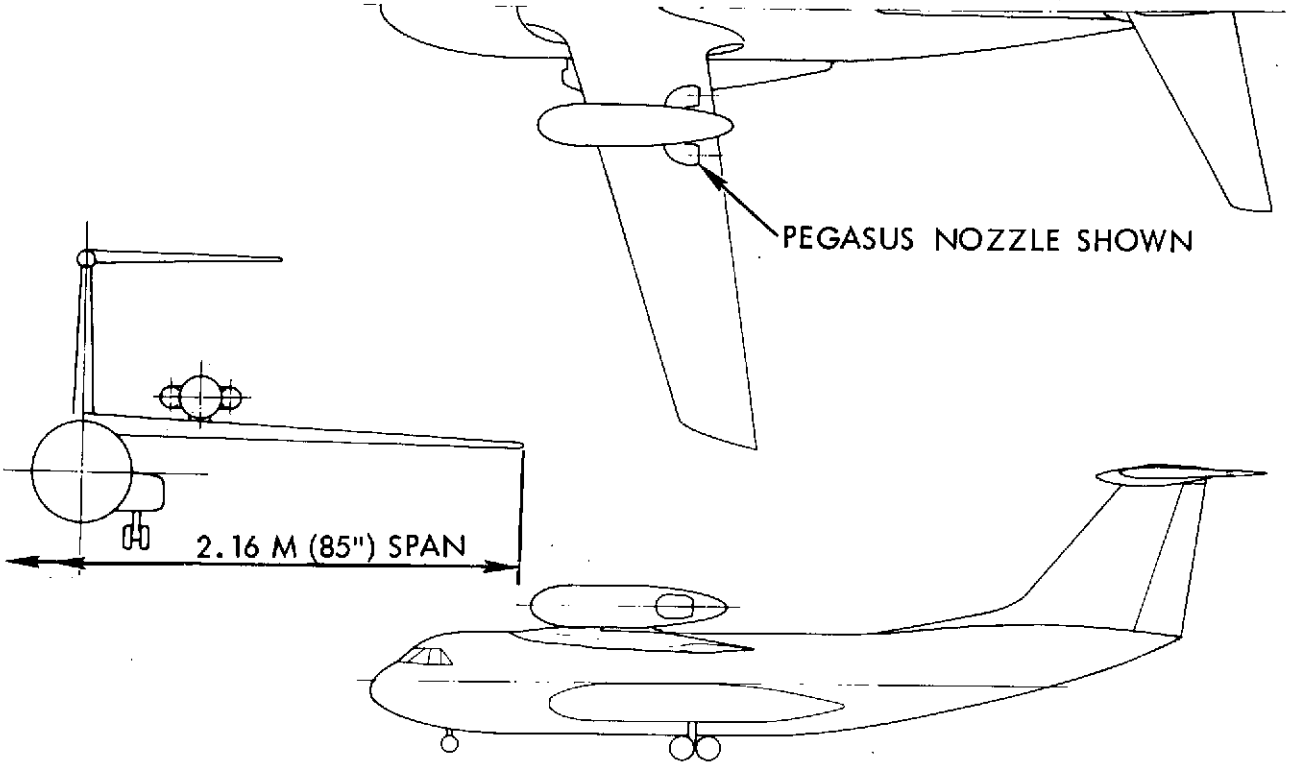

FIGURE 23: LOCKHEED POWERED LIFT MODEL
(HIGH WING)

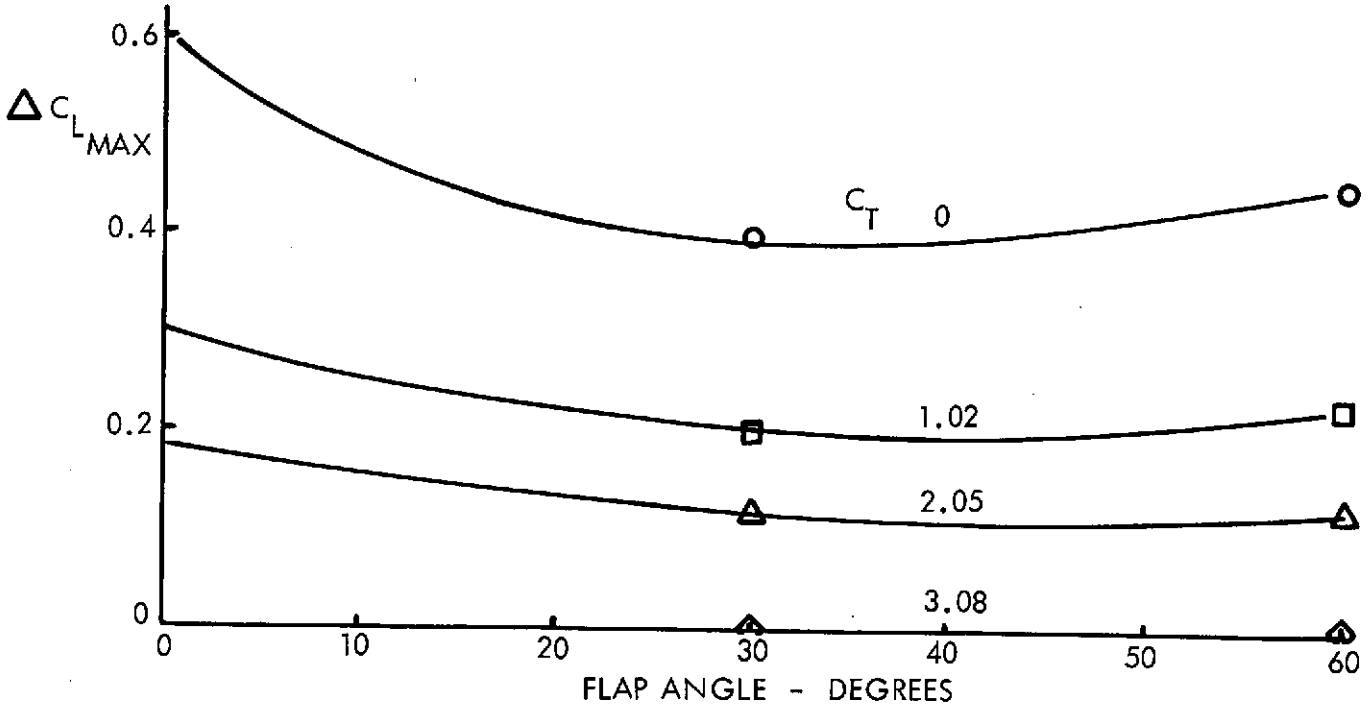

FIGURE 24: $\Delta C_{L_{MAX}}$ CORRECTION TO 107 TEST DATA

been applied to OTW data and IBF data as functions of OTW or IBF C_T values. In order to correct C_X for compatibility with C_L, the relatively parabolic ranges of C_X vs C_L have been extrapolated to higher C_L values compatible with revised $C_{L\ MAX}$'s as indicated in Figure 25 . Lateral and longitudinal trim corrections are small. $C_{X\ TRIM}$ is very small ($-0.001 \leq C_{X\ TRIM} \leq 0.001$) compared to C_X at all values of C_T and is ignored. $\Delta C_{L\ MAX}$ is accounted for by using slightly conservative $C_{L\ MAX}$ as predicted by linear superposition at flap angles of 30° and 60°.

For all initial aircraft optimization studies in this study, the effects of geometrical changes to aspect ratio, sweep and taper ratio have been accounted for by:

1. Correcting induced drag (or C_X force) for aspect ratio.
2. Assuming no sweep penalty on $C_{L\ MAX}$.
3. Assuming taper ratio effects can be compensated for by optimization of wing twist and high lift devices.

This approach permits the more significant effects of geometric variations to be included in the critical optimization while giving a slight advantage to the higher sweep angles and taper ratios. Results of the optimization studies verify that the above parametric simplifications do not significantly affect the selection of aspect ratio, sweep and taper for the baseline aircraft.

Empirical Methodology - Using Test 107 wind tunnel data, all engines operating or engine out data can be well approximated for various OTW/IBF thrust splits at approach or takeoff conditions by linearly superposing discrete OTW and IBF test results as follows:

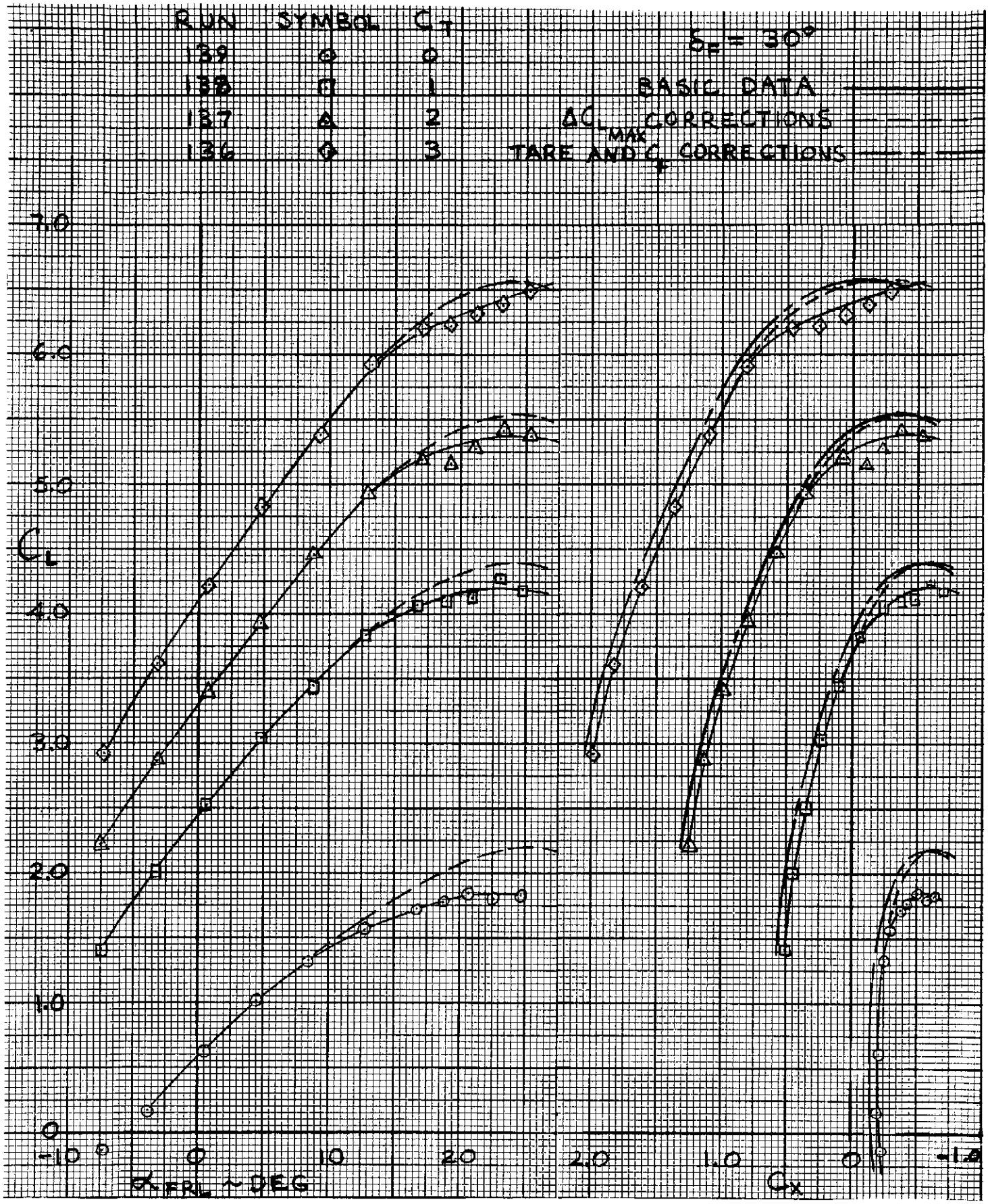

FIGURE 25: TEST 107 C_L AND C_X FOR OTW

(1) Define $C_{T_1} = \frac{T_{OTW}}{T_{TOTAL}} \times C_{T_{TOTAL}}$

$$C_{T_2} = \frac{T_{NET_{IBF}}}{T_{TOTAL}} \times C_{T_{TOTAL}}$$

where $C_T = T/qS$ and T denotes gross thrust.

(2) Also define S_o/S and S_I/S by:

S_o = Wing area spanned by OTW

S_I = Wing area spanned by IBF

S = Total wing area

(3) If IBF blowing is assumed to add to OTW blowing for region S_o, then define C_{T_1}' by

$$C_{T_1}' = C_{T_1} + C_{T_2} \times S_o/S_I$$

and C_{T_2}' by $C_{T_2}' = C_{T_2} \times (1 - S_o/S_I)$

(4) With the above definitions, hybrid (OTW/IBF) data may then be developed for the 2 engine configuration for various splits of OTW and IBF flow as follows:

(a) All Engines Operating

First, read values of C_L and C_X for OTW alone case from C_L or C_X vs. C_T curve at a given α and δ_{FLAP} as illustrated below:

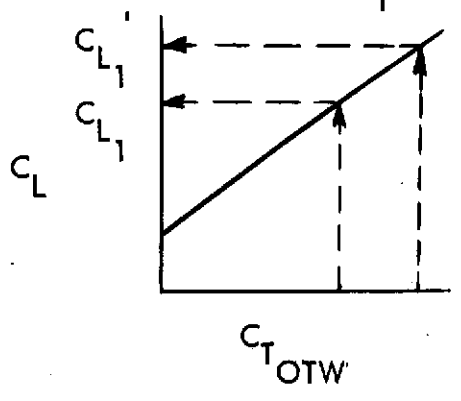

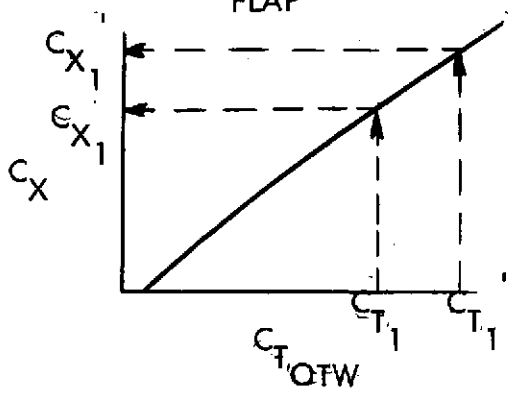

Depending on whether the OTW spanned portion of the wing has IBF or not, C_L and C_X are read at either C_T or CT'. Next, read values of ΔC_X vs. C_T curve at a given α and δ_{FLAP} as illustrated below:

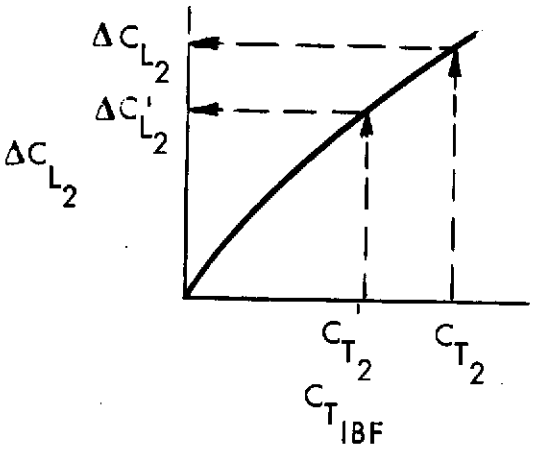

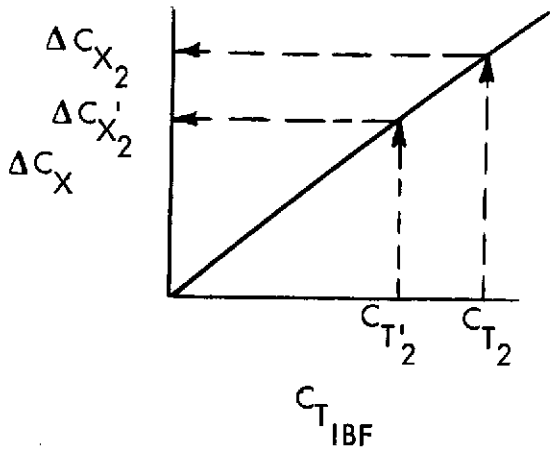

Finally the total C_L and C_X is derived by adding OTW and IBF effects as follows:

$$C_{L_{TOTAL}} = C_{L_1} + \Delta C_{L_2} \tag{1}$$

$$C_{X_{TOTAL}} = C_{X_1} + \Delta C_{X_2} \tag{2}$$

(b) One Engine Out

Engine out build-up of C_L and C_X proceeds similarly to build-up of all engines operating data. In this case, however, C_{L_1} is applied to one wing and $(C_{L_{C_T}} + C_{L_2})$ is applied to the other wing so that:

$$C_{L_{TOTAL}} = \frac{C_{L_1}}{2} + \frac{(C_{L_{C_T=0}} + C_{L_2})}{2} \tag{3}$$

$$C_{X_{TOTAL}} = \frac{C_{X_1}}{2} + \frac{(C_{X_{C_T=0}} + C_{X_2})}{2} \tag{4}$$

Lift carry-over effects are automatically accounted for since lift for the wing with OTW thrust is over-estimated by approximately the same amount as the lift is under-estimated for the wing with no OTW thrust. A slight deflection of the aft auxiliary IBF flap accomplishes trimmin in roll.

The above method of buildup has also been used to estimate 3-engine and 4-engine configuration data.

The validity of the linear superposition technique is demonstrated by the data shown in Figure 26. The hybrid data estimated by superposition as used in the present study show good agreement with corrected test 107 data in the C_L/α and C_L/C_X curves, while showing a small reduction in $C_{L\ MAX}$ values. The present study data base is compared in Figure 27 at 80/20 OTW/IBF thrust split with the initial systems study data for engine out conditions. Good agreement exists for the C_L/α relationship, but the present data base indicates a lower level of C_X at constant C_L.

OTW/IBF Comparison of Low Speed Data with Other Sources - Data from Lockheed Test No. 112/113 conducted in October 1973 indicated that no further change to the OTW/IBF slot nozzles as illustrated in Figure 28. Comparisons of the present study data base with other data sources are presented in Figure 29 through Figure 32. These comparisons demonstrate some conservatism in the present data base.

The results from the latest series of tests, Lockheed WT Test 119, have recently been released (Ref. 22). The model used in this test was a high wing configuration with aspect ratio 7.73 and 15 degrees sweep. The upper surface integrally mounted nacelles were tested with various nozzle configurations with nozzle aspect ratios from 4.0 to 11.4 and h/r values from 0.44 to 0.53. The optimum nozzle configuration (at a nozzle pressure ratio of 1.5 and 60° flap deflection) had a nozzle aspect ratio of 5.9 and an h/r of 0.53. Various fore and aft locations for the nozzle exit plane were tested. It has been concluded that edge tailoring at the nozzle exit is more important for C_L optimization than nozzle

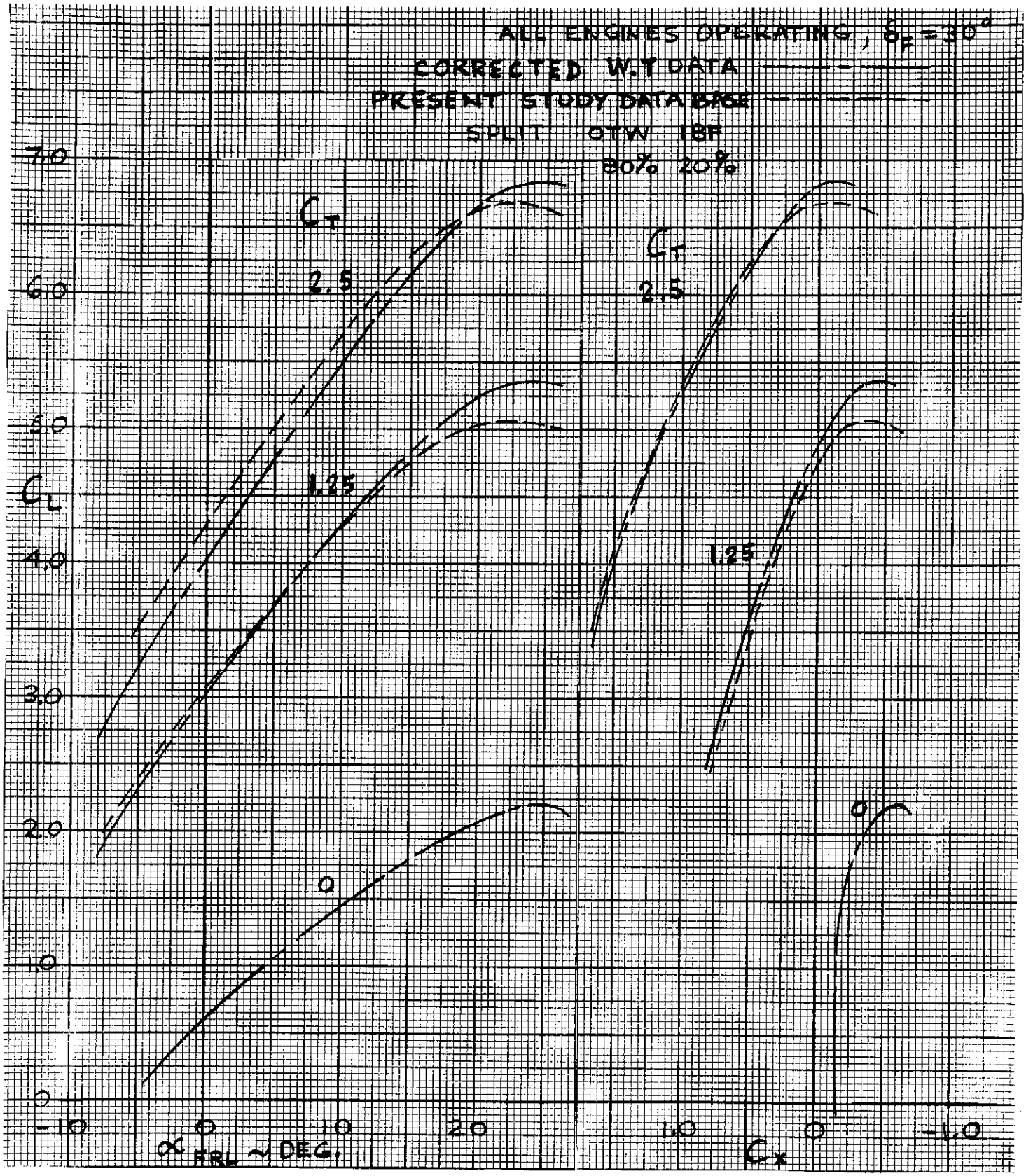

FIGURE 26: COMPARISON OF TEST 107 CORRECTED HIGH LIFT DATA WITH HYBRID DATA

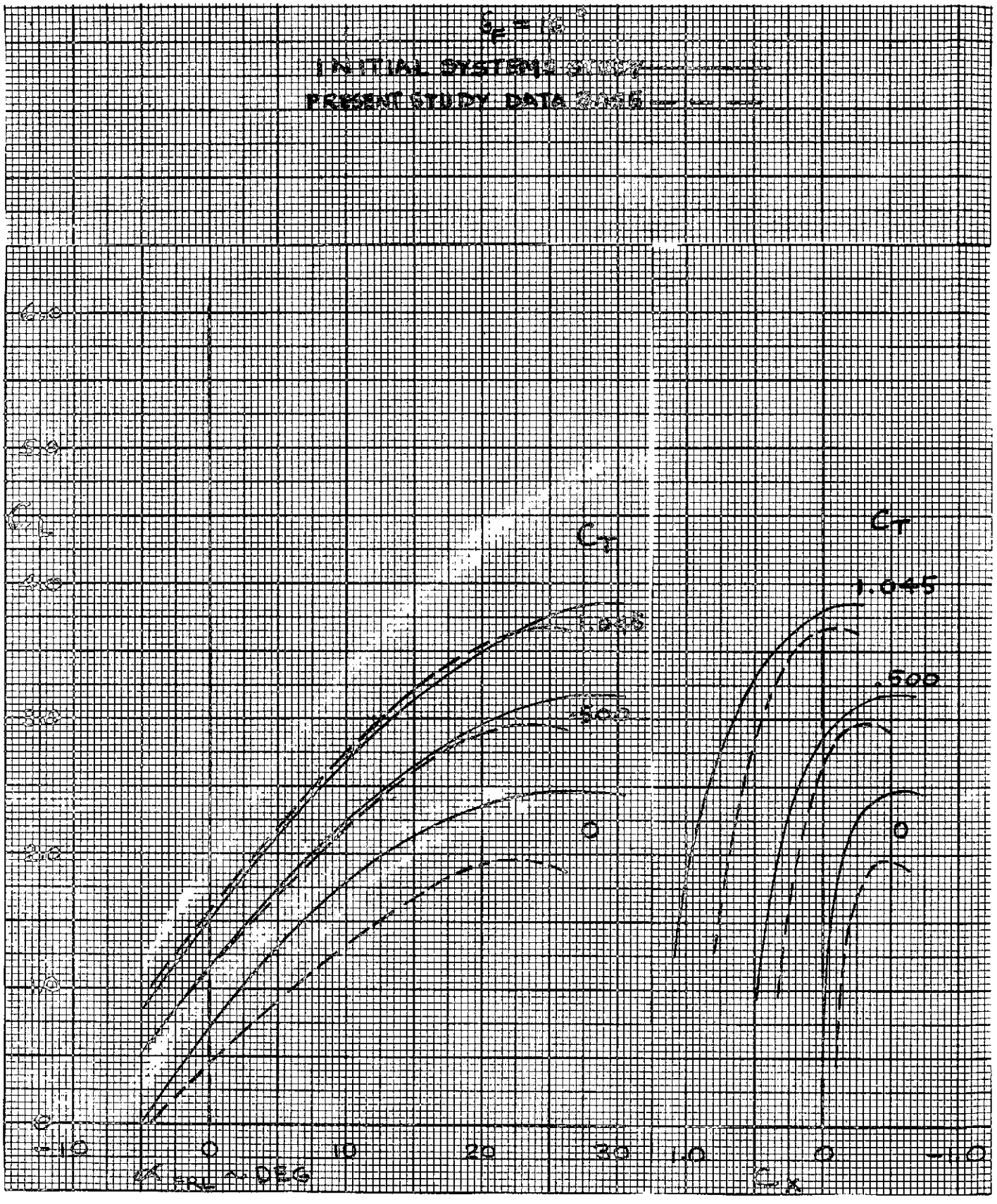

FIGURE 27: COMPARISON OF ESTIMATED ENGINE-OUT HYBRID DATA

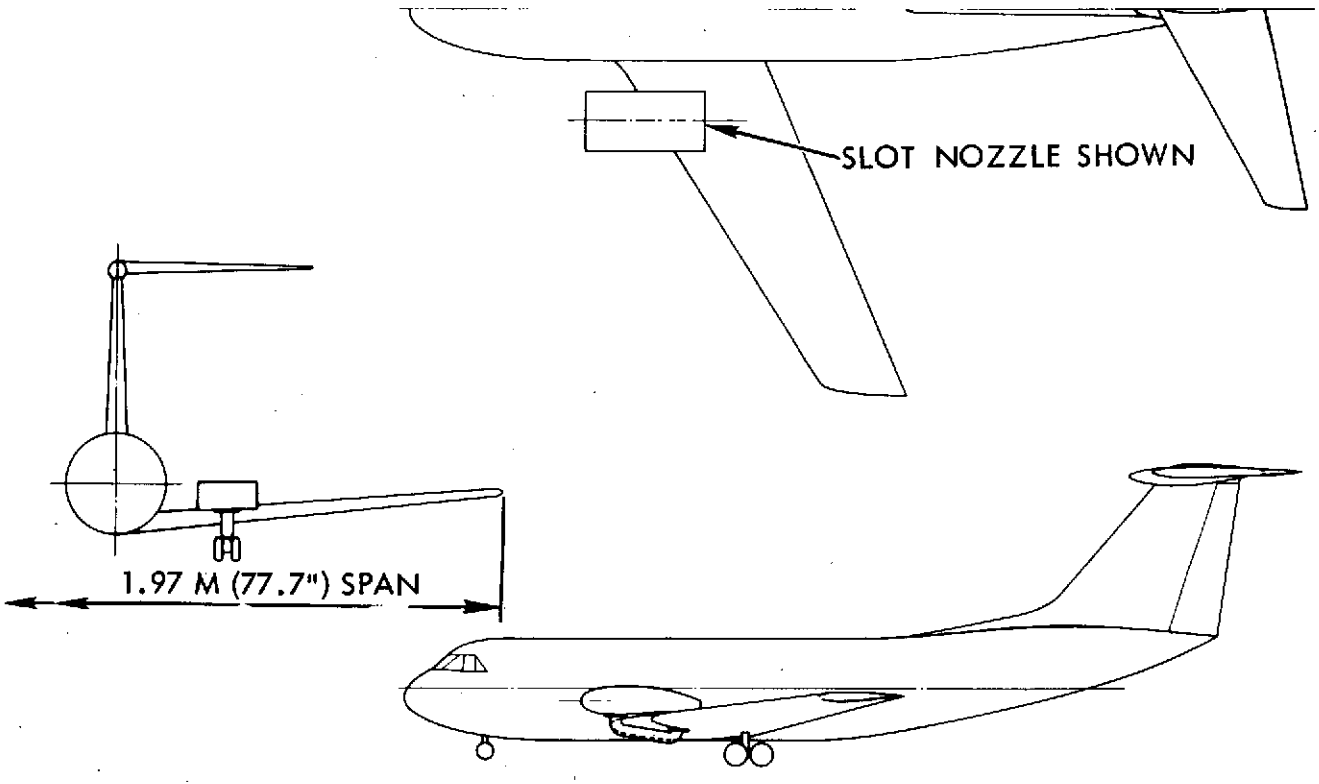

FIGURE 28: LOCKHEED POWERED LIFT MODEL
(LOW WING)

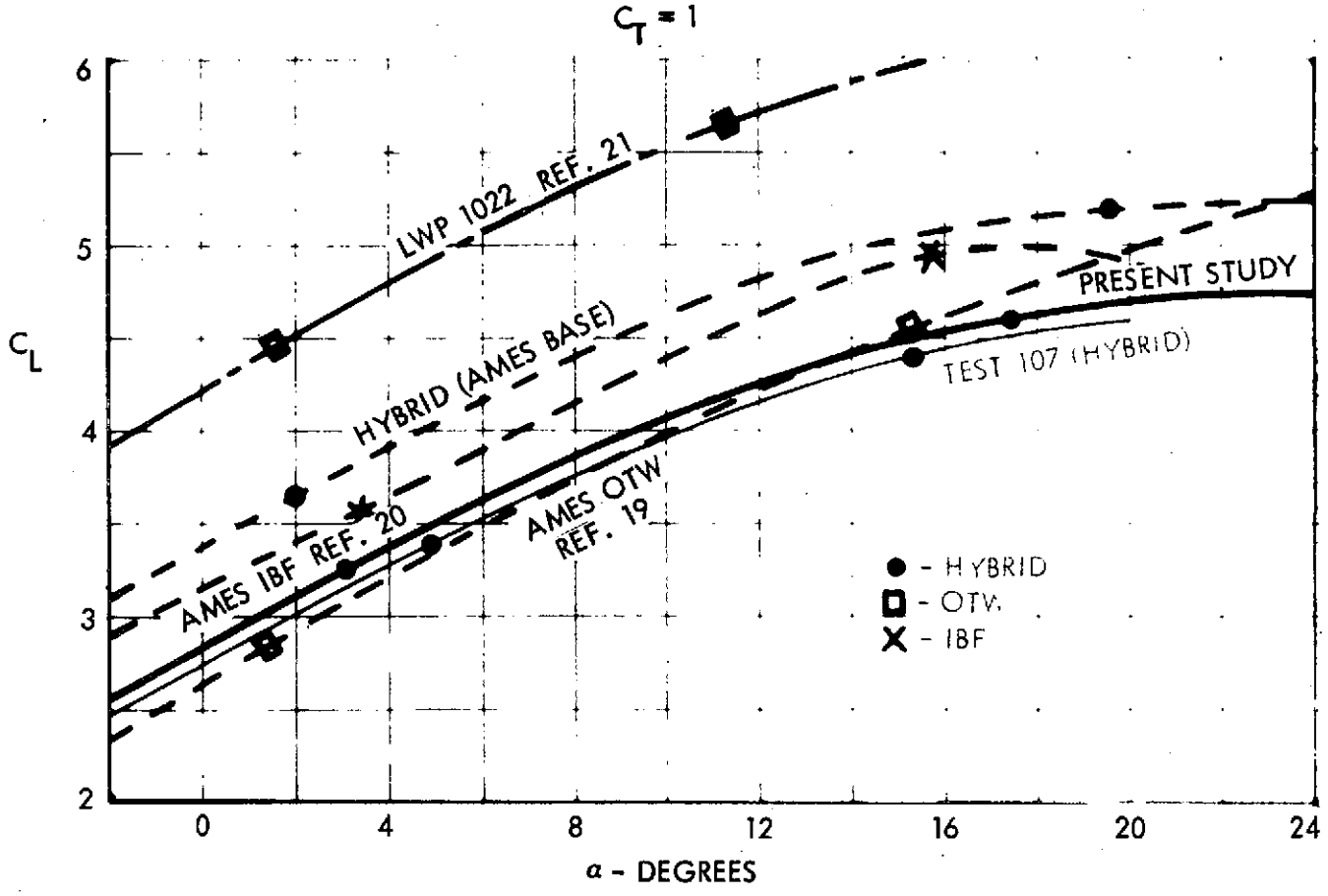

FIGURE 29: LIFT CURVE COMPARISON OF OTW AND IBF SYSTEMS

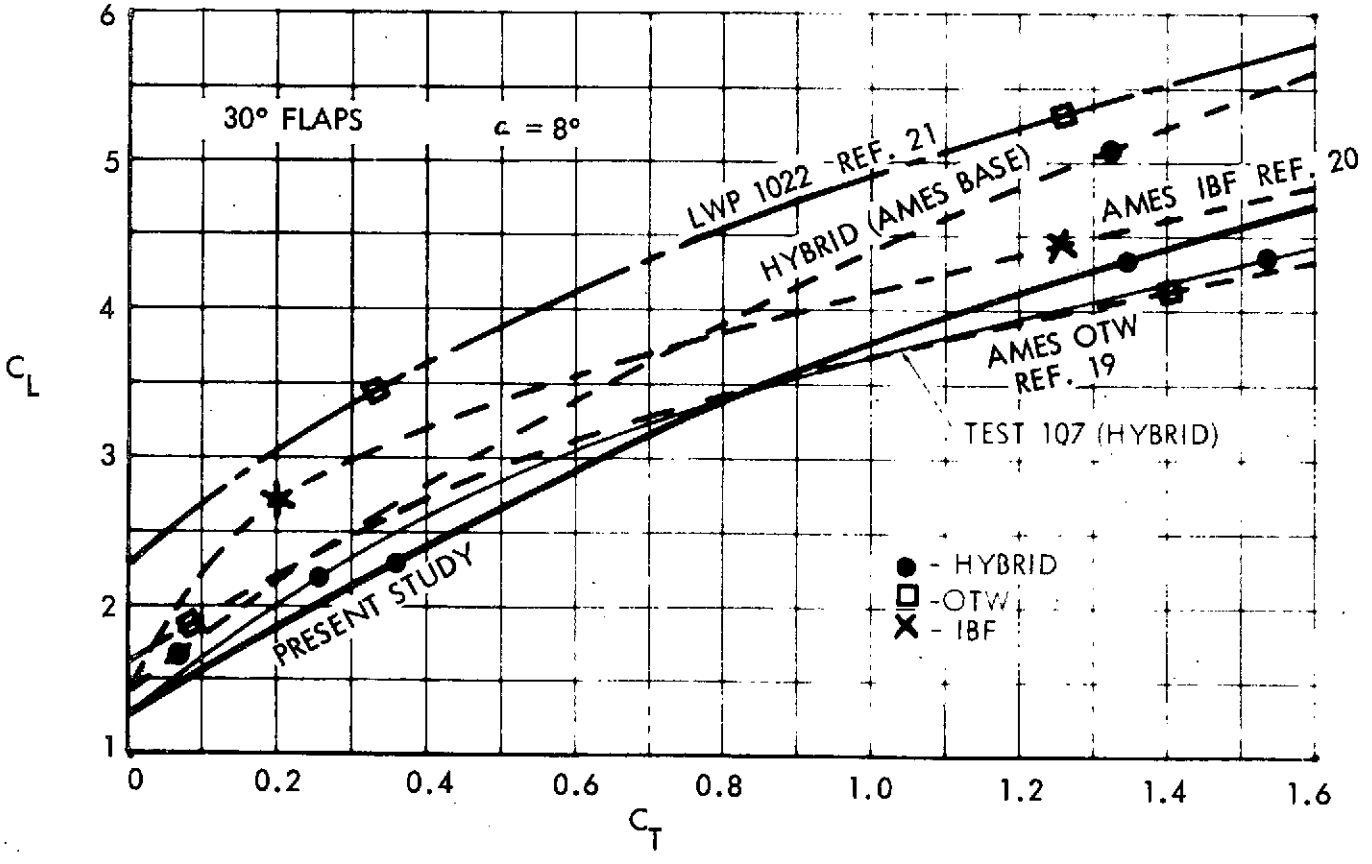

FIGURE 30: C_L VS C_T COMPARISON OF VARIOUS OTW AND IBF SYSTEMS

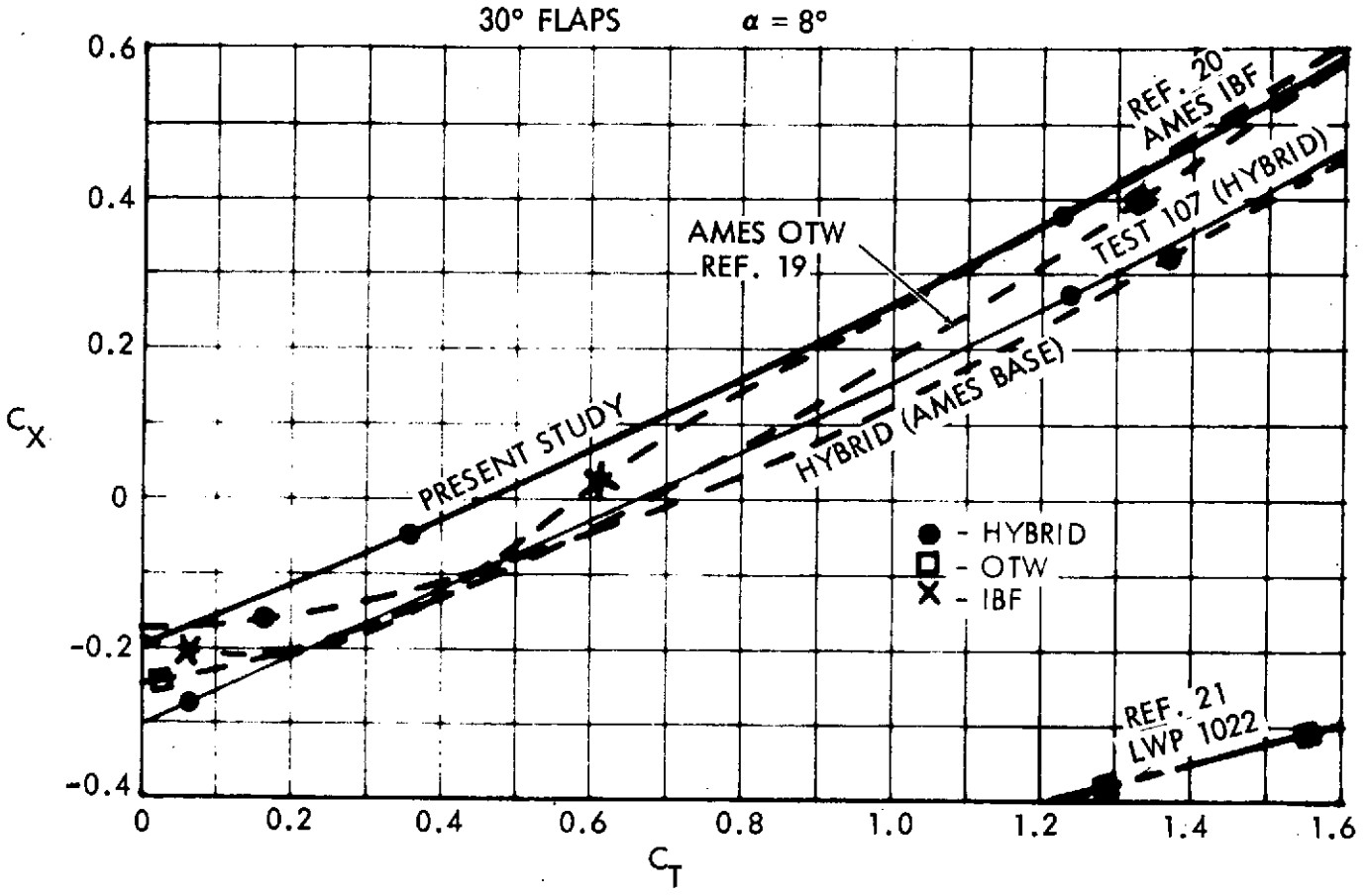

FIGURE 31: C_X VS C_T COMPARISON OF VARIOUS OTW AND IBF SYSTEMS

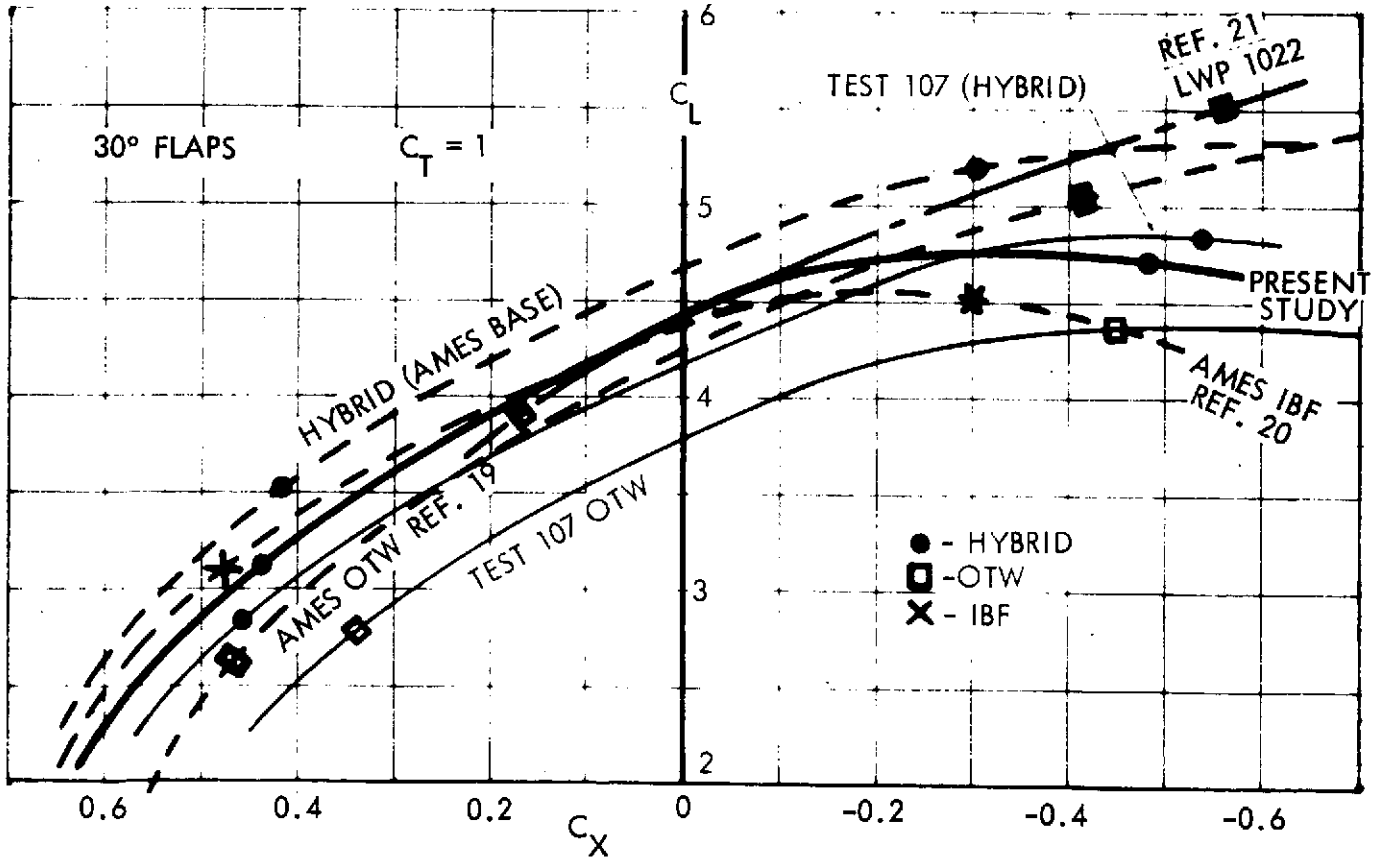

FIGURE 32: C_X VS C_L COMPARISON OF VARIOUS OTW AND IBF SYSTEMS

exit location. The selected nozzle had an upper surface deflector shield of 10° relative to the internal nozzle angle of 20°, giving a total of 30° impingement angle at the nozzle exit. A summary comparison of the present study data base with the results of Test 119 are shown in Figures 33 through 36. The data are compared for typical takeoff and landing flap settings of 22° and 60°, respectively. The figures indicate that the Test 119 results show improvements in C_L/α , C_L/C_T, C_L/C_X relationships and also in $C_{L\ MAX}$. The trends in these relationships are very consistent between the two sets of data. Thus, it is considered that when compared with the achievable low speed data levels for an optimum tailored nacelle nozzle, the present study data base is somewhat conservative.

A complete printout of the basic aspect ratio 7.73 low speed data is given in Figures 37 and 38 for engine out and both engines operating configurations. A summary of typical required takeoff and landing flap settings is presented in Table III.

A comparison of OTW/IBF and MF cruise drag polars at 0.8 Mach and 30,000 feet is shown in Figure 39. As indicated in the figure, the OTW/IBF cruise L/D exceeds that for the MF which is penalized by the low wing loading and resultant low C_L requirement.

4.3.3 High Speed Nacelle Tests

Lockheed-Georgia has initiated a combined analytical/experimental program designed to expand the relatively meager data base currently available for the OTW concept. This in-house technology program encompasses both the low-speed, high-lift, and the transonic cruise flight regimes. In the latter case, existing design data for achieving targeted cruise performance is almost non-existent. The published data on the drag implications of an overwing nacelle and its exhaust stream appear inconclusive. Reference 24 reports a series of preliminary wind tunnel tests conducted by the RAE which has measured an (apparently lift-dependent) drag increment associated with overwing nacelles in free-flow. It was further postulated that the reduction in spanwise lift distribution at the nacelle to which this could be attributed might be eliminated

$C_T = 1.0$

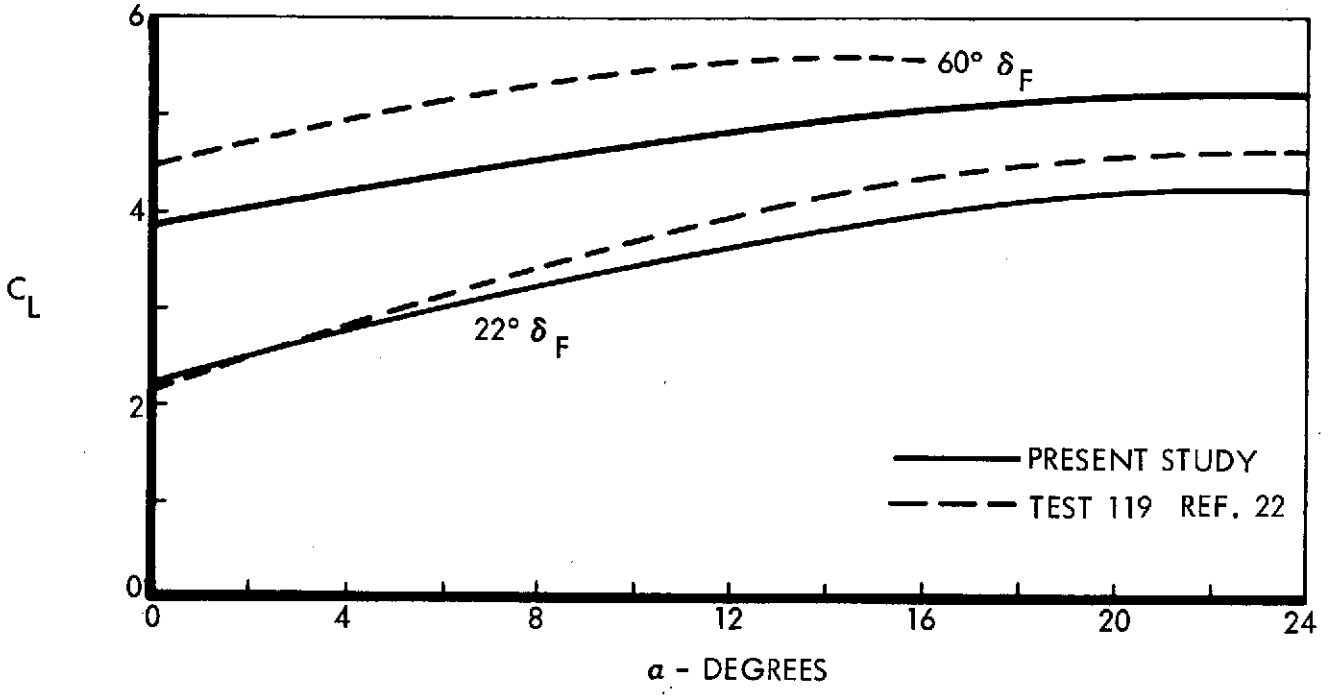

FIGURE 33: LIFT CURVE COMPARISON WITH GELAC TEST 119

$\alpha = 8°$

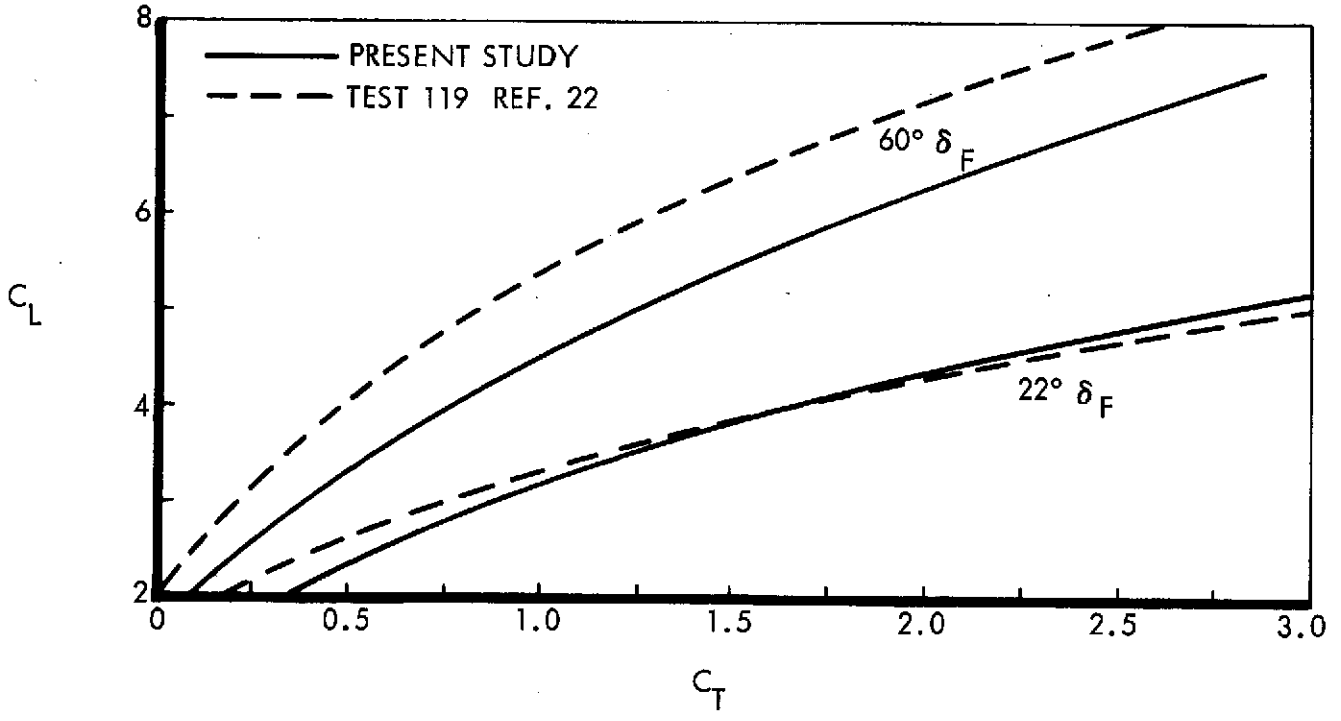

FIGURE 34: C_L VS C_T COMPARISON WITH GELAC TEST 119

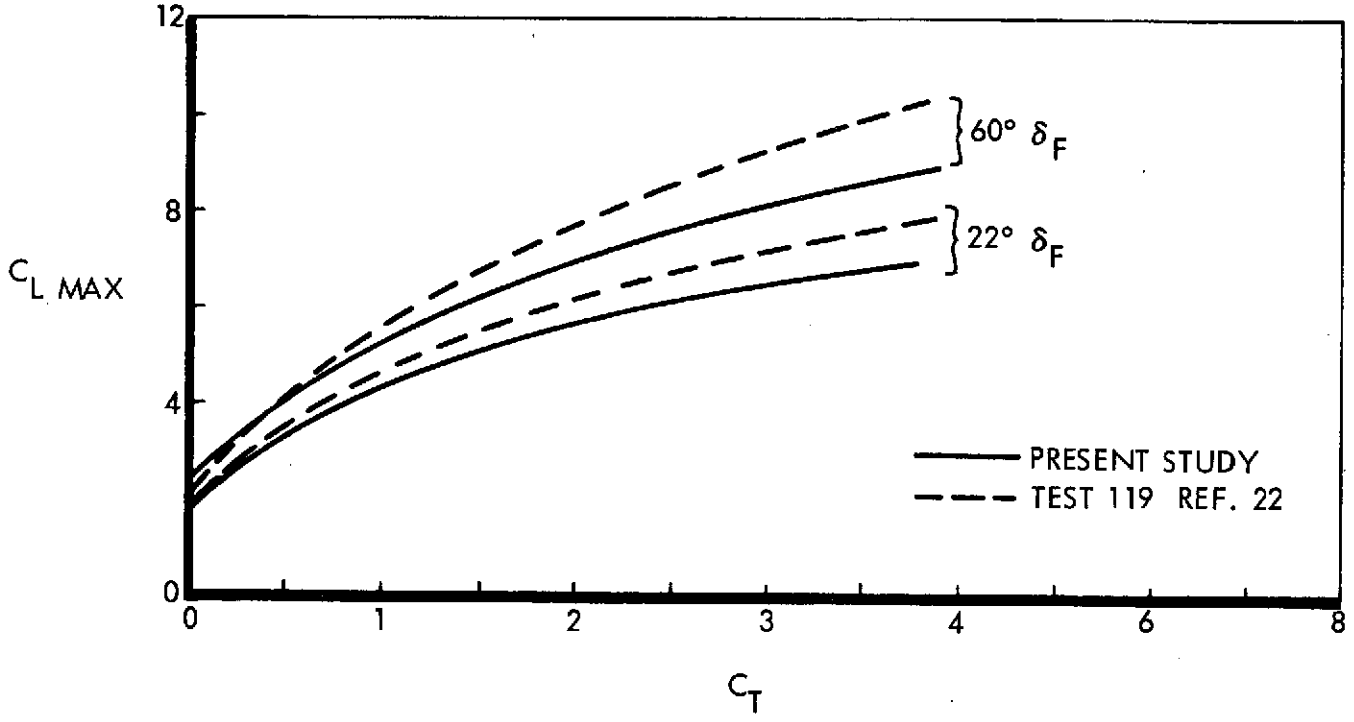

FIGURE 35: $C_{L\ MAX}$ VS C_T COMPARISON WITH GELAC TEST 119

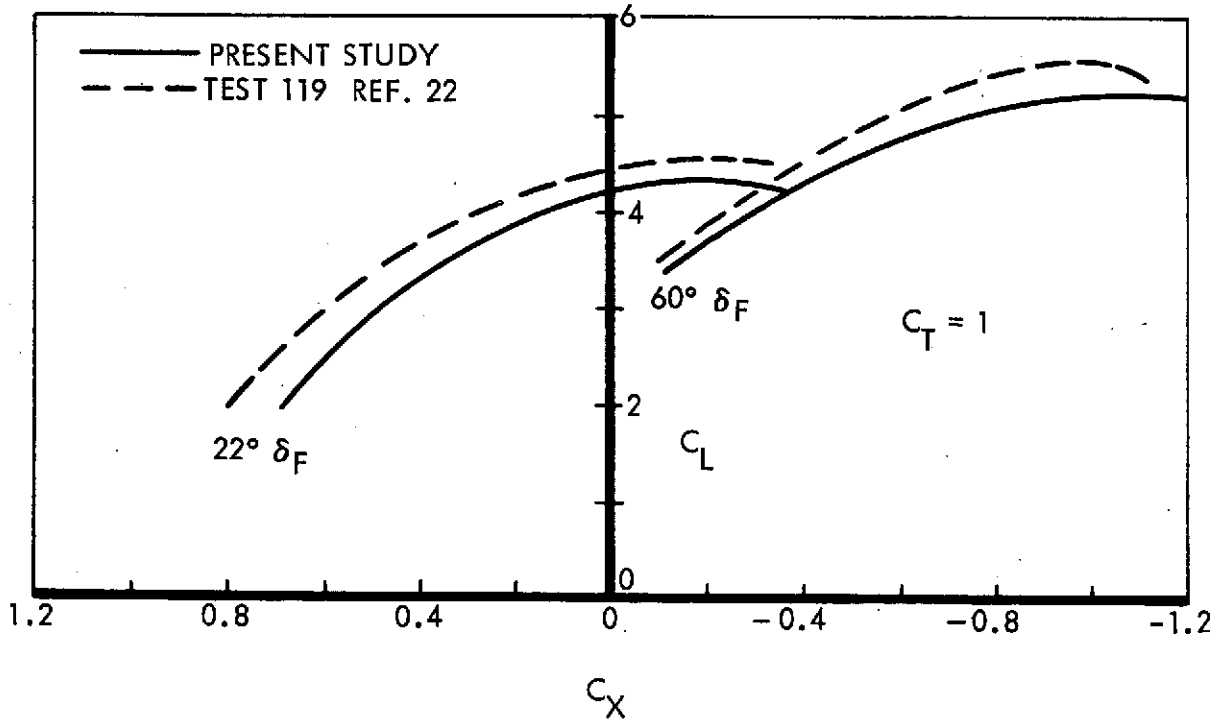

FIGURE 36: C_X VS C_L COMPARISON WITH GELAC TEST 119

δ_F	.00000						
C_T	.00000	.30000	.60000	1.20000			
α	.00000	8.00000	12.00000	16.00000	20.00000	24.00000	26.00000
C_L	.28000	1.04000	1.36500	1.63500	1.73500	1.52000	1.36000
	.38661	1.20869	1.57628	1.87702	2.04710	2.01678	1.89275
	.47674	1.35378	1.76016	2.08747	2.31831	2.43460	2.36181
	.60753	1.57314	2.04573	2.41370	2.73806	3.03340	3.10886
C_X	-.03966	-.08705	-.12409	-.23951	-.31806	-.42107	-.48305
	.25160	.18559	.12251	.01613	-.07779	-.20890	-.30632
	.54313	.46545	.39085	.29884	.18679	.04279	-.07781
	1.12681	1.04668	.99246	.94513	.78826	.65954	.53245
15.00000							
	.00000	.30000	.60000	1.20000			
	.00000	8.00000	12.00000	16.00000	20.00000	24.00000	26.00000
	.42500	1.14625	1.45562	1.73625	1.91062	1.91875	1.86000
	.89356	1.69861	2.05436	2.36154	2.55249	2.59893	2.53941
	1.26905	2.14536	2.54276	2.87223	3.08169	3.16334	3.11499
	1.74079	2.72205	3.18856	3.54976	3.80211	3.94687	3.95465
	-.09734	-.14061	-.16730	-.25304	-.34655	-.50767	-.61487
	.15578	.06702	.00271	-.09082	-.19073	-.37491	-.48218
	.41209	.28503	.19318	.09188	-.02079	-.22145	-.33163
	.93081	.74803	.63095	.51404	.35676	.14272	.01853
30.00000							
	.00000	.30000	.60000	1.20000			
	.00000	8.00000	12.00000	16.00000	20.00000	24.00000	26.00000
	.59000	1.29000	1.59000	1.87000	2.08000	2.21000	2.20500
	1.33183	2.10739	2.44584	2.74370	2.94271	3.02827	3.03301
	1.92943	2.76808	3.14092	3.45360	3.64778	3.70283	3.69509
	2.69193	3.61934	4.04878	4.38205	4.58497	4.62100	4.58143
	-.14950	-.19384	-.22013	-.28596	-.38240	-.56000	-.68019
	.03869	-.06848	-.13655	-.22292	-.32664	-.52885	-.63705
	.23690	.07356	-.02981	-.13825	-.25449	-.47883	-.58421
	.65502	.39833	.24336	.08607	-.07026	-.32985	-.45608
45.00000							
	.00000	.30000	.60000	1.20000			
	.00000	8.00000	12.00000	16.00000	20.00000	24.00000	26.00000
	.77500	1.47125	1.76812	2.03625	2.24312	2.39375	2.39500
	1.70141	2.43503	2.75072	3.02348	3.21777	3.30481	3.28350
	2.45787	3.22192	3.55463	3.83161	4.01657	4.05329	4.01210
	3.46094	4.26502	4.62638	4.91059	5.08665	5.06212	4.98919
	-.19604	-.24660	-.28242	-.33817	-.42562	-.57886	-.68009
	-.10048	-.22180	-.29617	-.38119	-.48657	-.67240	-.77315
	.01529	-.17168	-.28097	-.39461	-.51719	-.73251	-.83342
	.29495	-.00826	-.17658	-.34529	-.49851	-.76200	-.89492
60.00000							
	.00000	.30000	.60000	1.20000			
	.00000	8.00000	12.00000	16.00000	20.00000	24.00000	26.00000
	.98000	1.69000	1.99000	2.23500	2.40000	2.47000	2.43000
	2.00230	2.68153	2.96900	3.20088	3.37766	3.42853	3.38104
	2.85437	3.50689	3.78389	4.00624	4.18907	4.21436	4.15604
	4.04782	4.65909	4.92137	5.13537	5.30715	5.26790	5.17793
	-.23687	-.29872	-.35397	-.40952	-.47623	-.56477	-.61551
	-.26237	-.39361	-.47681	-.56633	-.67163	-.80600	-.89174
	-.25452	-.45266	-.56227	-.67916	-.81075	-.98419	-1.09609
	-.15299	-.47593	-.63308	-.78418	-.93160	-1.15721	-1.30132

ACCUM TTL=1 CORE=5120 CORE SEC=198 ACCUM CPU=1

FIGURE 37: OTW/IBF BASIC AERO DATA - ENGINE OUT

δ_F	.00000						
C_T	.00000	.60000	1.20000	2.40000			
α	.00000	8.00000	12.00000	16.00000	20.00000	24.00000	26.00000
C_L	.28000	1.04000	1.36500	1.63500	1.73500	1.52000	1.36000
	.48855	1.37031	1.77669	2.10578	2.34075	2.48184	2.39016
	.65476	1.63927	2.11186	2.48692	2.82781	3.22236	3.22223
	.86019	1.99316	2.55262	2.98031	3.44584	4.03944	4.29213
C_X	-.03966	-.08705	-.12409	-.23951	-.31806	-.42107	-.48305
	.54306	.45863	.36996	.26963	.16004	.00055	-.13293
	1.12659	1.01948	.90898	.82837	.68144	.49330	.31253
	2.29545	2.18563	2.12046	2.09289	1.85104	1.68207	1.47880
15.00000							
	.00000	.60000	1.20000	2.40000			
	.00000	8.00000	12.00000	16.00000	20.00000	24.00000	26.00000
	.42500	1.14625	1.45562	1.73625	1.91062	1.91875	1.86000
	1.34640	2.23409	2.63414	2.96728	3.17528	3.25948	3.19920
	2.05020	3.07695	3.55408	3.92996	4.17647	4.32943	4.29149
	2.80498	4.02774	4.61822	5.05032	5.38444	5.65701	5.73532
	-.09734	-.14061	-.16730	-.25304	-.34655	-.50767	-.61487
	.40898	.27582	.17575	.07247	-.03693	-.24433	-.35475
	.91994	.71307	.56327	.43852	.29435	.05342	-.07192
	1.94118	1.63244	1.45229	1.27206	1.00204	.73094	.54235
30.00000							
	.00000	.60000	1.20000	2.40000			
	.00000	8.00000	12.00000	16.00000	20.00000	24.00000	26.00000
	.59000	1.29000	1.59000	1.87000	2.08000	2.21000	2.20500
	2.04871	2.90035	3.27673	3.59296	3.78359	3.83042	3.78673
	3.16905	4.14842	4.59203	4.93948	5.12822	5.13130	5.06790
	4.39462	5.55776	6.10832	6.50319	6.74061	6.77438	6.72913
	-.14950	-.19384	-.22013	-.28596	-.38240	-.56000	-.68009
	.22961	.06145	-.04616	-.15419	-.26917	-.49611	-.59581
	.62972	.35430	.18255	.02709	-.12461	-.39516	-.49903
	1.45681	1.01248	.76216	.49537	.21970	-.11432	-.29719
45.00000							
	.00000	.60000	1.20000	2.40000			
	.00000	8.00000	12.00000	16.00000	20.00000	24.00000	26.00000
	.77500	1.47125	1.76812	2.03625	2.24312	2.39375	2.39500
	2.59546	3.36909	3.70446	3.98283	4.16567	4.19468	4.15274
	4.01129	4.85370	5.22570	5.51546	5.68306	5.62795	5.55175
	5.62912	6.58324	7.02292	7.33891	7.50236	7.39156	7.27355
	-.19604	-.24660	-.28242	-.33817	-.42562	-.57886	-.68009
	.00210	-.18785	-.29934	-.41414	-.54026	-.75781	-.85948
	.24794	-.06697	-.24403	-.41749	-.58520	-.85874	-.97468
	.82778	.30582	.02795	-.26031	-.51659	-.86813	-1.05129
60.00000							
	.00000	.60000	1.20000	2.40000			
	.00000	8.00000	12.00000	16.00000	20.00000	24.00000	26.00000
	.98000	1.69000	1.99000	2.23500	2.40000	2.47000	2.43000
	2.98655	3.64031	3.91735	4.13688	4.32152	4.35224	4.29725
	4.57694	5.19278	5.45510	5.65792	5.84097	5.81941	5.74276
	6.50846	7.10418	7.36201	7.55748	7.67367	7.50854	7.36859
	-.23687	-.29872	-.35397	-.40952	-.47623	-.56477	-.61561
	-.27571	-.47448	-.58616	-.70976	-.85240	-1.03140	-1.14781
	-.23140	-.55738	-.72306	-.90138	-1.09310	-1.34123	-1.50252
	.04279	-.50086	-.76390	-1.00829	-1.21843	-1.53845	-1.72630

ACCUM TIL=1 CORE=5120 CORE SEC=198 ACCUM CPU=1

ORIGINAL PAGE IS
OF POOR QUALITY

FIGURE 38: OTW/IBF FASIC AERO DATA - 2 ENGINES

TABLE III: TYPICAL OTW/IBF TAKEOFF AND LANDING FLAP SETTINGS

ENGINE FPR	$T/W_{T/O}$	$W/S_{T/O}$	FLAP SETTINGS (DEG.) TAKEOFF	LANDING	APPROACH
1.325	.480	90.	13.0	45	36
1.35	.479	90.	13.2	46	37
1.4	.471	90.	13.8	46	37
1.5	.471	95.	16.3	49	40

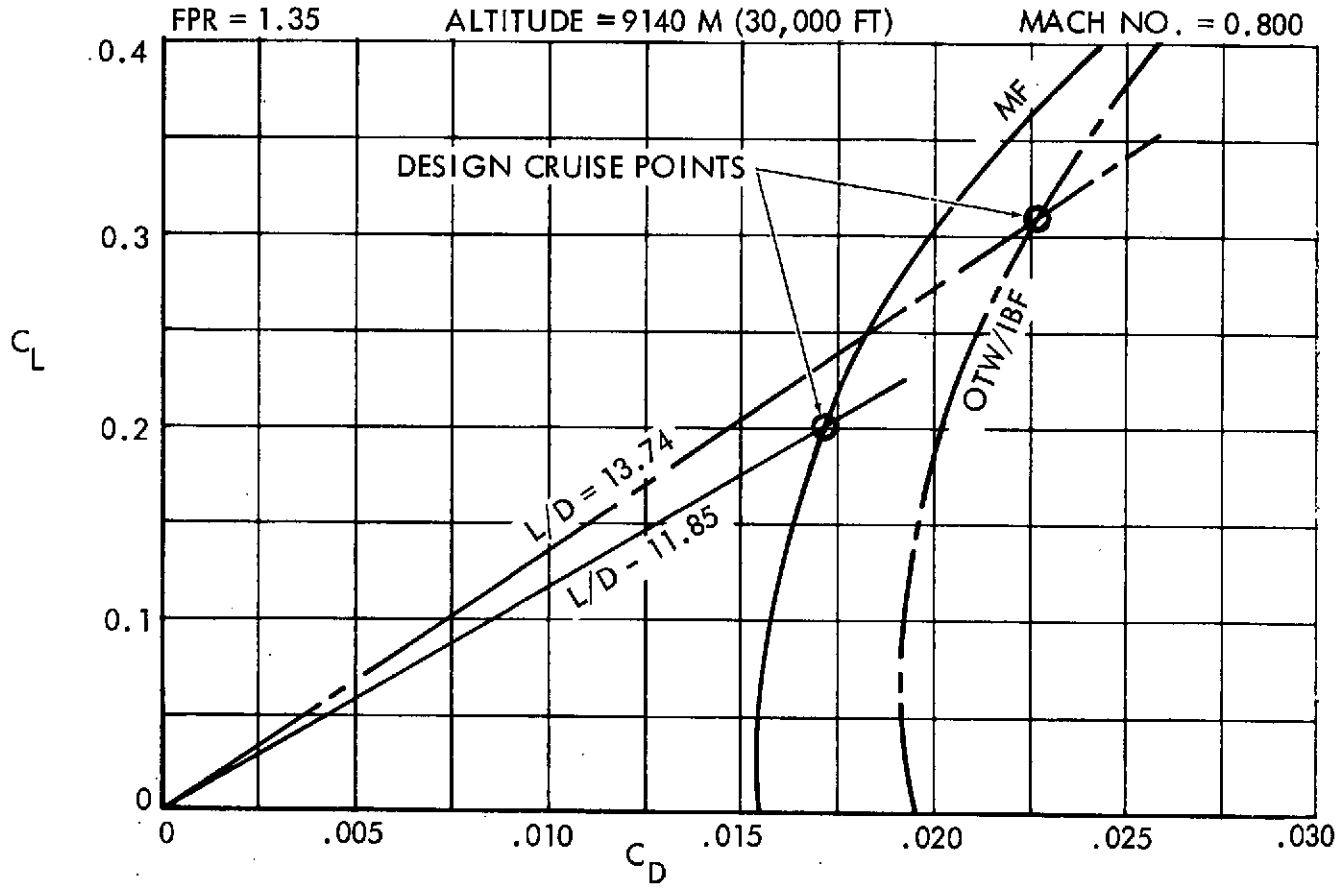

FIGURE 39: COMPARISON OF BASELINE OTW/IBF AND MF DRAG POLARS

by a correctly represented jet. Reference 24 presents no information on the effects of the overwing nacelle per se on the induced drag but does appear to confirm the favorable influence of a high pressure ratio jet (NPR - 2.0 to 2.6) in this respect. It is therefore reasonable to assume that the problem recorded by the RAE is at least tractable. However, the possibility of substantial interference drag arising from the overwing nacelle and jet-flow remains. Whereas the exhaust stream of a nominally low FPR engine is clearly subcritical under sea-level static conditions, the nozzle pressure ratio at representative cruise speeds and altitudes is generally supercritical as illustrated in Figure 19.The possible sources of high interference drag which an under-expanded sonic exhaust stream might create include:

- o Scrubbing drag over the exposed wing surface.
- o Shocks originating in the impingement of the jet on the wing surface at a finite angle as may be necessary for optimal Coanda turning.
- o Shocks originating at the sides of the nozzle exit plane due to the intrusion of an under-expanded jet into a supercritical wing flowregion which may precipitate significant flow separation.
- o The "two-dimensional" constraints imposed upon swept-wing streamlines by the axially directed jet.

Alleviation of these types of problems require a strong experimental program to be conducted under the guidelines of a supporting analytic capability. This section summarizes the current Lockheed-Georgia experimental program, including some of the more fundamental results.

Two wind tunnel tests of OTW nacelle configurations are scheduled for the current year. The first of these, which uses a full-span wing/body combined with circular flow-through nacelles, has just been completed. The second test, using shaped blowing nacelles mounted on a two-dimensional pressure wing is currently in progress. The full-span test was conducted in the Lockheed 4' X 4' blow-down facility using a force model 28 inches in wing span, a wing aspect ratio of 8 and 20 degrees of quarter-chord sweep. The basic objectives of this test were:

(1) To evaluate the aerodynamic penalties associated with positioning circular nacelles on the upper surface of a basic, unmodified wing.

(2) To evaluate the aerodynamic benefits and sensitivities associated with localized filleting of the wing/nacelle and with local changes in wing twist and camber.

(3) To evaluate the adequacy of existing analytical methods for predicting, interpreting and refining the aerodynamic quality of OTW configurations.

The various flow-through nacelle configurations included:

- A conventional underwing nacelle configuration (used primarily for comparative purposes.
- An upper-surface pylon-mounted nacelle representing a two-engine configuration.
- Intergral-type circular nacelles mounted directly to the wing upper surface in two- and four-engine configurations.

Other test variables considered placement of the single nacelles in inboard and outboard wing positions and the representation of the engine efflux by a hard-surface extension of the basic, flow-through nozzle. Lift, drag and moment data, as well as extensive flow visualization, were obtained across the Mach range of 0.5 - 0.75 at a constant Reynolds number of 3.5×10^6/MAC. A representative integrated nacelle configuration is shown in Figure 40 while a pylon mounted configuration is presented in Figure 41.

Typical drag results from tests of two nacelles mounted on the basic wing are shown in Figure 42 at an untrimmed lift coefficient of 0.40. Comparative data are provided for the underwing installation and are shown to be of a normal magnitude. As noted, exceptionally high drag increases were found when the nacelles were placed directly

FIGURE 40: UPPER SURFACE INTEGRATED NACELLES

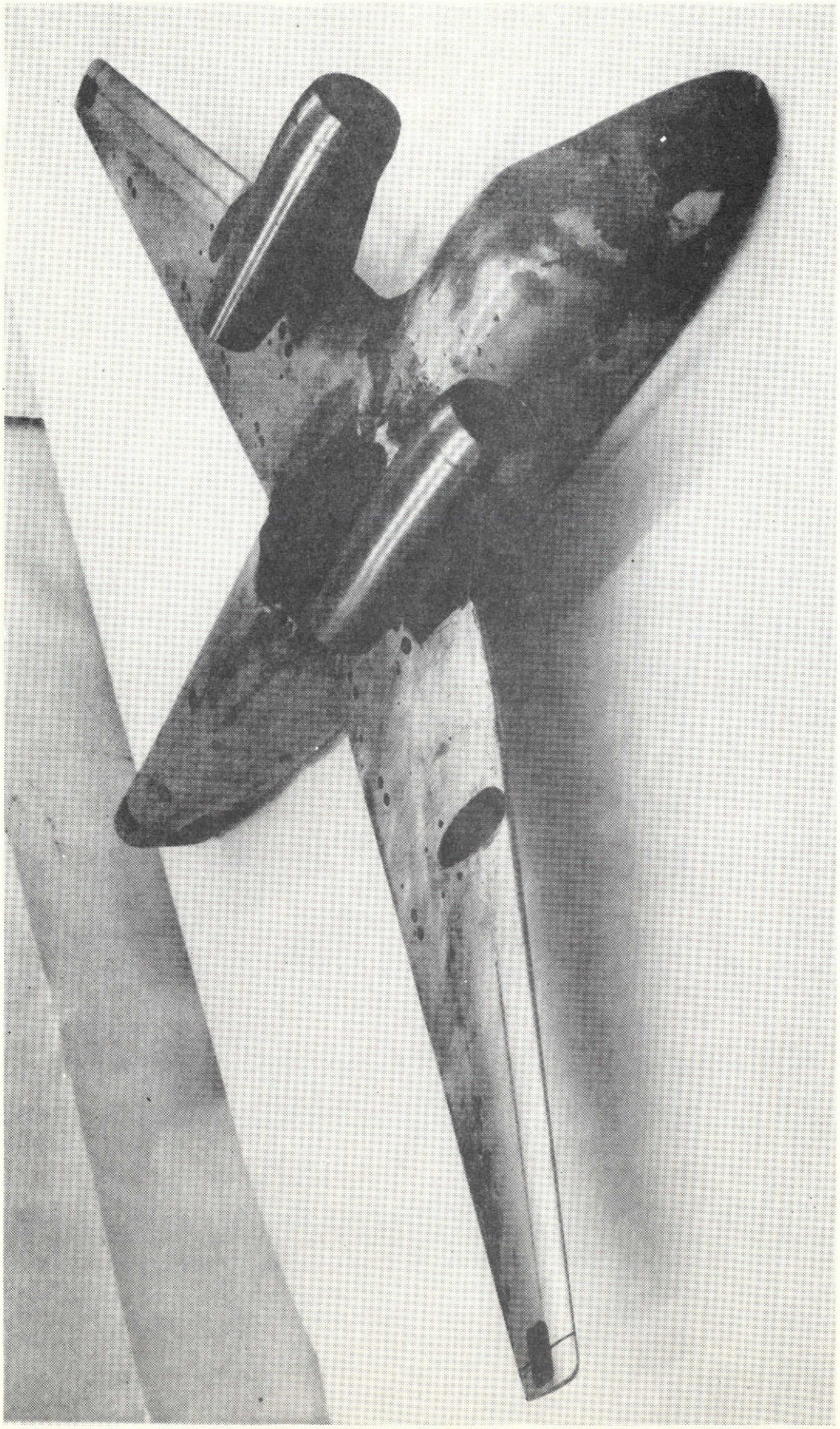

FIGURE 41: UPPER SURFACE PYLON NACELLES

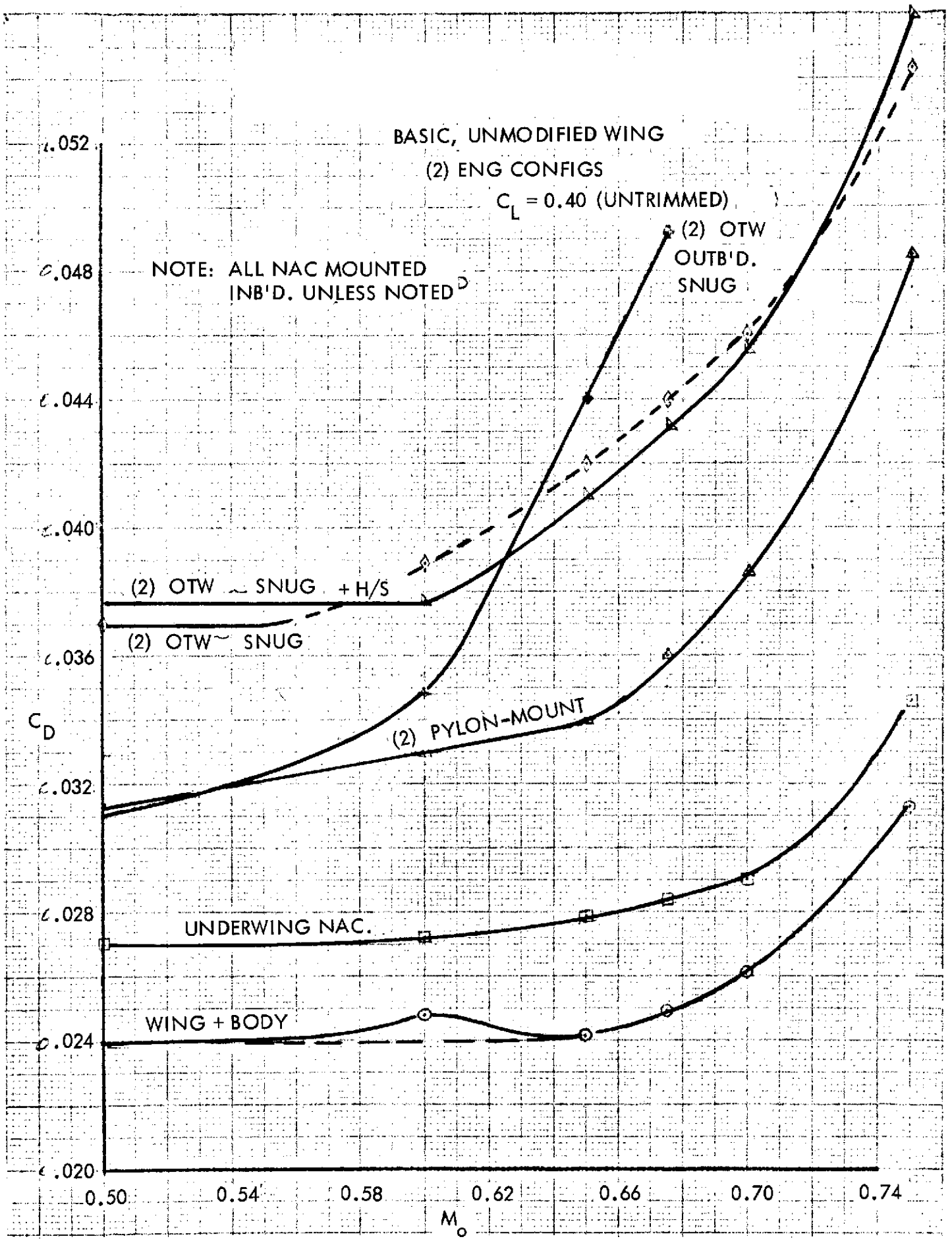

FIGURE 42: DRAG VARIATIONS OF VARIOUS NACELLE CONFIGURATIONS

onto the wing upper surface even at the lowest test Mach number; further deterioration in performance was observed as the Mach number was increased. Flow visualization techniques indicated the source of this drag problem to be extensive flow separation on the wing upper surface between the nacelle and fuselage. Tests of the four-engine configurations showed a greater spanwise extent of separated flow with resulting drag increments approximately double those shown for the two-engine cases. Drag levels found for the pylon-mounted nacelles were indicated to be less severe than those of the direct-mounting configurations at all Mach numbers. The controlling flow mechanism appeared to be a strong, vortex-like disturbance originating at the leading edge of the wing pylon juncture.

The second phase of this test was concerned with those local modifications, juncture filleting and wing camber or twist which tended to reduce the very high drag levels associated with the subject OTW configurations. The primary objective was to obtain drag levels for such configurations comparable to those of the underwing nacelle installation. Guided by earlier analytical studies, based on vortex-lattice modeling of the wing-body-nacelle, and supported by flow visulization studies, local modifications were made to the wing-nacelle contours with wax. It was recognized that this approach would result in a relatively poor aerodynamic surface over the modified portions of the model and thus create an unrepresentative drag increment. It was felt, however, that the overall drag changes to be noted would provide valuable insight into the sensitivity of the basic flow mechanisms, substantiate the guidance provided by the theory and would generally provide some indication of the drag increments associated with OTW arrangements.

Corresponding drag data obtained on the integral nacelles mounted on the modified (waxed) wing are shown in Figure 43 across the test Mach range. It is to be noted that a significant reduction in wing-body-nacelle drag level was rapidly achieved for all combinations shown. Flow visualization studies substantiated the implied improvements in the local flow. As anticipated, the wing alone, complete with the waxed-in surface modifications, incurred a substantial drag increase. Although not shown, the drag level obtained on the pylon-mounted nacelles as only slightly less than that found with the

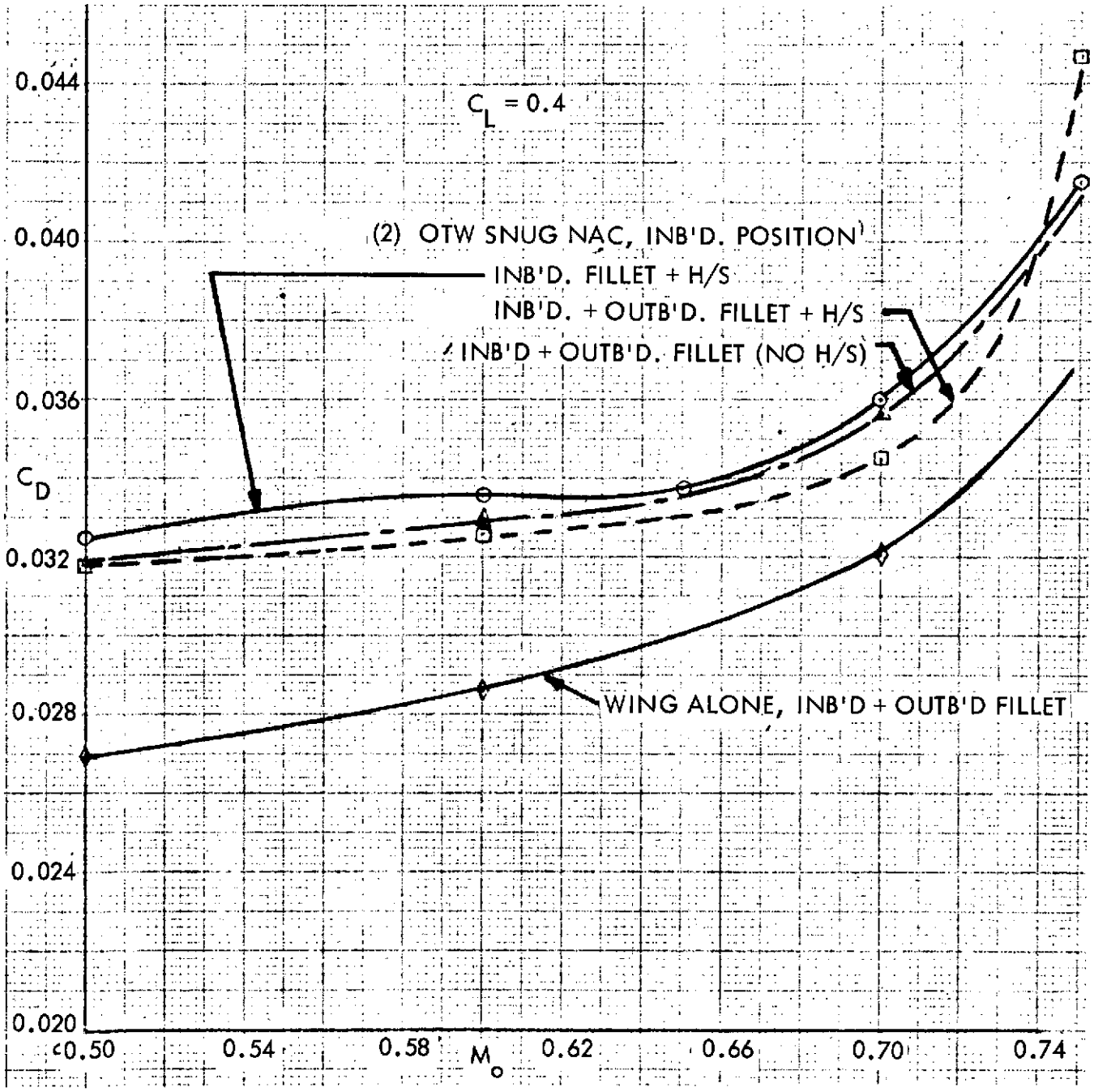

FIGURE 43: DRAG VARIATION OF INTEGRATED NACELLES ON MODIFIED (WAXED) WING

basic wing. Local contouring needed in the area of the wing leading edge for flow improvements required a stronger, more adhesive material than was afforded by the wax. Thus, the desired contouring could not be provided in the pylon-mounting case.

Direct, comparative data between the basic and modified wing results are shown in Figure 44 at a Mach number of 0.70. It is indicated here that from the standpoint of incremental nacelle drag, the upper-surface arrangement need be no worse than the underwing installation. The more important question, however, of the achievable drag level of the OTW installation was not directly answered by these tests inasmuch as the drag penalties of the waxed surface are unknown. The tests did indicate, however, that a properly combined theoretical/experimental approach provides a rapid and effective means of achieving significant improvements in the performance of the OTW system. A second generation test, based on the foregoing model modifications and theoretical analysis, will provide additional answers to the achievable drag levels of upper-surface nacelle configurations.

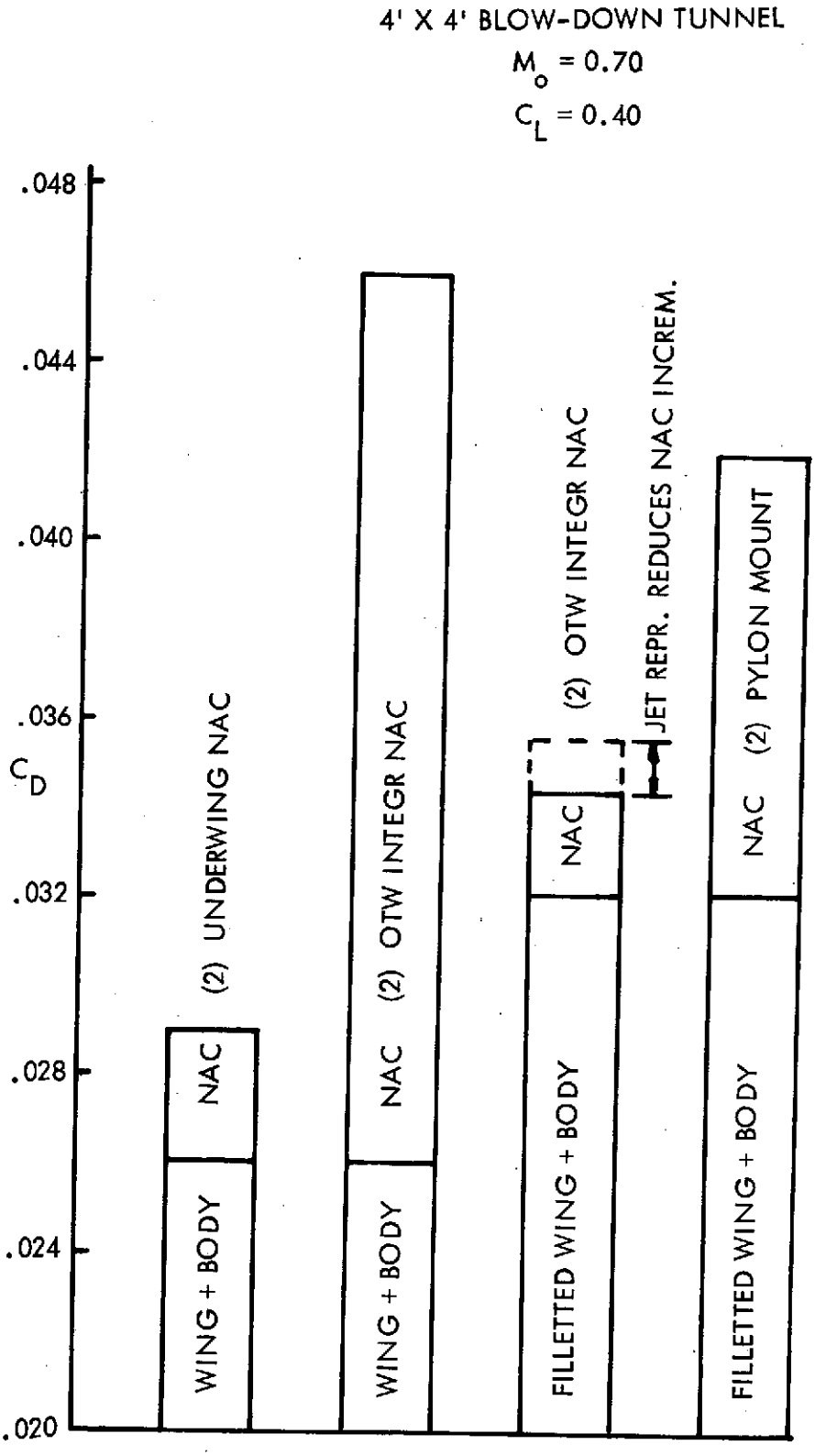

FIGURE 44: DRAG INCREMENTS FOR SEVERAL NAC/WING CONFIGURATIONS

4.4 OTW-IBF BASELINE MISSION VEHICLES

4.4.1 OTW-IBF Mass Flow Split

The variation of the proportions in which the fan mass flow is split between the OTW and IBF systems is a degree of freedom which is peculiar to the hybrid concept. The optimum is defined by the condition that the uninstalled engine thrust, i.e. engine size, be a minimum for a given field length and involves a compromise between the aerodynamically desirable split and the separate installation losses in each system. The optimum proportion is not a unique figure but a function of each parameter affecting either field performance or installation losses. It, therefore, is a function of FPR, aspect ratio, sweep angle, number of engines and, to a lesser degree, the spanwise nacelle location.

Typical 2, 3 and 4 engine IBF duct systems have been sized and their pressure losses analyzed to derive parametric duct loss data from which the preferred OTW-IBF mass flow split and the limits on installed thrust per unit wing area (T/S) could be defined for subsequent vehicle optimization. Figure 45 presents a schematic view of a representative two engine duct arrangement based upon a Coanda flap and four discrete chordwise ducts through the wing box from the fan bleed diffuser (not shown). The mass flow which can be diverted to the IBF system is heavily constrained by such consideration of the restricted duct space and the consequent pressure losses. Hence, increasing the duct mass flow (or Mach No.) produces diminishing returns in terms of IBF nozzle thrust as shown in Figure 46 and there is a well defined limit beyond which losses outweight gains in installed IBF thrust per unit wing area as indicated here. The typical variation of this limit with number of engines and FPR is also presented in Figure 46 . The corresponding variation of the total installed thrust (OTW plus IBF) required to meet a given field length with increasing IBF mass flow is indicated in Figure 47 from which the initial sharp reduction in T/W required for landing will be noted. This trend follows the establishment of attached flow over the flap and at higher IBF mass flows levels off as further IBF lift is derived from jet flap effects. Similar effects are detectable in the takeoff data but are less pronounced. Since the thrust recovery in the IBF system falls steadily as the IBF flow proportion increases, a specific "optimum" mass flow split can be identified at each wing loading at which the uninstalled thrust requirement is minimized. The OTW

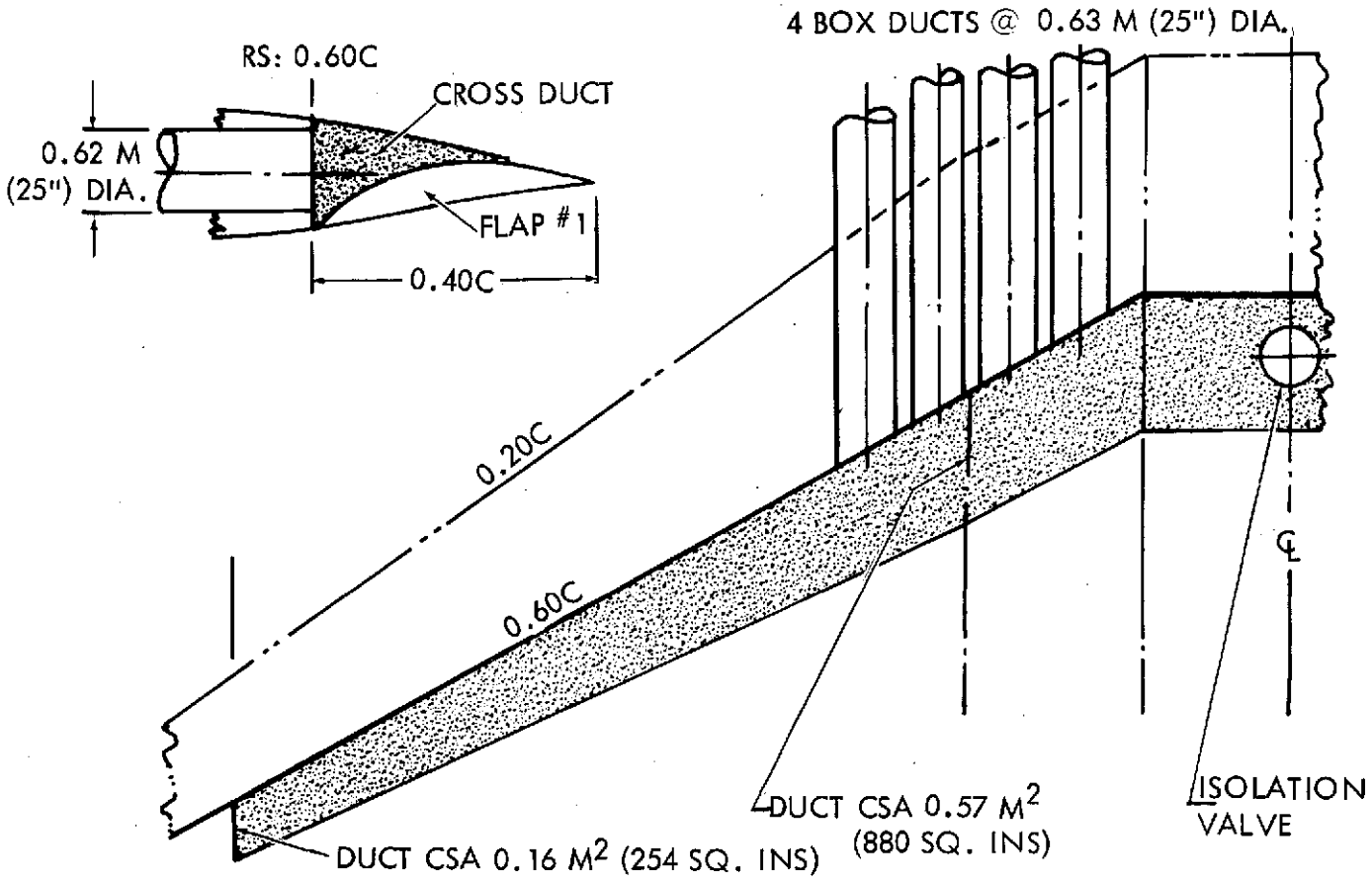

FIGURE 45: OTW/IBF - BASELINE FLAP AND DUCT CONFIGURATION

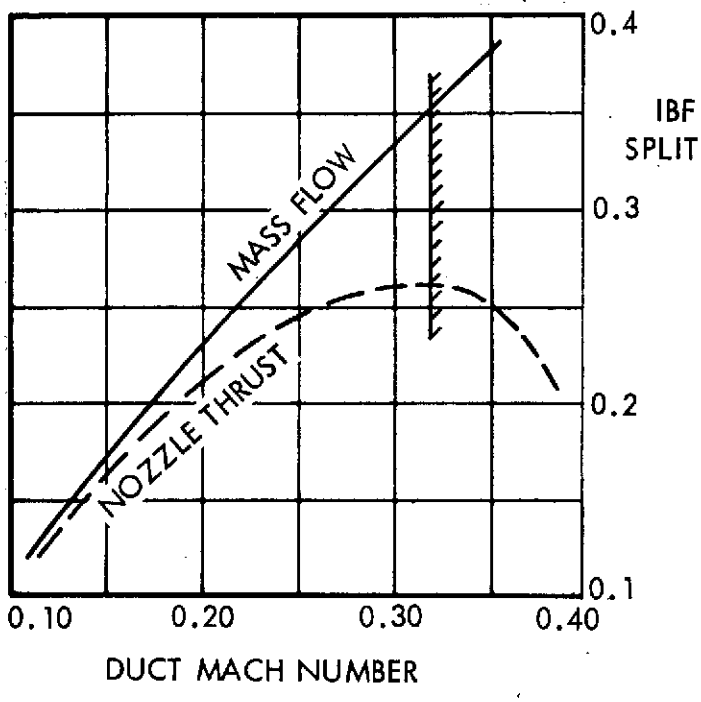

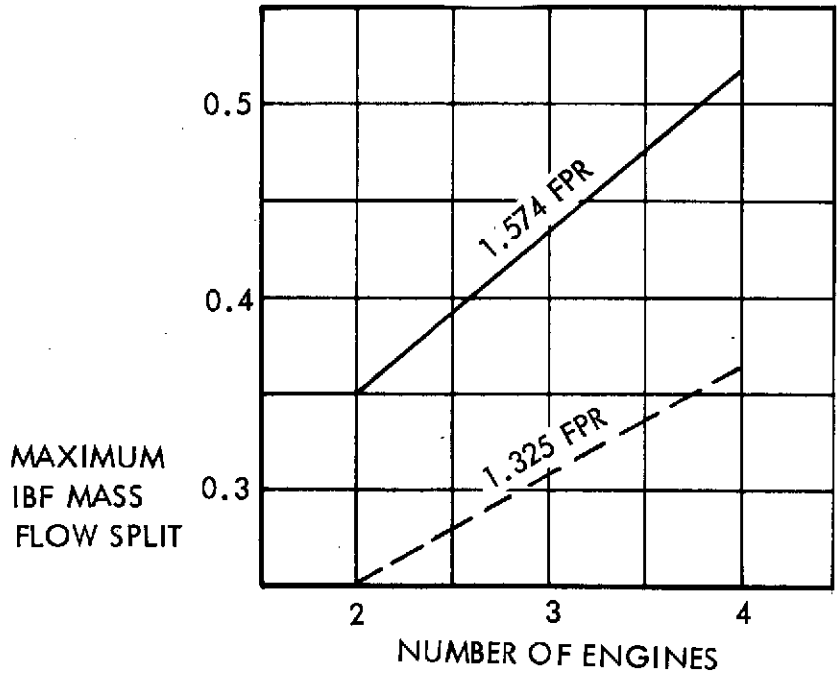

FIGURE 46: OTW/IBF - MAXIMUM IBF THRUST SPLIT

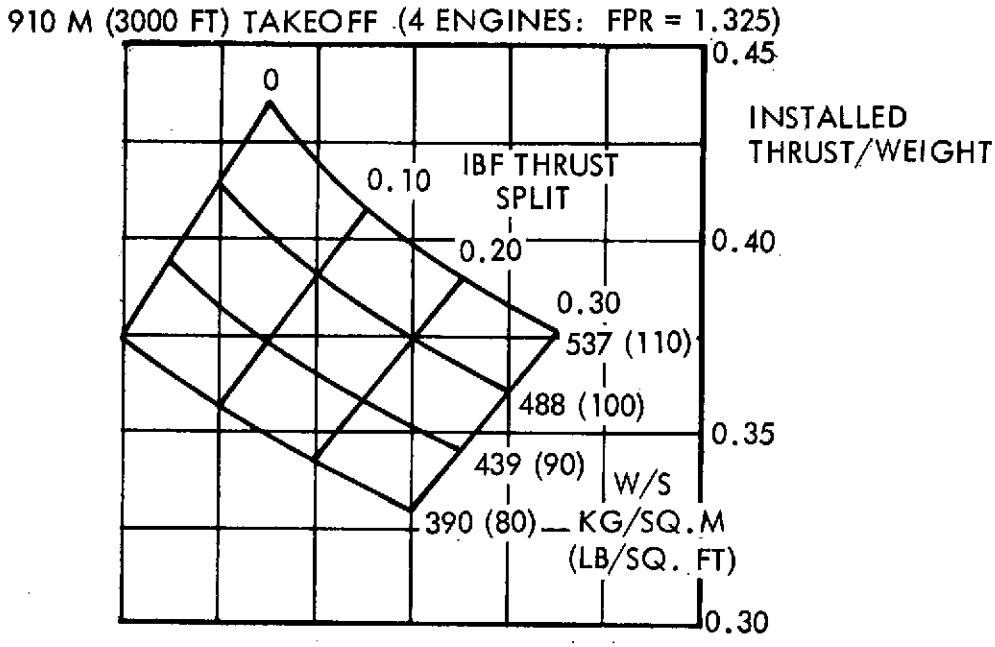

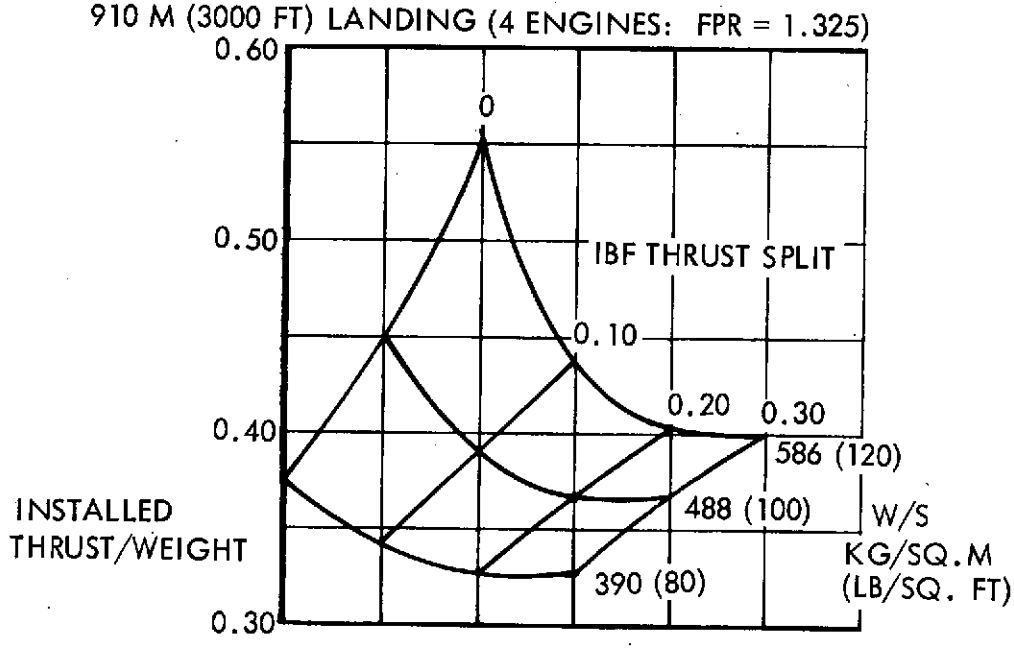

FIGURE 47: OTW/IBF - T/W VS W/S AND IBF THRUST SPLIT

thrust component is also limited by the ability of the flap to maintain attached Coanda flow and thus vector the OTW stream. Thus, with increasing wing loading, as the required thrust and flap setting increase according to Figures 47 and 48 ,respectively a point is reached at which Coanda separation precludes a further increase in both thrust and wing loading, i.e. a T/S limit is reached. When associated with the optimized mass flow split, the "optimum T/S limit" indicated in Figure 49 is defined beyond which no solution is possible other than by increasing IBF flow beyond its optimum value and accepting the increased system loss and lower efficiency. The upper bound to this process is reached when the IBF thrust is maximized as also shown in Figure 49. The "absolute T/S limit" in this instance corresponds to coincident maximum IBF and maximum OTW thrust components. Typical values of the optimum mass flow split and the "optimum" takeoff T/W for a 2 engine configuration are presented in Figure 50.

4.4.2 Optimum Number of Engines

Two, three, and four engine vehicles with representative aspect ratios at 30° sweep have been sized with optimized thrust splits as defined in the previous section. Figures 51 through 53 show the installed thrust to weight ratio at takeoff weight (T/W) and relative direct operating cost (DOC) plotted against wing loading at takeoff weight (W/S) for these configurations using FPR 1.325 variable-pitch and FPR 1.574 fixed-pitch fan engines. The figures show the T/W required to cruise at different cruise power settings (η_{PWR}) and takeoff from a 910 m. (3000 ft.) field length. The limitations on the combination of engine size and wing area from engine spacing, from installing ducts within the wing or from the ratio of the engine exhaust stream height to flap upper surface curvature are shown as a T/S limit on each figure. Since the wing loading of all the configurations was expected to be relatively high and part of the wing box would be used to accommodate ducting, the fuel volume limit is also shown. The selected airplanes are those configurations providing minimum direct operating cost within the limiting conditions and are identified on each figure. Comparisons of the attainable direct operating costs of the derived aircraft are presented in Figure 54 for the two fan pressure ratios between which the preferred engine may be expected to fall. Alternate engine production runs and cost assumptions are shown which may be regarded as representing either the use of an engine with both CTOL and STOL applications (1500 engines produced) or the use of a specialized

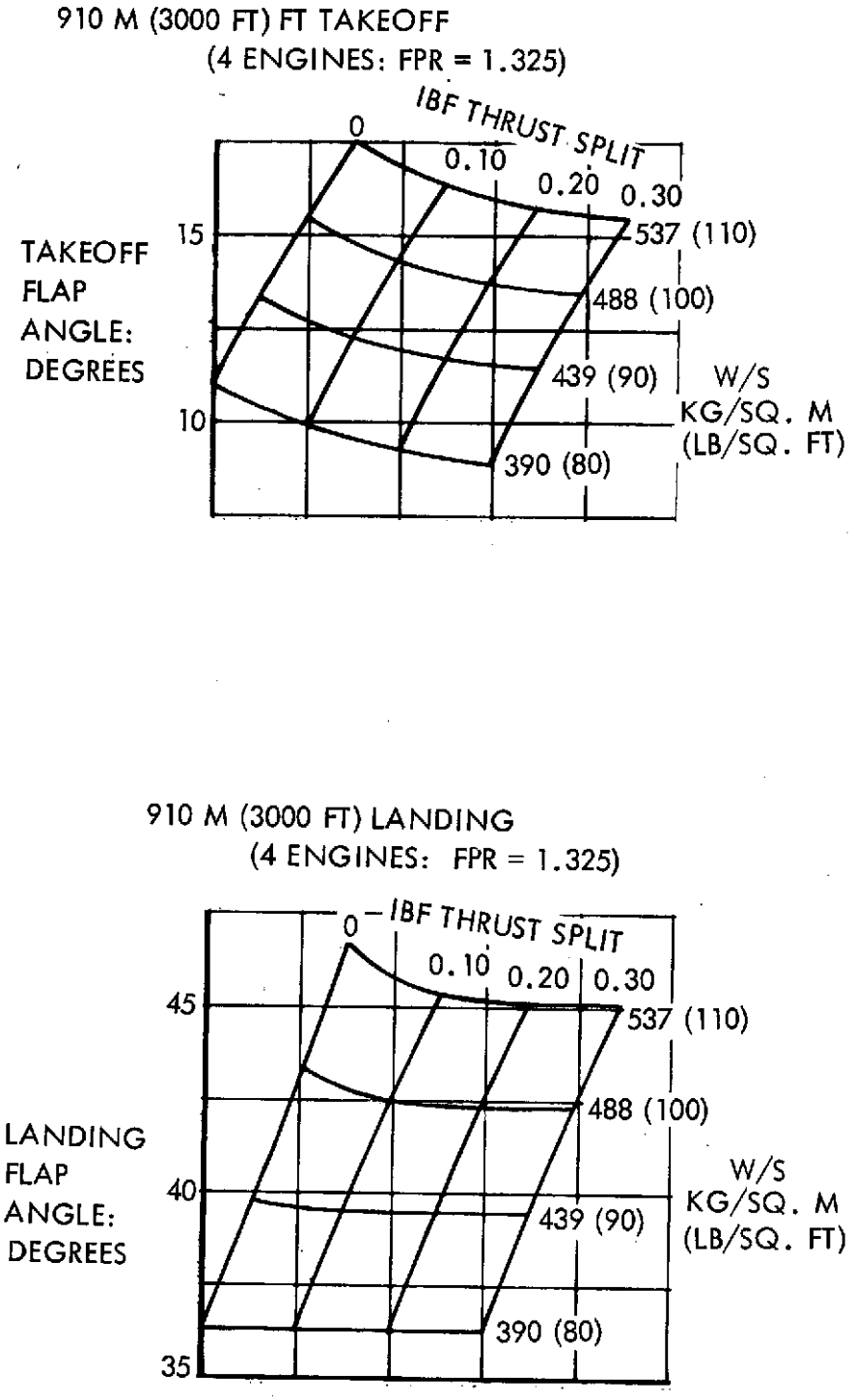

FIGURE 48: OTW/IBF - FLAP ANGLE REQUIREMENTS (4 ENGINES)

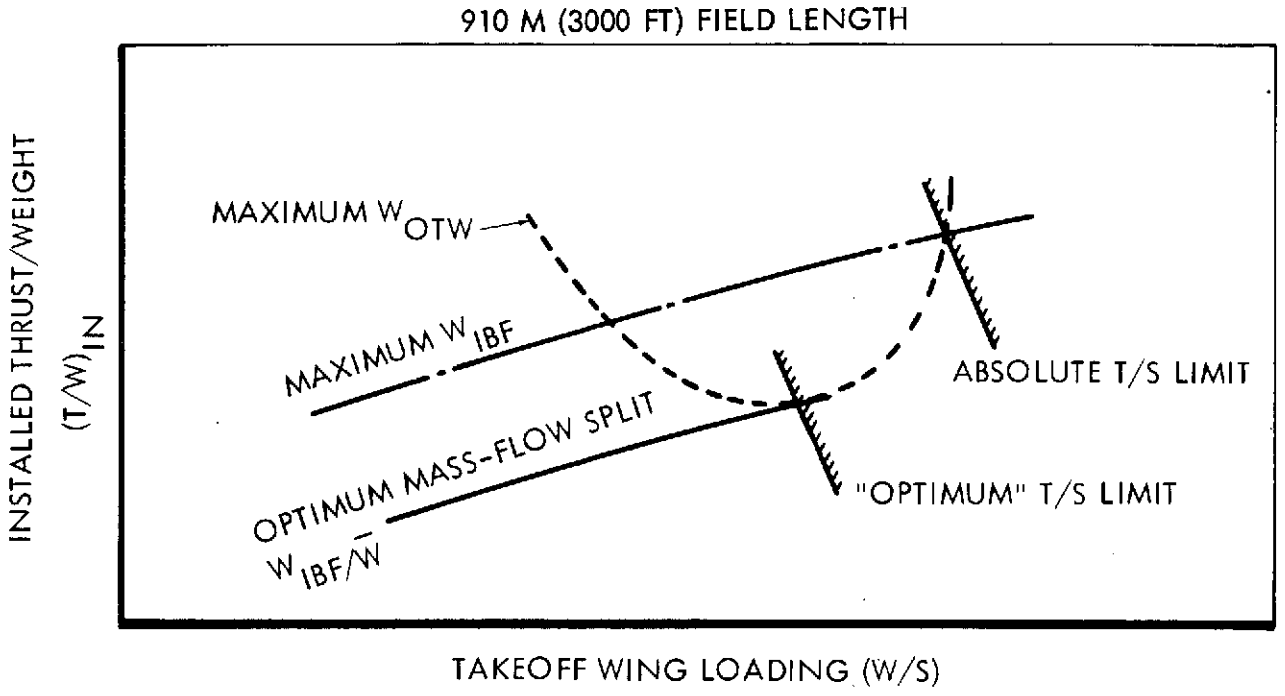

FIGURE 49: OTW/IBF: FIELD PERFORMANCE OPTIONS

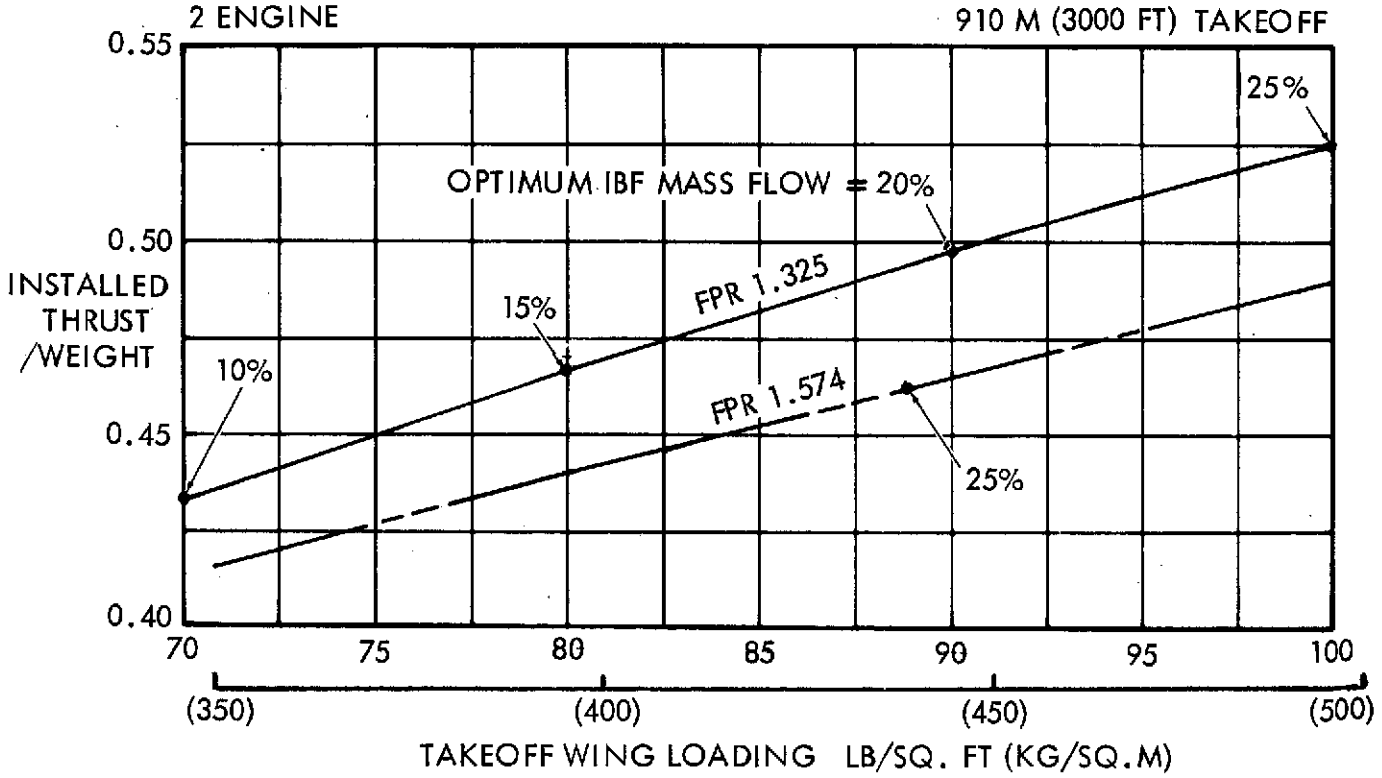

FIGURE 50: OTW/IBF - OPTIMUM IBF THRUST SPLIT

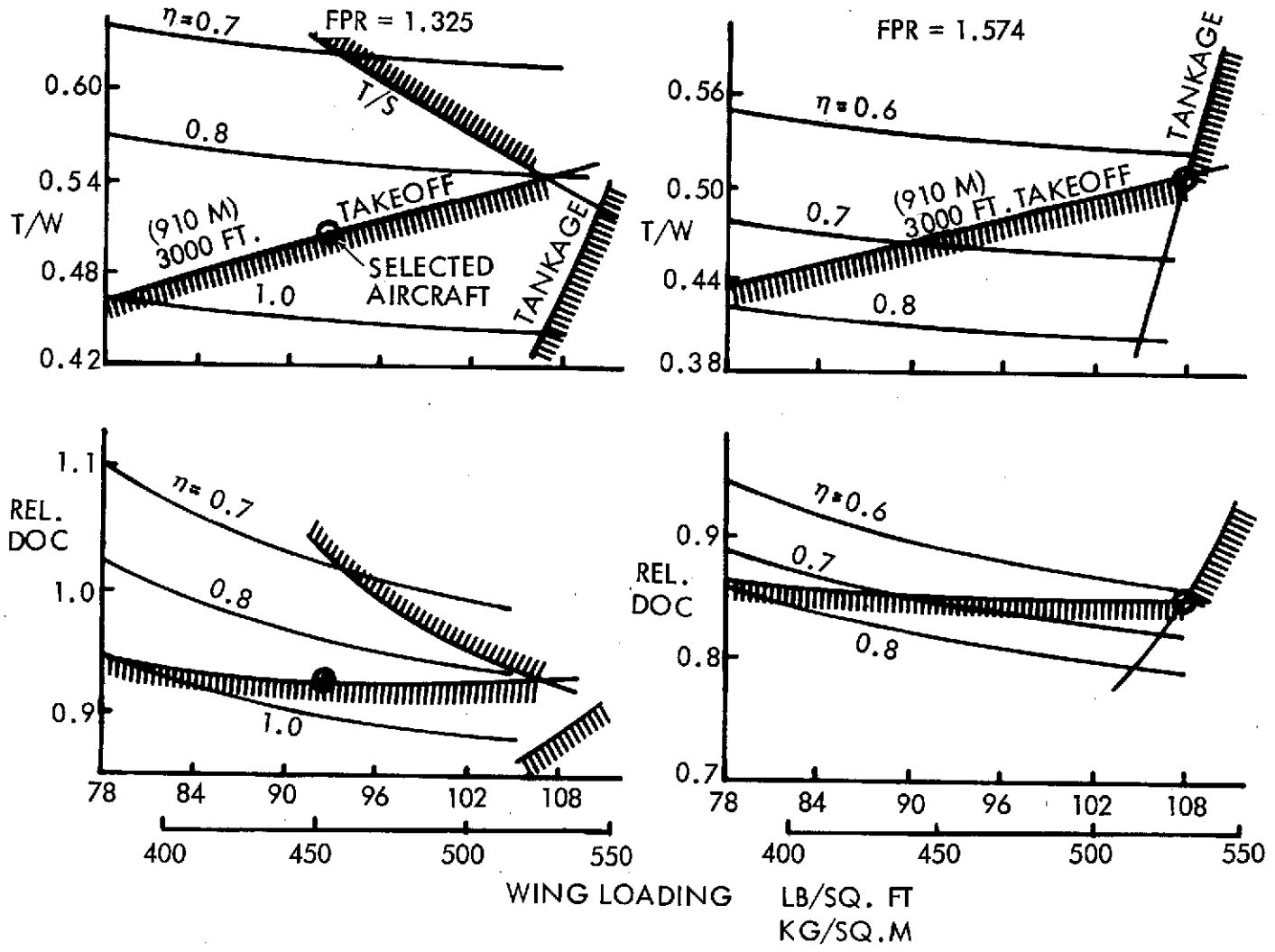

FIGURE 51: OTW/IBF - 2 ENGINE CONFIGURATION (AR = 7.0, 30° SWEEP)

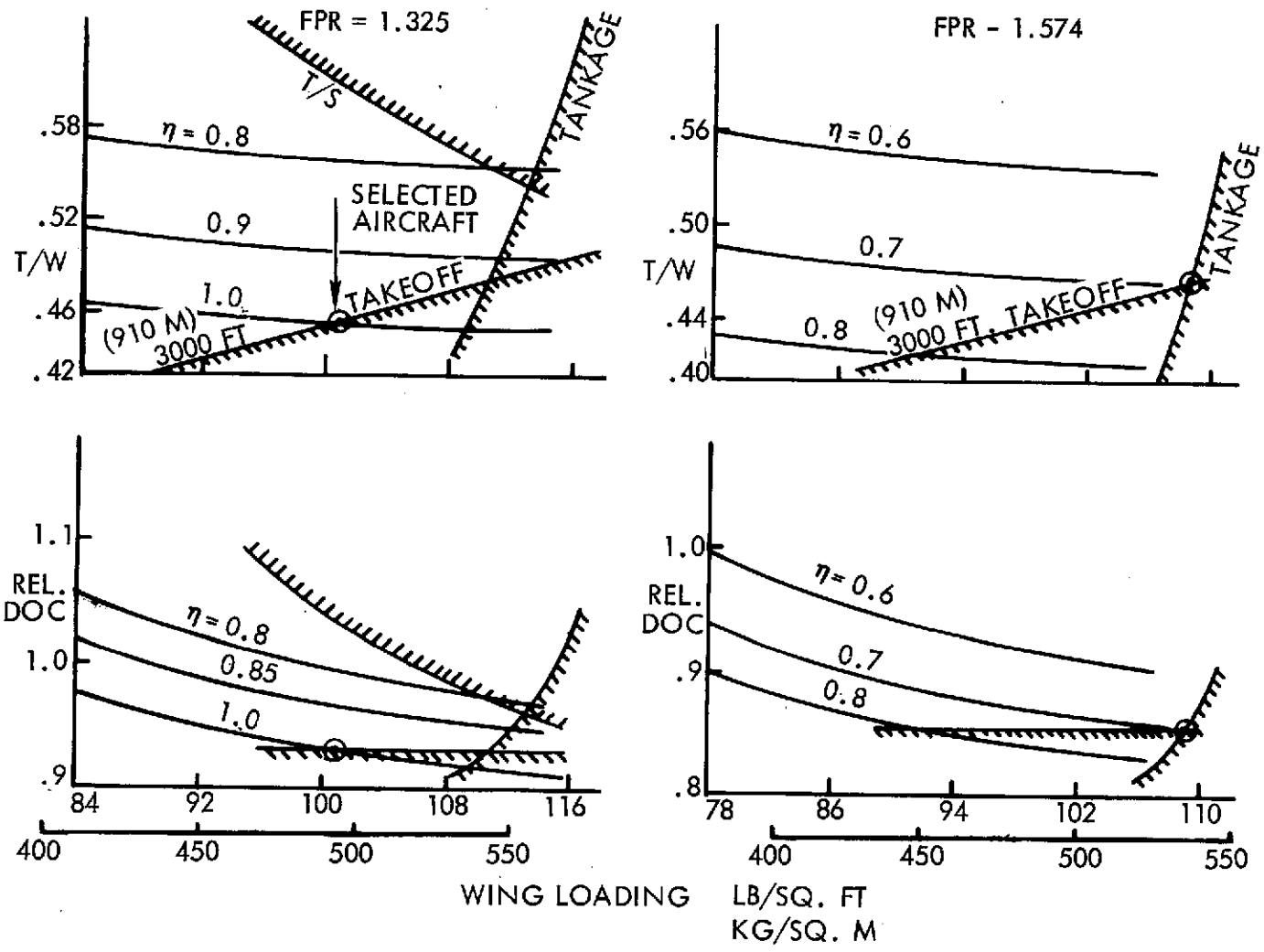

FIGURE 52: OTW/IBF - 3 ENGINE CONFIGURATIONS (AR = 6.75, 30° SWEEP)

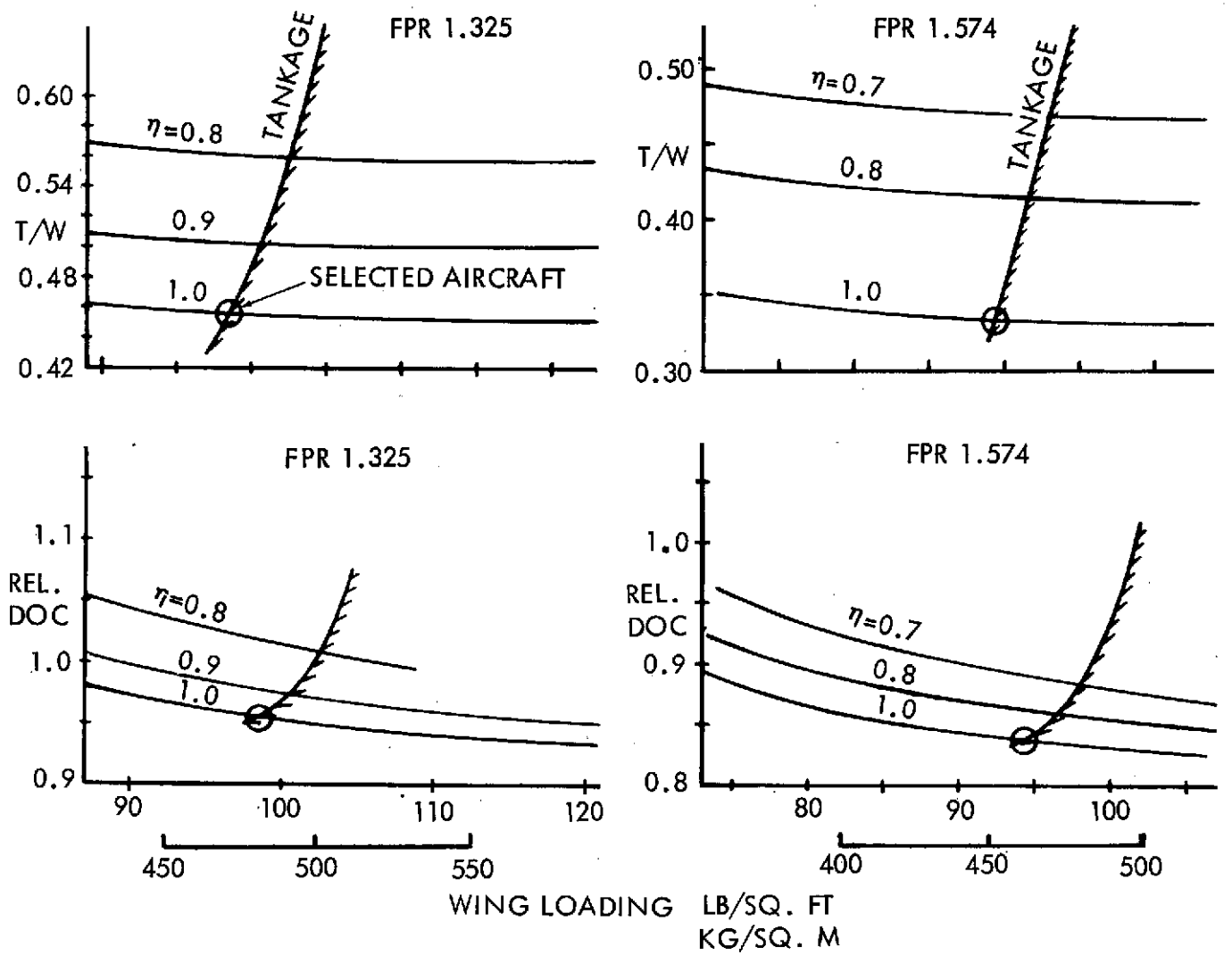

FIGURE 53: OTW/IBF - 4 ENGINE CONFIGURATIONS (AR = 6.5, 30° SWEEP)

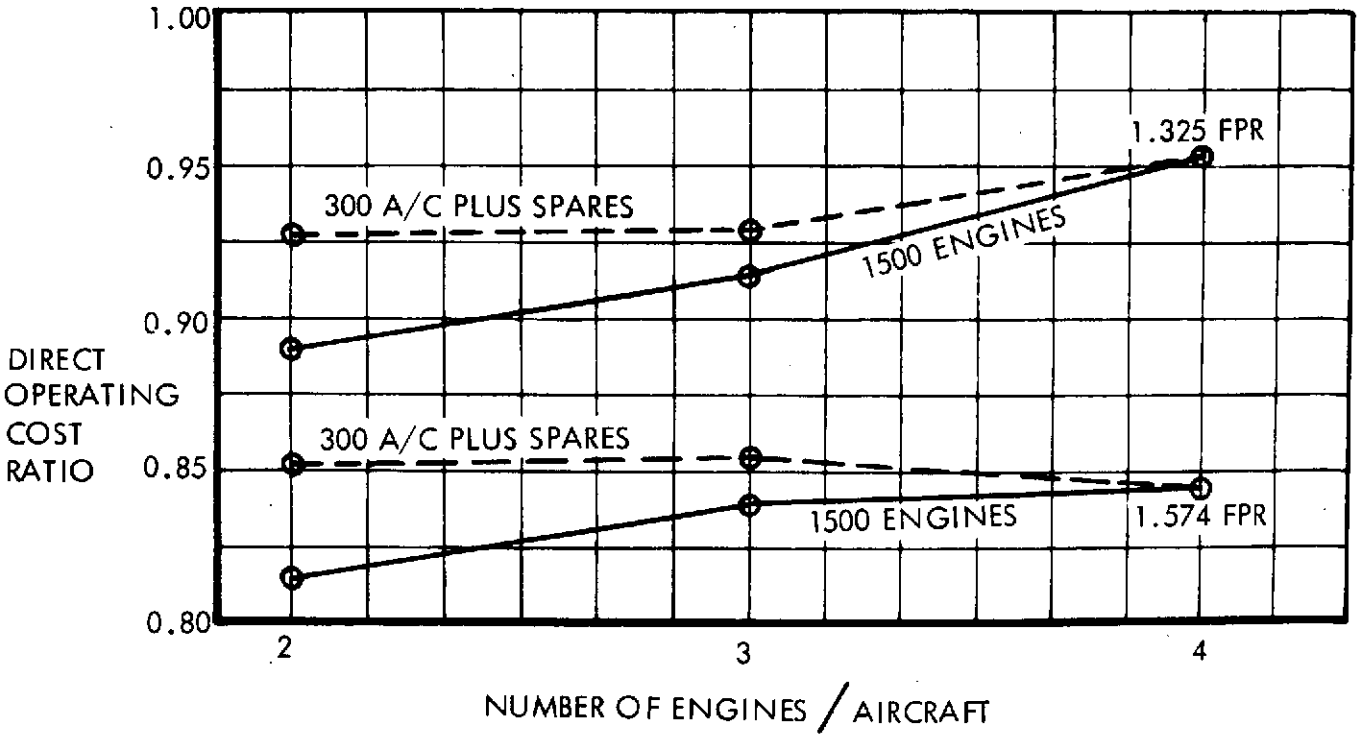

FIGURE 54: DOC VS NO. ENGINES

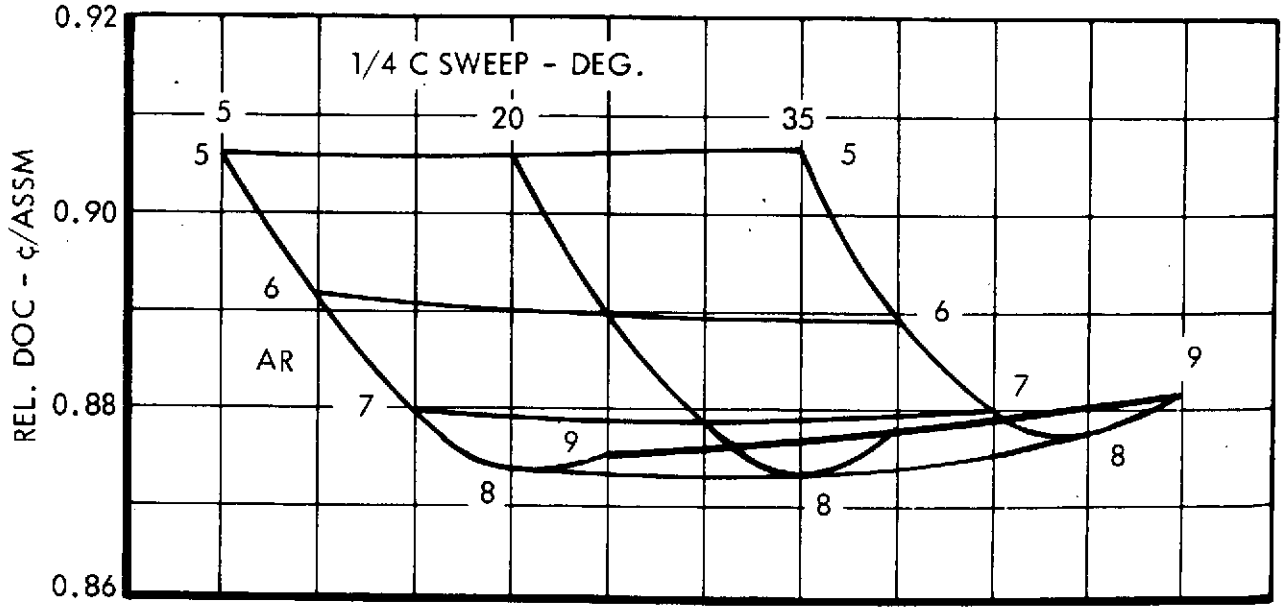

FIGURE 55: OTW/IBF TWIN DOC VS ASPECT RATIO AND SWEEP

STOL engine with no other immediate applications (300 aircraft sets plus spares). The 1.574 FPR engine shown is actually a "rubberized" RB.211 and therefore typical of current CTOL engines. From these data it has been concluded that the two engine configuration is generally superior to the other arrangements (at 1972 fuel prices) regardless of whether a CTOL or a STOL engine is used. The only possible exception is the slight advantage of the four engine arrangement with STOL engines at 1.574 FPR which is an improbable circumstance since there are already CTOL applications at this pressure ratio.

4.4.3 Optimum Aspect Ratio and Sweep

The variation with T/W and W/S of the preferred thrust split between the IBF and OTW systems has been determined for a number of combinations of aspect ratio and sweep. Two engine airplanes were then sized for minimum DOC-1 for a range of aspect ratios and sweep angles at a common fan pressure ratio of 1.325 with regard for the various design constraints as illustrated in Figure 51. These data are summarized in the variation of DOC-1 with aspect ratio and sweep selections shown in Figure 55. It has been concluded that DOC is relatively insensitive to sweepback but optimizes at about aspect ratio 8. Figures 56 and 57 show the variation of ramp gross weight and 500 N.M. mission fuel with aspect ratio for a range of sweepback angles. Ramp gross weight minimizes at about aspect ratio 7.5 to 7.8 while mission fuel continues to decrease with increase in aspect ratio but only slowly at aspect ratios higher than 7.5. An aspect ratio of 7.73 and sweepback of 20° were selected for further study of the 2-engine baseline mission vehicle.

4.4.4 Preferred Fan Pressure Ratio

Figure 58 presents the relative operating cost and noise levels at the FAR 36 measuring points of a family of two engine OTW-IBF vehicles as a function of the engine FPR. Each vehicle within this family has a 910 m. (3000 ft.) field performance which is predicated upon a near-optimum OTW-IBF thrust split at its respective FPR and is similarly identified with the optimum aspect ratio and sweep. From these data the FPR 1.35 engine with a fixed pitch fan has been selected (on the basis of comparing DOC vs noise level) as the preferred FPR for the derivation of the preferred baseline mission vehicle. This has implied the selection of one of two arbitrary noise levels for concept comparisons, i.e.

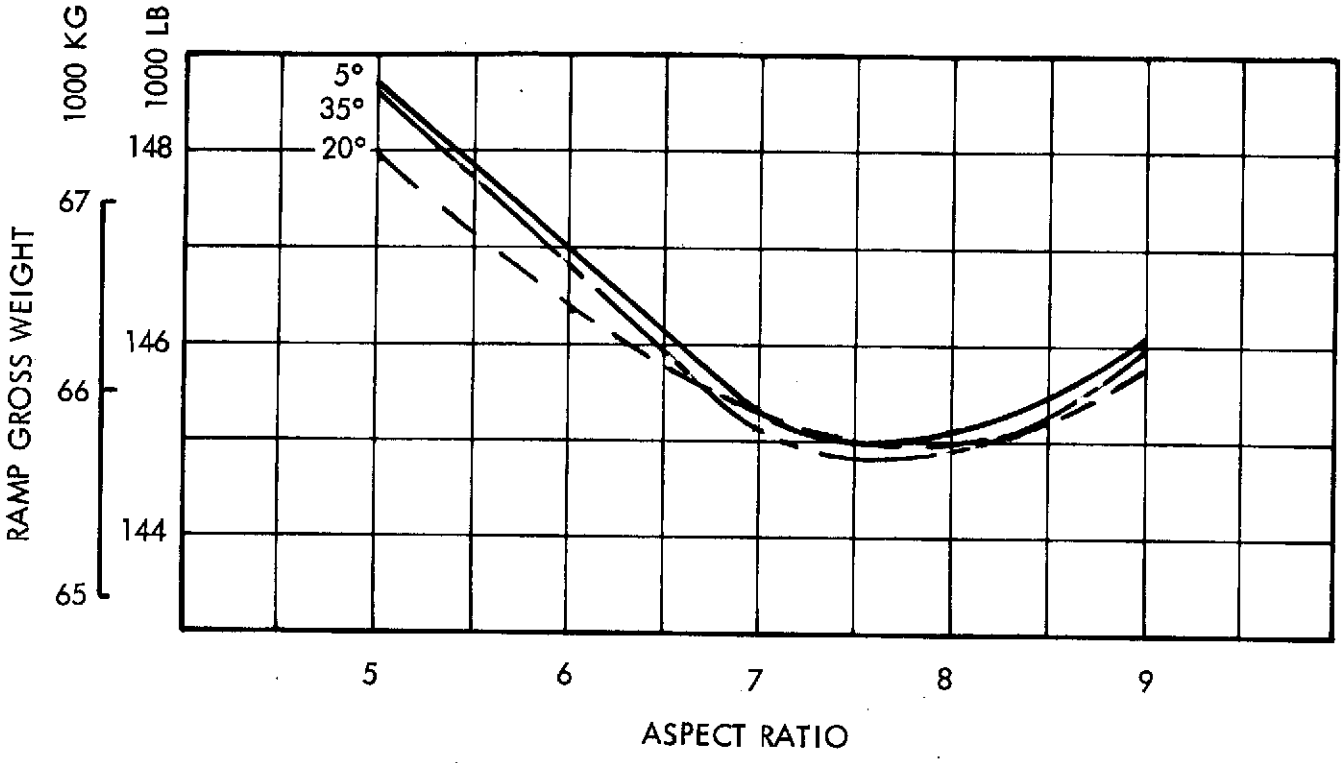

FIGURE 56: OTW/IBF TWIN - RAMP GROSS WEIGHT VS ASPECT RATIO (FPR 1.325)

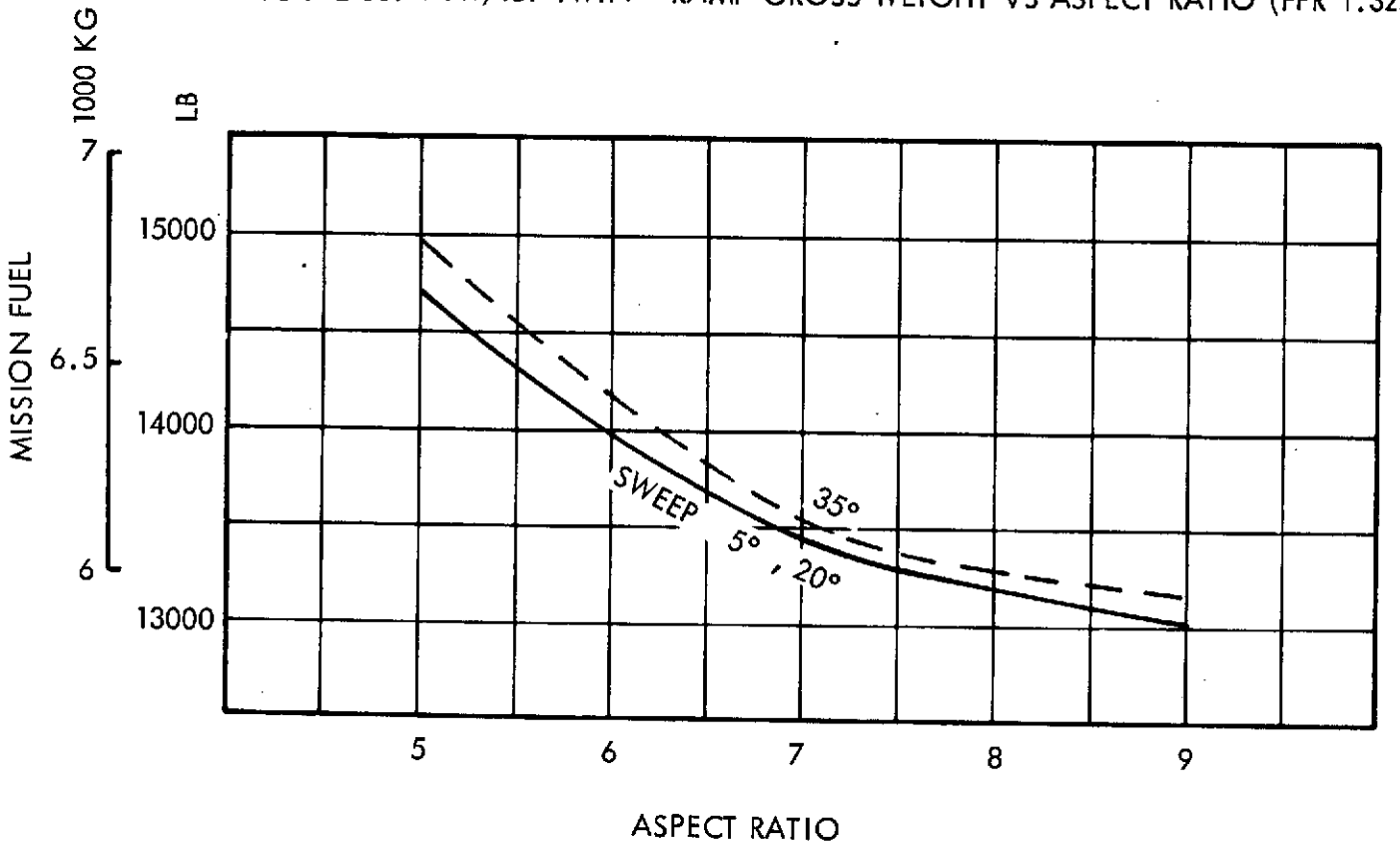

FIGURE 57: OTW/IBF TWIN - MISSION FUEL VS ASPECT RATIO (FPR 1.325)

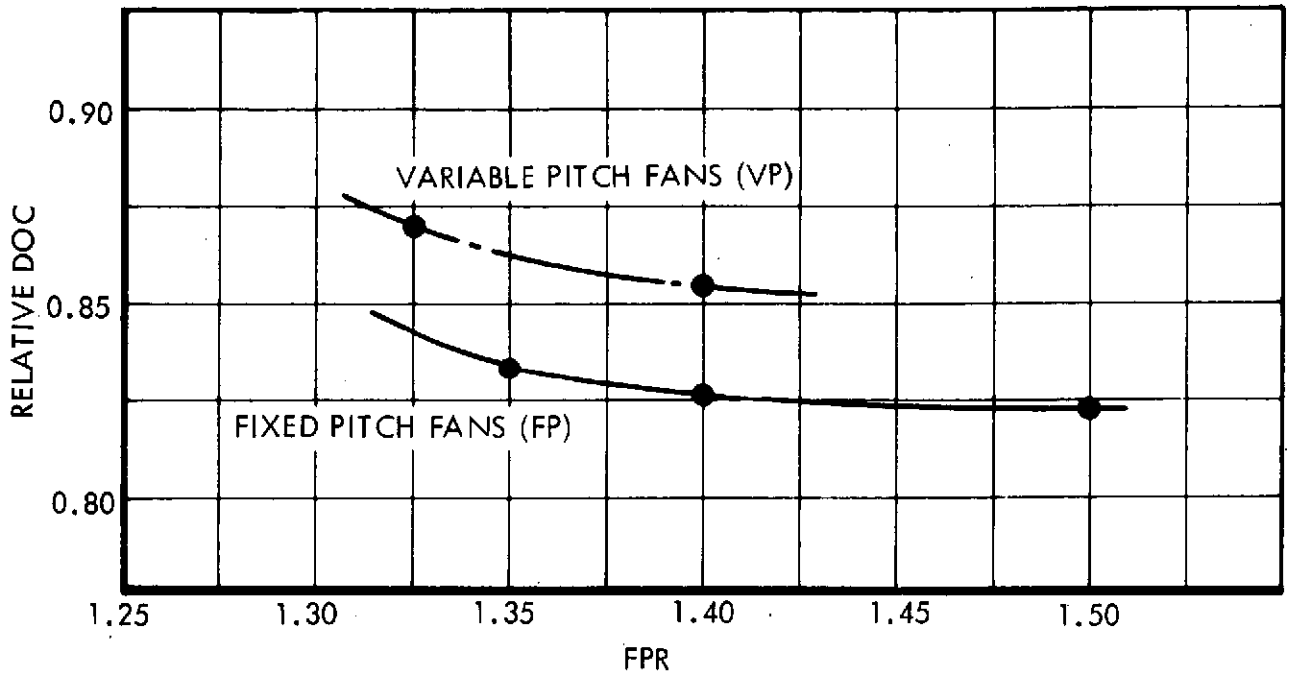

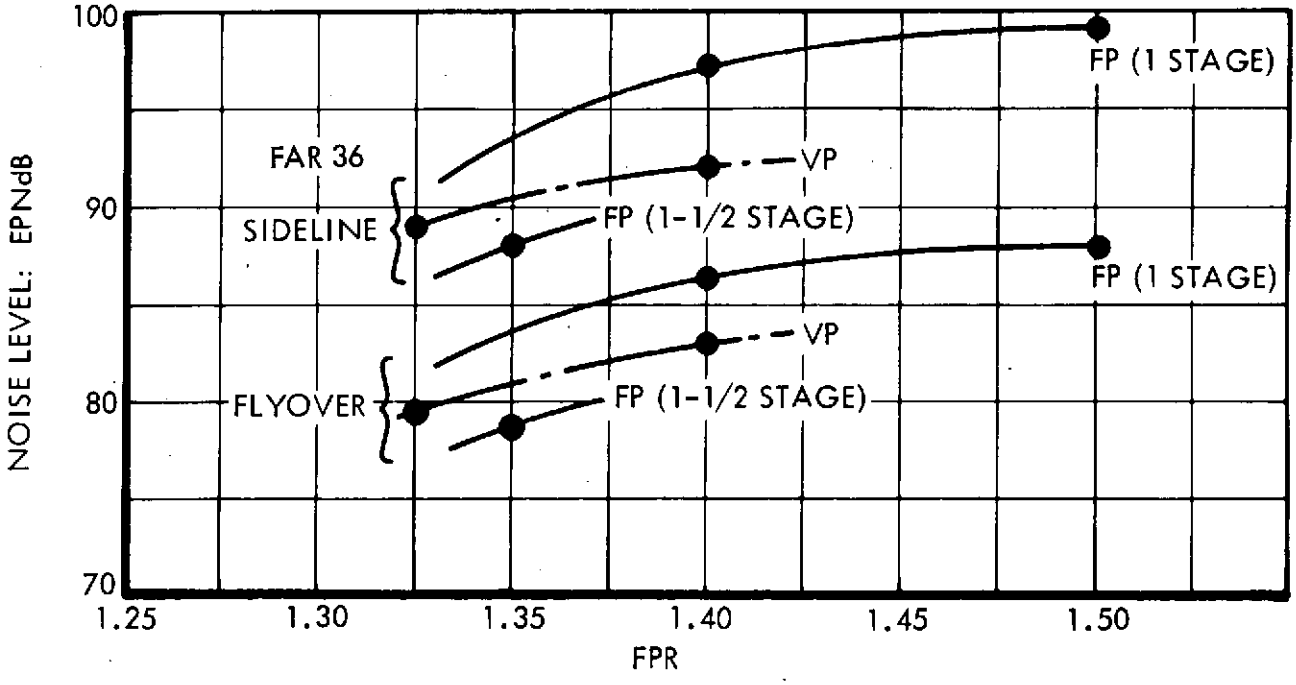

FIGURE 58: OTW/IBF TWIN: DOC AND NOISE LEVEL VS FPR

that corresponding to the preferred STOL engine; the second has been defined in general terms by the alternate use of a modern technology CTOL engine at FPR 1.47.

It should be emphasized that Figure 58 is based upon discrete engine points, having a common gas-generator technology but certain differences in fan design parameters. Hence, it is not possible to be dogmatic about the conclusions to be drawn. In particular, the VP fans have rather lower fan tip speeds than the single stage FP fans and the 1-1/2 stage FP fan has a still lower tip speed. However, it does appear that if a really useful reduction of 15-20 dB below FAR 36 requirements is to be attained without substantial DOC penalty, the best candidate is a 1.35 FPR engine with a 1-1/2 stage fixed pitch fan. Notwithstanding the advantages of the VP fan with regard to the ease of providing reverse thrust and quick throttle response, the additional weight, size and cost appear to be unacceptable in the OTW-IBF application. It should be noted that this conclusion is drawn in the context of the hybrid concept. The overwing nacelle requirements in this installation do not permit significant savings through the elimination of conventional thrust reversers. Hence, the added engine cost of the variable pitch feature is not compensated for by thrust reverser saving. (An under-wing nacelle, such as MF or EBF, does afford the tradeoff of variable-pitch cost against saving of nacelle thrust reversers.)

4.4.5 Selected Baseline Mission Vehicles

Figure 59 illustrates the derivation of the preferred configuration two-engine baseline vehicle in relation to its design constraints for a capacity payload range of 926 Km (500 n.mi.). A 3 view of this vehicle which is directly comparable with the 910 m. (3000 ft.) OTW-IBF derived in Reference 2 is presented in Figure 60.

Subsequent analysis of the OTW-IBF vehicle, as described, and with the structural provisions for alternate R/STOL operation with capacity payload over a 2780 Km (1500 n.mi.) range has yielded the comparative data presented in Table IV . It has been shown that despite the significant increase in operating weight empty which these provisions entail, the added operational flexibility permits a sufficiently enhanced annual utilization (from 2500 hours to 2980 hours) to reduce the DOC in the performance of the baseline

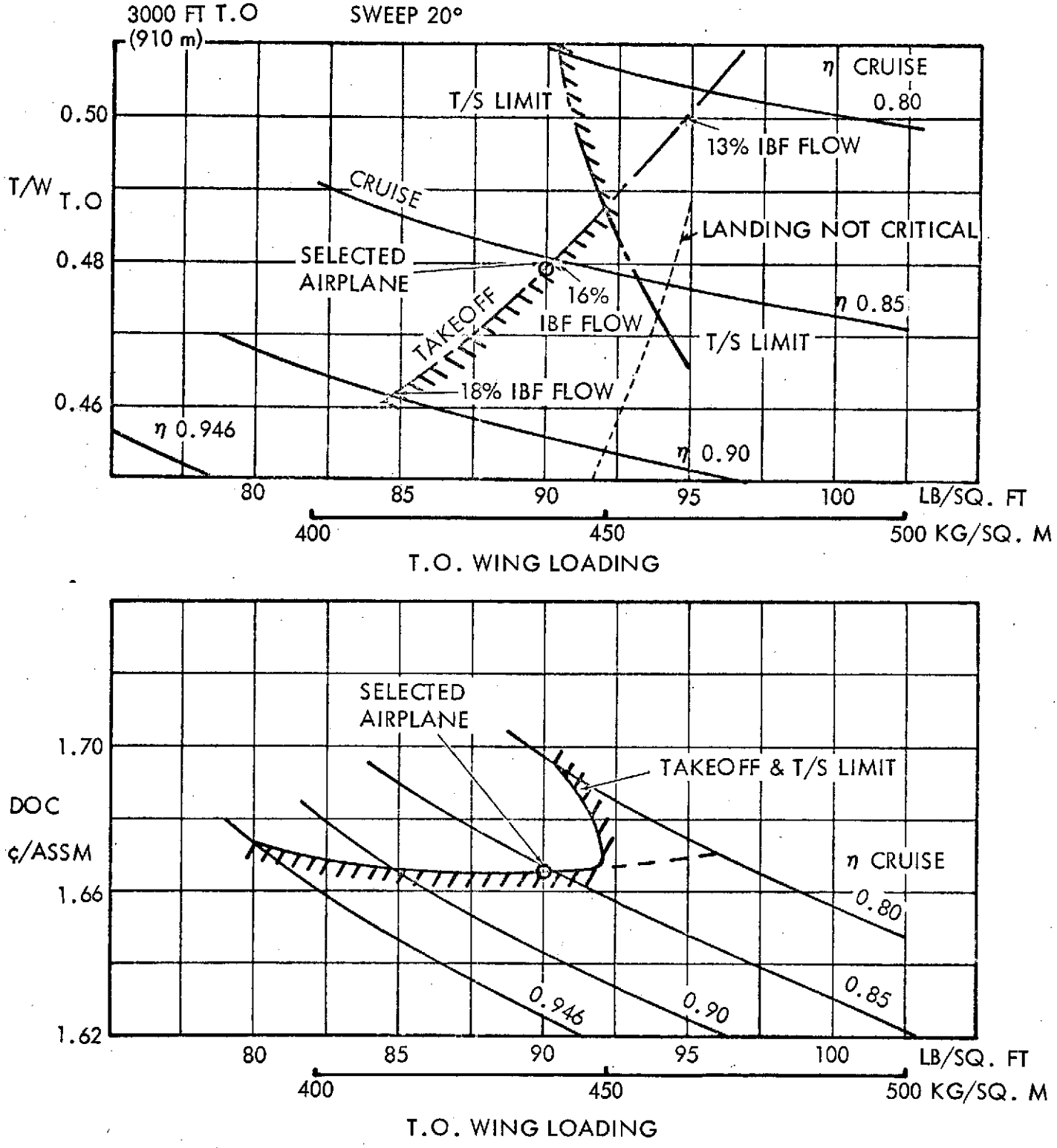

FIGURE 59: OTW/IBF TWIN - CRUISE AND TAKEOFF MATCHING (FPR 1.35; AR 7.73)

148 PASSENGERS

0.8 MACH

910 M (3000 FT) FIELD LENGTH

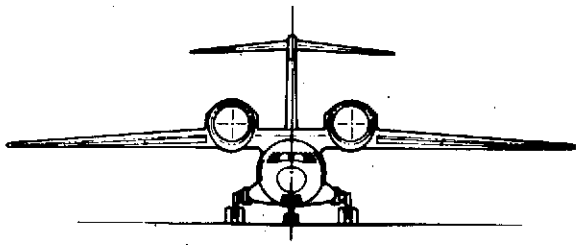

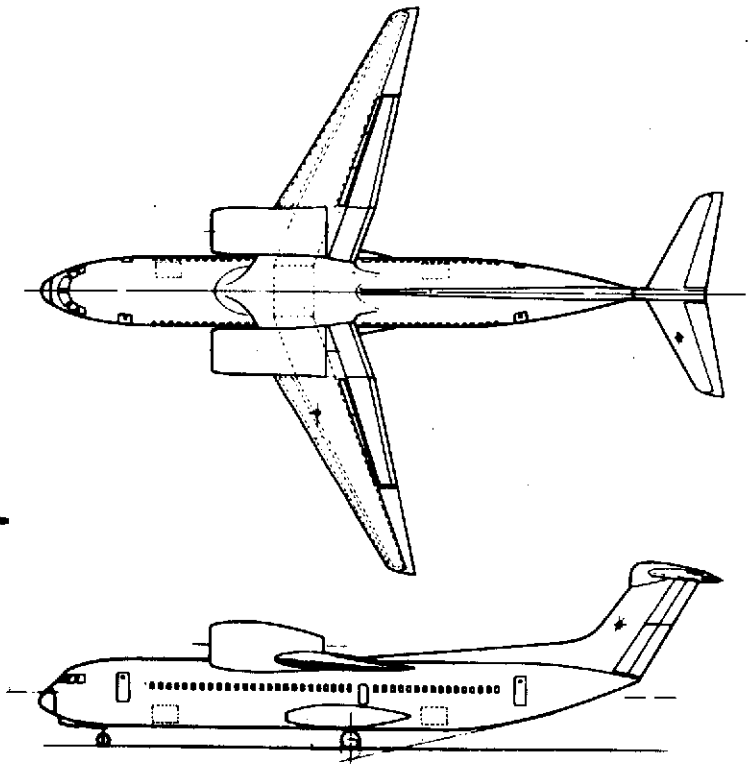

SPAN = 35.56 M (116.66')

LENGTH = 42.57 M (139.66')

HEIGHT = 11.78 M (38.66')

FIGURE 60: 910 M (3000 FT) OTW-IBF VEHICLE

TABLE IV: COMPARISON OF OTW-IBF STOL AND R/STOL VEHICLES

NO. ENGINES	2	FIELD LENGTH	910 m. (3000 FT.)
FAN PRESSURE RATIO	1.35 (FP)	NO. PASSENGERS	148
ASPECT RATIO	7.73	CRUISE SPEED	0.8 M
SWEEP ANGLE	20°	INITIAL CRUISE ALTITUDE	9140 m. (30,000 FT.)

	STOL	R/STOL	
RATED THRUST/ENGINE - KN - (LB)	161.8 (36,380)	175.5 (39,447)	
OPERATING WEIGHT EMPTY - Kg - (LB)	42,847 (94,460)	45,670 (100,684)	
STAGE LENGTH - Km - (N.MI.)	926 (500)	926 (500)	2,778 (1,500)
RAMP GROSS WEIGHT - Kg - (LB)	64,407 (141,990)	68,120 (150,176)	75,987 (167,520)
INSTALLED THRUST/WEIGHT - N/Kg - (LB/LB)	5.02 (0.479)	5.15 (0.490)	4.62 (0.440)
TAKEOFF WING LOADING - Kg/m^2 - (LB/SQ.FT.)	439 (90.0)	449 (92.0)	501 (102.7)
MISSION FUEL - Kg - (LB)	5,774 (12,730)	6,687 (14,742)	14,554 (32,086)
DIRECT OPERATING COST - ¢/ASSM			
(@ 2500 HRS. UTILIZATION)	1.666	1.728	1.322
(@ 2950 HRS. UTILIZATION)	-	1.595	-

```
 BASE 1.35FPR 150.NM HYBRID UPDATE NF0135SFCBD/03ROTWIBF 4/17/74        I1985=0      IVEC=0      ITR=1

STOL DISTANCE=30.  .FT   MACH= .80    RANGE=150  .NM   PAYLOAD= 30.40.LB    NO. OF SEATS=   148.

START CRUISE ALT=30.  .FT   SWEEP=20.  DEG   AR= 7.73   CDC=10.   CDMISC=   .0    DDM=.00

IVER=8   IMACH=4   IENG= 48  VBARH=VARIABLE  VBARV=VARIABLE  ETAPWR= .928  SFCFAC= 1.039    ETAMAX= 1.06
NO.ENG USED INITIAL CRUISE=2.     ENG COST FACTOR= .80       IGEAR=0     IRANGE=1     ULF= 3.750     CRUISE= 1
 WSP     S     TUN     PR  PRPI  RAMPWT     W2        W3        W4        W5        OWE       CL    L/D    FVR    RESV     FUEL     VBARH
FLTIM DSTZ3  ROC     N  T/W R  W/S R    ZFWR      TWTO5    TWLG5    W/S 5     TOS     TOC    DOC1  FVRCS  DOC2   DOC4      VBARV
 99.3 1622. 39447. 1.35 1.35 167520. 160562. 161112. 135796. 135434. 100684.  .353 15.09  .814   4406.  32086.    .922
 3.34 77.8  1495.   0    .480  102.7  1.00      .491      .491      92.0    45.18  13.13  .32   .643  1.543  1.984      .092

    DRAG BUILDUP, MACH NO. =   .80
 INITIAL CRUISE LIFT COEFFICIENT=   .353
CDWING  CDFUS  CDPYL  CDNAI  CDHOR  CDVER  CDPOD CDRUFF CDCOMP  CDTRM  CDMISC CDINT   CDO     CDI   CDTOT
.0051  .0 584 .00 .  .00 8  .0 114 .0  84  .  92  .   78 .0 1   .0  5  .  .    .0  78 .0173 .0 572 .0234
  WETTED AREA/WING AREA
WING=1.719 FUSELAGE=2.873 NACELLES=1.160 PYLON= .0   H TAIL= .381 V TAIL= .308 STOT/SREF=6.441

TOCWING     SWING         AR       TAPER      FUS LEN   FUS SWET   THRUST     SHOR       SVERT       DNAC       INVERT
    .1313   1622.48       7.73       .30      136.25    4661.38   39434.77    304.61     246.29       9.94        .00

    WWNG          WHOR          WVER          WFUS          WLG           WHYD          WSC           WPR
   18501.67       1868.16       1711.86       2 164.35      7035.84       1397.64       4192.91       13874.69
   WELEC          WAPU          WINSTR          WAV           WAC           WAI           WFUR          DUCTW
    1922.64        969.35          70.00       1250.00       2437.06        686.21       10656.00       1296.59
   WNAC          WPYL          WOPIT          WEMTY           OW            ZFW           AMPR           GW
   7371.22          .00        2653.81       98030.18      166683.98      13 023.98       83511. 3      167509.60
   SWING          AR          SWEEP          WGRSS          WFUEL          PAYLD          THRUST         TAPER
    1622.48        7.73          16.40       167519.93      36485.61       30 40.        394 7.49          .30
   TCROOT         TCTIP          SHOR          SVERT         FLENGTH        FUSAREA       DELPRESS        VDIVE
    13.91          10.63        304.61         246.29         136.25        4661.38          8.80        408.86
 RANGE/D.O.C. DATA
    RANGE      DOC1       DOC2       DOC4       DOC10
     500.      1.728      2.032      2.640      4.463

TOTAL COST OF
A/C LESS ENG  TOTAL ENG  COMPLETE A/C      FUEL50.
   6720875.    2110214.      8831089.       14742.
DOLLARS PER NAUTICAL MILE COST OF:
  CREW       FUEL       INSURANCE A/C LABOR A/C MATL ENG LABOR ENG MATL MTNCE BURDN DEPRECIATION TOTAL
     .557       .518        .196       .110       .101       .063       .160       .311       .928      2.945
    1500.      1.322       1.543      1.984      3.307
     400.      1.877       2.209      2.874      4.867
     300.      2.125       2.503      3.260      5.531
     200.      2.619       3.089      4.029      6.849

 99.3 1622. 39447. 1.35 1.35 167520. 160562. 161112. 135796. 135434. 100684.  .353 15.09 .814   4406.  32086.    .922
 3.34 77.8  1495.   0    .480  102.7  1.00      .491      .491      92.0    45.18  13.13 1.32  .643  1.543  1.984      .092
   1.0000     1.0000     1.000      1.000      1.00       1.0 00
   1.0000     1.0000     1.000       .8800     1.0        1.0 0
   1.000      1.0000     1.000      1.000      1.0         .00
DOVRS 00.00  FPOF 0.0 0.  FPUF 00  0  ERMD 0 00
 ***** TASK UNITS=1       ACCUM TTL=47     CORE=19968     CORE SEC=212      ACCUM CPU=94      ****
@COPY,S 1500M135HY2E/SIZ,1500M135HY2E/SIZRV1
FURPUR 0018-04/18-10:37
@COPY,S 1500M?
```

FIGURE 61: COMPUTER SIZING DATA: 2 ENGINE OTW-IBF @ 1.35 FPR, 910M (3000 FT) FIELD

```
 BASE 1.35FPR 1500NM HYBRID UPDATE NF0135SFCBD/03CROTWIBF 4/17/74        I1985=0      IVEC=0      ITR=1

STOL DISTANCE=2000.FT   MACH= .80   RANGE=1500.NM   PAYLOAD= 30340.LB   NO. OF SEATS=  148.

START CRUISE ALT=30000.FT   SWEEP=20.0DEG   AR=10.00   CDC=10.   CDMISC=   .00   DDM=.080

IVER=8    IMACH=4    IENG= 48  VBARH=VARIABLE  VBARV=VARIABLE  ETAPWR=1.000  SFCFAC= 1.000    ETAMAX= 1.060
NO.ENG USED INITIAL CRUISE=4.     ENG COST FACTOR=1.0000     IGEAR=0     IRANGE=1     ULF= 3.750    CRUISE= 1
 WSP     S     TUN     PR  PRPP RAMPWT     W2      W3      W4      W5      OWE      CL    L/D    AVG   RESV     FUEL    VBARH
FLTIM DST23  ROC     N  T/W R  W/S R   ZFWR    TWTO5   TWLG5   W/S 5    TOS     TOC    DOC1  FVRCS  DOC2  DOC4     VBARV
102.0 1517. 16758. 1.35 1.35 161360. 160546. 154754. 132688. 132380.  98084.  .363 15.83 .931   3949.  28980.    .907
 3.38104.9  1094.   0   .388  105.8  1.00     .429    .429     95.6   41.05  12.72 1.413 .751  1.613  2.012     .091

    DRAG BUILDUP, MACH NO. =   .8000
 INITIAL CRUISE LIFT COEFFICIENT=   .363
CDWING  CDFUS  CDPYL  CDNAI  CDHOR  CDVER  CDPOD CDRUFF CDCOMP  CDTRM  CDMISC CDINT   CDO    CDI   CDTOT
.00528 .00625 .00000 .00077 .00098 .00091 .00098 .00081 .00155 .00050 .00000 .00081 .01828 .00466 .02294
  WETTED AREA/WING AREA
WING=1.746 FUSELAGE=3.072 NACELLES=1.054 PYLON= .000 H TAIL= .319 V TAIL= .335 STOT/SREF=6.524

TOCWING    SWING        AR      TAPER     FUS LEN   FUS SWET  THRUST    SHOR      SVERT      DNAC      TRVERT
   .1272   1517.20     10.00       .30    136.25    4661.38  16758.79   238.31     249.26      6.48       .00

   WWNG          WHOR          WVER          WFUS          WLG          WHYD          WSC          WPP
  20384.37      1461.53       1732.54      22050.43      6777.12      1363.50      4090.50     11808.73
  WELEC         WAPU         WINSTR         WAV           WAC          WAI          WFUR         DUCTW
   1879.52       959.59        700.00      1250.00      2437.06      600.07      10656.00      1181.29
  WNAC          WPYL          WOPIT         WEMTY         OW           ZFW          AMPR         GW
   6156.66        .00         2527.03      95556.84     98083.87    128423.87     83019.74    161352.82
  SWING         AR           SWEEP         WGRSS        WFUEL        PAYLD        THRUST       TAPER
  1517.20      10.00          17.23      161360.08     32928.95     30340.00     16758.33        .30
 TCROOT        TCTIP         SHOR          SVERT        FLENGTH      FUSAREA      DELPRESS     VOLVE
  13.49        10.31         238.31        249.26        136.25      4661.38         8.80      408.86
 RANGE/D.O.C. DATA
   RANGE      DOC1       DOC2       DOC4       DOC10
   500.      1.867      2.146      2.704      4.378

TOTAL COST OF
A/C LESS ENG  TOTAL ENG  COMPLETE A/C     FUEL500
   6494375.    3127800.      9622175.      13510.
DOLLARS PER NAUTICAL MILE COST OF:
  CREW       FUEL       INSURANCE A/C LABOR A/C MAIL ENG LABOR ENG MATL MTNCE BUMDN DEPRECIATION TOTAL
   .571       .476        .220       .111       .099       .077       .242       .337      1.051      3.182
  1500.      1.413       1.613      2.012      3.210
   400.      2.035       2.341      2.954      4.792
   300.      2.313       2.664      3.367      5.474
   200.      2.870       3.310      4.190      6.831

102.0 1517. 16758. 1.35 1.35 161360. 160546. 154754. 132688. 132380.  98084.  .363 15.83 .931   3949.  28980.    .907
 3.38104.9  1094.   0   .388  105.8  1.00     .429    .429     95.6   41.05  12.72 1.413 .751  1.613  2.012     .091
   1.0000     1.0000     1.0000     1.0000     1.0000     1.0000
   1.0000     1.0000     1.0000      .8800     1.0000     1.0000
   1.0000     1.0000     1.0000     1.0000     1.0000      .0000
DOVRS 000000 FPOF 000000 FPUF 00.000 ERMD 0.000
***** TASK UNITS=1       ACCUM #TL=61     CORE=19968     CORE SEC=181     ACCUM CRU=138     *****
```

FIGURE 62: COMPUTER SIZING DATA: 4 ENGINE OTW-IBF @ 1.35 FPR, 610M (2000 FT) FIELD

```
 BASE 1.35FPR 1500NM HYBRID UPDATE NF0135SFCBD/03CROTWIBF 4/17/74        I1985=0      IVEC=0      ITR=1

STOL DISTANCE=3500.FT   MACH= .80   RANGE=1500.NM   PAYLOAD=  30340.LB   NO. OF SEATS=   148.

START CRUISE ALT=30000.FT   SWEEP=20.0DEG  AR= 7.73   CDC=10.   CDMISC=   .00   DDM=.080

IVER=8   IMACH=4   IENG= 48  VBARH=VARIABLE  VBARV=VARIABLE  ETAPWR= .976  SFCFAC= 1.01     ETAMAX= 1.060
NO.ENG USED INITIAL CRUISE=2.     ENG COST FACTOR= .800      IGEAR=0     IRANGE=1     ULF= 3.750     CRUISE= 1
 WSP     S     TUN      PR  PRPP RAMPWT     W2      W3      W4      W5      OWE     CL    L/D   FVM   RESV    FUEL    VBARH
FLTIM DST23  ROC     N  T/W R  W/S R   ZFWR    TWTO5   TWLG5   W/S 5    TOS     TOC    DOC1 FVMCS  DOC2   DOC4    VBARV
103.4 1496. 36038. 1.35 1.35 161552. 160677. 154671. 131301. 130970.  96487.  .368 15.07 .893   4145.  30582.   .90
 3.37100.7  1132.   0   .417  107.4  1.000    .464    .464     96.5    44.77  13.01 1.292 .699  1.502  1.923    .09

    DRAG BUILDUP, MACH NO. =   .8000
 INITIAL CRUISE LIFT COEFFICIENT=   .368
CDWING  CDFUS  CDPYL  CDNAI  CDHOR  CDVER  CDPOD CDRUFF CDCOMP  CDTRM  CDMISC CDINT   CDO     CDI   CDTOT
.00510 .00634 .00000 .00080 .00108 .00080 .00099 .00081 .001 c .0005  .0  .  .0 .81 .01822 .00620 .02442
  WETTED AREA/WING AREA
WING=1.706 FUSELAGE=3.116 NACELLES=1.149 PYLON= .000 H TAIL= .357 V TAIL= .289 STOT/SREF=6.617

TOCWING    SWING        AR      TAPER     FUS LEN   FUS SWET  THRUST    SHOW       SVERT      DNAC      TRVERT
    .1301  1495.85      7.73      .30     136.25    4661.38  36030.51   263.26     212.85      9.50        .0

    WWNG          WHOR          WVER          WFUS          WLG          WHYD          WSC          WBP
   17384.58       1614.53       1479.46      22032.05      6785.19      1364.57      4093.72     12673.96
   WELEC          WAPU          WINSTR        WAV           WAC          WAI          WFUR         DUCTW
    1880.86        959.90        700.00      1250.00      2437.06       668.30     10656.00      1197.29
   WNAC          WPYL          WOPIT         WEMTY         OW           ZFW          AMBR          GW
    6722.03          .00       2587.16      93899.53     96486.69     126826.69     80524.10     161553.08
   SWING          AR          SWEEP         WGRSS         WFUEL        PAYLD        THRUST       TAPER
    1495.85        7.73         16.40      161552.12     34726.39     30340.00     36038.41        .30
   TCROOT        TCTIP          SHOR          SVERT        FLENGTH      FUSAREA      DELPRESS      VDIVE
     13.79         10.54        263.26        212.85        136.25      4661.38         8.80     408.86
RANGE/D,O,C, DATA
   RANGE      DOC1       DOC2       DOC4       DOC10
    500.     1.702      1.997      2.585      4.351

TOTAL COST OF
A/C LESS ENG  TOTAL ENG  COMPLETE A/C     FUEL500
   6533447.    2044502.      8577949.      14276.
DOLLARS PER NAUTICAL MILE COST OF:
 CREW      FUEL      INSURANCE A/C LABOR A/C MATL ENG LABOR ENG MATL MINCE BURDN DEPRECIATION TOTAL
 .565       .502       .194       .107       .099       .060       .157       .302       .916     2.901
1500.      1.292      1.502      1.923      3.184
 400.      1.853      2.177      2.823      4.761
 300.      2.105      2.475      3.216      5.438
 200.      2.606      3.070      3.997      6.780

103.4 1496. 36038. 1.35 1.35 161552. 160677. 154671. 131301. 130970.  96487.  .368 15.07 .893   4145.  30582.   .90
 3.37100.7  1132.   0   .417  107.4  1.000    .464    .464     96.5    44.77  13.01 1.292 .699  1.502  1.923    .090
  1.0000     1.0000     1.0000     1.0000     1.0000     1.0000
  1.0000     1.0000     1.0000      .8800     1.00       1.0
  1.0000     1.0000     1.0000     1.0000     1.0        .000
DOVRS 000000 FPOF 000000 FPUF 000000 ERMD 00 00
***** TASK UNITS=1       ACCUM TIL=57     CORE=19968     CORE SEC=193      ACCUM CRU=127     ***
```

FIGURE 63: COMPUTER SIZING DATA: 2 ENGINE OTW-IBF @ 1.35 FPR, 1070M (3500 FT) FIELD

```
 BASELINE 1.47FPR 1500 NM HYB 2ENG UPDATE 4/19/74 NF0147SFCBD/03CROTWIBFI1985=0      IVEC=0      ITR=1

STOL DISTANCE=3000.FT   MACH= .80   RANGE=1500.NM   PAYLOAD=  30340.LB   NO. OF SEATS=   148.

START CRUISE ALT=30000.FT   SWEEP=20.0DEG   AR= 7.73   CDC=10.   CDMISC=   .00   DDM=.080

IVER=8   IMACH=4   IENG= 53  VBARH=VARIABLE  VBARV=VARIABLE  FTAPWR= .737  SFCFAC= 1.122     FTAMAX= 1.100
NO.ENG USED INITIAL CRUISE=2.     ENG COST FACTOR= .8000     IGEAR=2     IRANGE=1     HLF= 3.750     CRUISE= 1
 WSP     S     TUN     PP  PRPP RAMPWT    W2       W3       W4       W5       OWE      CL    L/D   FVR   RESV     FUEL     VBARH
FLTIM DST23  POC     N  T/W R  W/S R   ZFWR     TWTO5    TWLG5    W/S 5     TOS      TOC     DOC1 FVRCS  DOC2  DOC4     VBARV
103.2 1624. 38663. 1.47 1.47 173827. 172488. 167604. 137827. 137309. 102000.  .367 15.56 .932   4965.  36518.    .901
 3.29 39.2  3562.   0   .418  106.2  1.000    .472     .472     94.0   44.37  13.01 1.324 .736  1.575  2.077     .090

   DRAG BUILDUP, MACH NO. =   .8000
 INITIAL CRUISE LIFT COEFFICIENT=   .367
CDWING  CDFUS  CDPYL  CDNAI  CDHOR  CDVER  CDPOD CDRUFF CDCOMP  CDTRM  CDMISC CDINT   CDO     CDT   CDTOT
.00510 .00584 .00000 .00059 .00112 .00082 .00092 .00077 .00100 .00050 .00000 .00077 .01743 .00617 .02360
  WETTED AREA/WING AREA
WING=1.719 FUSFLAGE=2.870 NACELLES= .805 PYLON= .000 H TAIL= .373 V TAIL= .301 STOT/SREF=6.068

TOCWING    SWING        AR      TAPER     FUS LEN   FUS SWET  THRUST    SHOR      SVERT      DNAC      TPVERT
    .1301  1624.07      7.73      .30     136.25    4661.38  38662.53   298.15    241.07      9.14        .00

    WWNG          WHOR          WVER          WFUS          WLG           WHYD          WSC           WPP
     19448.16      1828.55       1675.57       19142.77      9417.95       1432.15       4296.44       15663.17
   WELEC         WAPU          WINSTR        WAV           WAC           WAI           WFUR          DUCTW
     1966.79       979.34        700.00        1250.00       2437.06       679.88        10656.00      1111.86
   WNAC          WPYL          WOPIT         WEMTY         OW            ZFW           AMPP          GW
     6537.54          .00        2776.37       99223.22      101999.59     132339.59     82561.08      173822.59
   SWING         AR            SWEEP         WGRSS         WFUEL         PAYLD         THRUST        TAPER
     1624.07       7.73          16.40         173827.08     41482.97      30340.00      38662.81          .30
   TCROOT        TCTIP         SHOR          SVERT         FLENGTH       FUSAREA       DELPRESS      VDIVE
       13.79         10.54         298.15        241.07        136.25        4661.38       8.80          408.86
 RANGE/D.O.C. DATA
    RANGE      DOC1      DOC2      DOC4      DOC10
      500.     1.707     2.053     2.744     4.818

TOTAL COST OF
A/C LESS ENG  TOTAL ENG  COMPLETE A/C     FUEL500
    6828663.    1902428.      8731090.      16770.
DOLLARS PER NAUTICAL MILE COST OF:
  CREW      FUEL      INSURANCE A/C LABOR A/C MATL ENG LABOR ENG MATL MTNCE BURDN DEPRECIATION TOTAL
     .539      .589      .187      .107      .101      .061      .141      .302      .883     2.910
    1500.     1.324     1.575     2.077     3.582
     400.     1.847     2.225     2.979     5.243
     300.     2.080     2.509     3.367     5.942
     200.     2.543     3.074     4.137     7.324

103.2 1624. 38663. 1.47 1.47 173827. 172488. 167604. 137827. 137309. 102000.  .367 15.56 .932   4965.  36518.    .901
 3.29 39.2  3562.   0   .418  106.2  1.000    .472     .472     94.0   44.37  13.01 1.324 .736  1.575  2.077     .090
   1.0000    1.0000    1.0000    1.0000    1.0000    1.0000
   1.0000    1.0000    1.0000     .8800    1.0000    1.0000
   1.0000    1.0000    1.0000    1.0000    1.0000     .0000
DOVRS 000000 FPOF 000000 FPUF 000000 ERMD 000000
***** TASK UNITS=1       ACCUM TTL=15     CORE=19968     CORE SEC=171     ACCUM CPU=33     *****
```

FIGURE 64: COMPUTER SIZING DATA: 2 ENGINE OTW-IBF @ 1.47 FPR, 910M (3000 FT) FIELD

926 Km (500 n.mi.) mission. Accordingly, the selected baseline mission vehicle at 1.35 FPR, in addition to its parametric variants at 610 m. and 1070m. field length (2000 ft. and 3500 ft.) and a 1.47 FPR vehicle at 1220m. (4000 ft.), has been defined with R/STOL capabilities. Computer-generated sizing data for each of these vehicles are presented in Figures 61 through 64.

4.5 OTW-IBF FUEL CONSERVATIVE VEHICLES

To achieve minimum fuel consumption rather than minimum DOC for the 926 Km (500 NM) mission, it is necessary to reoptimize the airplane configuration. The parameters involved are cruise Mach number, field length, engine FPR, number of engines, cruise power setting, cruise altitude, aspect ratio and wing loading. Consideration of the problem prior to actual computation gave some insight into the range of values to be considered for each parameter. At this time it was determined that 4-engine configurations would, in most cases, provide lower consumption than 2-engine configurations because of the better s.f.c. obtained from the lower total installed thrust combined with the use of higher cruise power settings. Accordingly, primary emphasis was placed on 4-engined configurations.

Airplanes were sized for the combinations of parameters defined in the following matrices:

FPR 1.25 (4-ENGINES):

Field Length	Cruise Mach No.	AR	Cruise Altitude 4570m (15,000')	6100m (20,000')	7620m (25,000')	9140m (30,000')
910m (3000')	0.55	10	X	X	X	
		12	X	X	X	
		14	X	X	X	
	0.6	14	X	X	X	
1220m (4000')	0.7	10	X	X	X	X
		12	X	X	X	X
1830m (6000')		14	X	X	X	X
	0.8	7.73		X	X	X
		10		X	X	X
		14		X	X	X

FPR 1.35 (4-ENGINES):

Field Length	Cruise Mach	AR	Cruise Altitude 6100m (20,000')	7320m (24,000')	8230m (27,000')	9140m (30,000')	10,060m (33,000')	10,970m (36,000')
610m (2000')	0.55	10	X	X	X			
		14	X	X	X			
	0.60	10	X	X	X	X		
910m (3000')		14	X	X	X	X		
	0.65	10		X	X	X	X	
1070m (3500')		14		X	X	X	X	
	0.70	10		X	X	X	X	
		14		X	X	X	X	
	0.75	10			X	X	X	X
		14			X	X	X	X
	0.8	7.73			X	X	X	
		10			X	X	X	
		14			X	X	X	

FPR 1.35 (2-ENGINES):

Field Length	Cruise Mach	AR	Cruise Altitude 7620m (25,000')	9140m (30,000')	10,060m (33,000')	10,970m (36,000')
610m (2000')	0.75	7	X	X		X
		7.73	X	X		X
		9	X	X		X
910m (3000')		12	X	X		X
		14	X	X		X
1070m (3500')	0.80	7.73		X		X
		9				X
	0.85	7.73		X	X	X

FPR 1.47 (4-ENGINES):

Field Length	Cruise Mach	AR	Cruise Altitude 6100m (20,000')	7320m (24,000')	8230m (27,000')	9140m (30,000')	10,000m (33,000')	10,970m (36,000')
910m (3000')	0.6	12	X	X	X			
		13	X	X	X			
		14	X	X	X			
	0.65	14		X	X	X		
1220m (4000')	0.70	14			X	X	X	
	0.75	14				X	X	X
1830m (6000')	0.80	7.73				X	X	X
		14				X	X	X

For each of the above design points, a range of cruise power settings was examined to determine the power setting providing minimum fuel consumption.

4.5.1 FPR 1.35 Configurations

Figures 65 through 69 illustrate example data for the 1.35 FPR fixed pitch fan engine which were generated by the sizing program/machine plotter and includes installed thrust to weight ratio at takeoff, 926 Km (500 NM) mission fuel, and direct operating cost at 11.5¢, 23¢, 46¢ and $1.15 per gallon of fuel plotted against wing loading at takeoff. The intersections of the takeoff (T/W_{INST}) requirement or the (T/S) limit, or the fuel capacity limit, whichever is most critical, on the T/W plot determines the wing loading and T/W_{INST} for each condition. Landing has not been found to be a critical requirement. Using this selected wing loading the equivalent points on the other parameter plots can be located, thus generating the lines shown as 914m. (3000 ft) fuel, 914m (3000 ft) DOC-1, etc. From these data, the minimum value of mission fuel and DOC at various fuel prices can be obtained for a given field length. The process was repeated for all the combinations of parameters previously discussed.

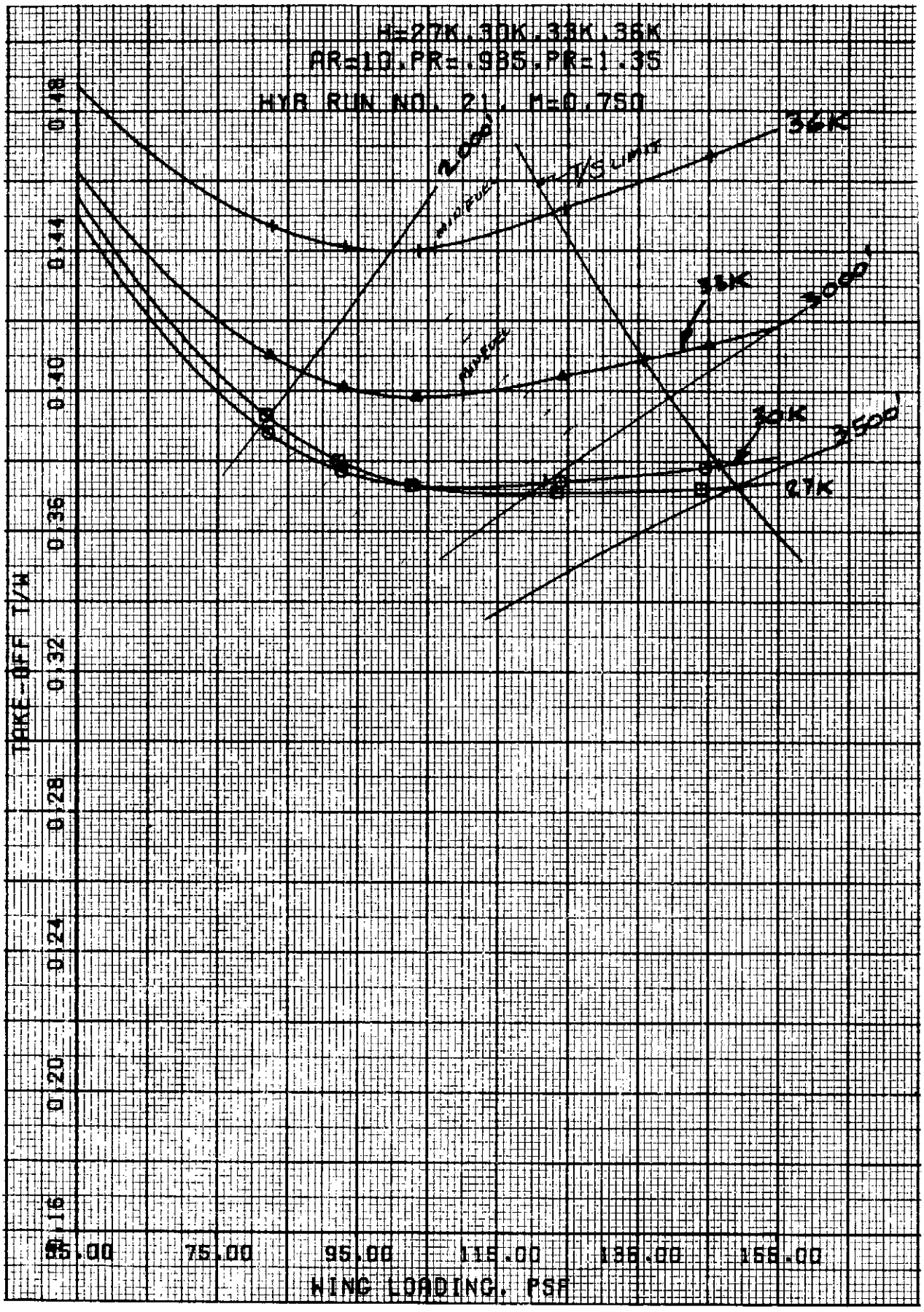

FIGURE 65: TYPICAL COMPUTER SIZING GRAPHIC OUTPUT (1)

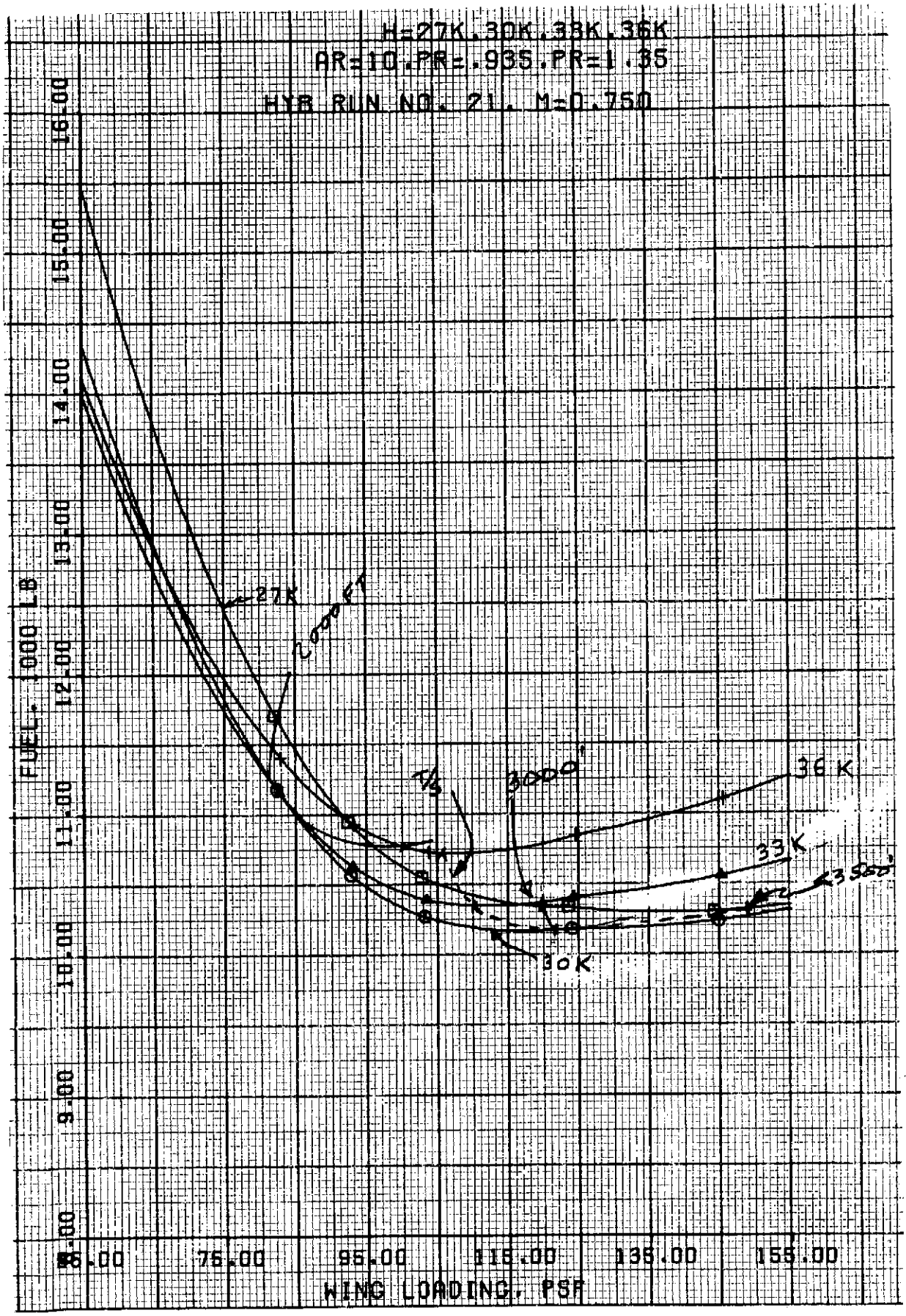

FIGURE 66: TYPICAL COMPUTER SIZING GRAPHIC OUTPUT (2)

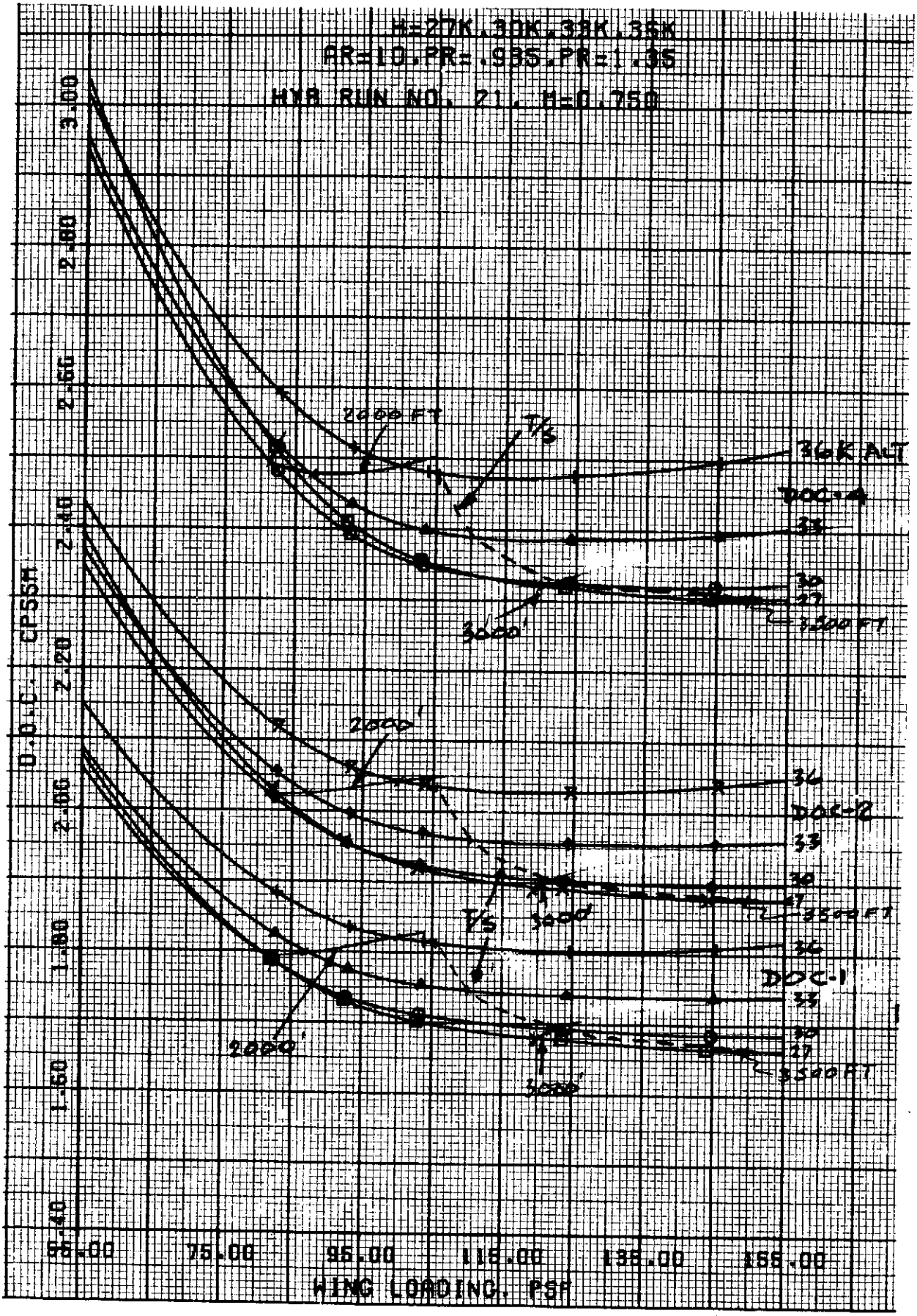

FIGURE 67: TYPICAL COMPUTER SIZING GRAPHIC OUTPUT (3)

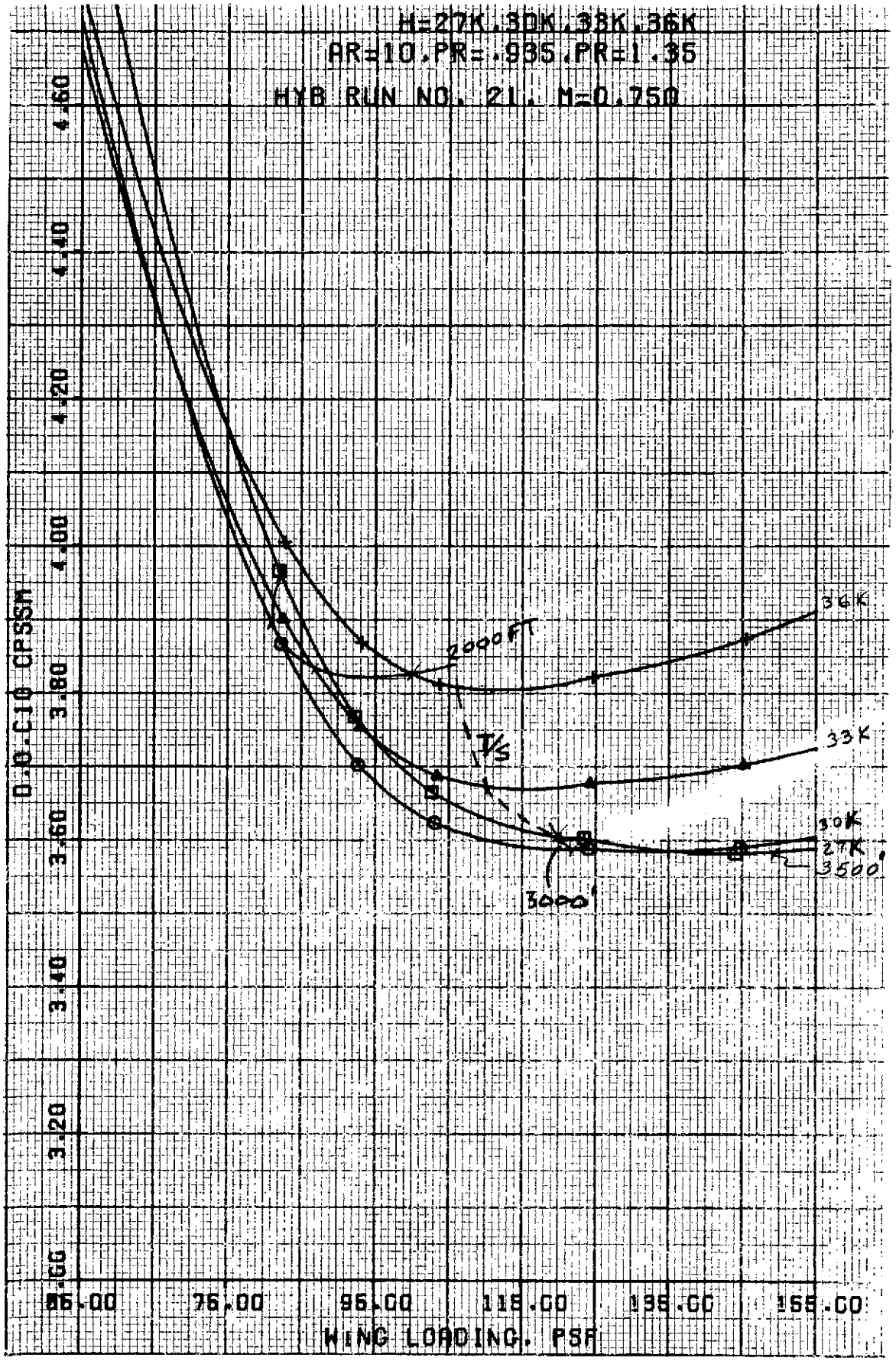

FIGURE 68: TYPICAL COMPUTER SIZING GRAPHIC OUTPUT (4)

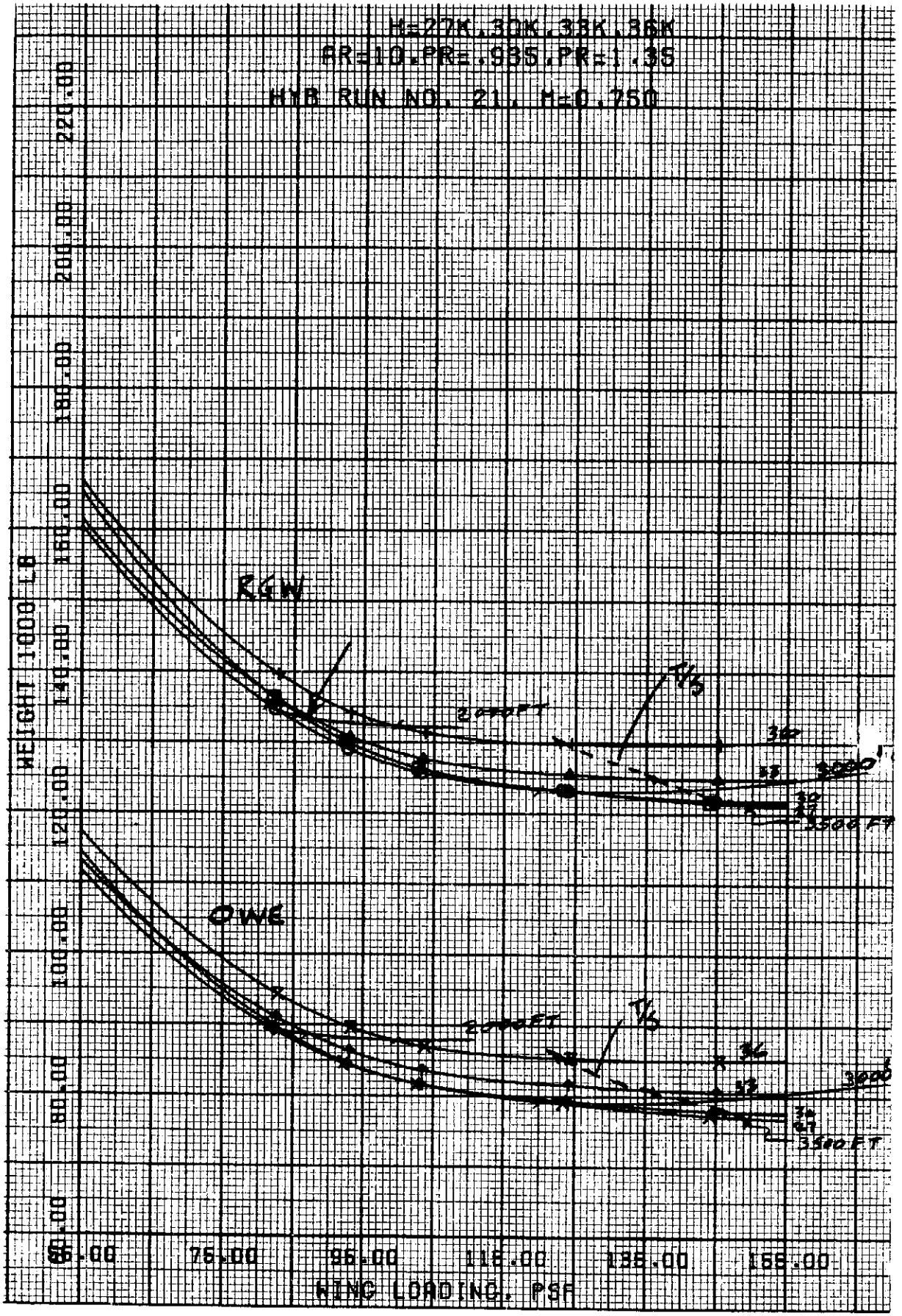

FIGURE 69: TYPICAL COMPUTER SIZING GRAPHIC OUTPUT (5)

Figure 70 presents mission fuel versus cruise altitude and aspect ratio for each cruise Mach number for a 610m (2000 ft) field length, 4-engine configuration. The figure indicates that aspect ratio 14 is optimum for all Mach numbers. The highest altitude studied provides the minimum fuel consumption and it might have been worthwhile to compute additional altitudes for 0.65 and 0.6 M to obtain the absolute minimum value. However, it should be noted that optimum DOC's for these speeds are not competitive with other speeds except at fuel costs of 10 times 1972 price levels. Figures 71 through 74 show DOC at fuel costs of 11.5¢, 23¢, 46¢ and $1.15 gallon for the same range of aspect ratios, cruise altitudes and Mach numbers. From these figures the optimum combination of aspect ratio, cruise altitude and Mach number can be determined at each fuel cost and the sensitivity to any of the parameters evaluated. For example, from Figure 71 at M = 0.70 the DOC, based on 11.5¢/gallon is insensitive to aspect ratio and cruise altitude variation whereas from Figure 73 the effect of increasing the fuel cost to 46¢/gallon "opens out" the carpet, showing the relative sensitivity of the DOC to both aspect ratio and cruise altitude. Comparison of Figures 71 through 74 also reveals the change in optimum Mach number with increase in fuel cost. Figure 71 indicates 0.8 M provides minimum DOC at 11.5¢/gallon while the other figures indicate 0.75 at 23¢, 0.7 at 46¢ and approximately 0.65 to 0.7 at $1.15.

Similar data were developed for 910m and 1070m (3000 and 3500 feet) field lengths. It is significant that in some cases the airplanes were so cruise-critical that it was not possible to match the cruise requirement to the field performance requirement. For example, all of the 0.75M configurations cruising at altitudes higher than 8230m (27,000 ft) have field length capability better than 1067m (3500 ft) and all the 0.8M airplanes have better than 914m (3000 ft) field performance. Even at 0.7M the configuration designed for the higher altitudes are overpowered at sea-level and have field performance better than required.

C3

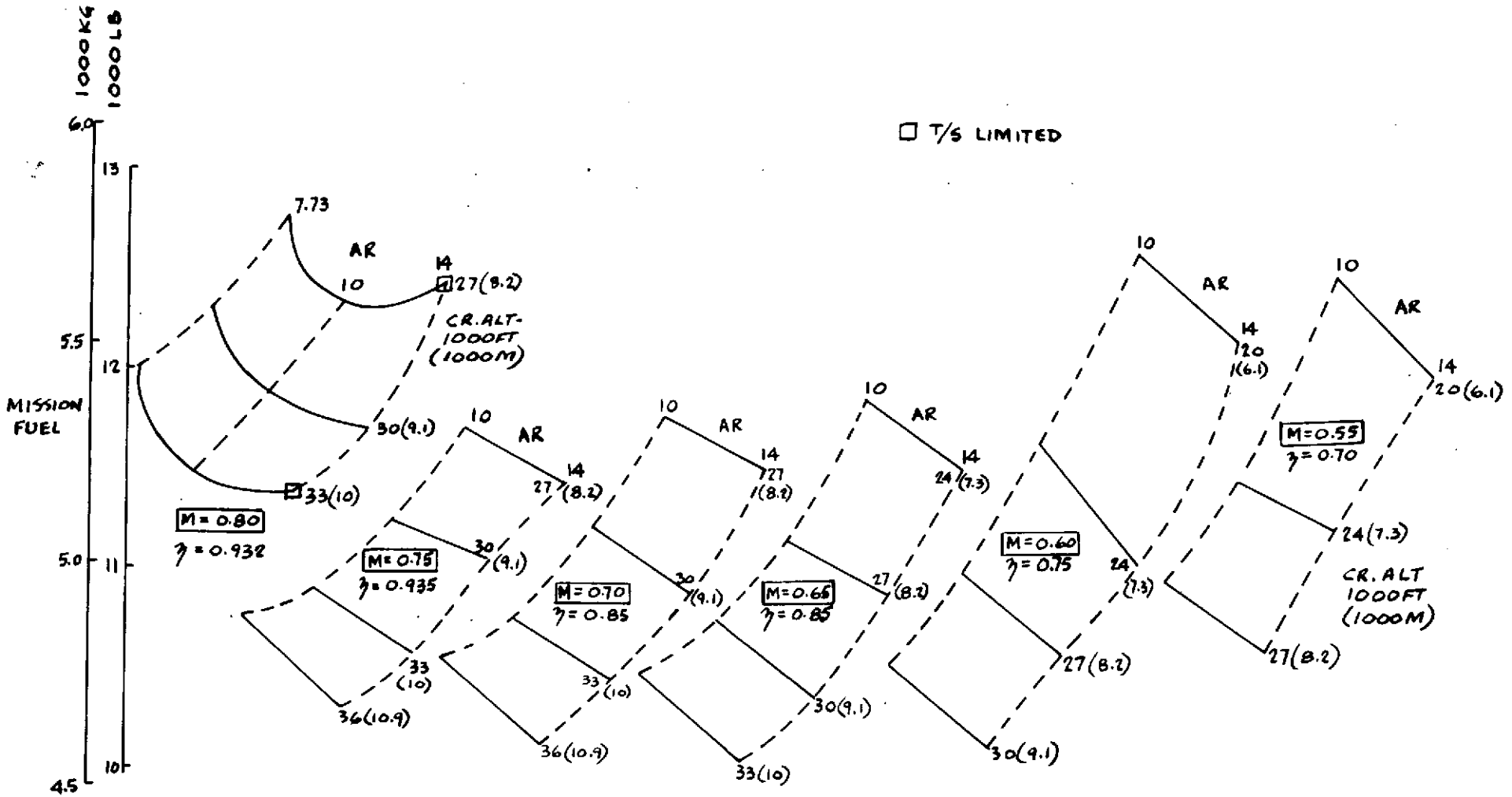

FIGURE 70: OTW/IBF 1.35 FPR MISSION FUEL VS ASPECT RATIO AND CRUISE ALTITUDE (MACH 0.55, 0.60, 0.65, 0.70, 0.75 AND 0.80) AT 2000 FT. FIELD LENGTH, 4-ENGINE

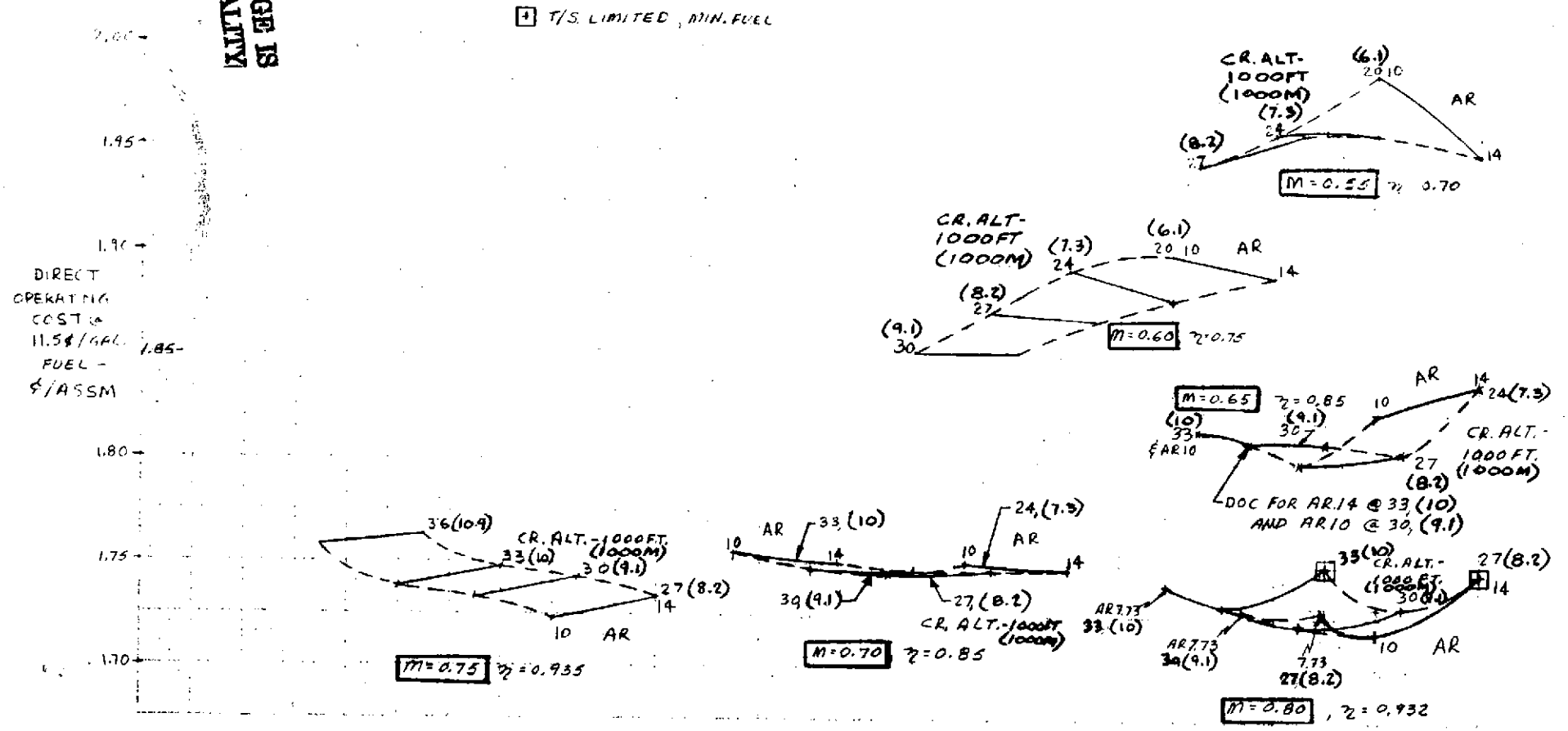

FIGURE 71: OTW/IBF 1.35 FPR DIRECT OPERATING COST @ 11.5¢/GAL. FUEL VS ASPECT RATIO AND CRUISE ALTITUDE (MACH 0.55, 0.60, 0.65, 0.70, 0.75 AND 0.80) AT 2000 FT. FIELD LENGTH, 4-ENGINE

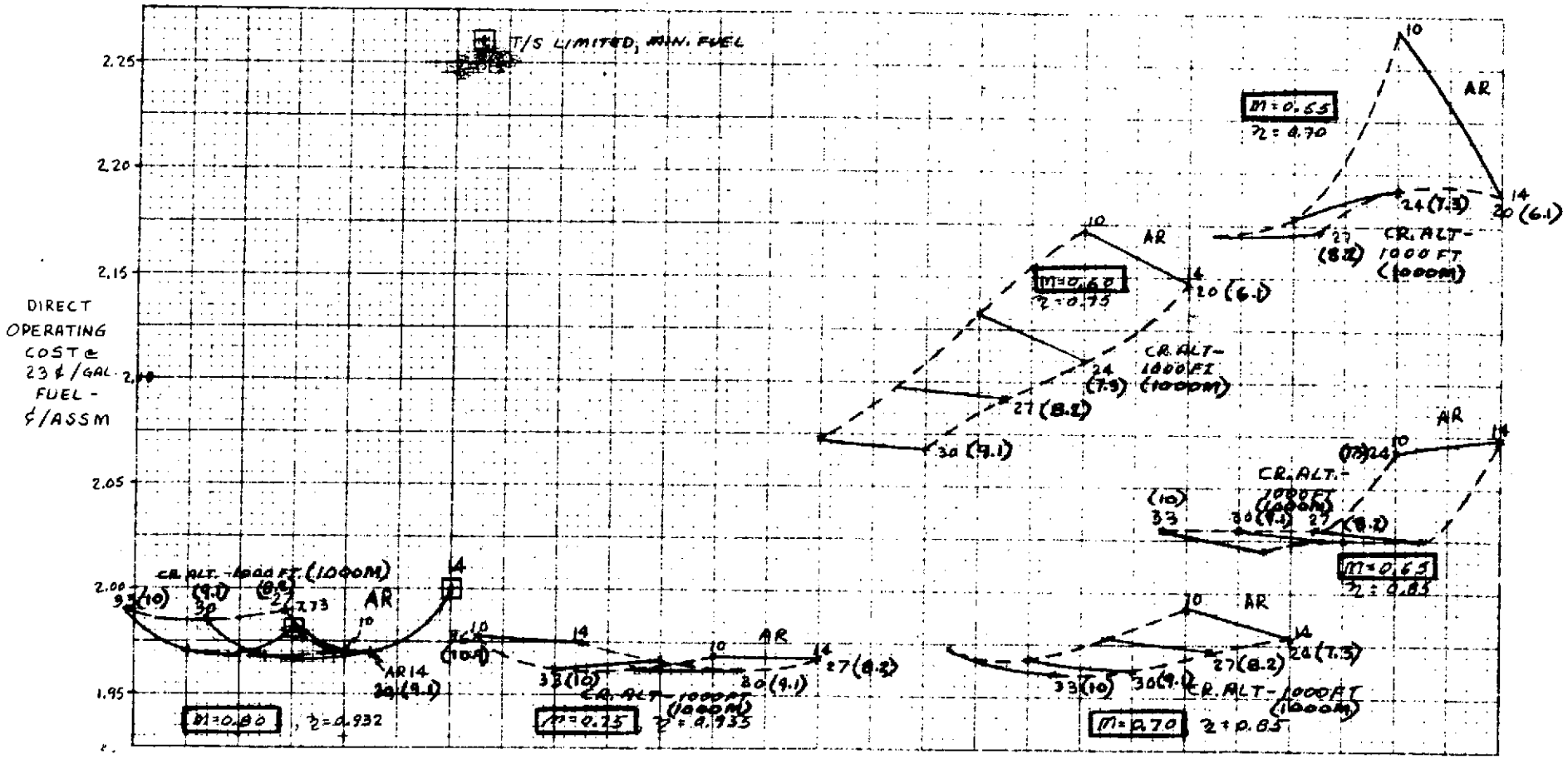

FIGURE 72: OTW/IBF 1.35 FPR DIRECT OPERATING COST @ 23¢/GAL. FUEL VS ASPECT RATIO AND CRUISE ALTITUDE (MACH 0.55, 0.60, 0.65, 0.70, 0.75 AND 0.80) AT 2000 FT. FIELD LENGTH, 4-ENGINE

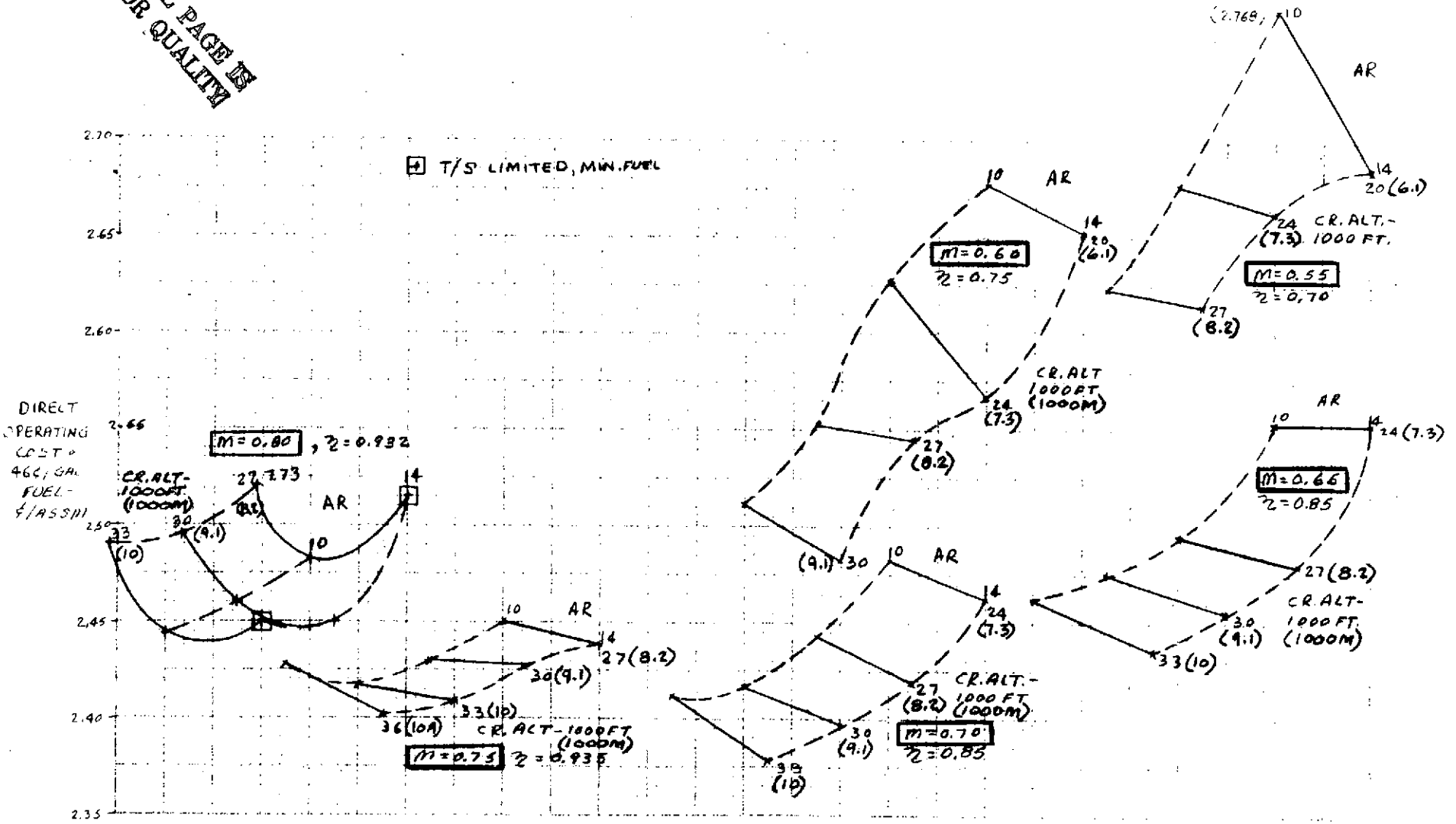

FIGURE 73: OTW/IBF 1.35 FPR DIRECT OPERATING COST @ 46¢/GAL. FUEL VS ASPECT RATIO AND CRUISE ALTITUDE (MACH 0.55, 0.60, 0.65, 0.70, 0.75 AND 0.80) AT 2000 FT. FIELD LENGTH, 4-ENGINE

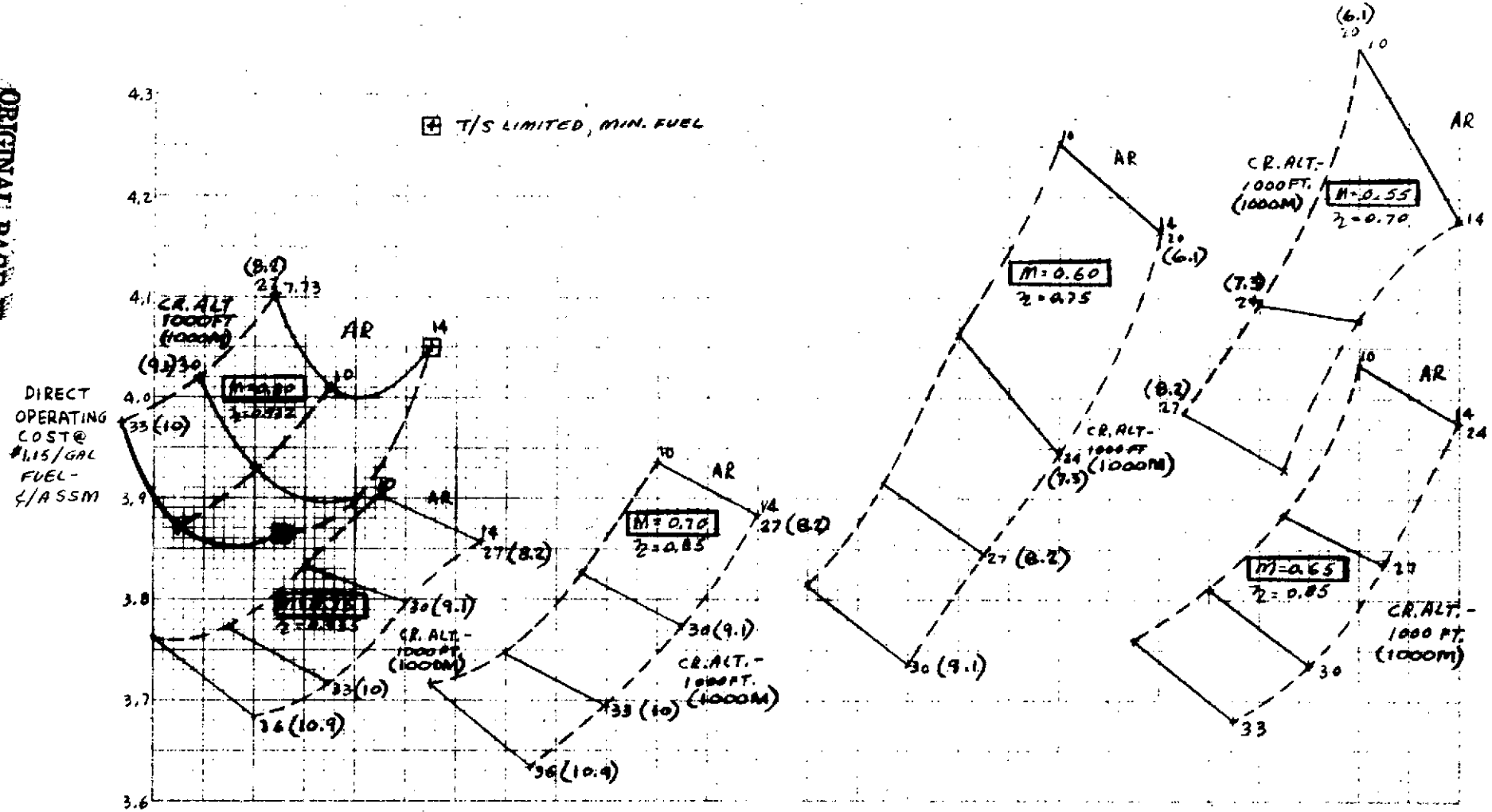

FIGURE 74: OTW/IBF 1.35 FPR DIRECT OPERATING COST @ $1.15/GAL. FUEL VS ASPECT RATIO AND CRUISE ALTITUDE (MACH 0.55, 0.60, 0.65, 0.70, 0.75 AND 0.80) AT 2000 FT. FIELD LENGTH, 4-ENGINE

From these data the following figures and discussion have been prepared. Figure 75 presents fuel required for a 926 Km (500 NM) mission plotted against cruise Mach number for airplanes having 610m, 910m and 1070m (2000, 3000 and 3500 ft respectively) field length capability. Two-engined and four-engined cases are represented and in each case the solid line indicates airplanes optimized for minimum fuel consumption while the dashed line indicates airplanes optimized for minimum DOC at a fuel cost of 23¢/gallon (DOC-2). It can be concluded that the 4-engine configurations provide minimum fuel consumption at all Mach numbers and field lengths. The reasons for the differences between the minimum fuel and minimum DOC-2 airplanes are varied. For example, consider the 610m (2000 ft) field length, 4-engine configuration shown in Figure 75 At 0.55M the minimum fuel at aspect ratio 10 is slightly better on DOC than the aspect ratio 14 design which is about 159 Kg (350 lb) better on fuel consumption. At 0.6, 0.65 and 0.7M the minimum fuel and minimum DOC designs are identical. At 0.75M the minimum fuel optimizes at AR 14 and 10,970m (36,000 ft) whereas DOC 2 optimizes at AR 10 and 10,060m (33,000 ft). At 0.8 M similar differences in AR and cruise altitude account for the difference in fuel consumption. Considering the 910m (3000 ft) and 1070m (3500 ft) field lengths at speeds above Mach 0.7, T/S limits begin to restrict aspect ratio and wing loading selection which results in the minimum fuel and minimum DOC airplanes being identical. Note at the higher Mach numbers airplanes cannot be matched to 1070m (3500 ft) field length.

Figure 76 presents DOC at 23¢/gallon (DOC-2) versus design cruise Mach number for 760m, 910m, and 1070m (2500, 3000 and 3500 ft respectively) field lengths for 2- and 4-engine configurations. The differences in DOC between the minimum fuel and minimum DOC designs are small except at 1070m (3500 ft) where the Δ DOC amounts to approximately 2% below 0.7 M. At 610m and 910m (2000 and 3000 ft) field length, the 4-engine configuration is best while at 1070m (3500 ft) and Mach numbers higher than 0.77 the 2-engine configuration provides minimum DOC. Note that the DOC buckets at .70 to .74 for 610m (2000 ft), 0.72 for 910m (3000 ft) and

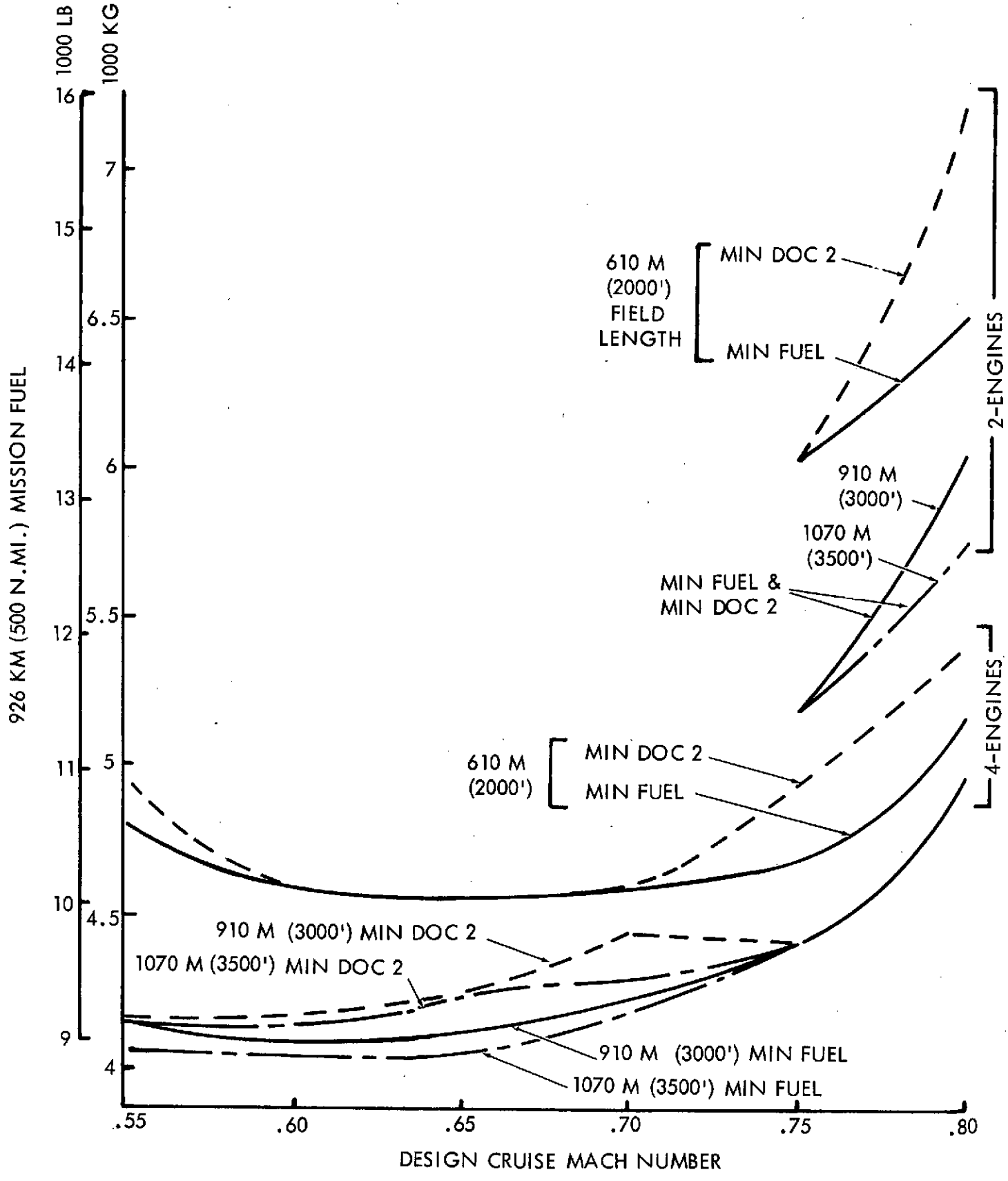

FIGURE 75: MISSION FUEL VS DESIGN CRUISE MACH NUMBER
1.35 FPR OTW/IBF

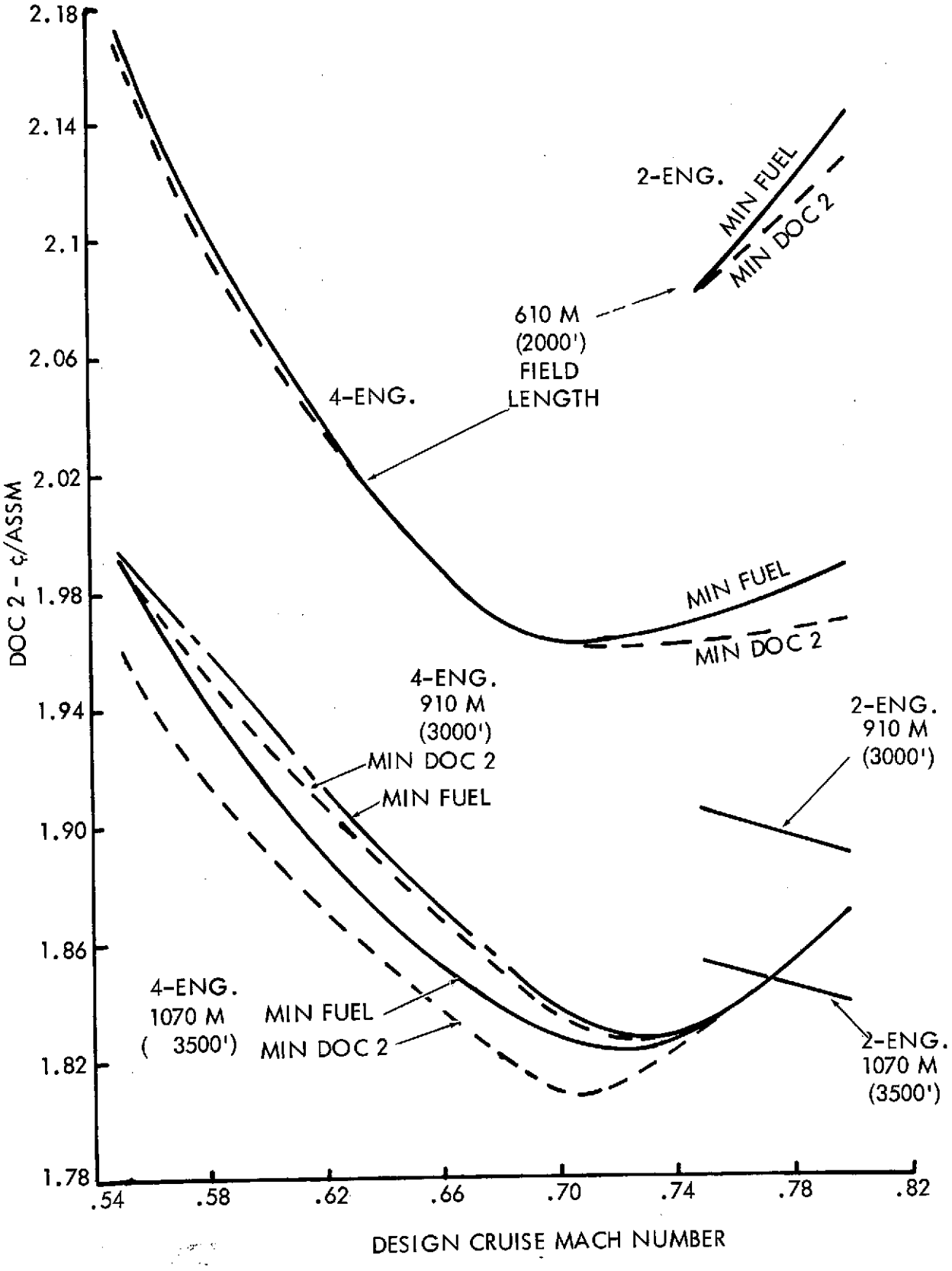

FIGURE 76: 1.35 FPR OTW/IBF DOC-2 VS DESIGN CRUISE MACH NUMBER

approximately 0.71 for 1070m (3500 ft), the 1070m (3500 ft) bucket being affected by the T/S limit. It could be that the 1070m (3500 ft) value would be higher if the T/S limit is a steeper change. Figure 77 presents DOC at varying fuel costs plotted against design cruise Mach number for 2- and 4-engine configurations at 910m (3000 ft). The 4-engine designs provide lower DOC's at all Mach numbers and fuel costs except at Mach numbers above 0.78 at a fuel cost of 11.5¢/gallon. The dashed line shows the optimum design cruise Mach number for each fuel cost. Note that the optimum at 11.5¢/gallon is 0.8 since the 2-engine configuration provides approximately equal DOC at a more desirable speed. Figure 78 shows relative DOC plotted against cruise altitude at optimum aspect ratio and Mach number for that altitude and for varying fuel costs and 910m (3000 ft) field length. Connecting the bucket points show the trend in optimum cruise altitude with variation in fuel cost. A similar plot is shown in Figure 79 to determine optimum aspect ratio variation with fuel cost. As indicated, the aspect ratio for minimum DOC at 11.5¢/gallon is 7.73 for the 2-engined configuration. For the 4-engine configuration, the optimum is AR 11 at 11.5¢, 12.25 at 23¢ and 14 at 46¢ and $1.15/gallon. Figure 80 plots wing loading versus fuel cost factor for the airplanes optimized to provide minimum DOC at the particular fuel cost.

Sensitivity Studies - A number of sensitivity studies have been conducted to determine the effect of variations of compressibility drag, airfoil technology, sweep angle, weight saving and cost increase. Figure 81 presents the effect of compressibility drag variation on DOC-1, mission fuel, wing loading and thickness to chord ratio at 0.75 M. The results confirm that the choice of 2 counts, used in the general program, does provide minimum DOC and minimum fuel. Figure 82 presents similar data for variation in airfoil technology, as defined by Δ drag divergence Mach number (DDM). The level used for the general sizing program is 0.080 Δ DDM which is confirmed in the figure as producing the minimum DOC and minimum fuel consumption. Figure 83 shows similar plots for variation in sweep angle. The value chosen for the general sizing program is 10° up to 0.75 M. The figure shows DOC and mission fuel to be relatively insensitive to sweep angle. Figure 84 presents DOC at 11.5¢, 23¢, 46¢ and $1.15/gallon of fuel plotted against percent structure weight saving and percent airframe cost increase.

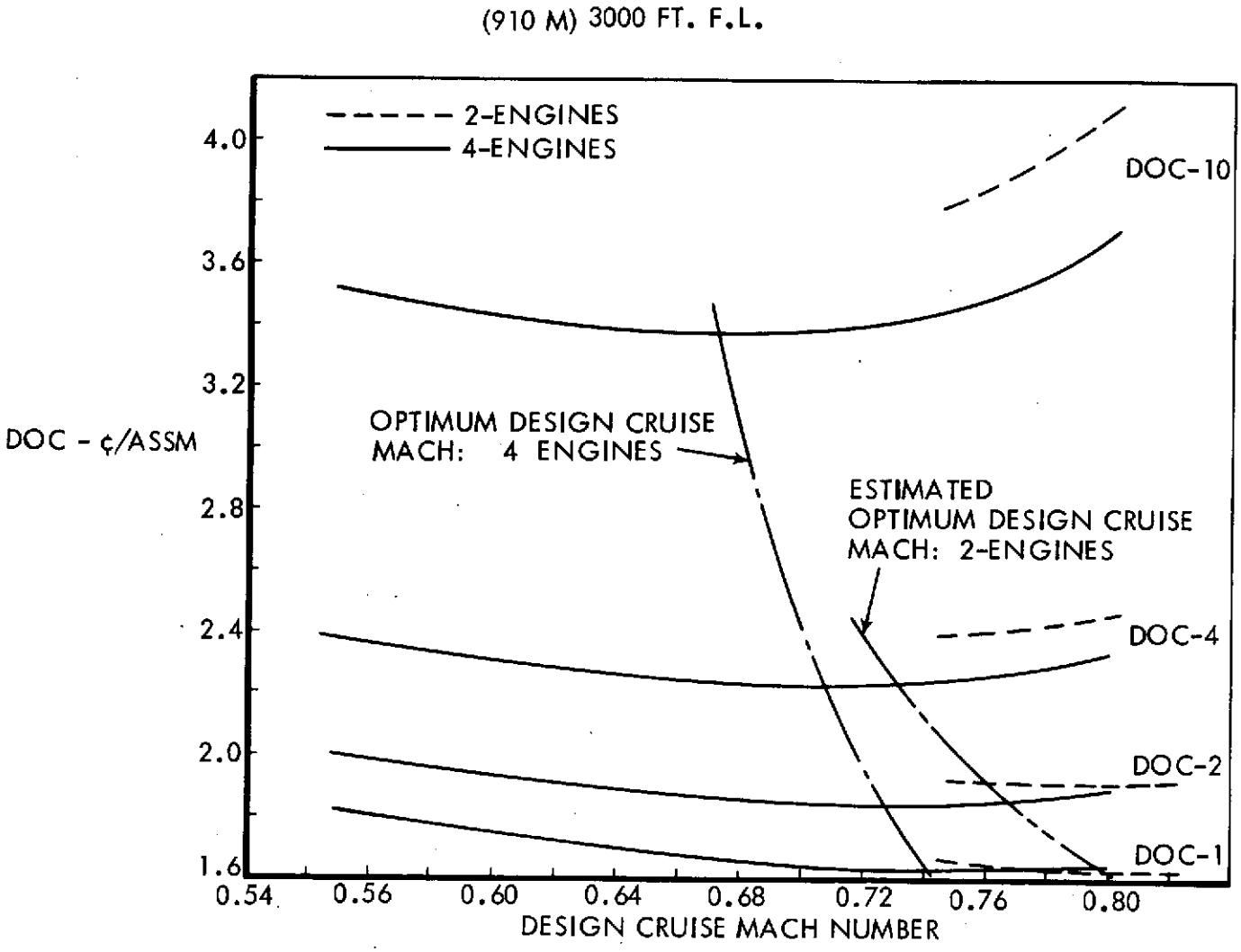

FIGURE 77: 1.35 FPR OTW/IBF: EFFECT OF FUEL PRICE ON OPTIMUM DESIGN CRUISE SPEED

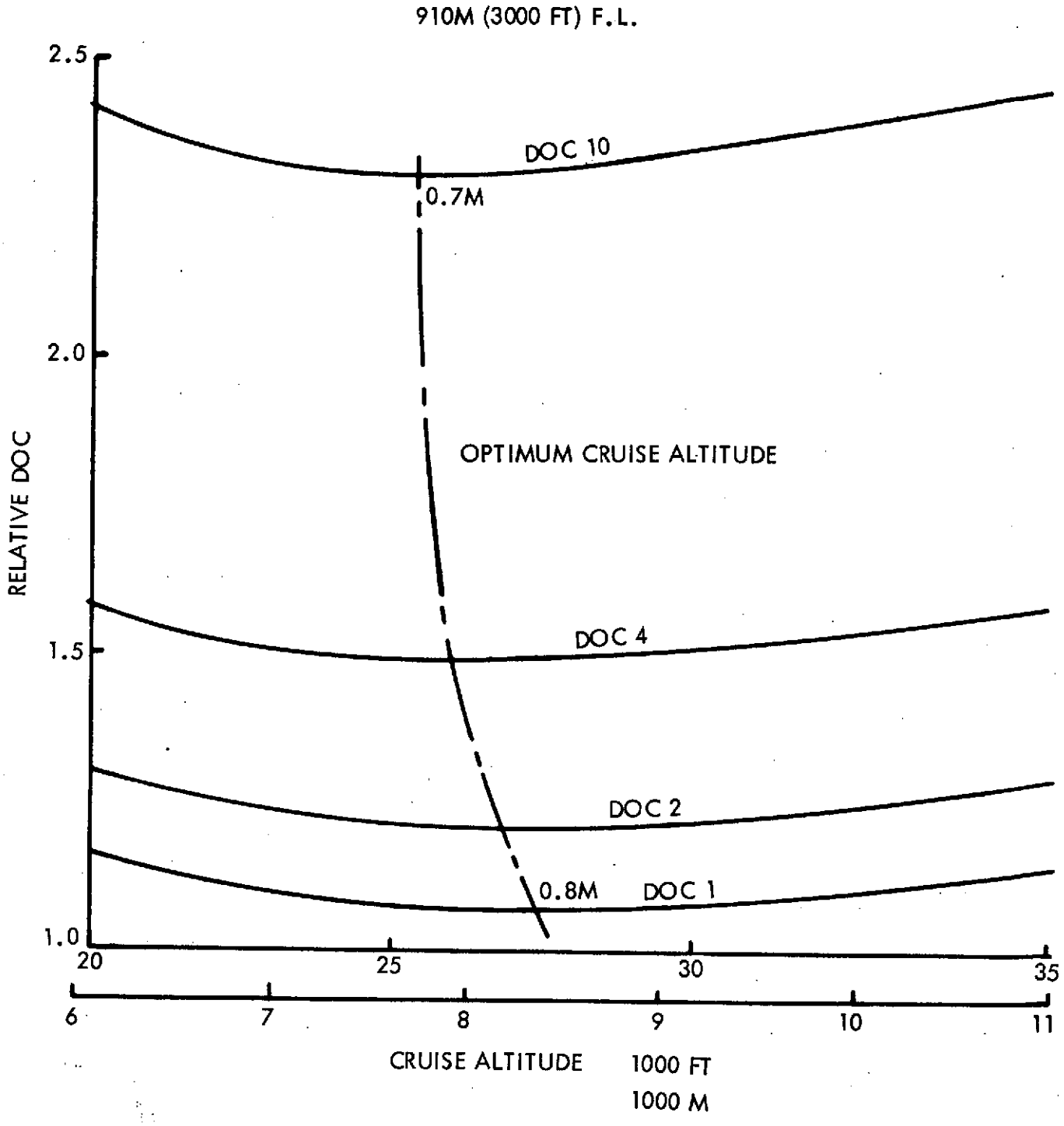

FIGURE 78: 1.35 FPR OTW/IBF: EFFECT OF FUEL COST ON OPTIMUM DESIGN CRUISE ALTITUDE

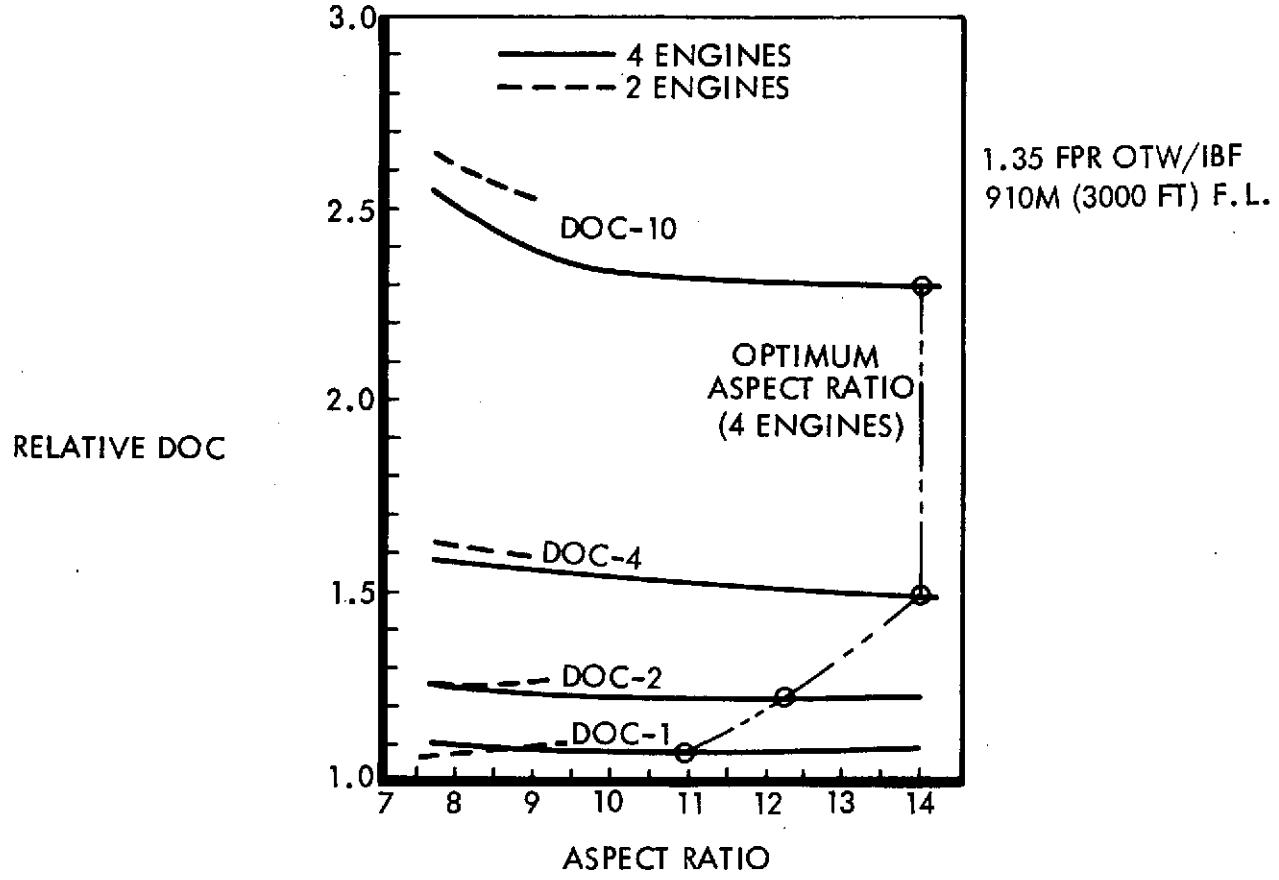

FIGURE 79: EFFECT OF FUEL PRICE ON ASPECT RATIO OPTIMIZATION

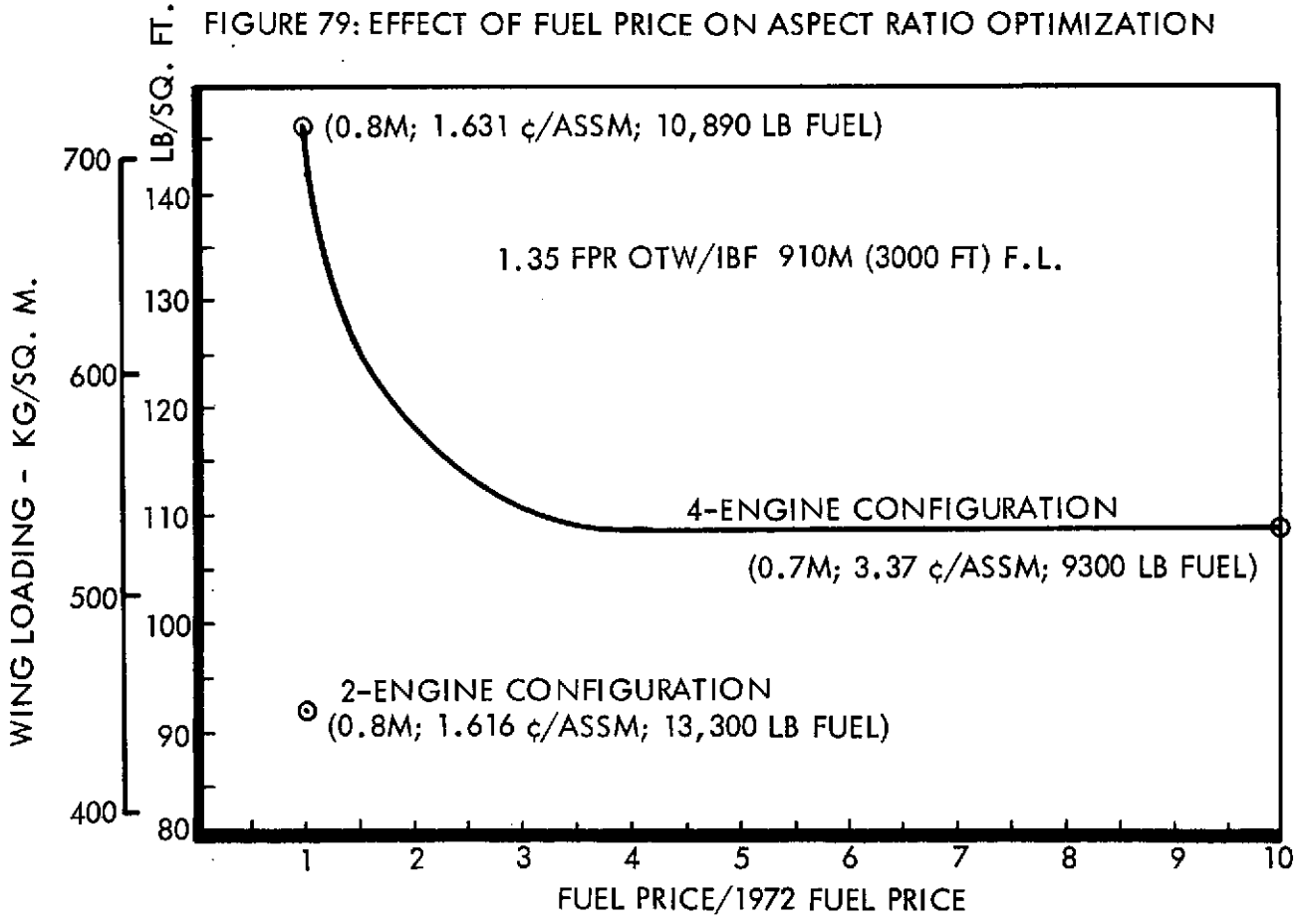

FIGURE 80: WING LOADING FOR MINIMUM DOC VS FUEL PRICE

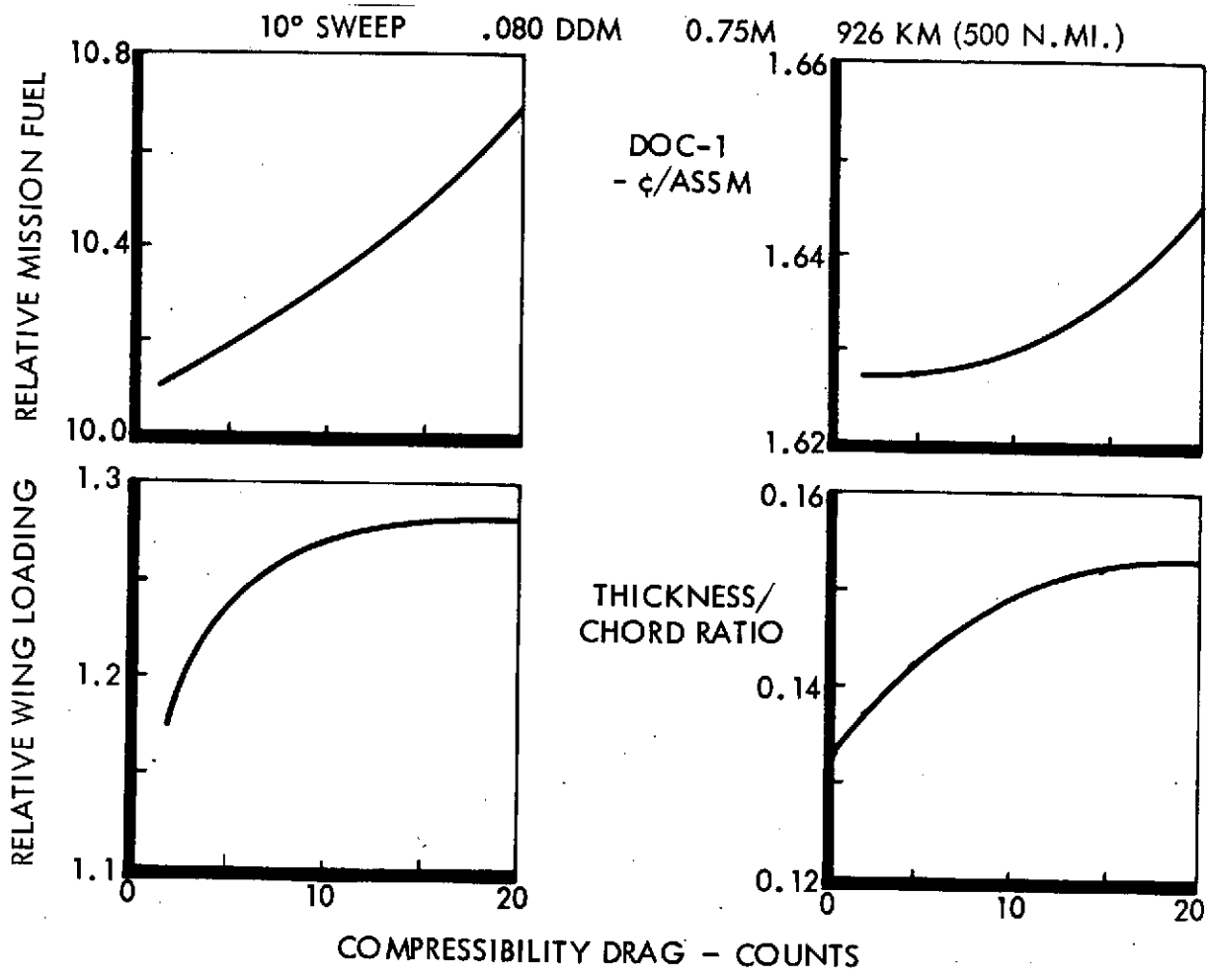

FIGURE 81: SENSITIVITY TO COMPRESSIBILITY DRAG (1.35 FPR OTW/IBF)

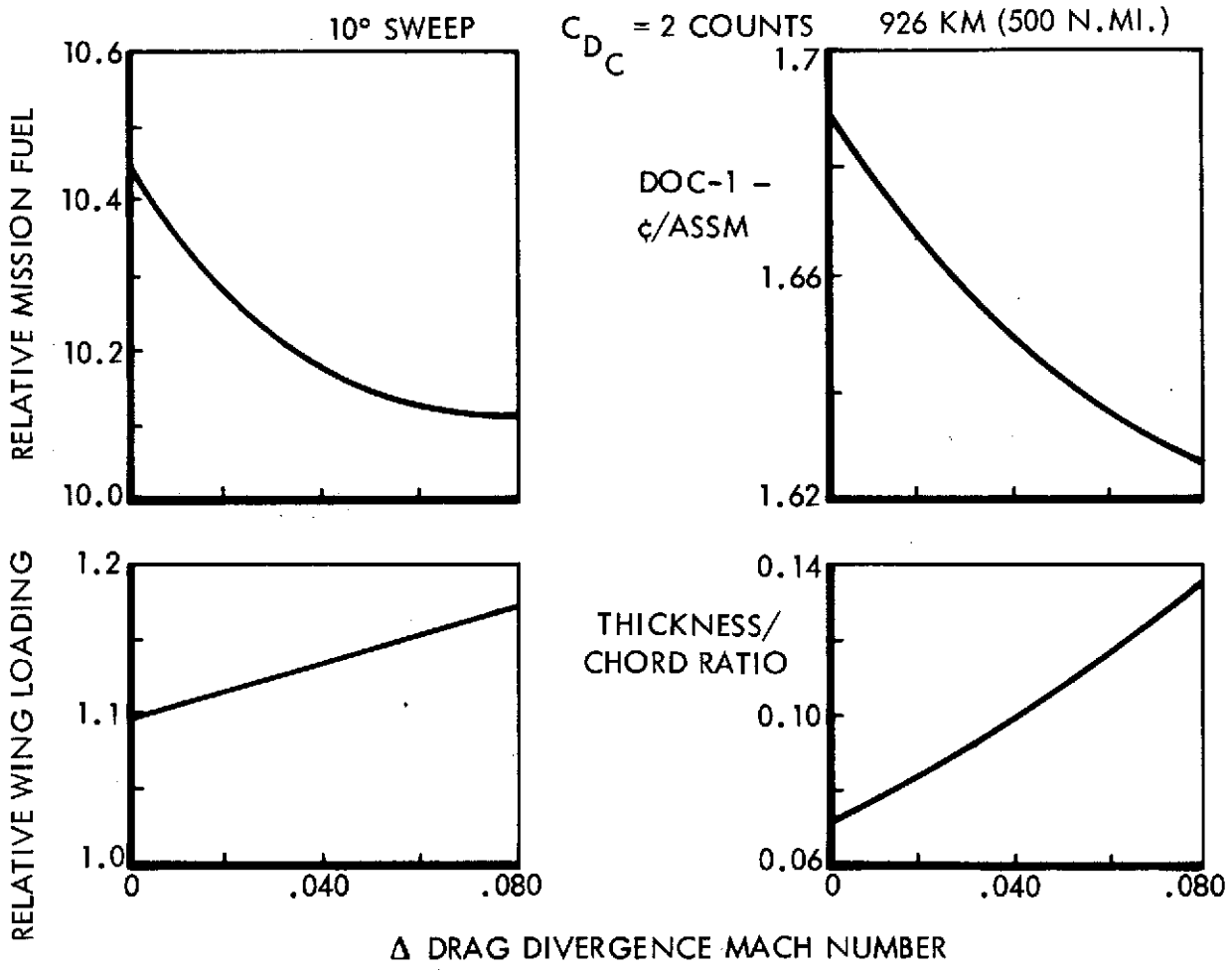

FIGURE 82: SENSITIVITY TO AIRFOIL TECHNOLOGY (1.35 FPR OTW/IBF)

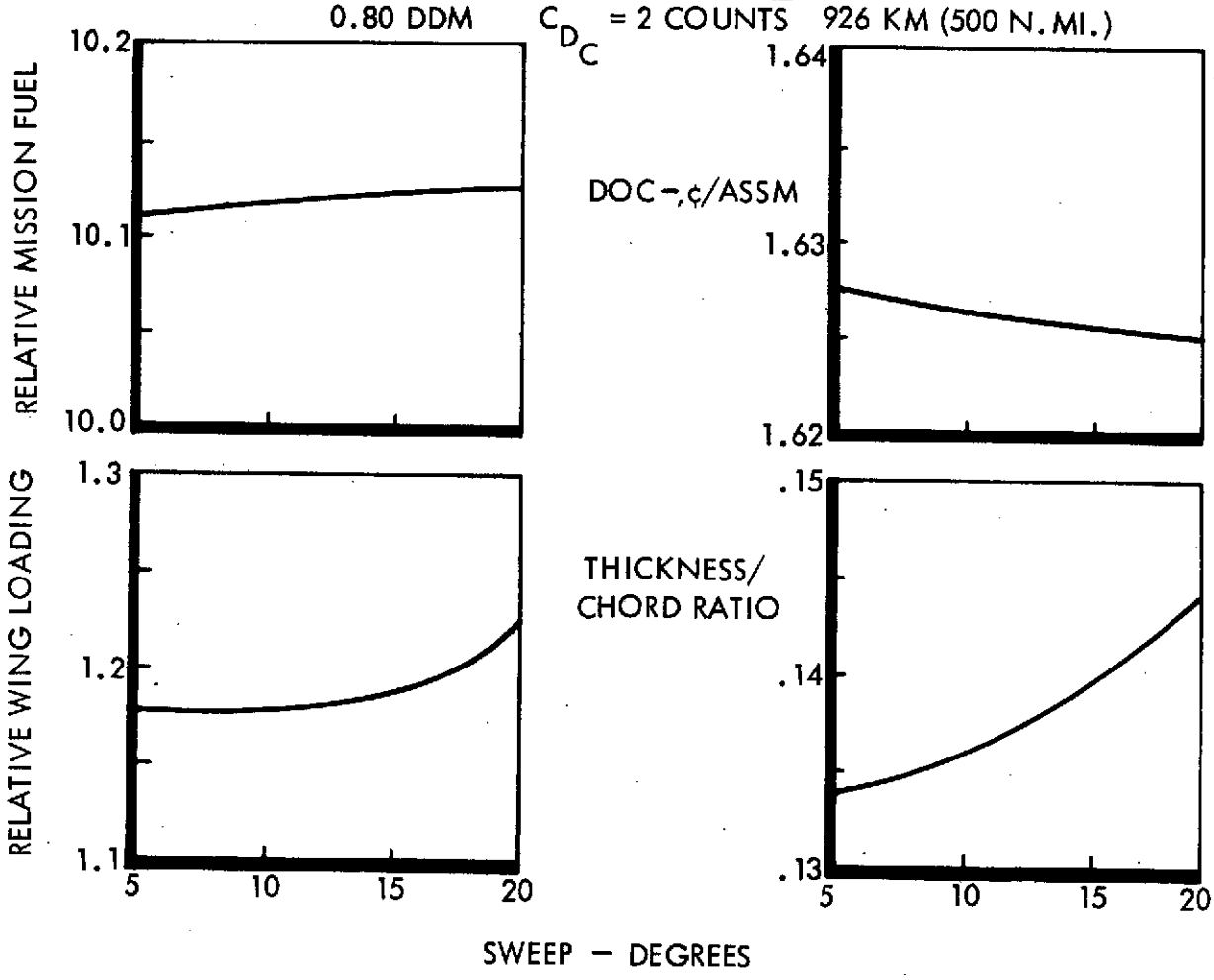

FIGURE 83: SENSITIVITY TO SWEEP ANGLE (1.35 FPR OTW/18F)

1.35 FPR; 4-ENGINE HYBRID; 0.75 M; 910M (3000 FT) F.L.

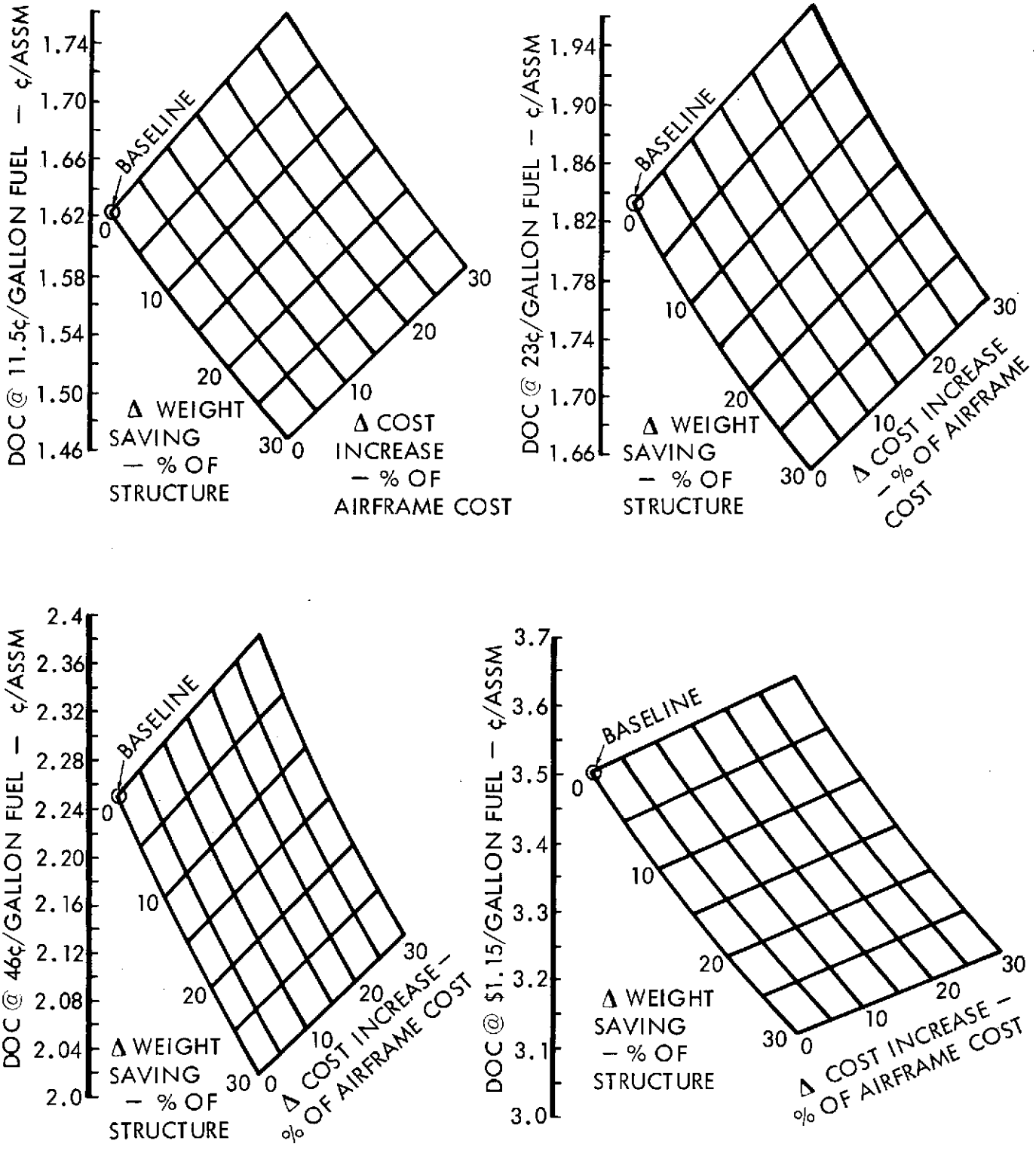

FIGURE 84: SENSITIVITY OF DIRECT OPERATING COST TO WEIGHT SAVING AND COST INCREASE

These data can be used, for example, to determine the effect of composites on the DOC at different fuel costs if the weight saving and cost increase due to the use of composites are known. The charts indicate, for example, that at the pre-energy crisis fuel cost of 11.5¢/gallon and an airframe cost increase of 30 percent, due to composites, the structure weight must be reduced by at least 23 percent to make any improvement in DOC. However, at a fuel cost of 46¢/gallon and a 30% increase in airframe cost it is only necessary to reduce the structure weight by more than 15 percent to start improving DOC. Thus, it can be accepted that an increase in fuel cost improves the case for the use of composities.

4.5.2 FPR 1.25 Configurations

Similar data to those described for the FPR 1.35 configurations were generated for the 1.25 FPR configurations. At the time this portion of the study was being conducted, emphasis was on minimum mission fuel consumption and therefore only 4-engine configurations were sized. Because of the lower cost/lb of thrust of larger engines, it could be that 2-engine configurations with this high lapse rate engine could have a lower DOC. However, since only 4-engine configurations have been sized, comparisons of fan pressure ratio effects have been conducted with only 4-engine configurations while comparisons of 2- and 4-engine configurations have been conducted with the 1.35 FPR engine.

Figure 85 presents mission fuel versus cruise altitude for 610m (2000 ft) and 910m (3000 ft) field performance and Mach numbers of 0.7, 0.75 and 0.8. All except the 0.7 M, 910m (3000 ft) field length optimized at 9,450m to 10,060m (31,000 to 33,000 ft) altitude. Note that there is little difference between $\leq$ 610m (2000 ft) and 910m (3000 ft) field performance at 0.8 M primarily because the $\leq$ 910m (3000 ft) design points have field lengths closely approaching 610m (2000 ft); this is due to the criticality of the cruise power requirement with this low FPR, high lapse rate engine. The difference between the field lengths is greater at 0.75 M and quite

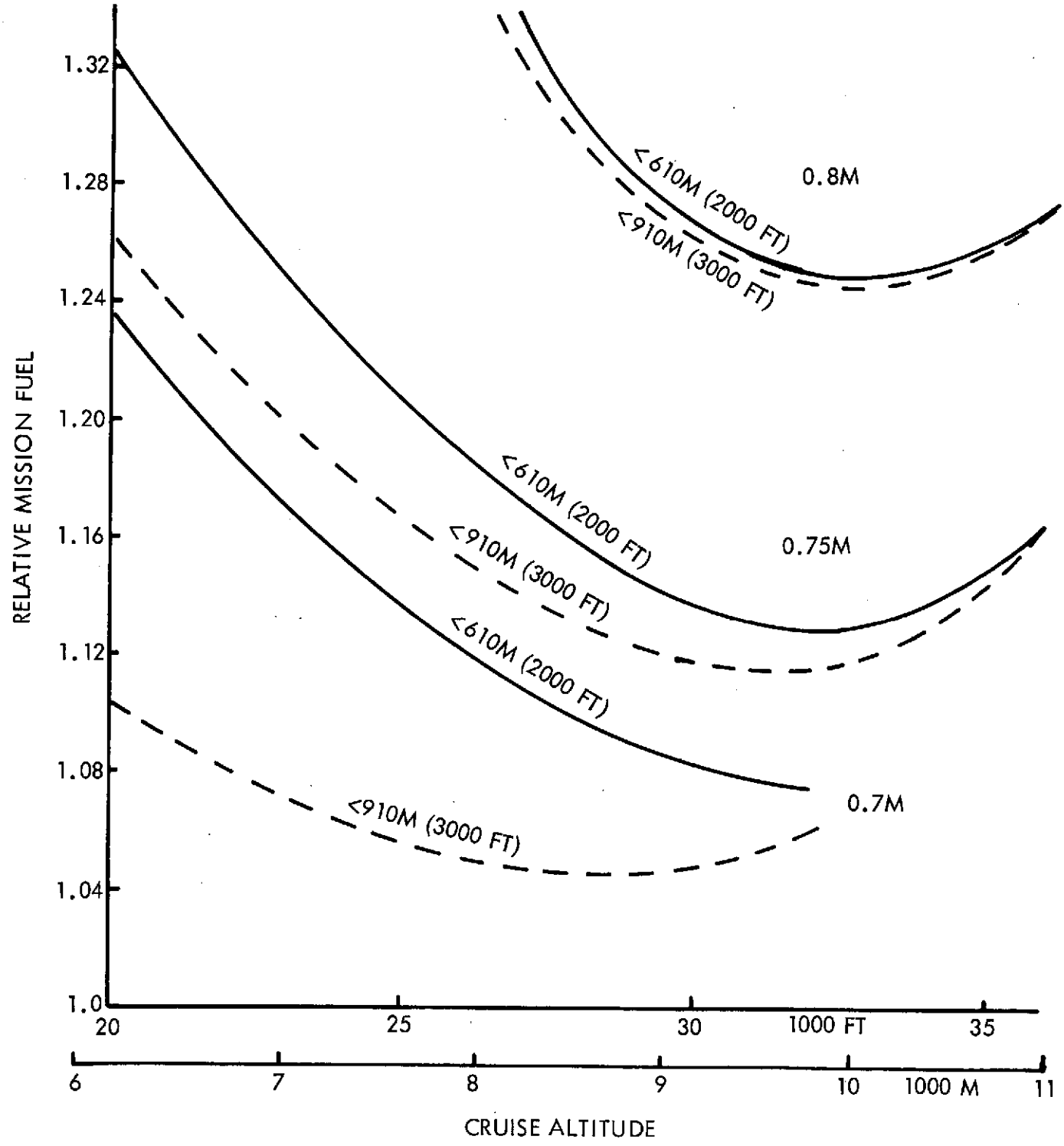

FIGURE 85: 1.25 FPR OTW/IBF - MISSION FUEL VS CRUISE ALTITUDE - (FOUR-ENGINES)

marked at 0.7 M, particularly at the lower altitudes. Figure 86 presents DOC at 11.5¢/gallon of fuel versus cruise altitude for ≺ 610m (2000 ft) and ≺ 910m (3000 ft) field performance and 0.8 M, 0.75 M and 0.7 M. The most apparent observation is that the optima are at the opposite end of the altitude scale to the minimum fuel points of Figure 85. As for the fuel case, the difference in DOC at 0.8 M for ≺ 610m (2000 ft) and ≺ 910m (3000 ft) is relatively small but is quite large at 0.7 M.

Figures 87 and 88 present similar data for DOC based on 23¢ and 46¢/gallon of fuel respectively. Note the large increase in DOC but also note the change in optimum altitude as fuel price increases. For example, at 0.75 M and ≺ 910m (3000 ft) field length, the optimum altitude changes from less than 6710 m (22,000 ft) at 23¢/gallon to 8530 m (28,000 ft) at 46¢/gallon. The optimum altitude for fuel economy is 9450 m (31,000 ft) from Figure 85. As would be expected, the point designs for minimum fuel and minimum DOC get closer together as the fuel cost/gallon increases.

Figure 89 shows mission fuel versus design cruise Mach number for 610m (2000 ft), ≺ 910m (3000 ft) and ≺ 1070m (3500 ft) field lengths for airplanes optimized for "minimum fuel" and those designed for minimum DOC at 23¢/gallon of fuel. At 0.8 M the minimum fuel and minimum DOC airplanes coincide. Also at 0.8 M airplanes cannot be optimized and have longer than 640m (2100 ft) field lengths. As the Mach number is reduced, airplanes can be optimized and have longer field lengths than 610m (2000 ft) as shown on the figure. The difference in fuel consumption between the minimum fuel and minimum DOC airplanes increases with decrease in Mach number and is still decreasing at 0.5M.

Figure 90 plots DOC at 11.5¢/gallon of fuel against design cruise Mach number for field lengths of ≺ 610m (2000 ft), ≺ 910m (3000 ft) and ≺ 1070m (3500 ft) for

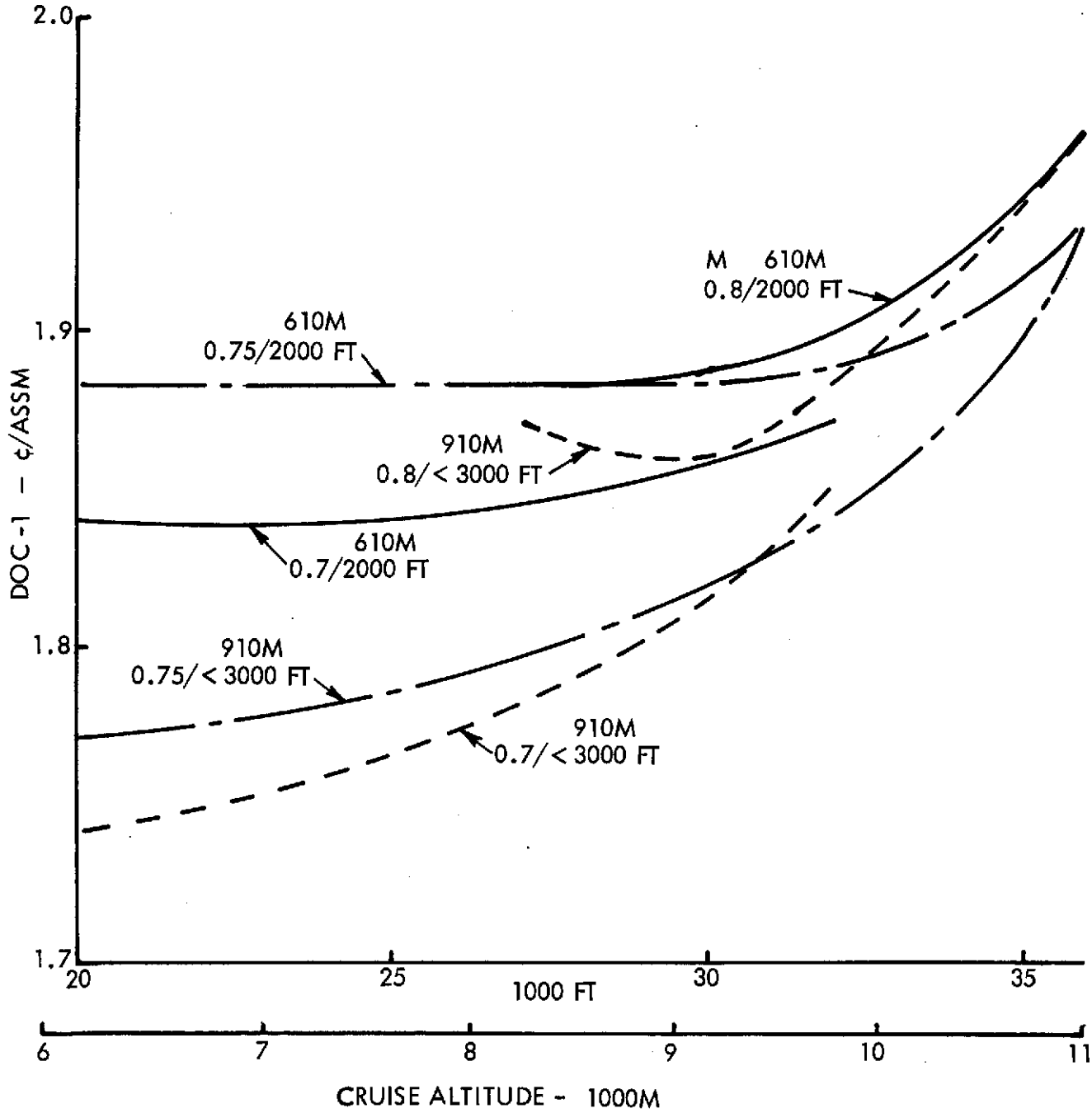

FIGURE 86: 1.25 FPR OTW/IBF - DOC -1 VS CRUISE ALTITUDE (4-ENGINES)

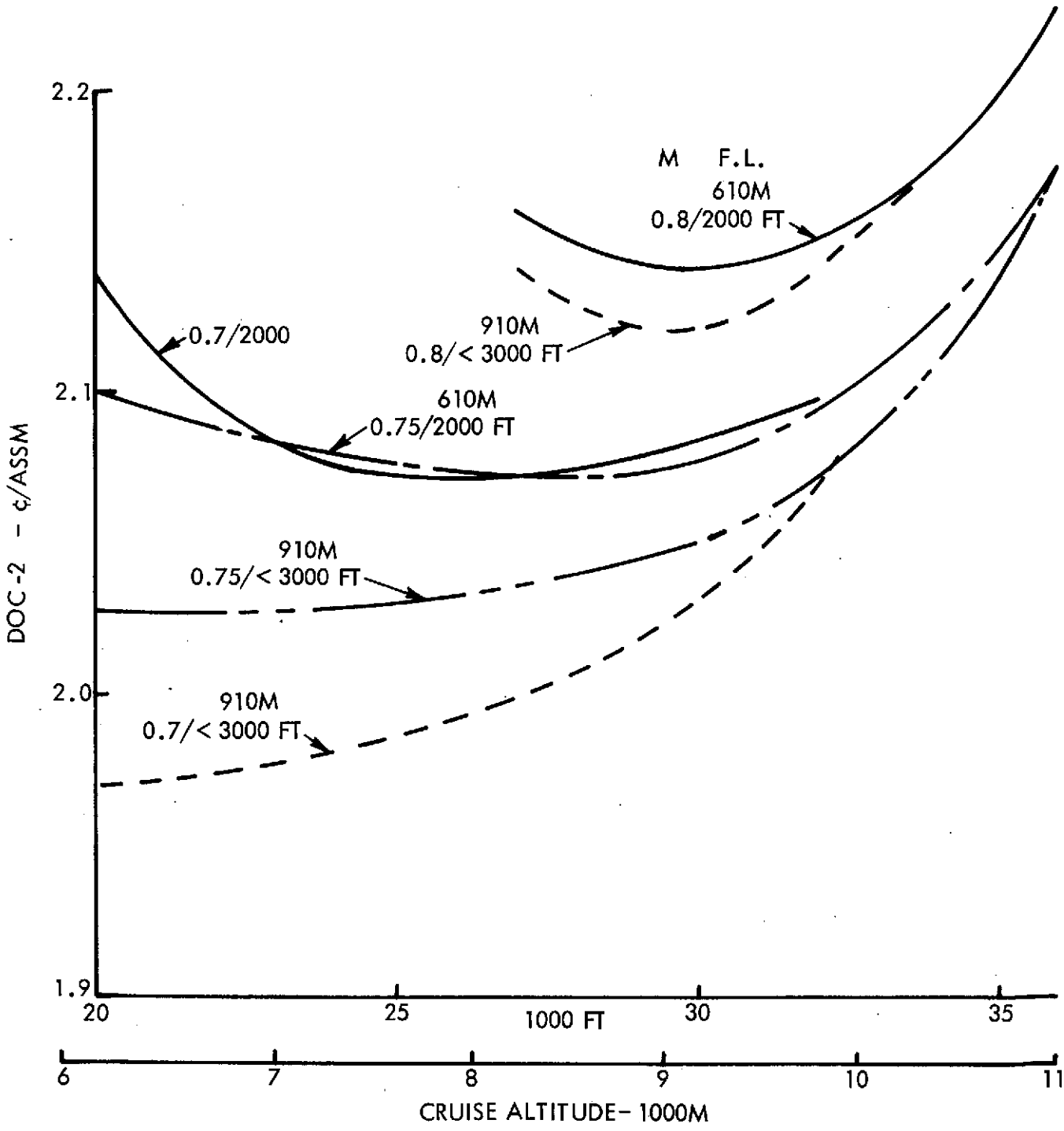

FIGURE 87: 1.25 FPR OTW/IBF - DOC -2 VS CRUISE ALTITUDE (4-ENGINES)

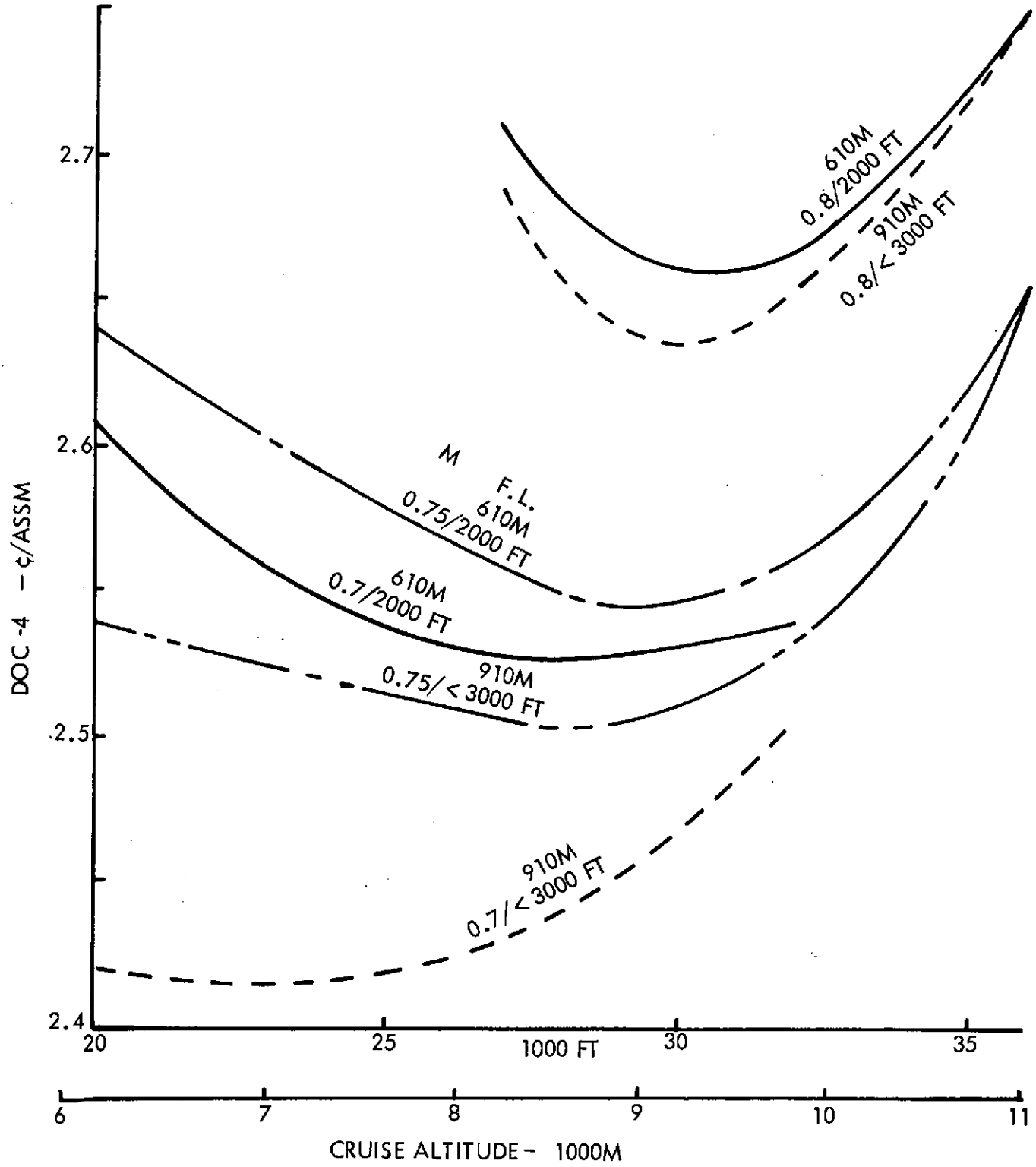

FIGURE 88: 1.25 FPR OTW/IBF - DOC - 4 VS CRUISE ALTITUDE (4-ENGINES)

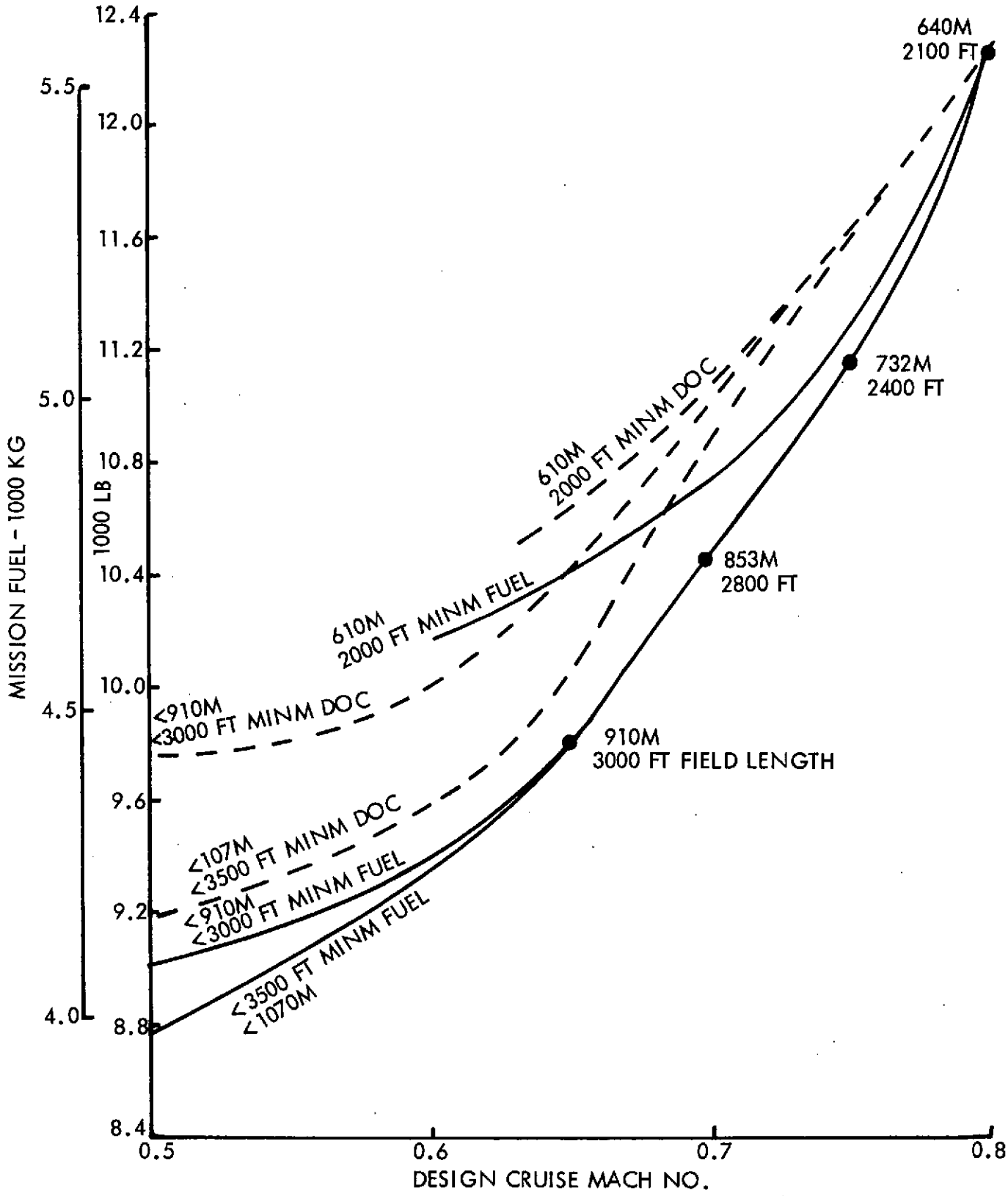

FIGURE 89: 1.25 FPR OTW/IBF - MISSION FUEL VS CRUISE MACH NO. (FOUR-ENGINES)

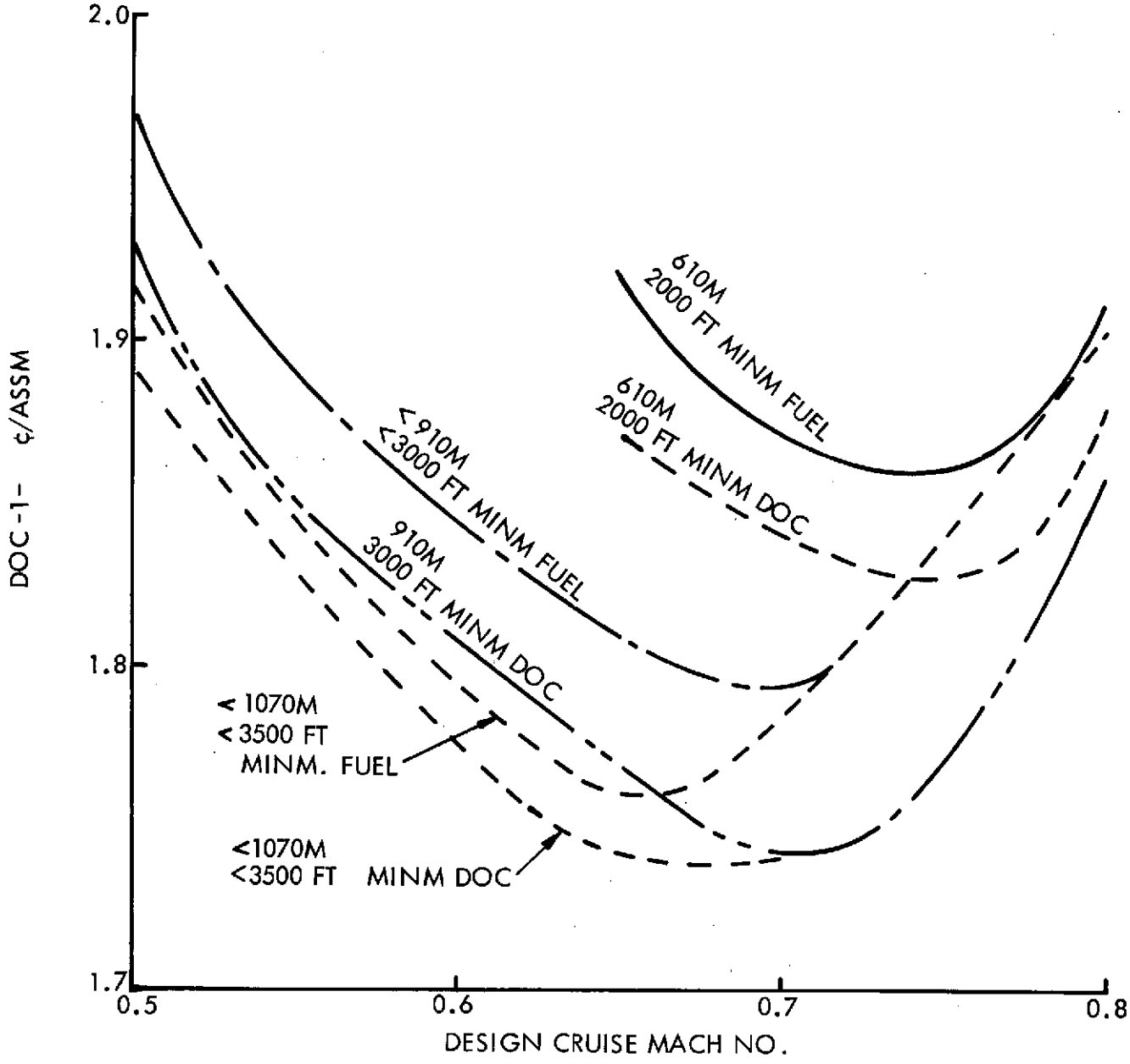

FIGURE 90: 1.25 FPR OTW/IBF - DOC-1 VS CRUISE MACH NO (4-ENGINES)

minimum fuel airplanes. Note that whereas fuel consumption continued to decrease with Mach number down to 0.5 M, the DOC buckets at 0.75 M for the 610m (2000 ft) designs, 0.7 M for the ≤910m (3000 ft) points and approximately 0.68 M for the ≤1070m (3500 ft) airplanes. Figures 91 and 92 present similar data to Figure 90 but for fuel costs of 23¢ and 46¢/gallon respectively. Note by comparison of the three figures that the Mach number at which the bucket occurs reduces with increase in fuel cost; for example, the 610m (2000 ft) buckets occur at 0.75 M for 11.5¢/gallon but reduce to 0.7 M at 46¢/gallon. Note also how the minimum fuel and minimum DOC curves are much closer together at 46¢/gallon than they are at 11.5¢/gallon.

4.5.3 FPR 1.47 Configurations

It was shown in Section 4.5.1 for the 1.35 FPR configuration that the 4-engine configuration provided the minimum fuel for 926Km (500 NM) mission for all Mach numbers and field lengths and also provided the lowest DOC at all Mach numbers, fuel costs and field lengths except 0.8 M, 910m (3000 ft) field and 11.5¢/gallon and 0.77 M, 1070m (3,500 ft) field and 23¢/gallon. Because of the relatively low lapse rate with altitude of the 1.47 FPR engine, these configurations will be less cruise critical than configurations using the 1.35 FPR engine and will therefore favor a 4-engined configuration even more than the 1.35 FPR. Sizing studies were therefore limited to the 4-engine configuration. The relatively high pressure ratio of this engine results in a smaller height of engine nozzle and smaller ducts for the IBF flow, which together eliminate (T/S) as a practical limit on wing loading. Similarly, the smaller ducts make the configurations less likely to be fuel volume critical.

The original data generated for these configurations used a constant dive speed (V_D) in the routine, which made the slower airplanes slightly pessimistic. This does not affect the optimizations of cruise altitude, aspect ratio and cruise power setting but does

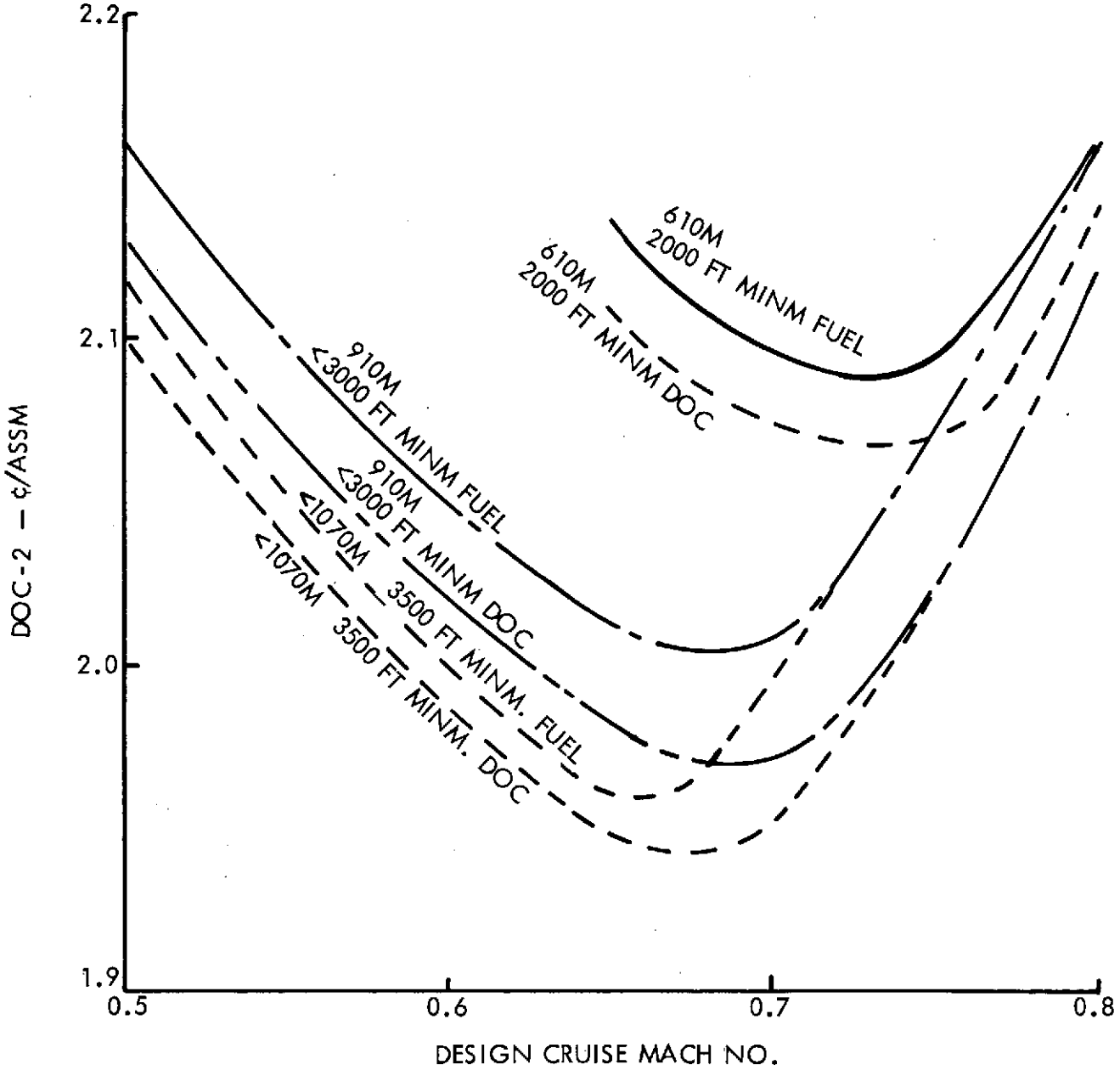

FIGURE 91: 1.25 FPR OTW/IBF - DOC (2) VS CRUISE MACH NO. (4-ENGINES)

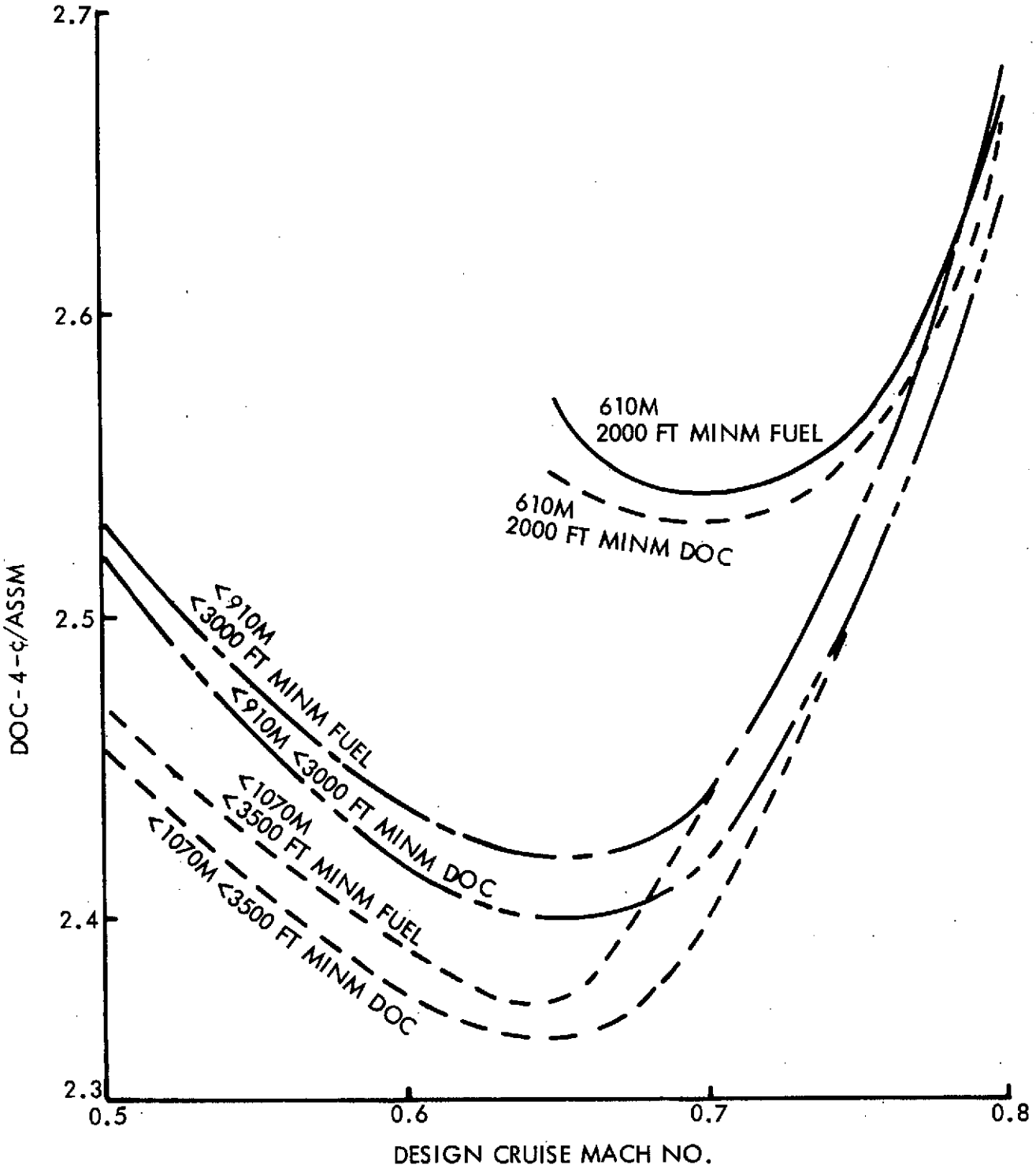

FIGURE 92: 1.25 FPR OTW/IBF - DOC -4 VS CRUISE MACH NO. (4-ENGINES)

affect the absolute value of mission fuel and DOC. The "constant" V_D data were therefore used to select the optimum cases, for each field length and Mach number, which were then recomputed. To avoid confusion, none of the "constant" V_D data is included in this report with the result that the amount of data presented is less than for the other FPRs.

At all Mach numbers and all field lengths studied, mission fuel minimized at the highest aspect ratio (AR 14). The optimum cruise altitude for minimum fuel varied with cruise Mach number and field length as shown below:

Cruise Speed M	Altitude @ Field Length 910m (3000')	1220m (4000')	1830m (6000')
0.8	10,970m (36,000')	10,360m (34,000')	9750m (32,000')
0.7	10,060m (33,000')	9450m (31,000')	8840m (29,000')
0.65	10,060m (33,000')	9140m (30,000')	8530m (28,000')
0.6	9140m (30,000')	8230m (27,000')	7620m (25,000')

The aspect ratio for minimum DOC varies with fuel cost, Mach number and field length as follows:

Cruise Speed	AR @ Field Length 910m (3000')	1220m (4000')	1830m (6000')
@ 11.5¢/gallon:			
0.8 M	8	8 - 14*	14
0.6 M	12	12	14
@ 46¢/gallon:			
0.8 M	Aspect ratio optimized at 14 for		
0.6 M	all cases.		

* Insensitive to aspect ratio.

The cruise altitude for minimum DOC varies with fuel cost, Mach number and field length as follows:

Cruise Speed	Cruise Altitude @ Field Length		
	910m (3000')	1220m (4000')	1830m (6000')
@ 11.5¢/gallon:			
0.8 M	9140m (30,000')	9140m (30,000')	9140m (30,000')
0.7 M	8230m (27,000')	8230m (27,000')	8230m (27,000')
0.6 M	6100 - 8230m (20-27,000')	6100m (20,000')	6100m (20,000')
@ 46¢/gallon:			
0.8 M	9140-10,970m (30-36,000')	9140-10,060m (30-33,000')	9140m (30,000')
0.7 M	9140m (30,000')	9140m (30,000')	8840m (29,000')
0.6 M	8230m (27,000')	7320-8230m (24-27,000')	6710m (22,000')

The variation of wing loading with field length and Mach number is shown in Figure 93

Figure 94 presents fuel required for a 500 NM mission plotted against cruise Mach number for airplanes having field lengths of 910m (3000 ft), 1220m (4000 ft) and 1830m (6000 ft) field length capability. The solid lines indicate airplanes optimized for minimum DOC at a fuel cost of 23¢/gallon (DOC-2). Minimum fuel consumption appears to occur at 0.64 to 0.66 M for all field lengths. At this speed the minimum fuel and minimum DOC-2 configurations are identical. As Mach number progressively increases, the fuel penalty for optimizing for DOC also increases until at 0.8 M the penalty at 910 m (3000 ft) is 204 Kg (450 lb or 3.7%). This penalty reduces with increase in field length until at 1830m (6000 ft) the configurations are again identical.

Figure 95 presents DOC at 23¢/gallon plotted against design cruise Mach number for the same cases as the foregoing. The Mach number at which the DOC bucket occurs increases with increase in field length for both the minimum fuel and minimum

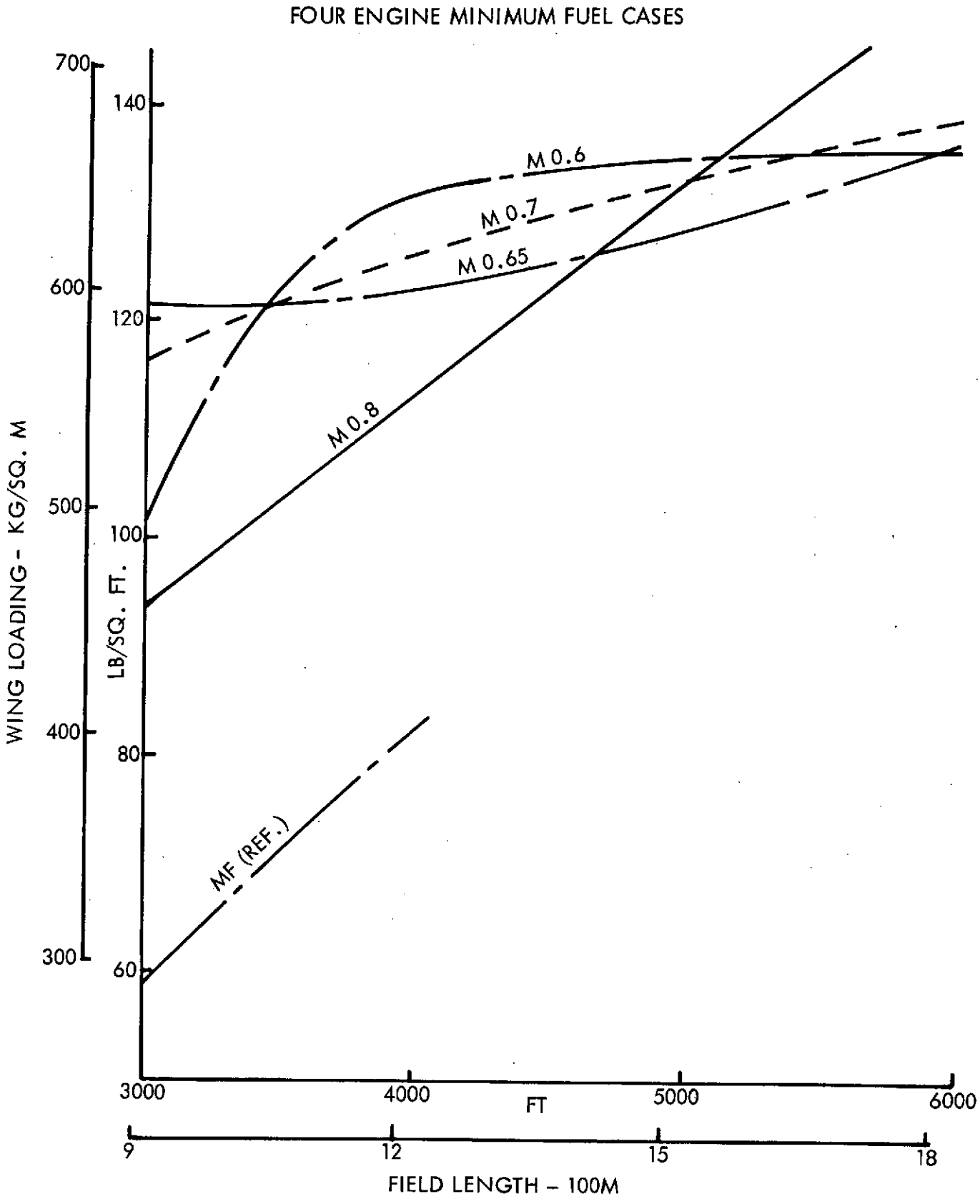

FIGURE 93: OTW/IBF: WING LOADING VS FIELD LENGTH & CRUISE SPEED

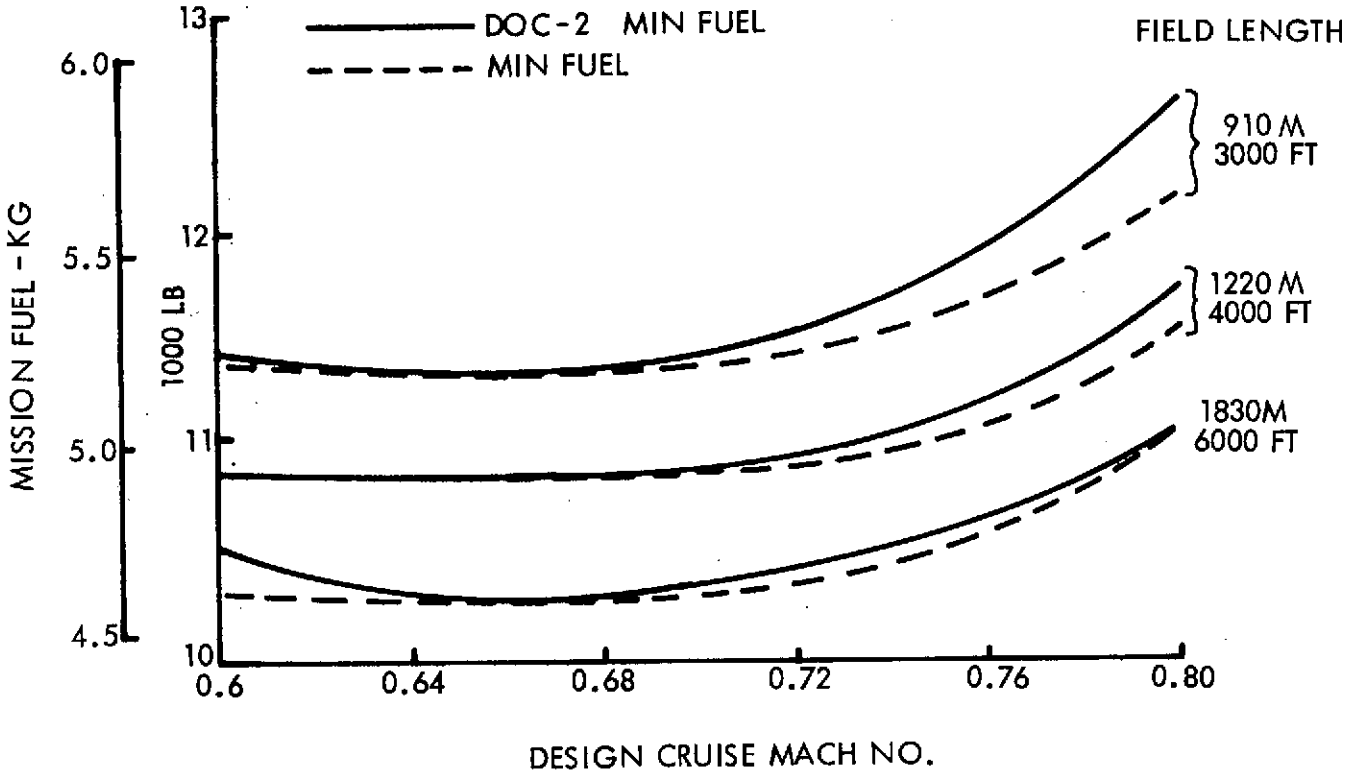

FIGURE 94: 1.47 FPR OTW/IBF: MISSION FUEL VS MACH NO.

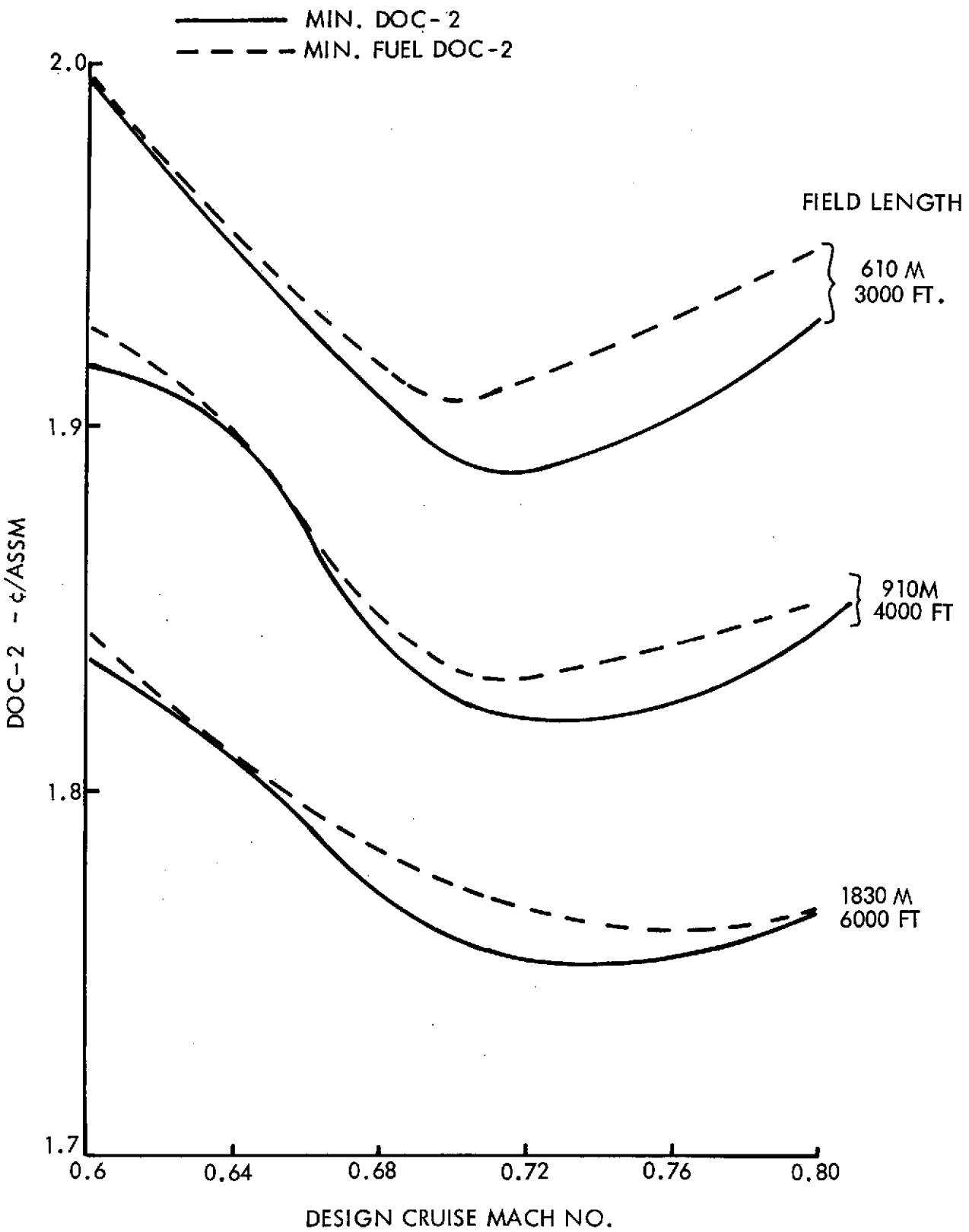

FIGURE 95: 1.47 FPR OTW/IBF: DOC-2 VS MACH NO.

DOC cases. The lowest Mach number at which the DOC bucket occurs is 0.7 M for the 910m (3000 ft) minimum fuel case increasing gradually to 0.76 for the 1830m (6000 ft) case compared with 0.64 to 0.66 to obtain absolute minimum fuel consumption. The advantage of a 3.7% fuel saving at 0.8 M and 910m (3000 ft) is offset by a 1% increase in DOC again reducing with increase in field length.

4.6 OTW-IBF MISSION PERFORMANCE

In order to validate the parametric performance data which forms the basis for the major part of the current study, detailed mission performance data have been computed using more refined methodology. These data have been found to show good correlation with the corresponding parametric performance for the range of airframe configurations and engine types under consideration. As an example of the detailed data obtained, this section presents mission performance for the baseline OTW/IBF aircraft.

4.6.1 Take-Off Performance

The take-off ground rules used in the current study are the same as those used in reference 2, and are outlined in Section 3.2. The optimum OTW-IBF mass flow split is closely represented by by the more convenient use of a standard 15 percent split for the 2000 ft. and 3000 ft. field length designs, and 10 percent for designs with longer field lengths. The absolete optimum split is a variable depending upon aspect ratio, wing loading, FPR and other configuration-oriented parameters. However, the take-off thrust loading requirement is relatively insensitive to small deviations from that optimum which permits the computational savings of the adopted approach. Based on the aerodynamic data presented in Section 4.3, take-off T/W versus W/S relationships have been calculated and are shown in Figure 96 for various field lengths, aspect ratios and numbers of engines. These characteristics have been developed by optimizing the flap settings to minimize T/W at a given W/S. Take-off operational envelopes at the 926km (500 n.m.) mission take-off weight are presented in Figure 97 for the baseline 910m (3000 ft.) OTW/IBF design having two 1.35 FPR engines and a 7.73 aspect ratio. The figure indicates that the airplane has an engine-out second segment climb gradient of 1.37 degrees which just meets the FAR XX requirements. Lift-off occurs at 106 KTAS at an angle of attack of 15 degrees. The take-off field length versus gross weight is shown in Figure 98.

4.6.2 Take-Off Climbout Profiles

Various climbout techniques have been studied in order to minimize the take-off noise footprint areas. The take-off climbout profile shown in Figure 99 for the baseline

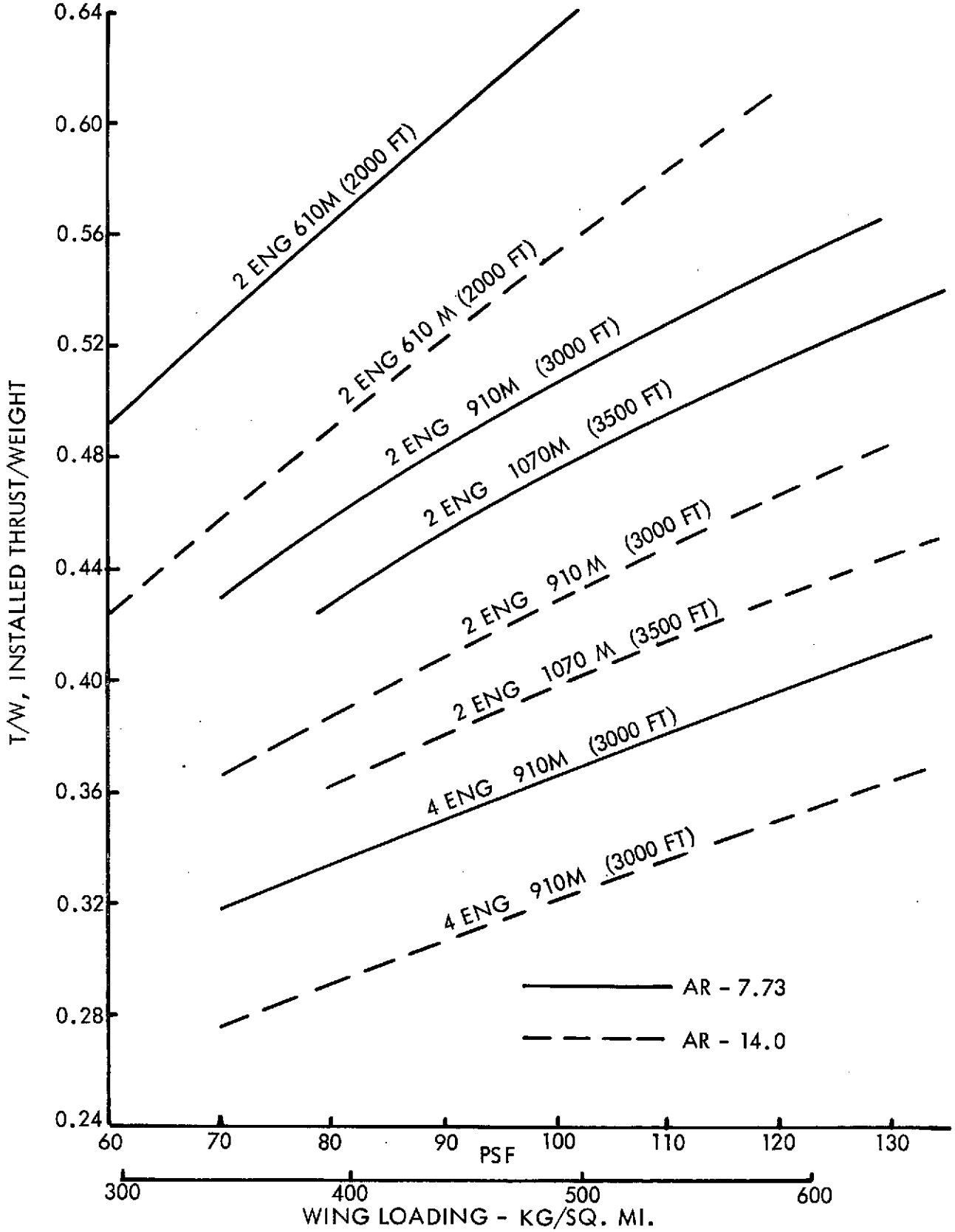

FIGURE 96: GENERALIZED T/W REQUIRED FOR TAKEOFF
(910M, 3000 FT, 1.35 FPR OTW/IBF)

GROSS WEIGHT = 142,500 LB.
67,360 KG

FLAPS = 12.7°

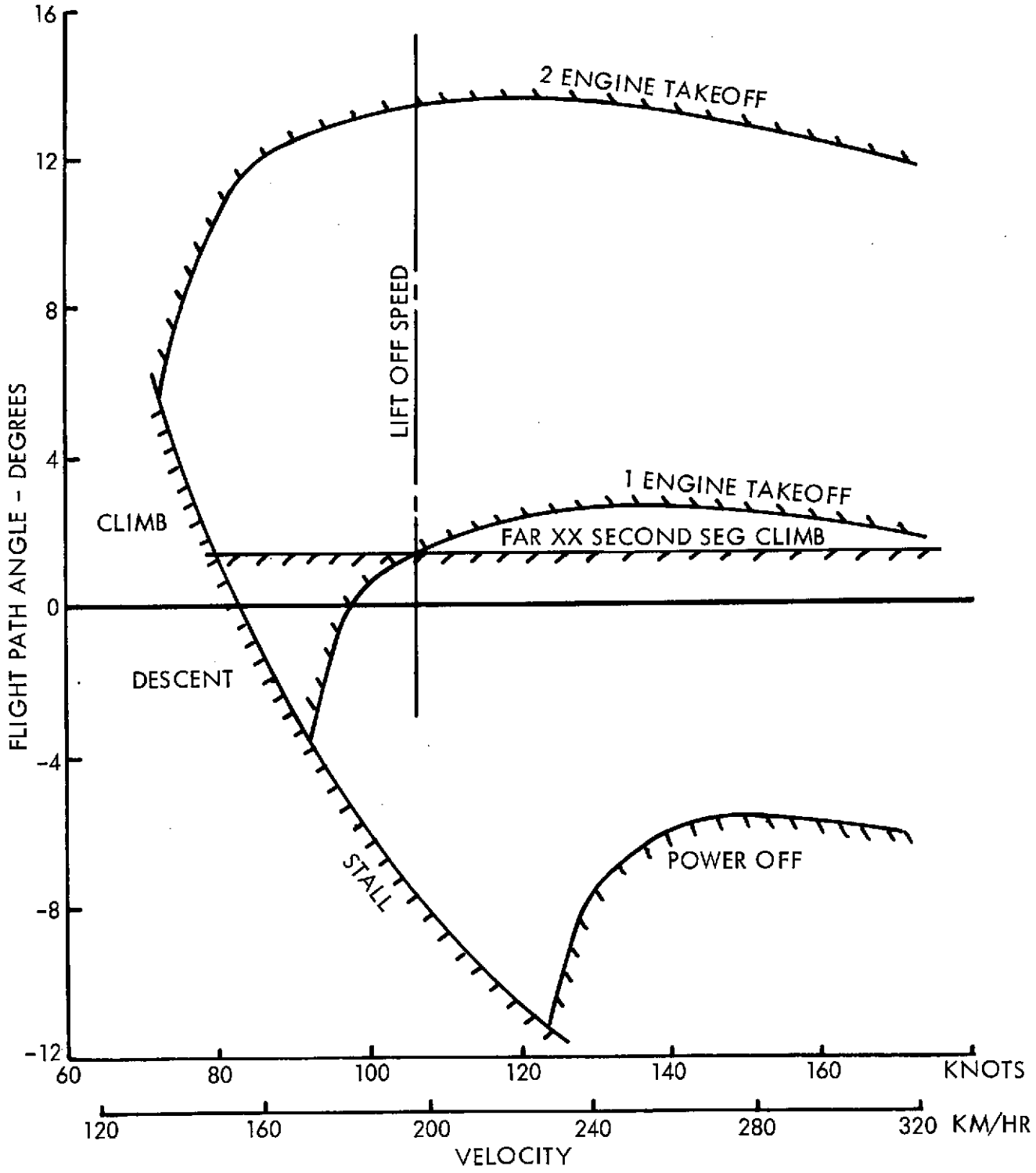

FIGURE 97: TAKE-OFF OPERATIONAL ENVELOPE
1.35 FPR OTW/IBF, 910M (3000 FT. F.L.)

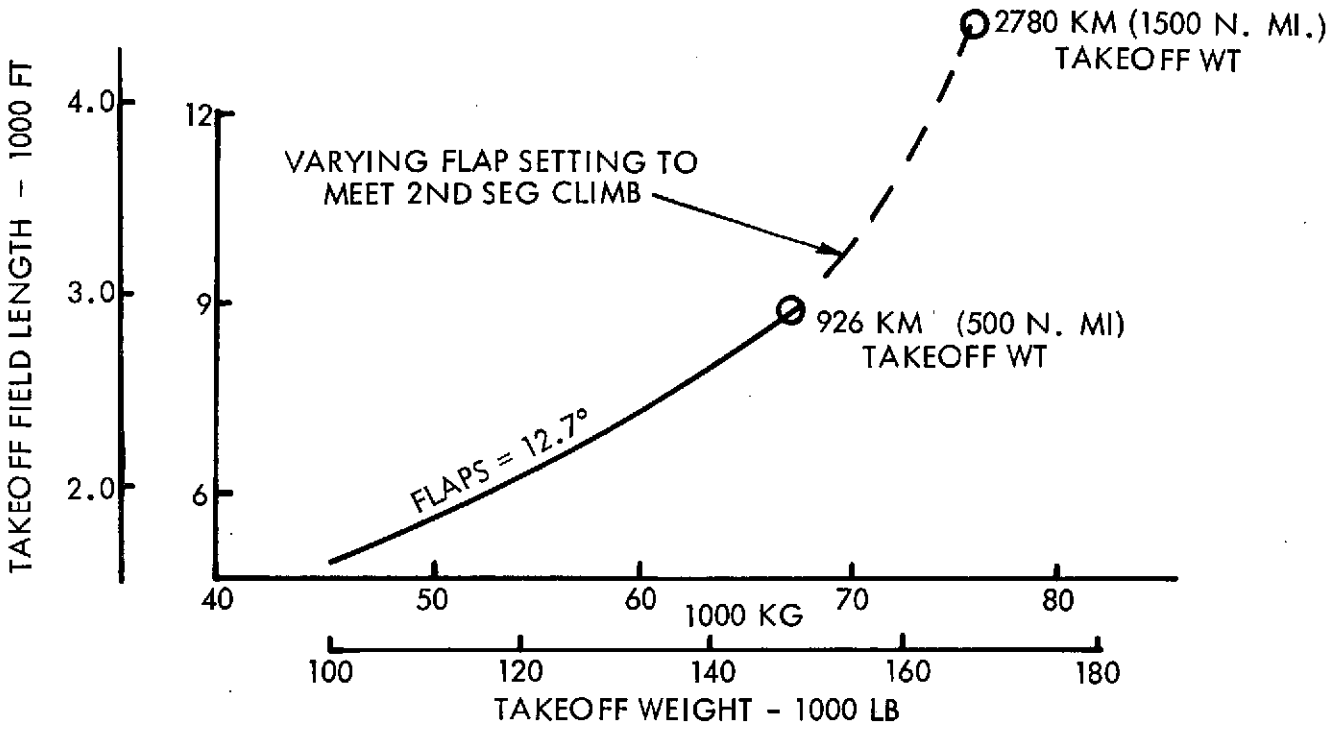

FIGURE 98: TAKEOFF PERFORMANCE - 1.35 KG FPR OTW/IBF @ 910M (3000 FT) F.L.

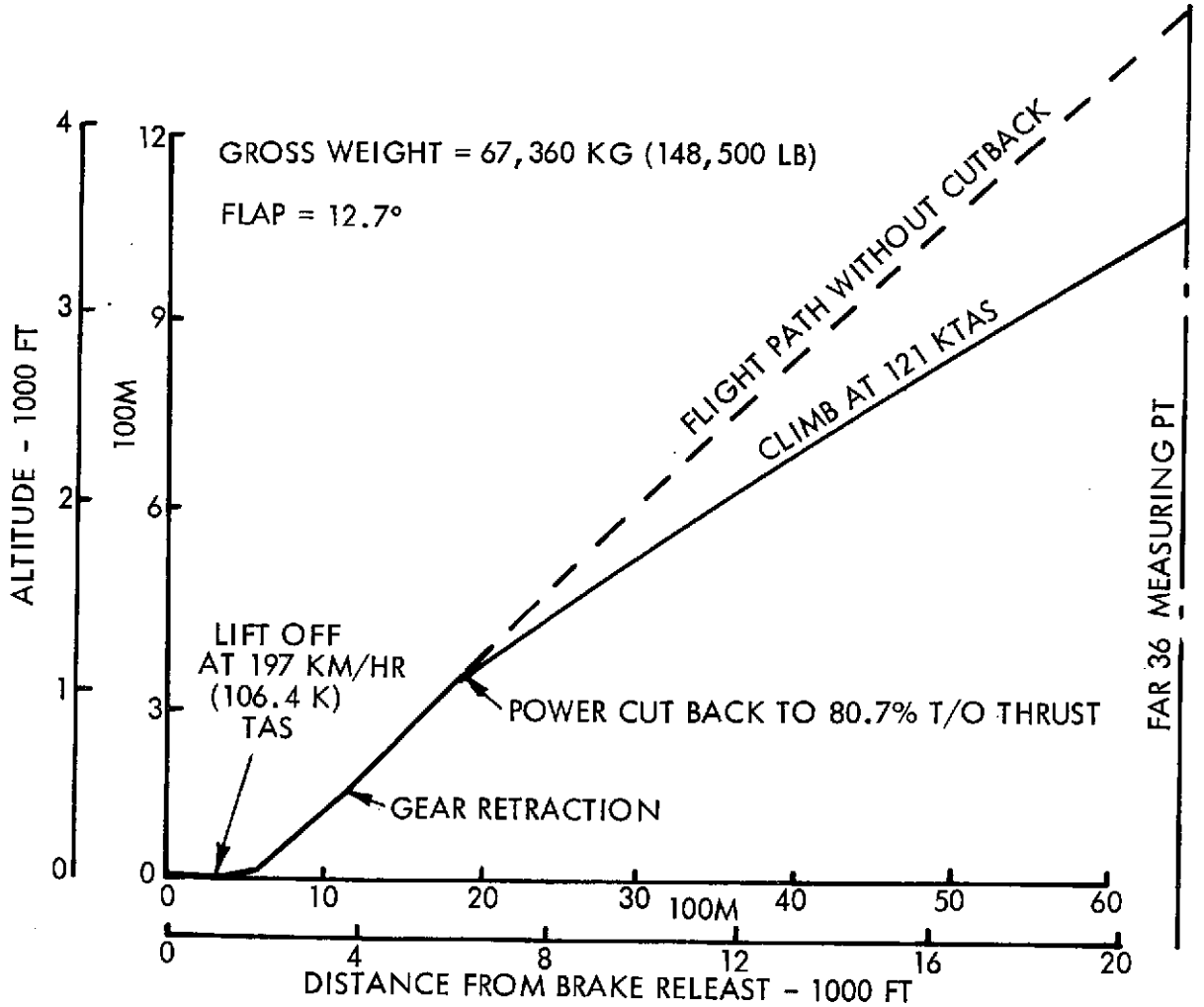

FIGURE 99: TAKEOFF CLIMBOUT PROFILE 910M (3000 FT) 1.35 FPR OTW/IBF

aircraft uses the technique adopted for all aircraft take-off noise analyses. Gear retraction is assumed to occur 10 seconds after passing the 10.7m (35 foot) screen, during which interval the aircraft accelerates 27.8km/hr. (15 KTAS). From this point the climb is continued with all engines at maximum take-off thrust and the flaps maintained at the take-off setting, until the FAR 36 minimum height for power cutback is attained. At this point, power is reduced to the level which permits zero climb gradient in the event of engine failure. The climb is then continued, maintaining the take-off flap setting, to the FAR 36 measuring point of 6.5km (3.5 n.m.) from brake release. For the baseline aircraft the height at this point is 1070m (3500 ft) above the runway.

4.6.3 Mission Flight Profiles

The basic flight profile used throughout the study for sizing, costing, and ROI analyses is presented in Figure 100. Mission data for the baseline aircraft operating at 926km (500 n.m.) mission is given in the form of a computer pointout in Figure 101. Payload-range performance is shown in Figure 102.

4.6.4 Landing Performance

The landing ground rules used in the current study are given in Section 3.2 and are unchanged from those used in reference 2. Landing field length for the baseline aircraft is shown as a function of gross weight in Figure 103. Significant parameters for the landing approach profile used in the baseline aircraft noise analyses are:

Flap Setting	46 degrees
Glideslope	5.2 degrees
Approach Speed	182.2 km/hr. (98.4 KTAS)
Power Setting	38 percent
Flare Distance	125m (410 feet)
Ground Roll	455m (1390 ft)
Approach C_L	3.00
Angle of Attack	6.9 degrees

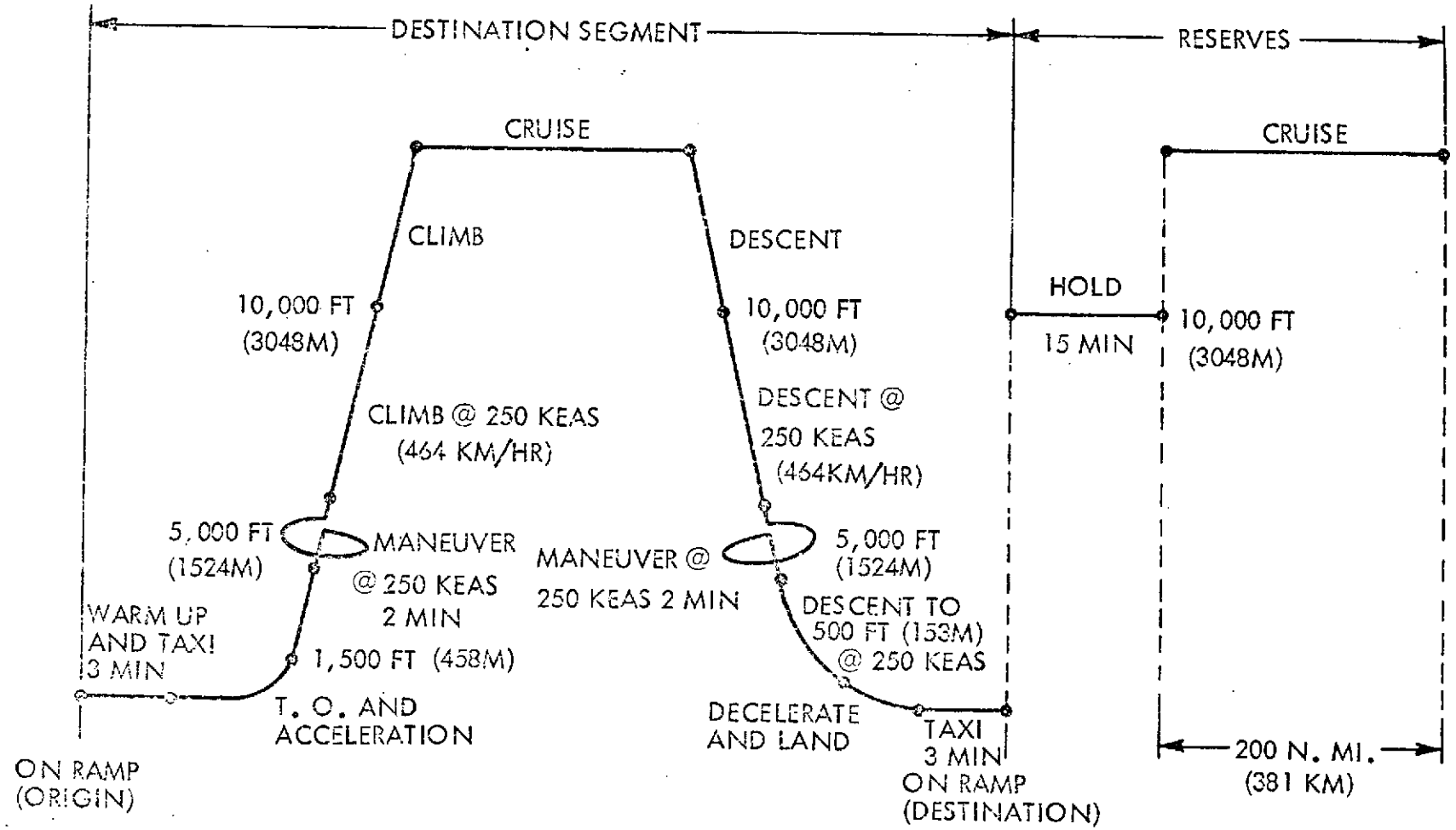

FIGURE 100: 4.96 FLIGHT PROFILE (INCLUDING RESERVES)

MISSION SUMMARY

2 ENG BASELINE 1.35 HYB - 1500 NM .80 MACH 30000 FT - 4/9/74

RANGE = 500.N MI CRUISE MACH = .800 CRUISE ALTITUDE = 30000. FT
PAYLOAD = 30340. LB NO. PASSENGERS = 148. IENG = 48

FLIGHT TIME= 1.324 BLOCK TIME= 1.391 BLOCK SPEED=359.6 BLOCK FUEL= 12189.
RESERVE FUEL= 5401. D.O.C.= 1.692 CENTS PER SEAT STATUTE MILE

MISSION SEGMENTS

1. WARM-UP AND TAKE-OFF

RAMP WT (LB)	WARM-UP/ G.M. TIME (MIN)	TAKE-OFF TIME (MIN)	WUTO FUEL (LB)
148532.	2.00	1.00	956.

2. HOLD AND CLIMB TO CRUISE ALTITUDE

START CLIMB WT (LB)	CLIMB TIME (HR)	CLIMB FUEL (LB)	CLIMB DISTANCE (N MI)
147576.	.361	3493.	107.4

3. CRUISE SEGMENT

START CRUISE WT (LB)	CRUISE TIME (HR)	CRUISE FUEL (LB)	CRUISE DISTANCE (N MI)
144133.	.698	6148.	329.2

4. DESCENT 1 TO 20000 FT

START WT (LB)	DESCENT TIME (HR)	DESCENT FUEL (LB)	DESCENT DISTANCE (N MI)
137984.	.040	215.	19.2

5. DESCENT 2 TO 10000 FT

START WT (LB)	DESCENT TIME (HR)	DESCENT FUEL (LB)	DESCENT DISTANCE (N MI)
137769.	.049	257.	19.1

6. DESCENT 3 TO 5000 FT

START WT (LB)	DESCENT TIME (HR)	DESCENT FUEL (LB)	DESCENT DISTANCE (N MI)
137512.	.047	197.	13.2

7. HOLD AT 5000 FT

START HOLD WT (LB)	HOLD TIME (MIN)	HOLD FUEL (LB)	HOLD DISTANCE (N MI)
137314.	2.000	259.	.0

8. DESCENT 4 TO 500 FT

START WT (LB)	DESCENT TIME (HR)	DESCENT FUEL (LB)	DESCENT DISTANCE (N MI)
137055.	.046	201.	11.9

9. APPROACH AND LANDING

START WT (LB)	APPROACH TIME (MIN)	APPROACH FUEL (LB)	LANDING WT (LB)
136854.	2.00	361.	136493.

RESERVE FUEL

EXTENDED RANGE (N MI)	FUEL REQ (LB)	LOITER TIME (MIN)	FUEL REQ (LB)	FUEL MIL (LB)
200.0	3551.	15.00	1850.	0.

FIGURE 101: MISSION SUMMARY: 1.35 OTW/IBF @ 910M (3000 FT) F.L.

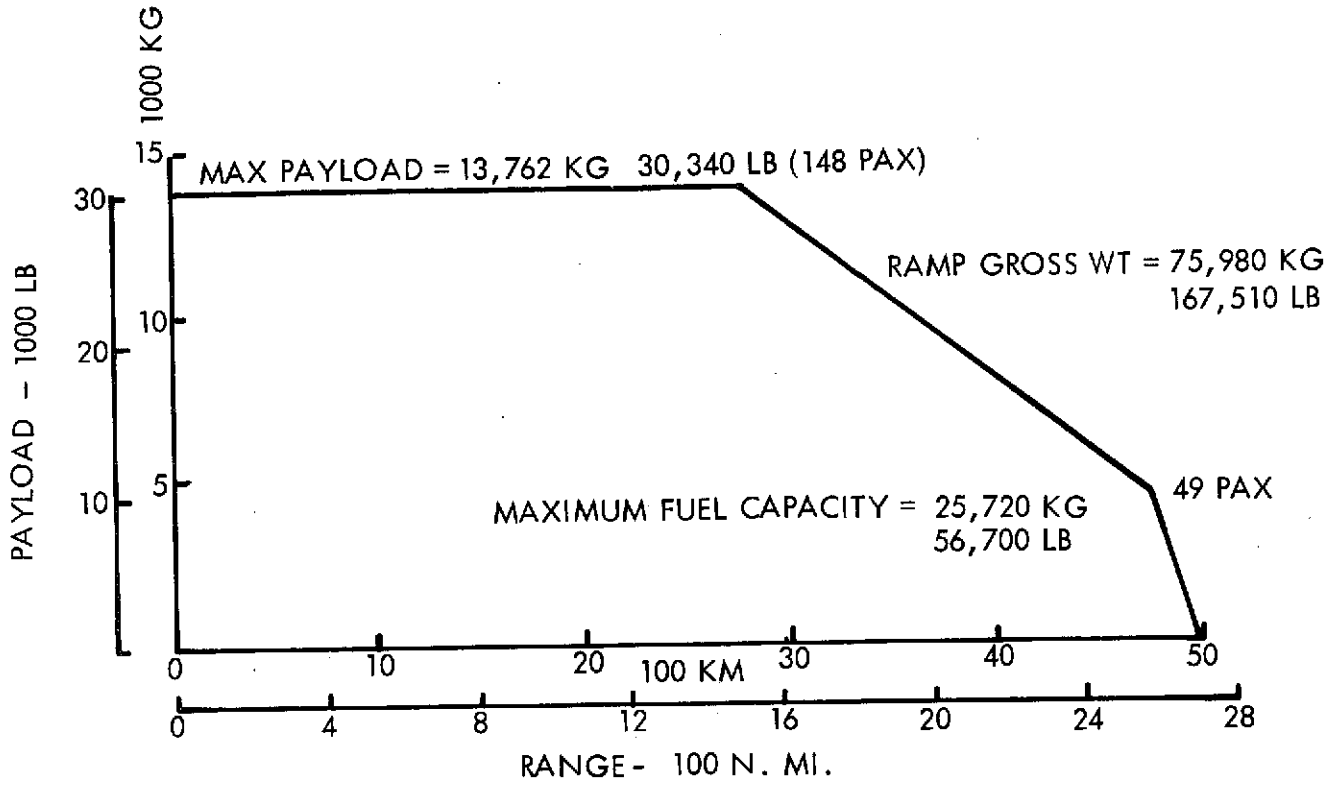

FIGURE 102: PAYLOAD-RANGE: 1.35 FPR OTW/IBF 910M 3000 FT

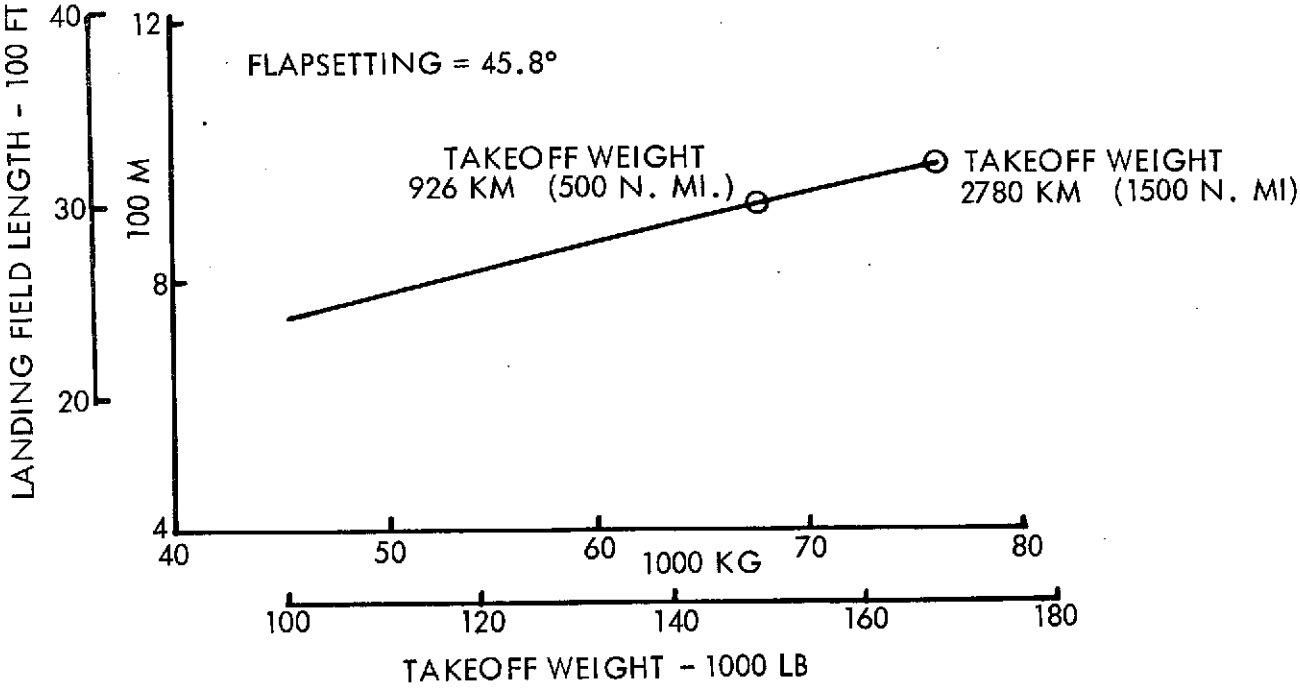

FIGURE 103: LANDING PERFORMANCE - 1.35 FPR OTW/IBF

4.6.5 Off-Design Operation

To illustrate the effect on mission fuel and DOC of operating the airplane at other Mach numbers and altitudes than its design optimum, additional mission performance was computed for the baseline 1.35 FPR OTW/IBF airplane. The specific points identified in Figure 104 represent the design point airplanes for 926 Km (500 N. Mi) STOL mission (lower point), and for the combined 926 KM (500 N. Mi)/ 2780 Km (1500 N. Mi) R/STOL mission (upper point). The penalty for the R/STOL capability is approximately 400 lb of fuel for the 926 Km (500 N. Mi) mission. Reducing the altitude from the design point of the combined mission airplane increases fuel consumption rapidly. Lowering the speed to 0.75M results in a small reduction in fuel consumption, while increasing altitude at the reduced Mach number further reduces the fuel used. However, decreasing the speed and increasing the altitude also increases the block-time as shown in Figure 105 . Decreasing the altitude decreases the block-time due to the better climb performance at the lower altitudes.

The combined effects of the changes in fuel consumption and block-time on DOC are shown in Figure 106. Considering a utilization of 2500 hours/year, the DOC -1 of the R/STOL airplane is 1.7 £/ASSM compared with 1.62 £/ASSM or the STOL-only airplane. Because of small differences in the climb routines of the sizing and mission programs and because the airplane is compromised to meet the longer range operation, the 926 KM (500 N. Mi) DOC-1 reduces slightly as altitude is reduced. In other words, the reduction in block-time is more than offsetting the increase in fuel consumption effect on the DOC.

The 2500 hour utilization is based on a 926 Km (500 N. Mi) range capability. Increasing the capacity payload range to 2780 Km (1500 N. Mi) increases the flexibility of the vehicle and permits greater utilization. In order to achieve the same DOC at 926 Km (500 N. Mi) for the R/STOL airplane as that which can be achieved by the STOL-only airplane , requires an increase in utilization to 2940 hours. The added flexibility of route scheduling and the use of some longer routes will allow this

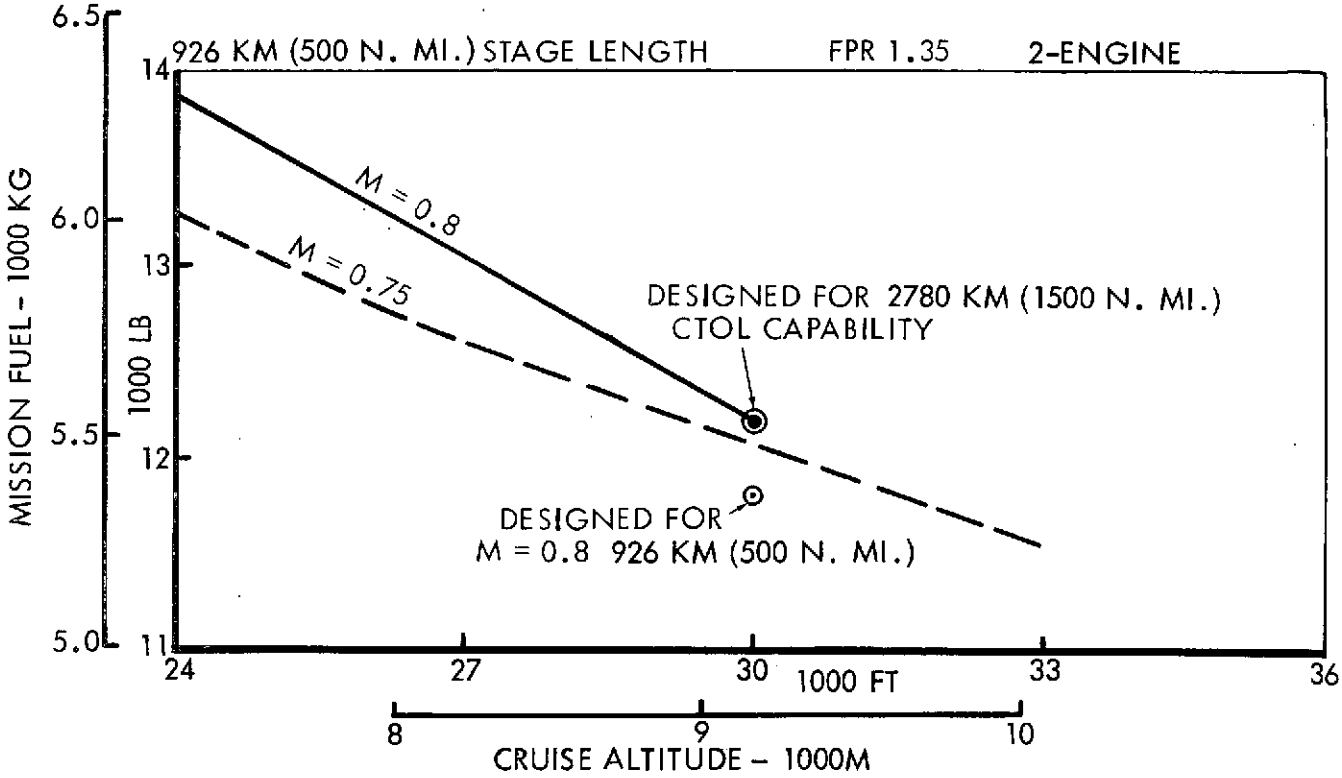

FIGURE 104: FUEL VS ALTITUDE AND CRUISE SPEED, OFF-DESIGN OPERATION: 1.35 FPR OTW/IBF; 910M (3000 FT) F.L.

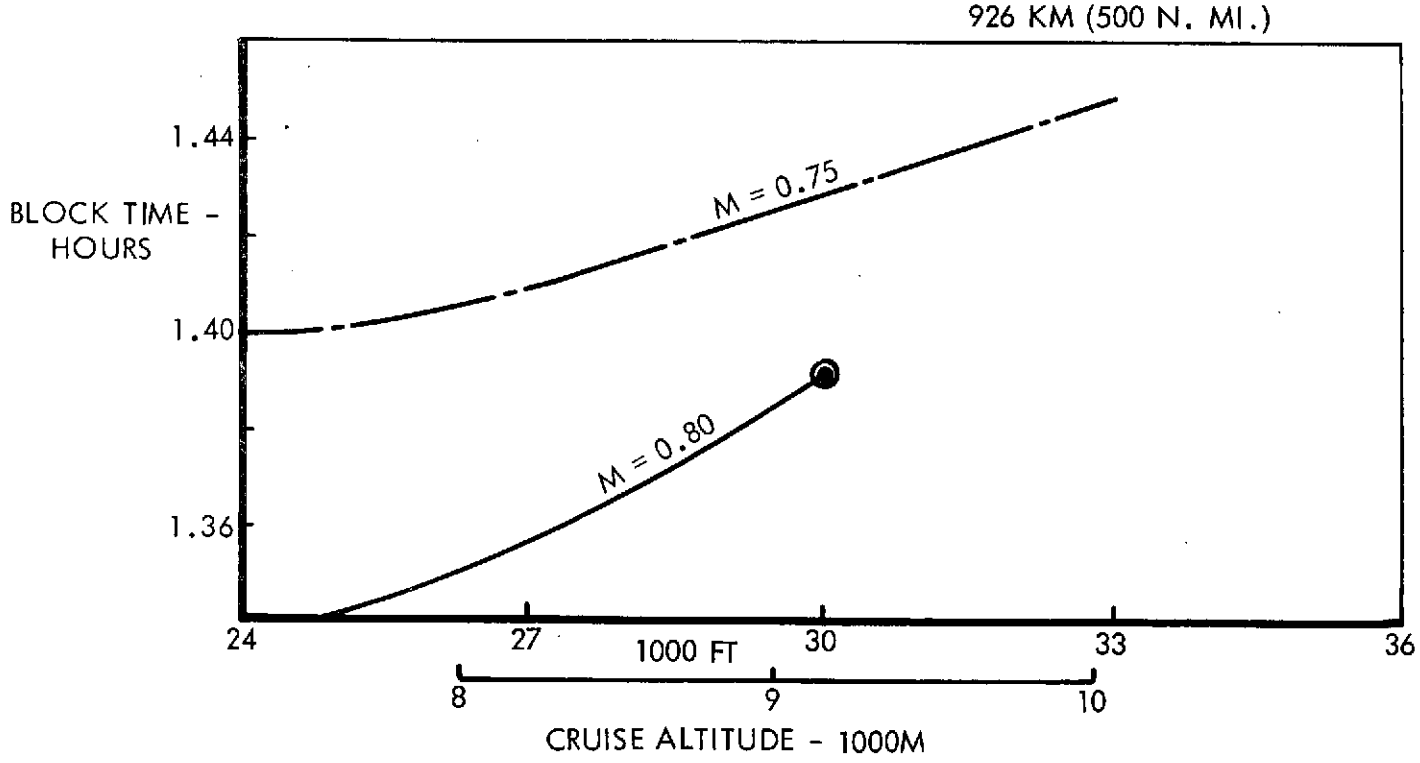

FIGURE 105: BLOCK TIME VS ALTITUDE AND CRUISE SPEED: OFF-DESIGN OPERATION 1.35 FPR OTW/IBF; 910M (3000 FT) F.L.

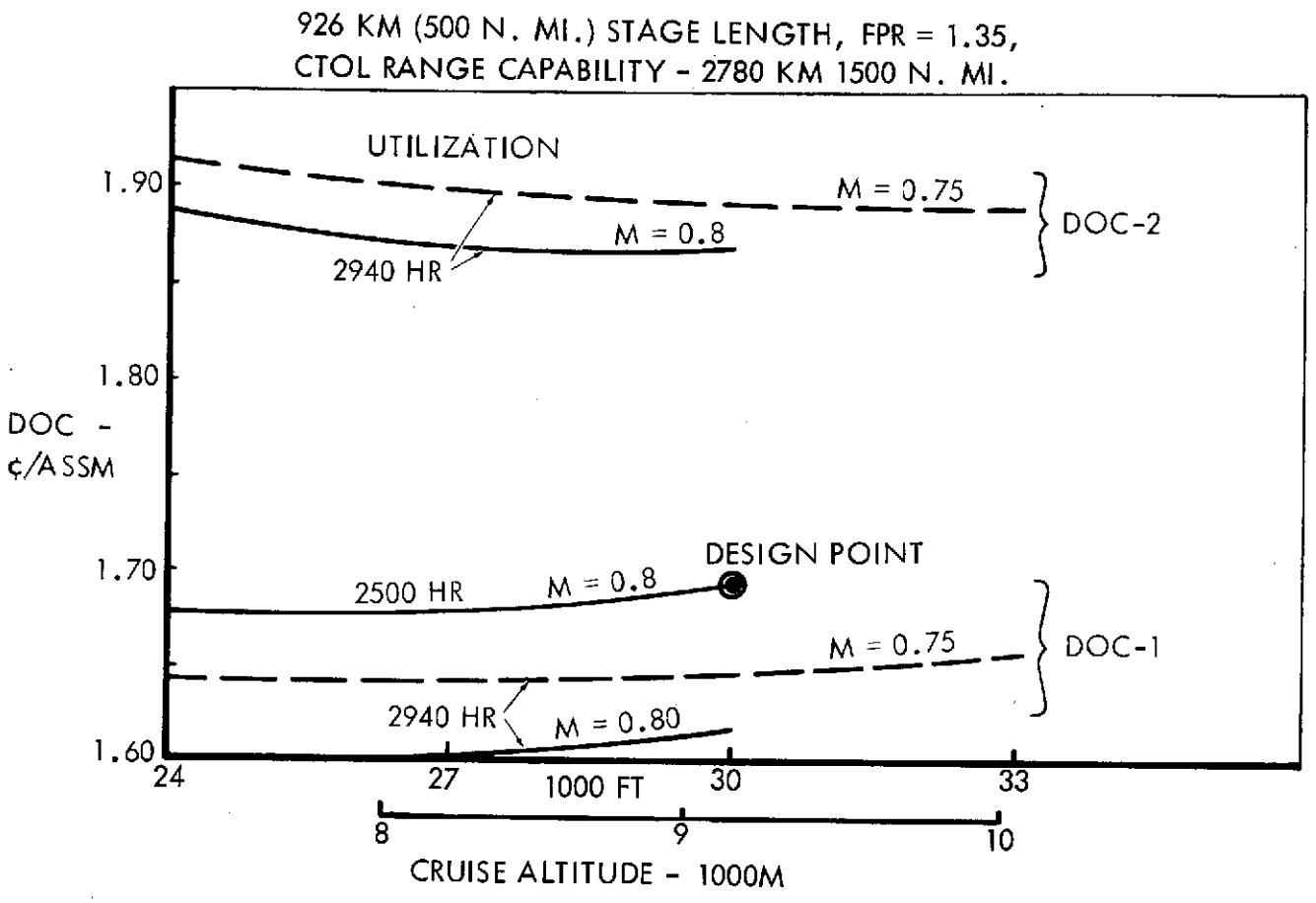

FIGURE 106: DOC VS ALTITUDE AND CRUISE SPEED OFF-DESIGN OPERATION: OTW/IBF 910M (3000 FT) F. L.

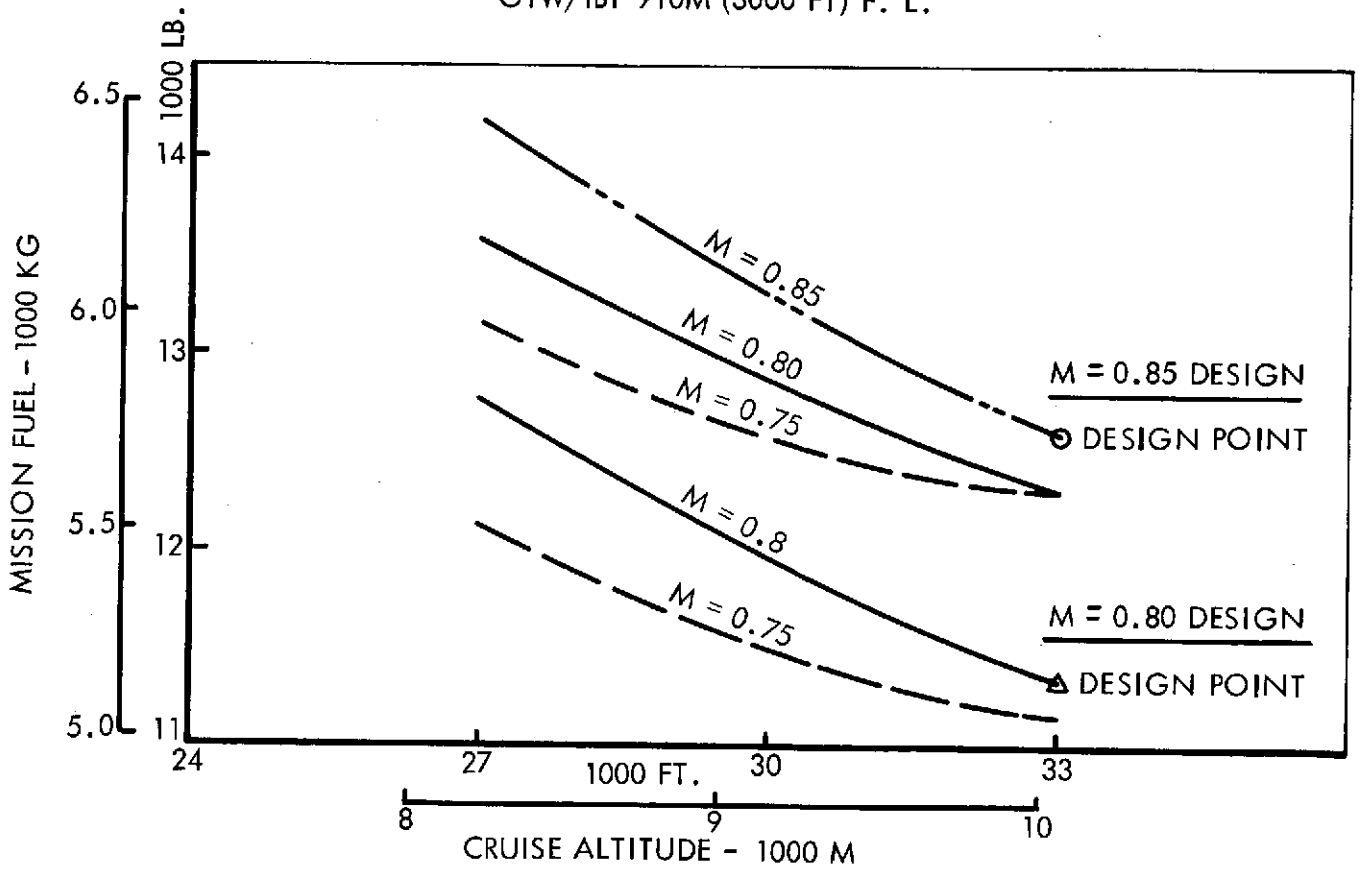

FIGURE 107: FUEL VS ALTITUDE AND CRUISE SPEED, OFF-DESIGN OPERATION: 1.47 FPR OTW/IBF @ 910M (3000 FT) F.L.

utilization to be achieved as discussed in Section 9.0. Although Figure 104 shows a decrease in fuel consumption by decreasing speed and increasing altitude, it is not sufficient to improve DOC-2 as can be seen in the upper portion of Figure 106.

Figure 107 illustrates a similar point by comparing two designs, one optimized for 0.85M and the other optimized for 0.80M, both at 10,060m (33,000 ft) cruise altitude. Operation of the 0.85M design at 0.8M or even 0.75M does not lower the fuel consumption down to the level of the airplane actually optimized for operation at 0.8M. Figure 108 shows the increase in DOC-1 and DOC-2 due to operating off the design points. Attempting to fly a 0.85M design at 0.8M results in a 9% fuel penalty, and a 5% DOC penalty relative to the airplane actually optimized for 0.8M.

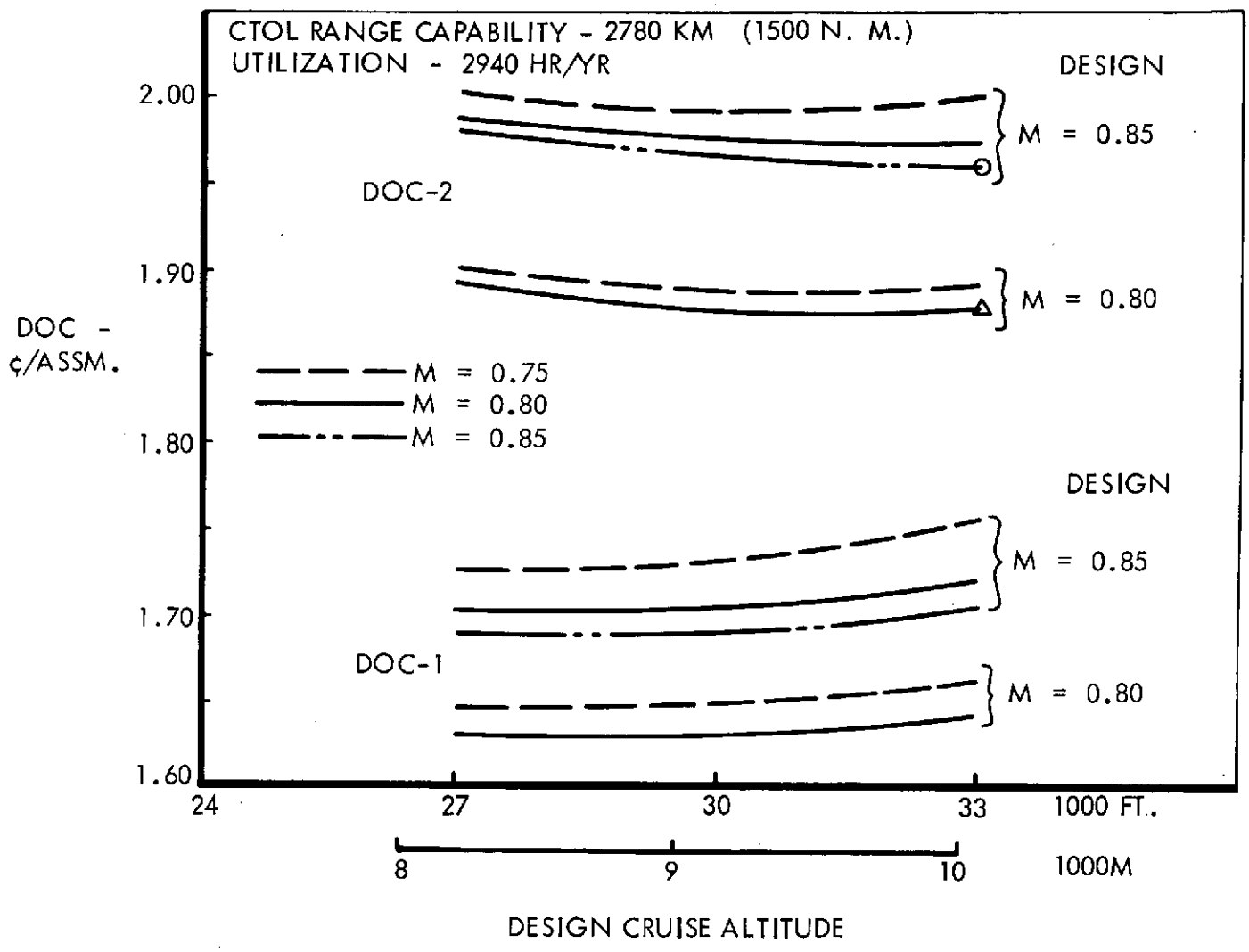

FIGURE 108 DOC VS ALTITUDE AND CRUISE SPEED, OFF DESIGN OPERATION: 1.47 FPR OTW/IBF @ 910M (3000 FT) F.L.

4.7 OTW-IBF HANDLING AND RIDE QUALITIES

The handling and ride characteristics of the selected baseline mission configuration for 1.35 FPR and 910m. (3000 ft.) field length have been compared with the selected criteria developed in Ref. 2. The purpose and design philosophy have been discussed in Section 3.3 and Ref. 2. Since the baseline configuration has an aspect ratio of 7.73 whereas the fuel conservative configurations identified in Section 4.5 have aspect ratios of 10-14, the gust response and ride quality data presented here will tend to be slightly optimistic for the latter vehicles with higher lift curve slopes at the similar field lengths and wing loadings. However, at the longer field lengths the increased wing loading will compensate for this effect. The qualitative conclusions presented here may be taken to be applicable to all vehicles.

The unique features of a two engine over the wing and internally blown flap configuration for STOL performance lead to a great deal of importance being placed on the engine out possibility. The ducting arrangement developed for this emergency condition has shown that the concept is indeed feasible. Particular emphasis in the analysis has been placed on a six degree of freedom program to insure adequate consideration of cross coupling during engine out and gust response.

4.7.1 OTW-IBF Handling Qualities

Longitudinal - The selected horizontal tail volume coefficient of 1.0 provides a 20 percent MAC allowable travel of the center of gravity. The aft C.G. limit is at 45 percent MAC and there is a 4 percent static margin at that point with a thrust coefficient of 0.5 which approximately corresponds to approach power. The landing phase is tail critical and as before there is a pitch acceleration capability of 0.3 rad/sec^2 at the aft C.G. after trim is provided. The downwash used in this analysis was taken from Lockheed tunnel test of a similar configuration. The required $C_{L\ MAX}$ of the horizontal tail is 2.1. Reference 2 shows that inverted camber and a geared elevator with slot are required for this tail lift coefficient to be achieved.

The unaugmented short term mode dynamic characteristics are compared to the MIL-F-83300 criteria in Figure 109. This critical aft C.G. landing approach meets the criteria. Due to the narrow margin and the aperiodic nature of this mode, an augmentation system is needed to insure adequate handling characteristics and low pilot work load.

Lateral-Directional - Directional control is provided by a 40 percent double hinged rudder which deflects to a maximum of 60 degrees. This control with the selected vertical tail volume coefficient of 0.1 provides a yaw acceleration capability of 0.174 rad/sec^2 approximately 18.5 Km/hr. (10 knots) below approach speed. The six degree of freedom analysis which follows shows that this is adequate for trimming a single engine failure in a 46 Km/Hr. (25 knot) crosswind (equivalent to a sideslip of 15 degrees) with 30 percent control power left for maneuver.

The lateral control required to meet the instantaneous roll capability of 0.42 rad/sec^2 calls for a roll coefficient of 0.23. Reference 15 shows that this requires a BLC type aileron. The six degree of freedom analysis will show that 25 percent of the roll control is available for maneuver after trimming for an engine out with the most adverse 46 Km/hr. (25 knot) crosswind.

The dynamic characteristics of the dutch roll mode are compared to MIL-F-83300 in Figure 110 . The unstable mode has a time to double amplitude of 5 seconds and will require an augmentation system. The spiral mode is stable and the roll time constant is 1.1 seconds.

Six Degree of Freedom Analysis - The longitudinal aerodynamic characteristics of the parametric program were combined with the estimated lateral-directional aerodynamic and propulsive system characteristics in a six degree of freedom digital computer program. The estimated lateral-directional trends are from recent Lockheed wind tunnel tests on similar configurations. Particular attention has been focused on an engine failure and

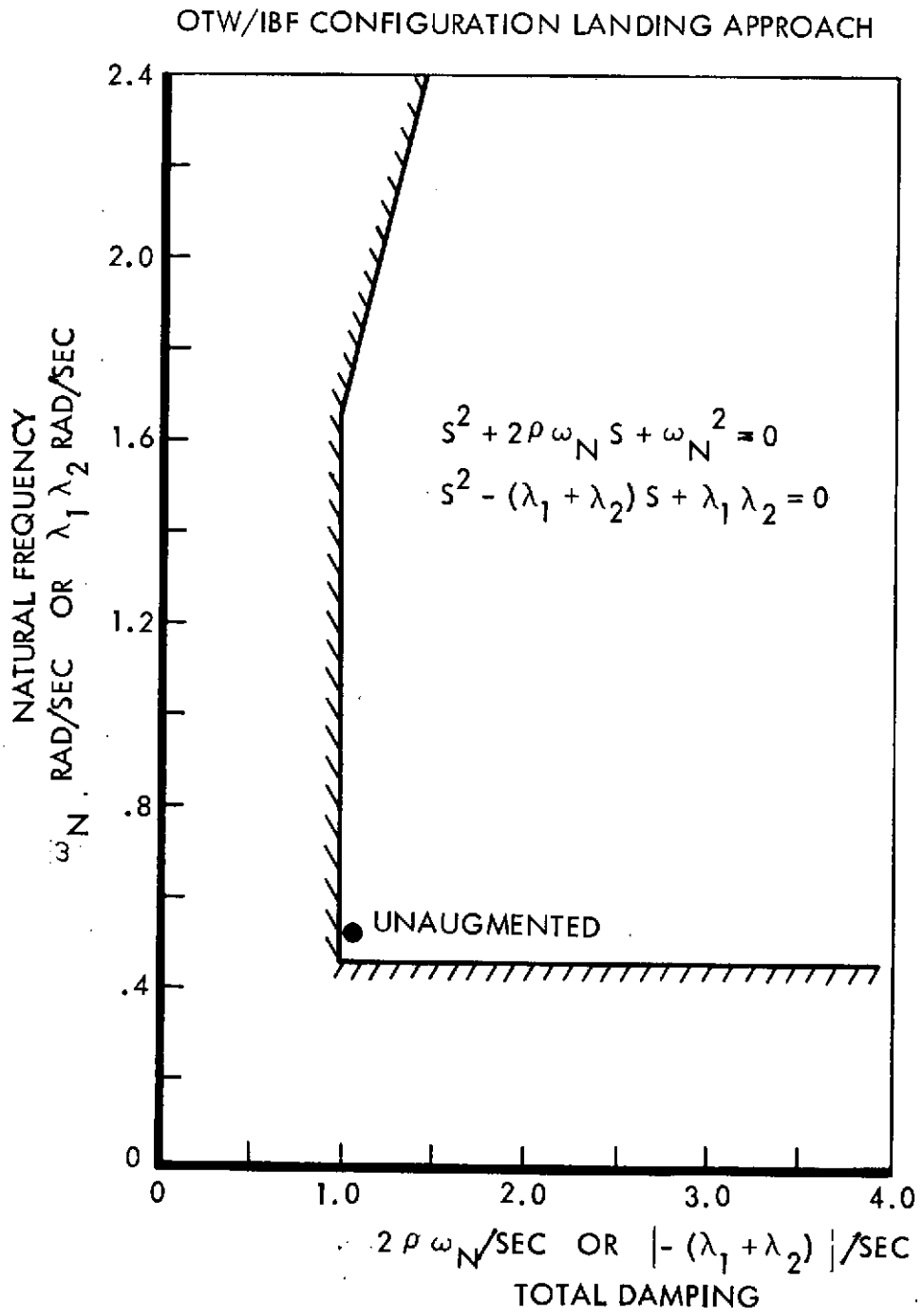

FIGURE 109: LONGITUDINAL SHORT TERM MODE REQUIREMENTS

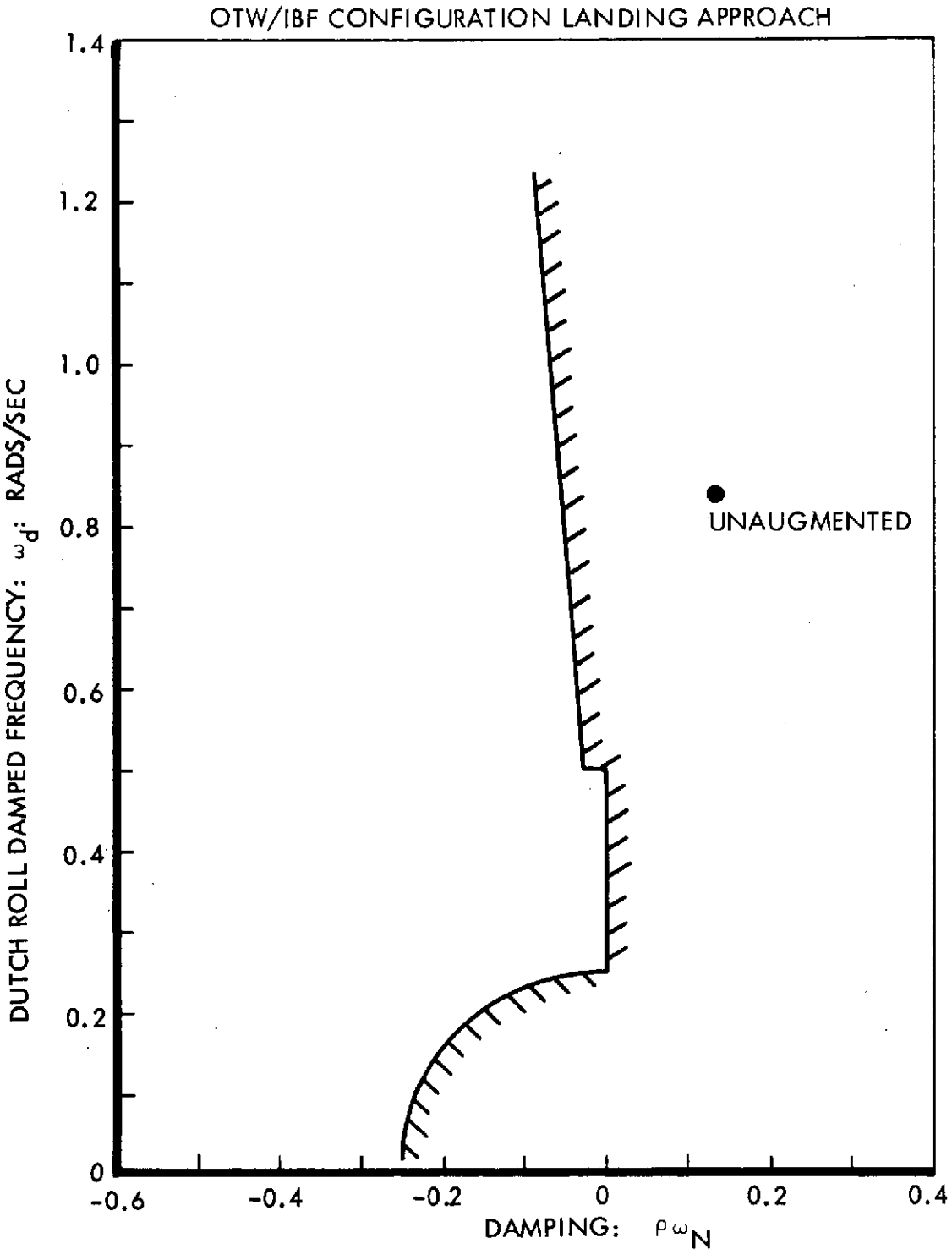

FIGURE 110: LATERAL DIRECTIONAL REQUIREMENTS

the ensuing requirements to handle it. The details of the mixed flow system are discussed in Section 4.10 of this report; in brief however, the system is such that if an engine fails, the internal blowing and trailing edge blowing is retained on that side of the aircraft by cross ducting. At the same time, the trailing edge blowing is stopped on the side of the good engine where the over-the-wing blowing remains. Lateral control as previously described requires boundary layer control and that is maintained with an inoperative engine.

The flight condition analyzed was the landing approach starting from a trimmed condition at 177 Km/hr. (95.4 knots) at an altitude of 305m. (1000 ft.) on a glide slope of 5.2 degrees. These conditions were taken from the results of the aerodynamic study and are required to meet the designated field performance.

The six degree of freedom program was used to analyze the following three situations:

- o Aircraft response to a sudden engine failure
- o Aircraft minimum control speed
- o Aircraft response to gust.

Each of these is discussed in turn in subsequent paragraphs.

Aircraft Response to a Sudden Engine Failure - Time histories of some of the most important flight parameters are presented in Figures 111 and 112 for a two second delay in reaction time to a sudden engine failure. At zero time a sudden engine failure has occurred on the port engine and the starboard engine (together with all controls) is set for normal trim glide slope. The corrective actions taken were purely arbitrary from several trial and error runs and were not pre-programmed (as if a system were trying to maintain conditions or correct the failure). If a stability augmentation system (SAS) were employed the magnitude of the control deflections would be reduced considerably and a much greater recognition time could be allowed. The elapsed time of 1 second for engine spool up is considered realistic and is indicated in the curve of thrust coefficient, (CT).

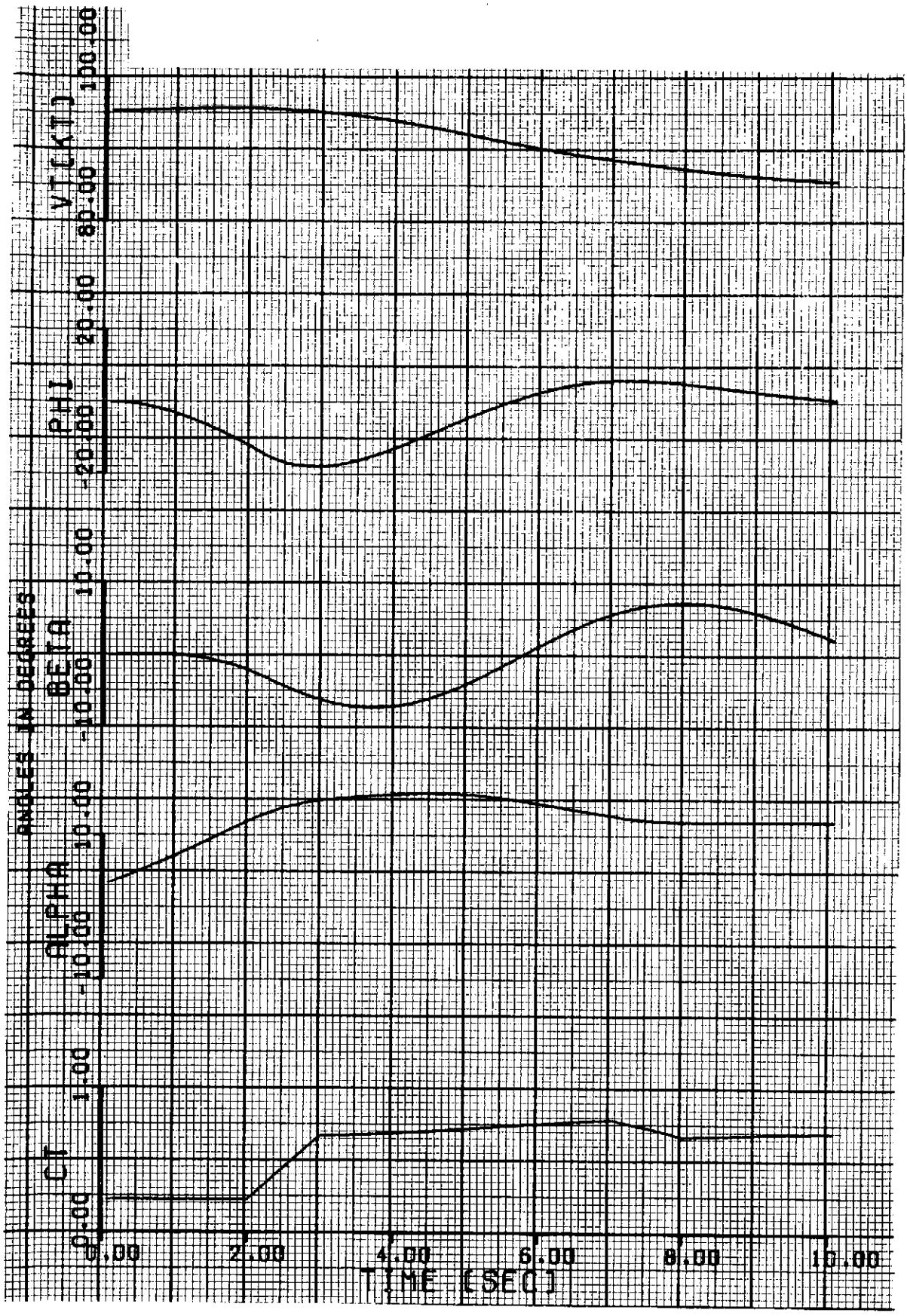

FIGURE 111: RESPONSE TO ENGINE FAILURE (CORRECTIVE ACTION AFTER 2 SECONDS) (1)

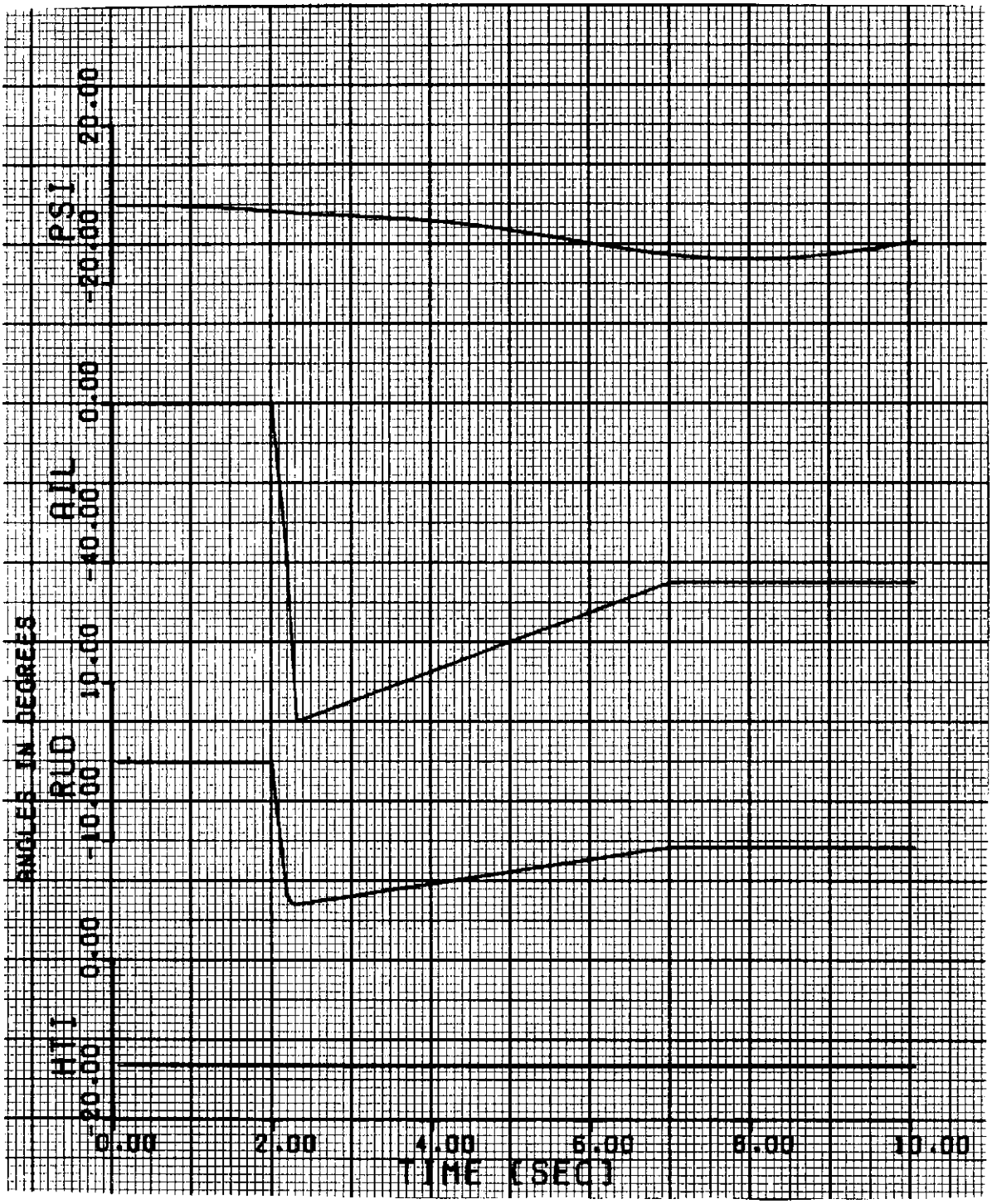

FIGURE 112: RESPONSE TO ENGINE FAILURE (CORRECTIVE ACTION AFTER 2 SECONDS) (2)

The aileron required from trim is approximately 56% of the total available, leaving an adequate margin for control after trim. Full aileron was applied in 0.3 seconds for immediate bank angle correction and was then eased off to the trim settings. (Trim angle PHI for BETA = 0 is -0.43 degrees). The rudder required for trim with zero sideslip is only 18% of that available. Eighteen degrees of rudder were applied immediately and then gradually reduced to trim. The resulting excursions with a time delay of two seconds do not seem prohibitive and would be reduced with SAS. Maximum deviations of the ALPHA, BETA, and heading angles were 13, 8 and 12 degrees, respectively. Longitudinal correction was not applied, but proper action could reduce the 17 Km/hr. (9 knot) speed loss.

The action taken, after a recognition and reaction time of one second, and the ensueing aircraft motions are presented in Figures 113 and 114 . The applied control deflections were decreased to 65 and 25 percent of the available aileron and rudder. The excursions in bank, sideslip, and heading were drastically reduced. An attempt at a longitudinal check maneuver was applied during this run. Additional trial runs could provide the optimum corrective action rather than this arbitrary selection. The speed loss was only 11 Km/hr. (6 kts) and this occurred with throttle being reduced too quick (7 sec.) and the flight path degradation being corrected too quickly.

In conclusion, an engine failure does appear manageable even with arbitrary course corrections. Sophisticated augmentation systems would substantially reduce the aircraft excursions.

Minimum Control Speed - The OTW/IBF configuration was trimmed with the port engine out and maximum power on the starboard engine at various speeds. At each speed, trim was established at various sideslip angles to determine the effect of bank and sideslip on the required controls. Figure 115 presents the required controls for trim at the normal approach speed. The maximum available deflections of aileron and rudder are 80 and 60 degrees, respectively. Therefore, it is possible to trim at sideslip angles of $\pm$ 30 degrees without depleting the available control. If the bank angle were limited

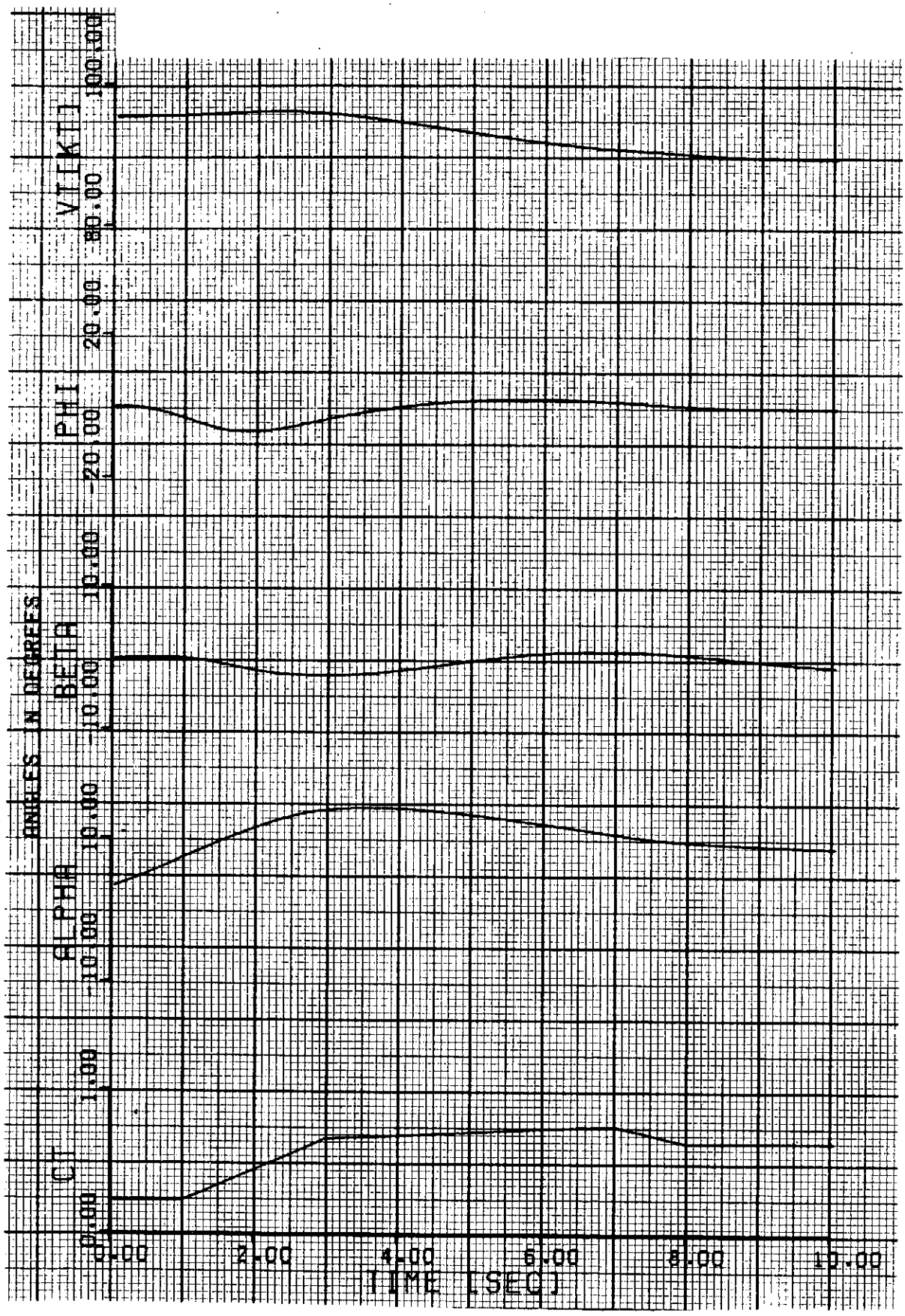

FIGURE 113: RESPONSE TO ENGINE FAILURE (CORRECTIVE ACTION AFTER 1 SECOND) (1)

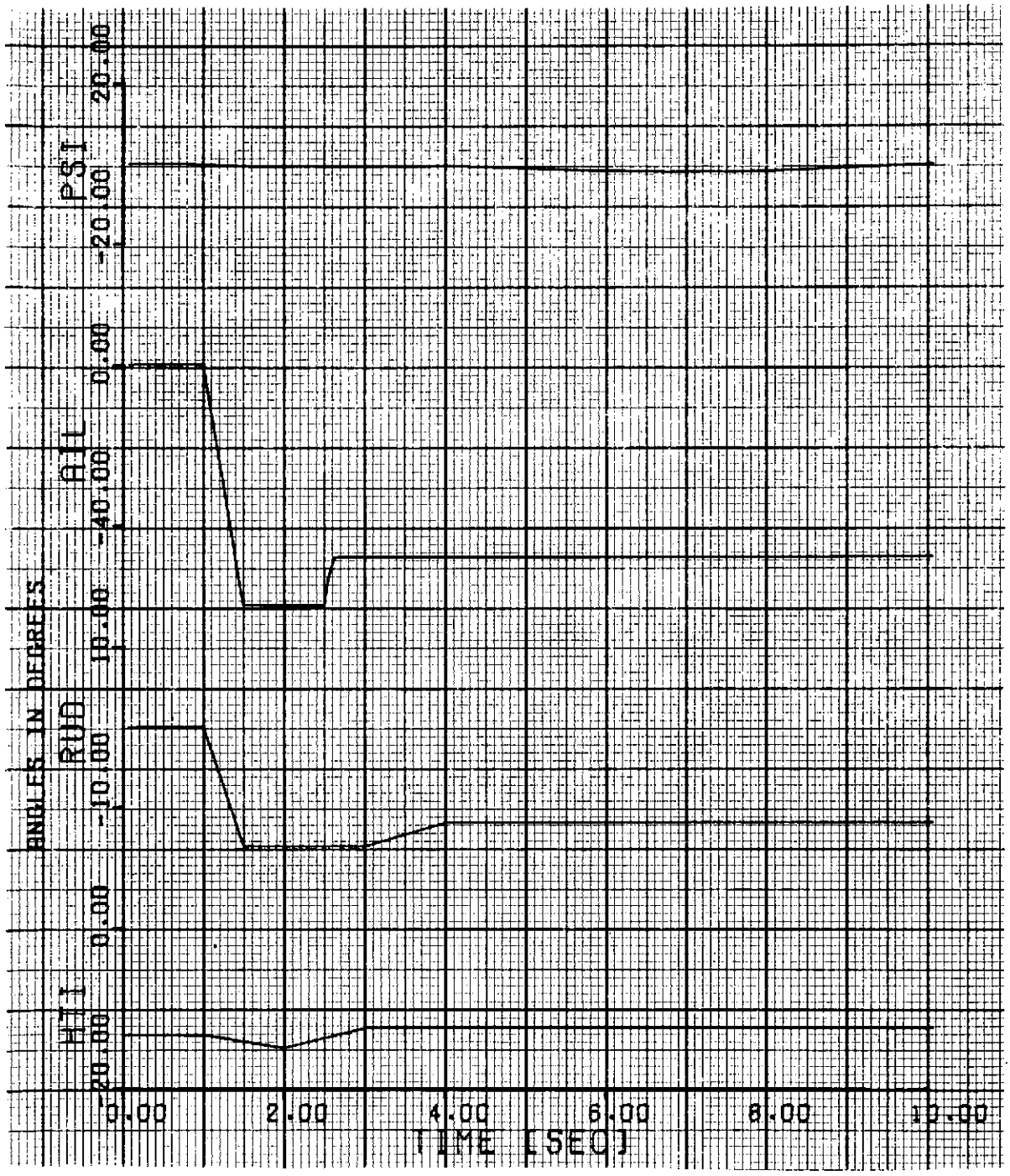

FIGURE 114: RESPONSE TO ENGINE FAILURE (CORRECTIVE ACTION AFTER 1 SECOND) (2)

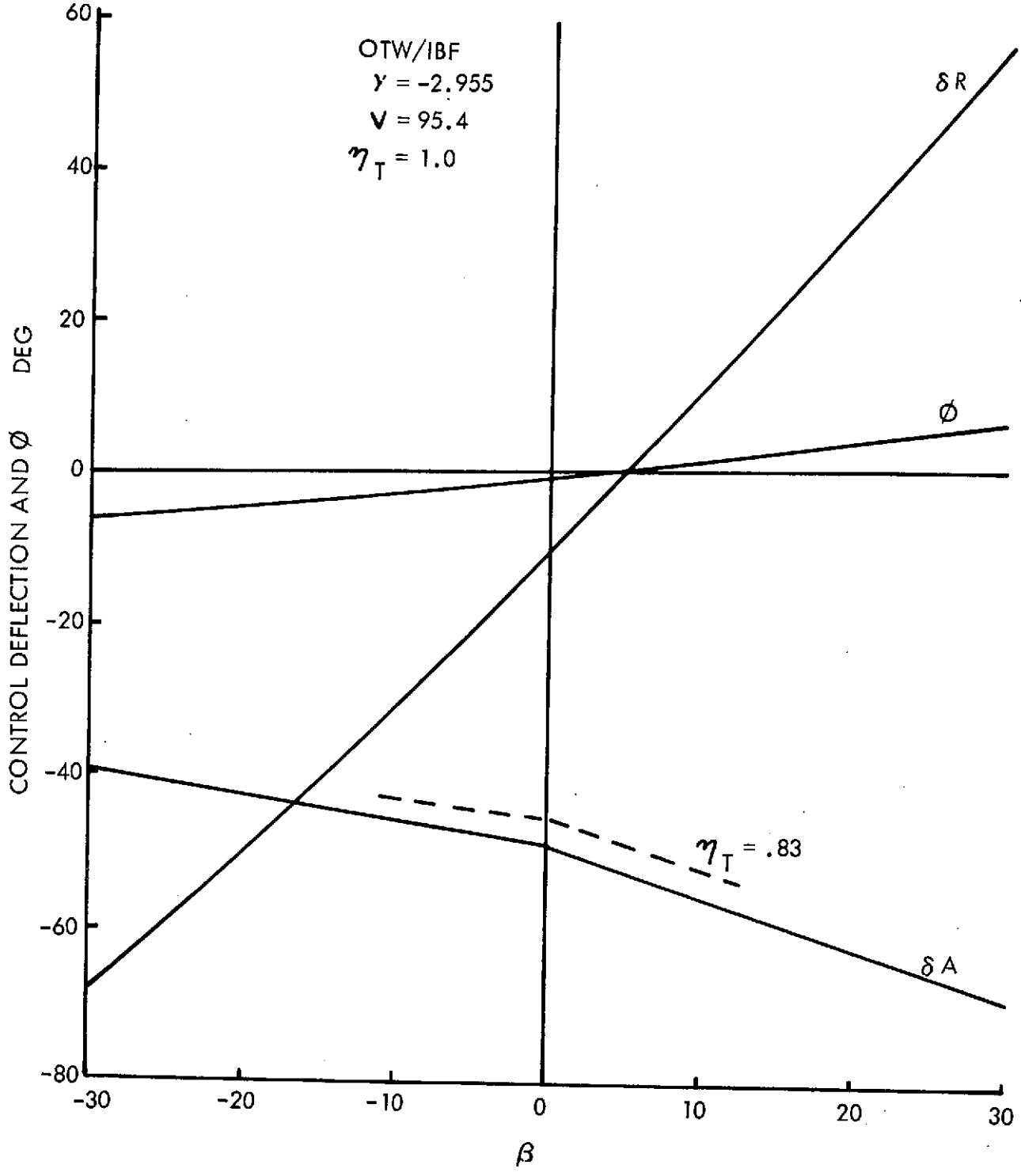

FIGURE 115: CONTROL ANGLES TO TRIM FAILED ENGINE

to 5 degrees, the range of sideslip angles for trim would be -25 to +20 degrees. (MIL-F-8785B suggests the limit of 5 degrees away from the dead engine.) If control is limited to 75% of that available, the maximum sideslip would be -18 degrees as limited by rudder and -17 degrees limited by aileron. The effect of thrust is shown by the slight decrease in required aileron, if thrust is reduced to that required to maintain the landing glide slope.

Figure 116 shows the effect of speed on the required trim control. The aileron becomes critical in all cases if sideslip is limited to 10 degrees. The aircraft can be trimmed at a sideslip of zero to a speed 20 percent lower than the normal approach speed with 75 percent of the available control. Minimum control speed does not appear to present a problem with respect to operational requirements.

Aircraft Response to Gust - The response to vertical and lateral gusts are presented in Figures 117 and 118 . The aircraft was again unaugmented with respect to stability and all controls were fixed.

A sharp edge vertical gust of a constant 3.05m./sec. (10 ft./sec.) applied at the end of 1 second is presented in Figures 117 and 118 . The gust time history is shown as WG in Figure 118 . The aircraft response to a vertical gust patterned after MIL-F-8785B requirements is presented in Figures 119 and 120 . The gust occurs over a 6 second interval with a peak velocity of 5.12m./sec. (16.8 ft./sec.) at 3 seconds. The response to both of these gusts appears normal and should not present any real problems. The velocity loss was 7.4 Km/hr. (4 kts.) for the latter case.

Aircraft response to a sharp edged lateral gust of 3.05m./sec. (10 ft./sec.) applied and left constant after 1 second is shown in Figures 121 and 122 . The lateral gust time history is presented as VG in Figure 122 . Roll and yaw appear stable with the yaw excursion going to 8 degrees. Response to a lateral gust patterned from MIL-F-8785B requirements is presented in Figures 123 and 124 . This gust reaches 7.62m./sec. (25 ft./sec.) in 7.7 seconds and appears to be too great for this configuration.

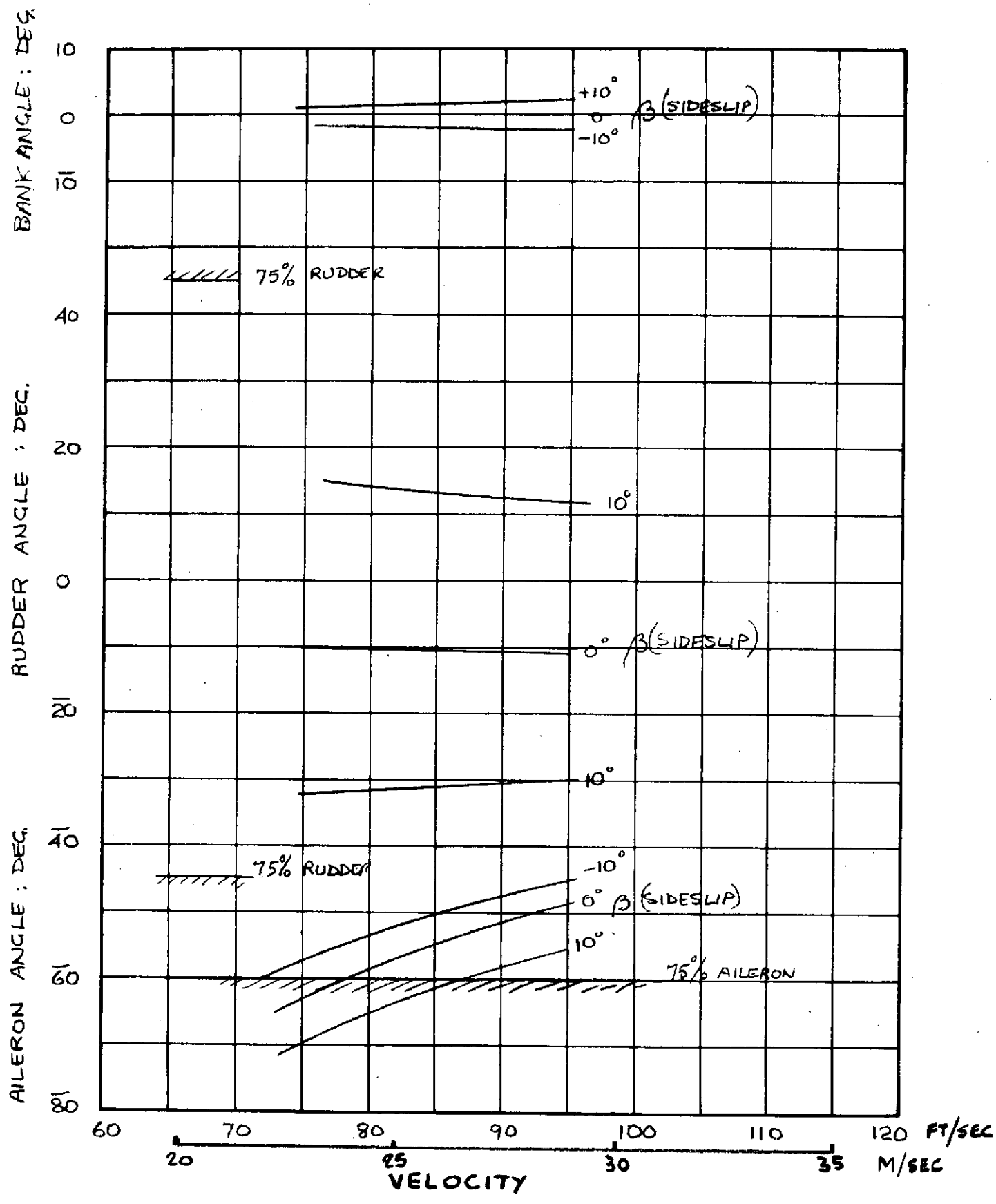

FIGURE 116: 4.112 TRIMMED CONDITIONS (1 ENGINE OUT) VS. SPEED

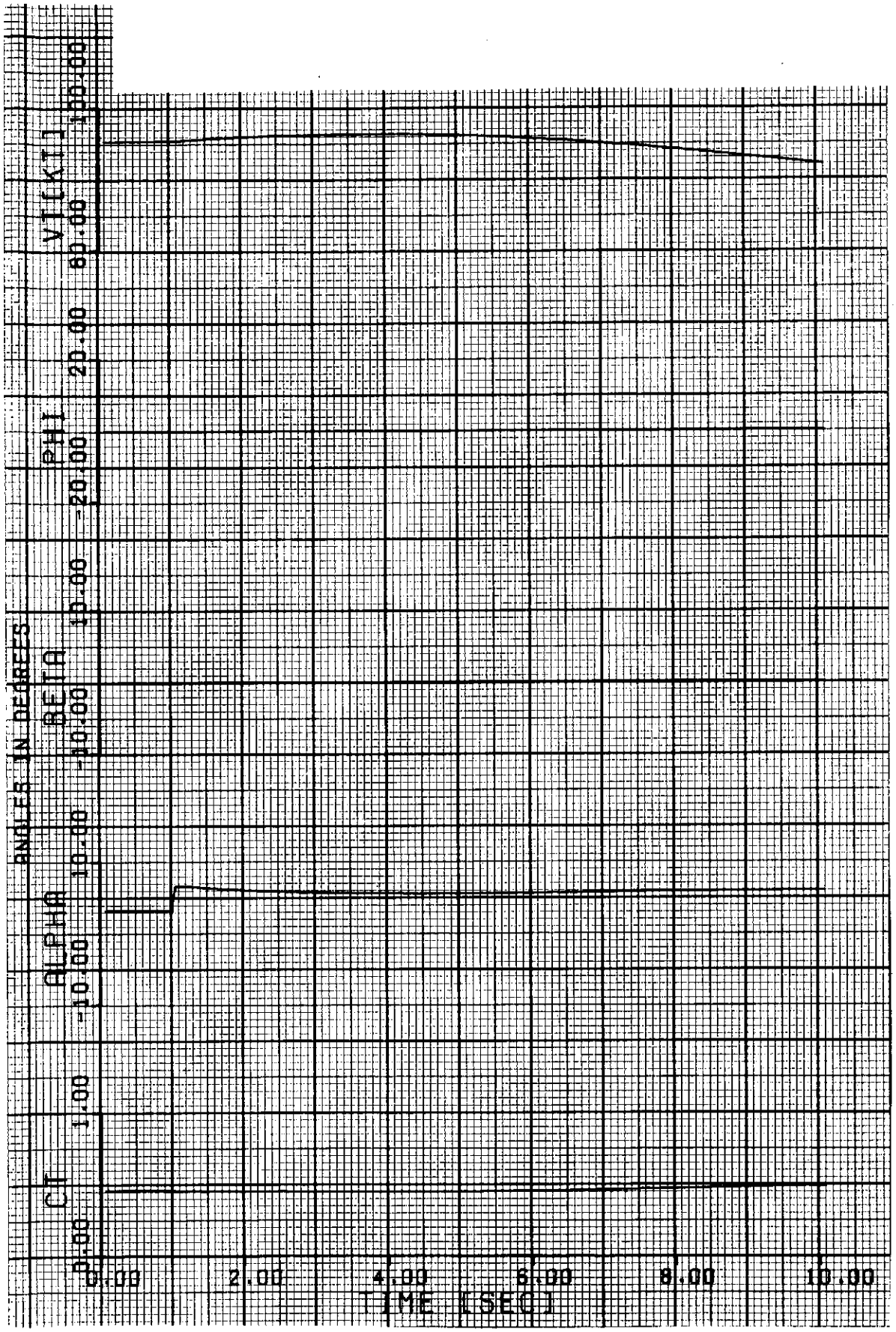

FIGURE 117: RESPONSE TO 3.05 M/SEC (10 FPS) VERTICAL GUST (1)

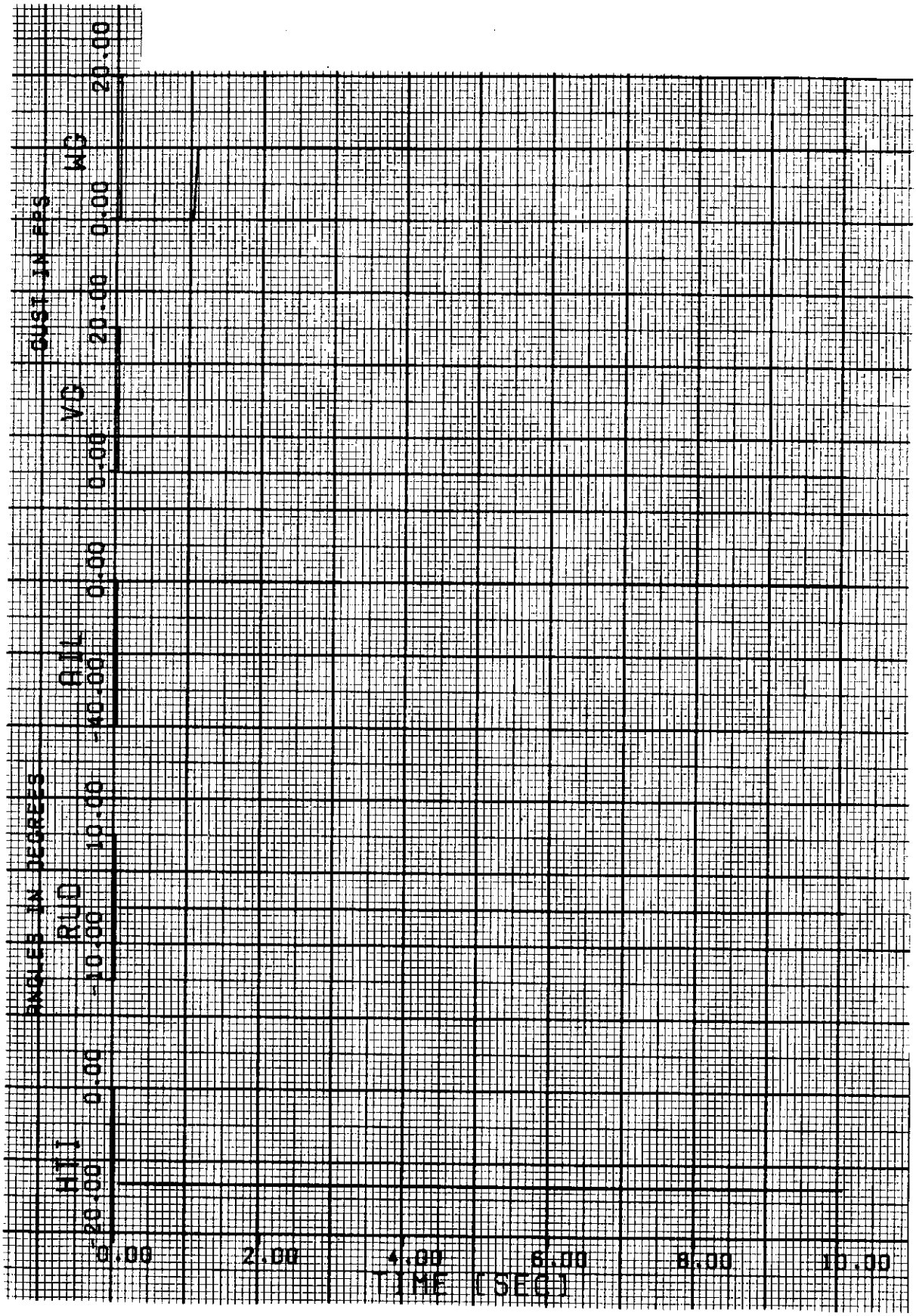

FIGURE 118: RESPONSE TO 3.05 M/SEC (10 FPS) VERTICAL GUST (2)

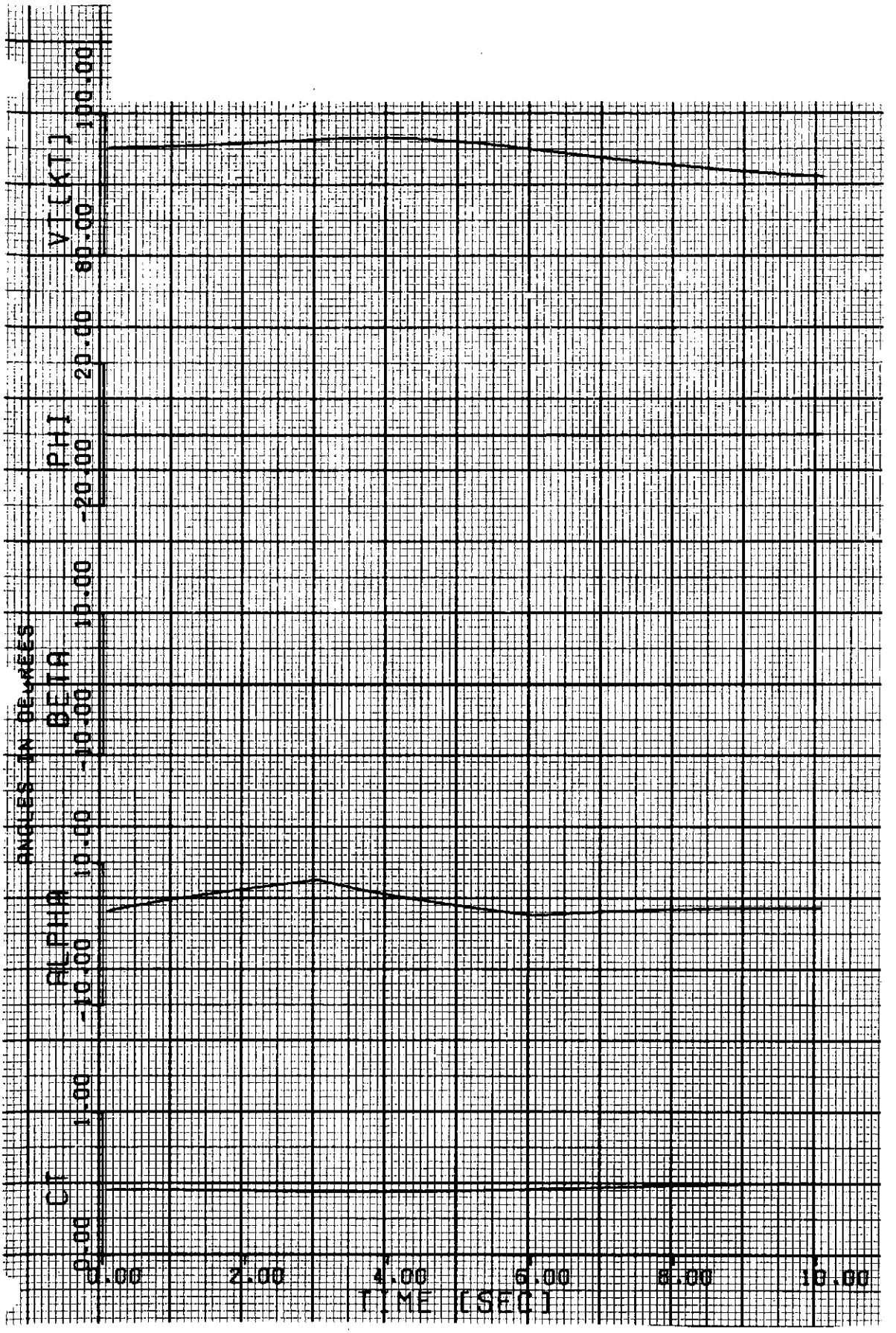

FIGURE 119: RESPONSE TO MIL-F-8785 VERTICAL GUST (1)

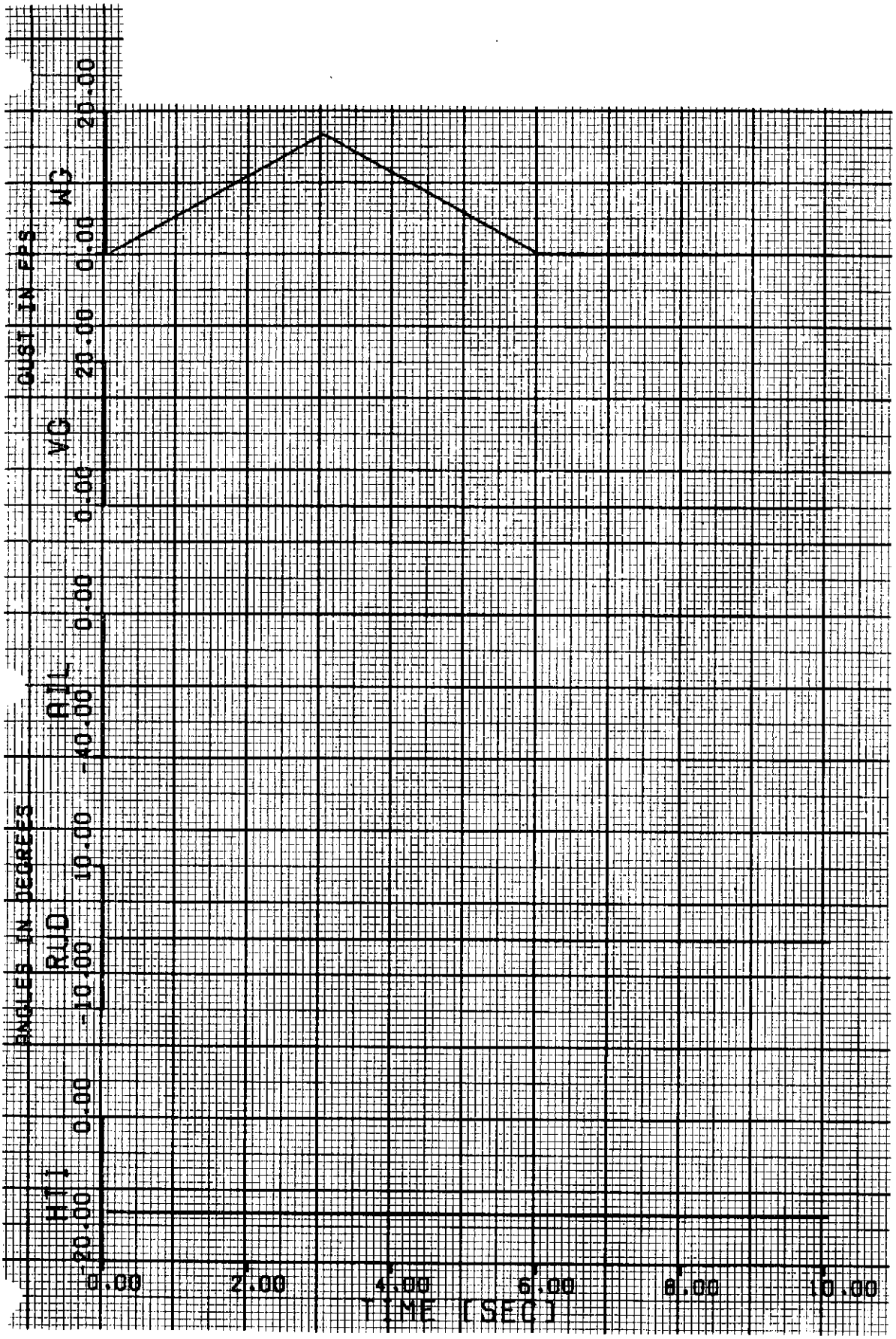

FIGURE 120: RESPONSE TO MIL-F-8785 VERTICAL GUST (2)

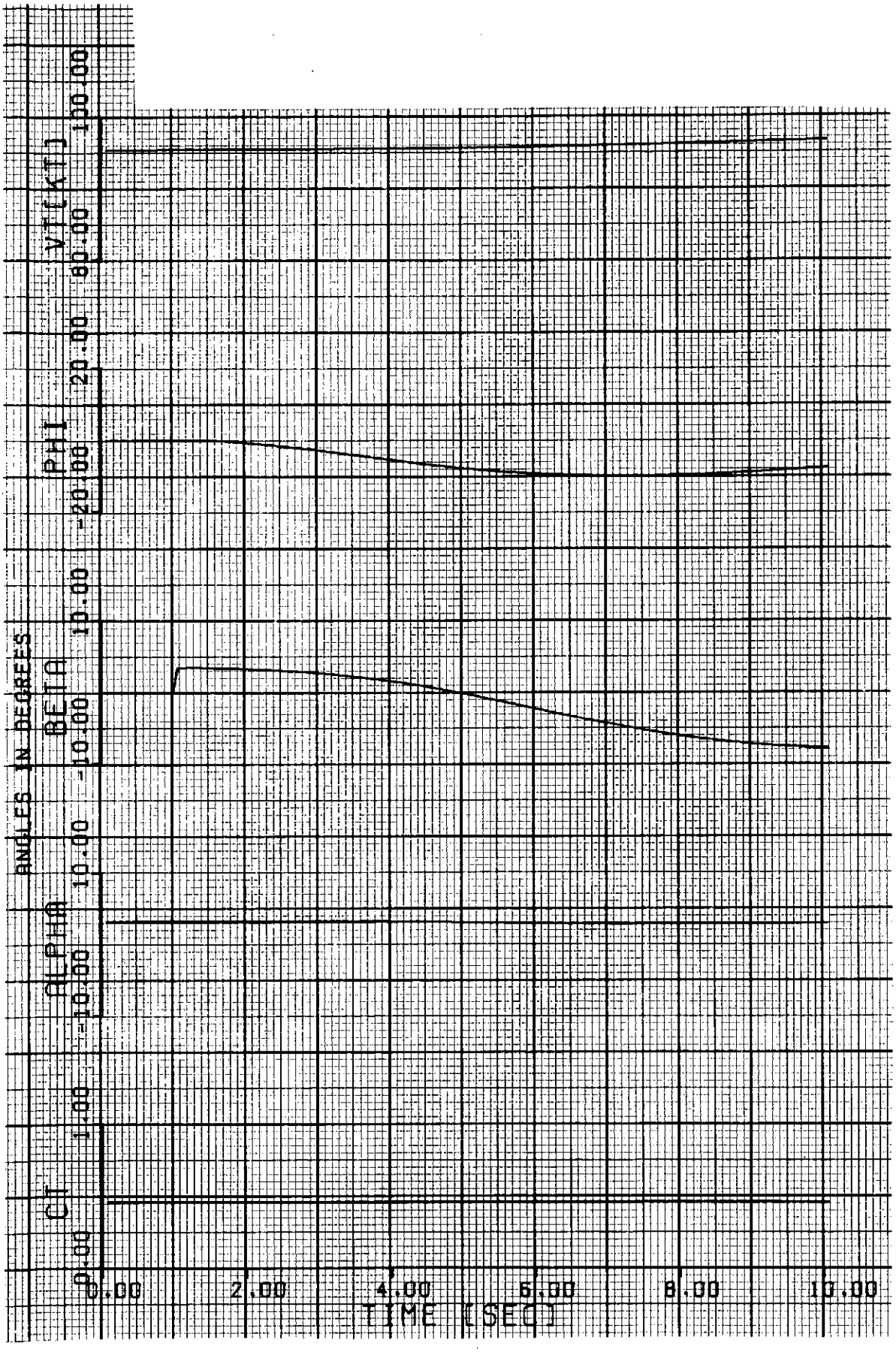

FIGURE 121: RESPONSE TO 3.05 M/SEC (10 FPS) LATERAL GUST (1)

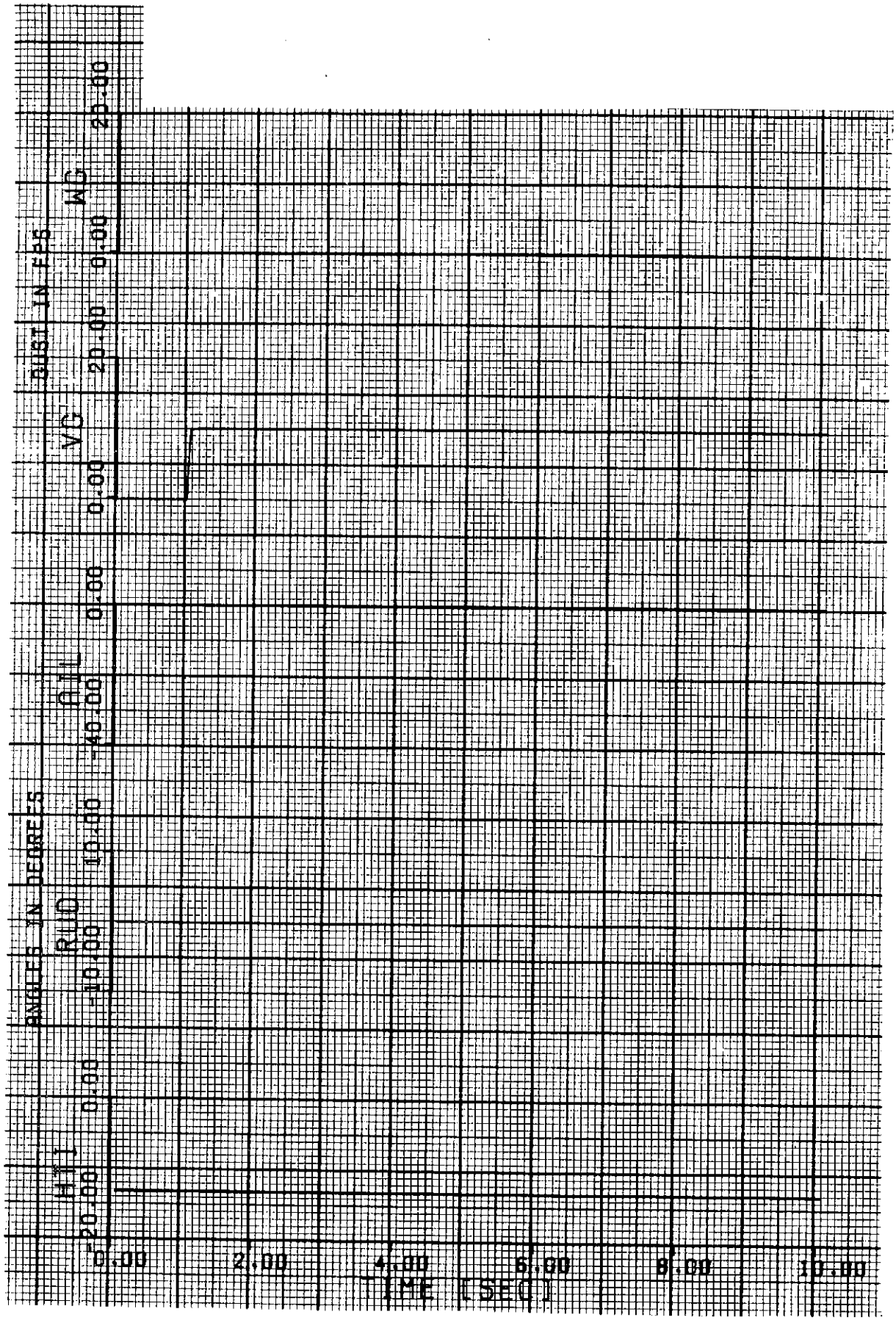

FIGURE 122: RESPONSE TO 3.05 M/SEC (10 FPS) LATERAL GUST (2)

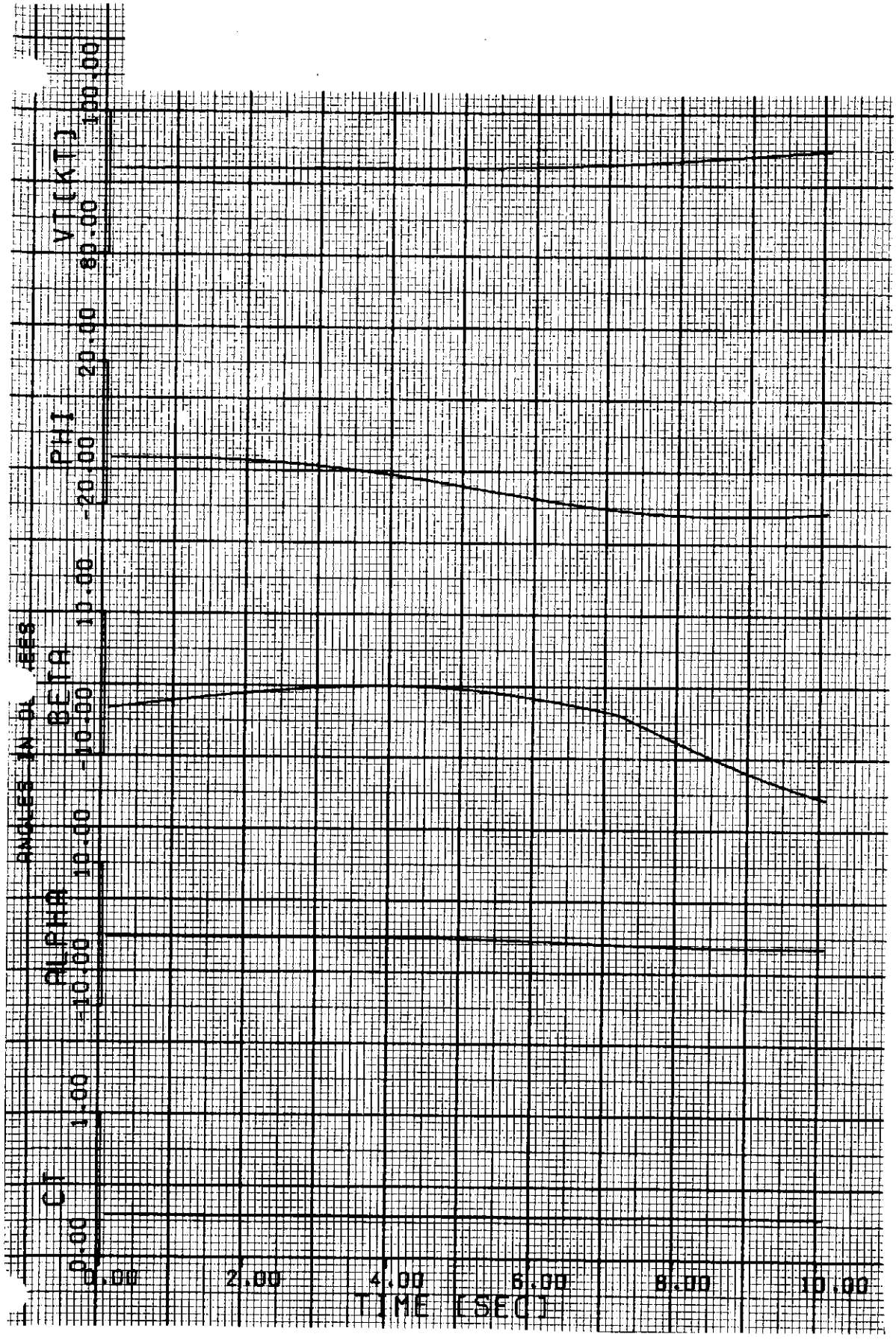

FIGURE 123: RESPONSE TO MIL-F-8785 LATERAL GUST (1)

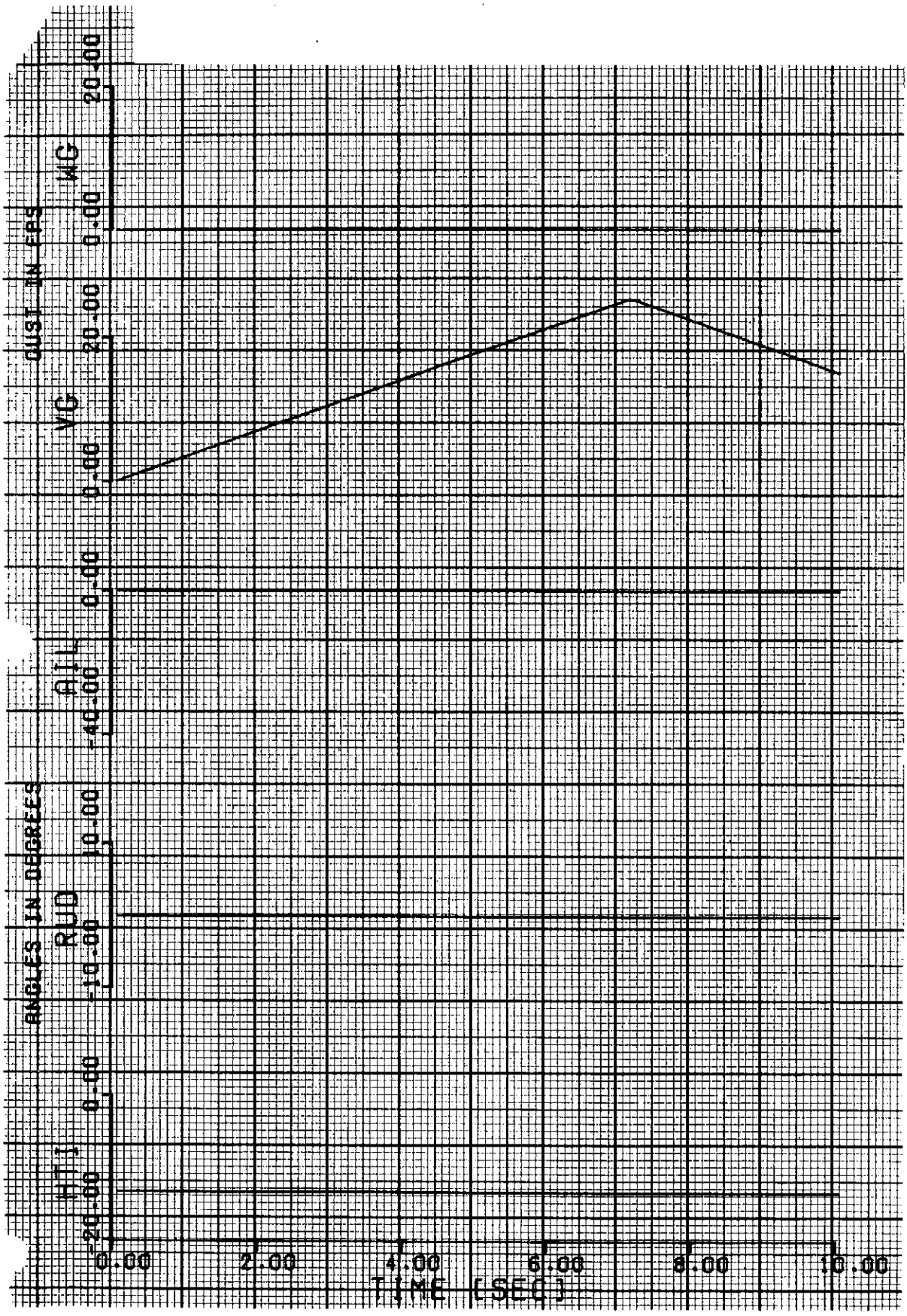

FIGURE 124: RESPONSE TO MIL-F-8785 LATERAL GUST (2)

Sideslip reaches 15 degrees at the end of 10 seconds and a stability augmentation system would probably be required to effectively handle the gust.

4.7.2 OTW/IBF Ride Qualities

The ride quality characteristics of the rigid, unaugmented stability OTW/IBF configuration are presented in Figures 125 and 126. The longitudinal results in Figure 125 show that the only criteron exceeded is the RMS acceleration σ_g allowable for the descent case. A longitudinal SAS (stability augmentation system) will probably bring this level close to the criteria.

The discomfort level of σ_g adopted by Gelac for the flight case is 0.178. This means that the stated acceleration over the frequency range 0.1 to 10. cps could be tolerated for several minutes without providing noticeable discomfort. Since the expected operational time in this descent phase of the flight regime is only expected to be 12 minutes, the ride characteristics will probably be acceptable.

Lateral-directional ride characteristics are presented in Figure 126 . These characteristics are similar to those found in reference 2. Lateral acceleration presents no real problem and the criteria are easily met. The rotational criteria are considered too stringent but will probably be met with a conventional SAS for all conditions (except roll) during the landing approach.

In conclusion, a ride control system, as such, would not be required to provide acceptable ride characteristics for the OTW/IBF configuration.

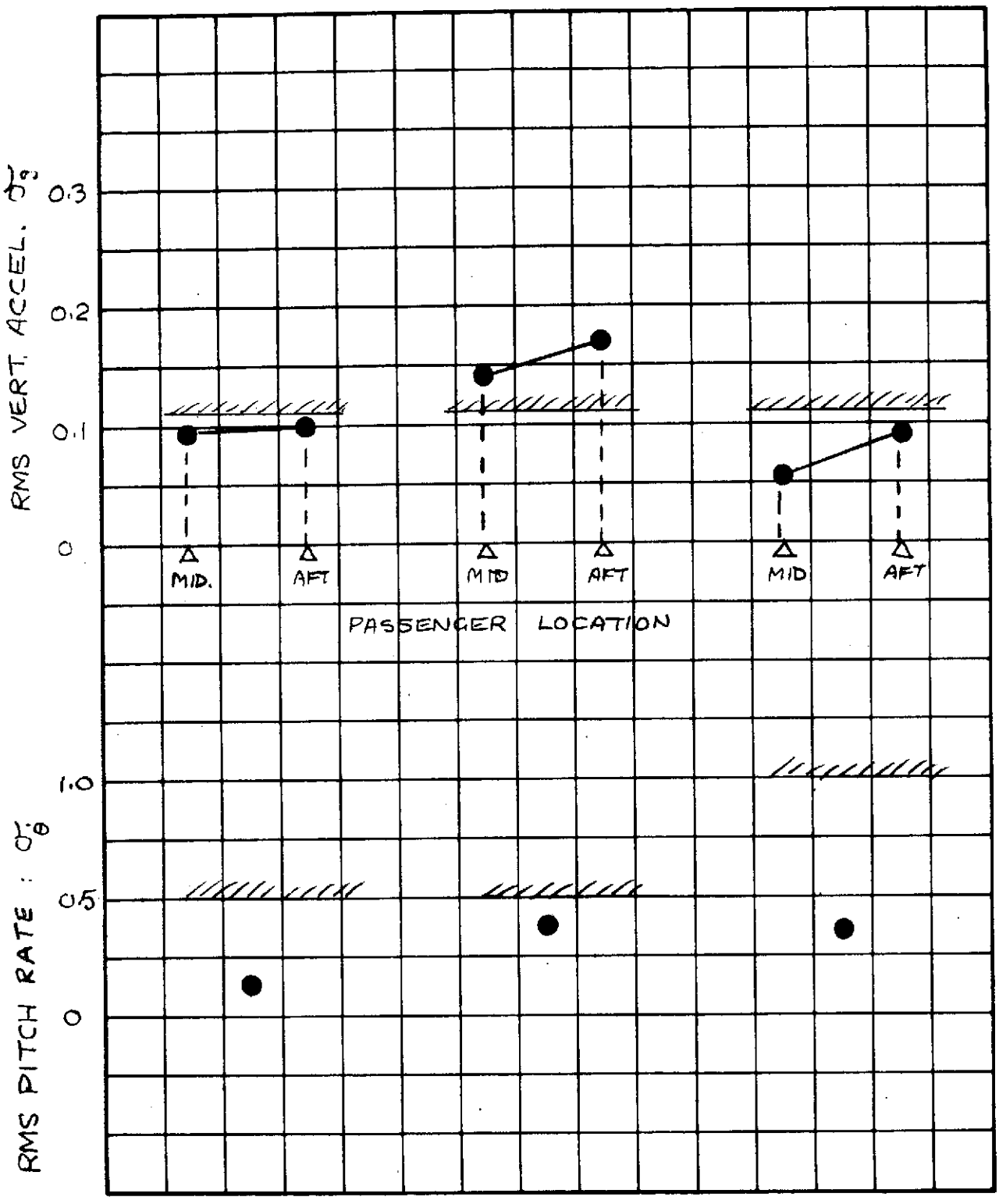

FIGURE 125: OTW/IBF LONGITUDINAL RIDE QUALITIES

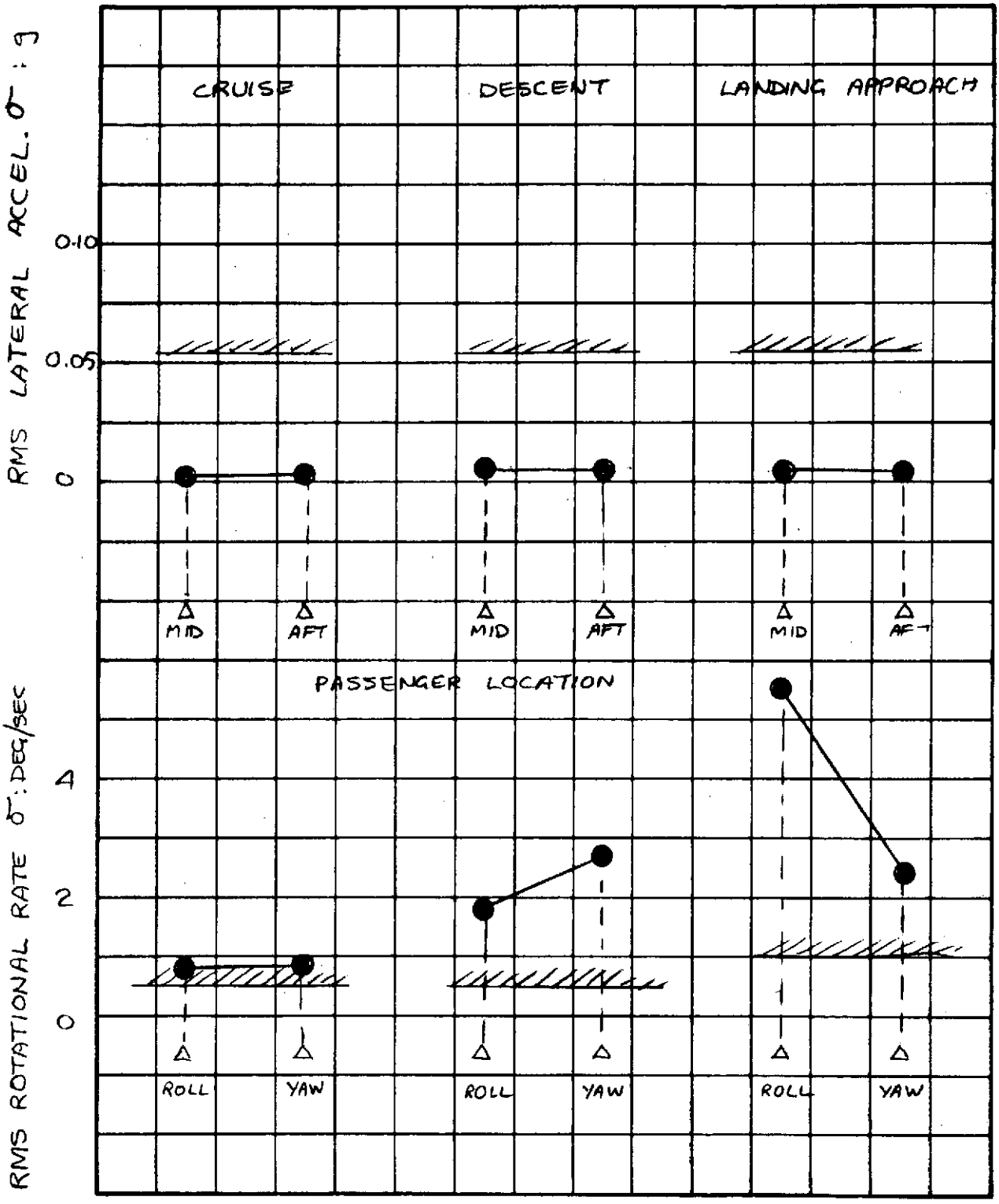

FIGURE 126: OTW/IBF LATERAL RIDE QUALITIES

4.8 OTW-IBF WEIGHT AND BALANCE

In the studies reported here, the primary objective in the weight area was to examine the weight estimation logic within the vehicle sizing computer program to obtain more accurate sensitivity to the various aircraft parameters. This involved a survey of the logic used in the computer programs and design point weight analyses for the nacelles, wing box, flaps, ailerons, air ducts, and other miscellaneous items. The following sections summarize these weight studies and present the weight equations used. It should be noted that standard U.S. units rather than metric units are to be used in their application, but all output data is quoted in both units. The weight estimation logic used in the derivation of OTW-IBF vehicle configurations was modified for the wing and bleed air distribution weight components based upon design point analyses and nacelle and propulsion weight variations were derived for each candidate engine baseline.

4.8.1 Wing Weight

The wing weight logic incorporated in the present computer program essentially uses Lockheed statistical wing weight equations (as derived from contemporary aircraft) with increments for special features as derived from base point analyses for the OTW/IBF flaps, ailerons, bleed air ducts, and wing box weight effects. The following outlines the resulting logic for the OTW/IBF wing weight.

(a) Basic Wing Weight (W_{W_O}) - This weight is derived from the equation identified by Figure 127 and using the nomenclature on this figure W_{W_O} is identified as follows:

$$W_{W_O} = W_W - (3.3\, S_P + 3.28\, (S_{LED})^{1.13})$$

For these studies, the fixed identities are:

W_R = Relief Weight = Nacelle + Pylon + Propulsion - Fuel System

N = Ultimate Load Factor = 1.5 X 2.5 = 3.75

TS = Design Tension Stress = 27.6 KN/cm^2 (40,000 psi)

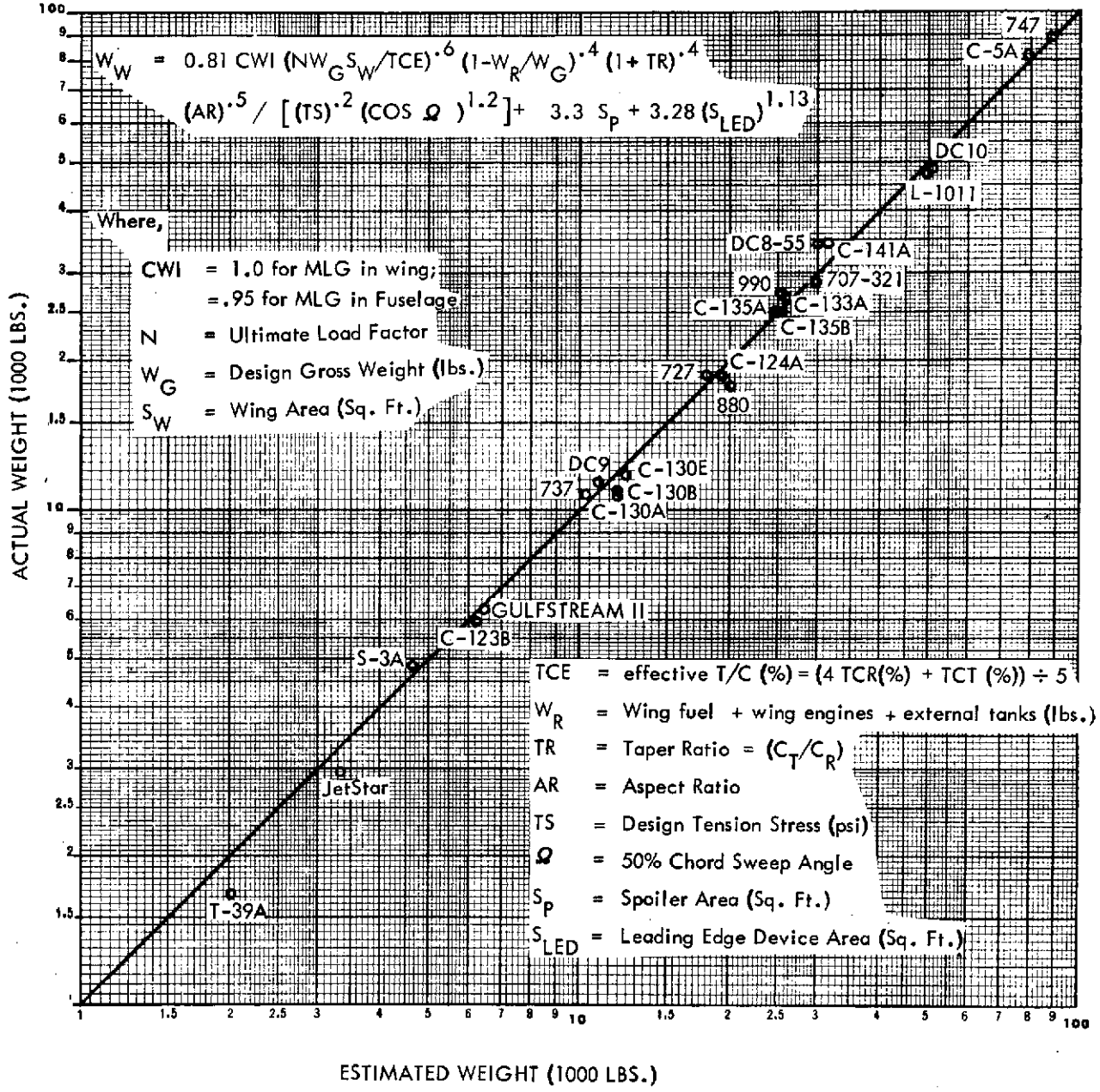

FIGURE 127: WING WEIGHT ESTIMATE CORRELATION

Ω = Sweep of 50% chord

$$= \text{Tan}^{-1}\left[\text{Tan}\ \Omega 1/4C + (TR-1) \div (AR \times (TR + 1))\right]$$

Where, Ω 1/4C = sweep angle of wing quarter-chord line.

(b) Basic Secondary Structure (W_{SEC_O}) - This weight item is the amount of secondary structure for a conventional transport aircraft wing. It represents the fixed leading edge and trailing edge structure, doors, and wing root fairing. The following relationship has been derived from contemporary aircraft data:

$$W_{SEC_O} = 0.85\ S_W + 65.\ (S_W/AR)^{0.5} \div (1 + TR)$$

(c) Basic Trailing Edge Flaps (W_{TF_O}) - The basic wing weight is assumed to contain a basic flap weight equivalent to a Fowler flap. This basic flap was estimated using the equation identified in Figure 128 (i.e. $W_{TF_O} = W_{TF}$). For these studies, the parameters in this equation are self-explanatory except for V_F, S_F, TCF and K_{TF} which are identified as follows:

- V_F = 370 Km/hr (200 KEAS) = Flap Design Airpseed
- S_F = retracted flap planform area

  $S_F = \epsilon_F\ (\eta_{F_O} - \eta_{F_I})\ (FCR)\ (S_W) \quad (1 + TR)$

  ϵ_F = flap chord to total wing chord ratio = 0.4

  η_{F_O} and η_{F_I} = outboard and inboard ends of the flap panels in fraction of wing semi-span.

  $FCR = 2 - (1 - TR)(\eta_{F_O} + \eta_{F_I})$ = chord ratio factor
- TCF = Wing T/C ratio at flap centroid (%)

  $TCF = \left[2X\ TCR - (TCR - TCT \times TR)\ (\eta_{F_O} + \eta_{F_I})\right] \div FCR$
- K_{TF} = Flap Configuration Factor which is identified on Figure 128; a value of 1.0 is assumed for the basic flap weight.

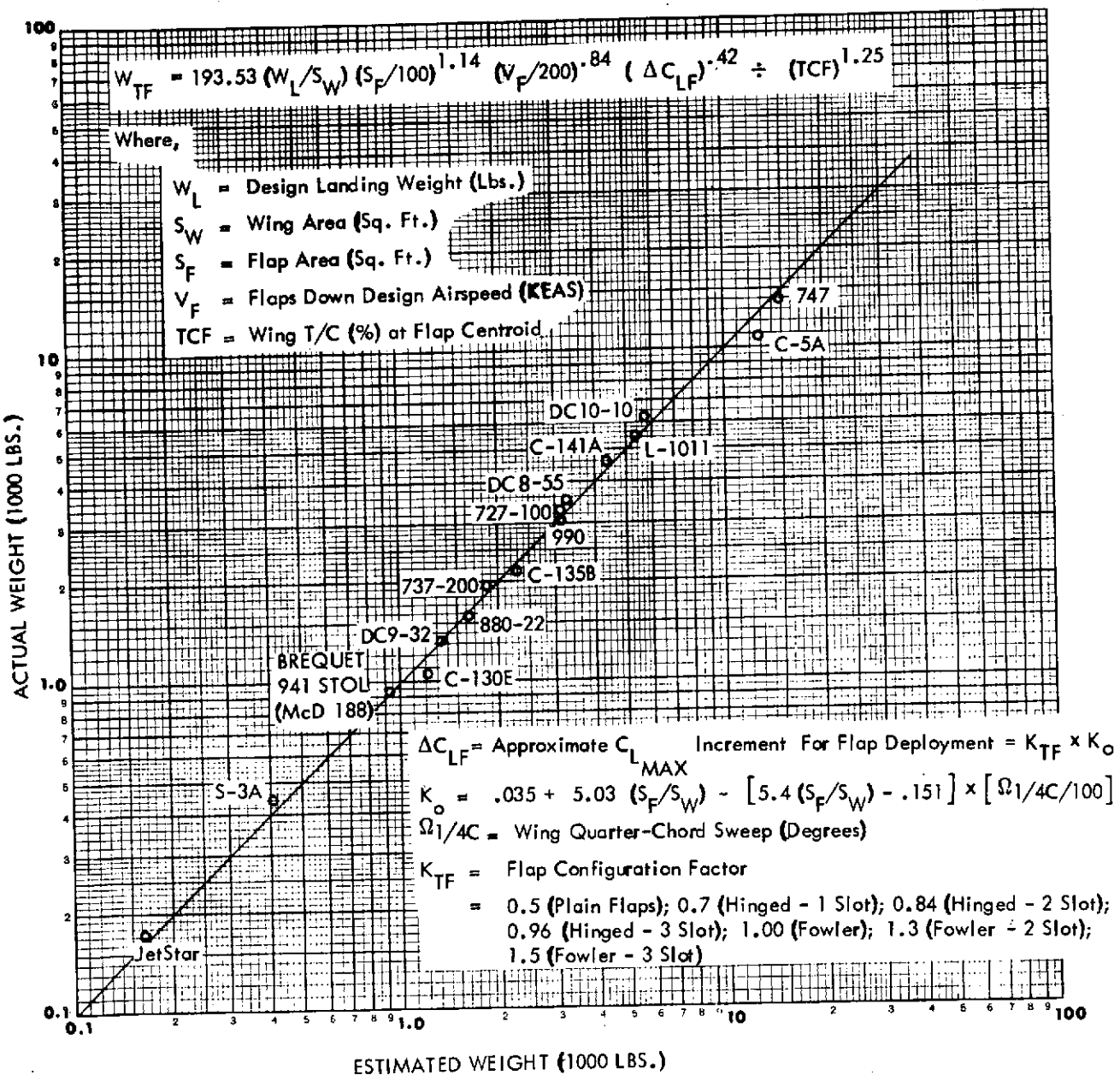

FIGURE 128: TRAILING EDGE FLAP WEIGHT ESTIMATE CORRELATION

(d) Basic Aileron (W_{AIL_O}) - The basic wing weight is assumed to contain a basic aileron weight determined as follows:

$$W_{AIL_O} = 6.58 \times 0.53 \times S_W$$

(e) Basic Wing Box Weight (W_{BOX_O}) - From the foregoing, the basic wing box weight is determined next as follows:

$$W_{BOX_O} = W_{W_O} - W_{SEC_O} - W_{TF_O} - W_{AIL_O}$$

(f) OTW/IBF Control Surfaces - An analysis was conducted for an OTW/IBF configuration to determine the weight associated with the leading and trailing edge flaps and ailerons in the following manner. Preliminary loads and stress analyses were performed on this configuration which resulted in the flap and aileron weights summarized by Table V. Reflecting these data in parametric form for use in the weight estimation logic results in the following relationships:

- Trailing Edge Flaps

$K_{TF} = 3.04$ as derived for the study configuration

$$W_{TF} = W_{TF_O} \times (K_{TF})^{.42}$$

- Ailerons

$$S_{AIL} = \epsilon_{AIL} (1 - \eta_{F_O}) \left[2 - (1 - TR)(1 + \eta_{F_O})\right] S_W \div (1 + TR)$$

ϵ_{AIL} = aileron chord to total wing chord ratio = 0.4

$(W/S)_{AIL} = 45.8$ Kg/m^2 (9.37 psf) as derived for the study configuration

$$W_{AIL} = 9.37 \times S_{AIL}$$

The leading edge flap weight was determined using the conventional wing leading edge flap weight relationship, which is as follows:

TABLE V: - OTW/IBF FLAP AND AILERON WEIGHT STUDY SUMMARY

	WEIGHT Kg (LBS)	AREA m^2 (SQ. FT.)
I. TRAILING EDGE FLAPS		
(a) Inboard Flaps 65.57 Kg/m^2 (13.43 psf)	1295 (2856 lb)	19.75 (212.6)
o Upper Forward Flap	527 (1162)	
o Lower Forward Flap	367 (808)	
o Aft Flap	103 (228)	
o Support Fittings	249 (550)	
o Fixed Trailing Edge Panels	29 (64)	
o Fairings and Seals	20 (44)	
(b) Outboard Flaps 58.30 Kg/m^2 (11.94 psf)	1029 (2268)	17.65 (190.0)
o Upper Forward Flap	375 (826)	
o Lower Forward Flap	284 (626)	
o Aft Flap	131 (288)	
o Support Fittings	198 (436)	
o Fixed Trailing Edge Panels	25 (56)	
o Fairings and Seals	16 (36)	
Total Trailing Edge Flaps	2324 (5124 lb)	37.40 (402.6)
(W/S - 2324 ÷ 37.40 = 62.16 Kg/m^2 (12.73 psf)		
II. AILERON/FLAPERON		
(a) Movable Aft Panels	222 (490)	
(b) Lower Support Panels	86 (190)	
(c) Upper Panels	29 (64)	
(d) Support Fittings	76 (168)	
Total Aileron	414 (912)	9.04 (97.3)
(W/S = 45.75 Kg/m^2 (9.37 psf)		

$$S_{LED} = \epsilon_{LED} (1 - \eta_{FI}) \left[2 - (1 - TR)(1 + \eta_{FI})\right] \times S_W \div (1 + TR)$$

ϵ_{LED} = leading edge flap chord to total wing chord ratio = 0.18

$$W_{LED} = 3.28 (S_{LED})^{1.13}$$

The spoiler weight was determined using the conventional wing spoiler weight relationship, which is as follows:

$$S_P = \epsilon_{SP} \times (\eta_{F_O} - \eta_{SP_I}) \left[2 - (1 - TR)(\eta_{F_O} + \eta_{SP_I})\right] \times S_W \div (1 + TR)$$

ϵ_{SP} = spoiler chord to total wing chord ratio = 0.0 for the OTW/IBF configuration.

η_{SPI} = inboard end of the spoiler panels in fraction of wing semi-span (the outboard end is assumed to coincide with outboard end of the flaps)

$$W_{SP} = 3.3 S_P$$

The control surface weight is now identical as follows:

$$W_{CS} = W_{TF} + W_{AIL} + W_{LED} + W_{SP}$$

(g) <u>OTW/IBF Wing Secondary Structure</u> - Since the flaps and ailerons occupy the entire space behind the wing rear beam, the weight for the OTW/IBF configurations fixed trailing edge structure would be zero. To reflect this effect in a general equation, the following relationship was used:

$$W_{SEC} = 0.85 (K_{LE} + K_{TE}) S_W + 65 (S_W \div AR)^{0.5} \div (1 + TR)$$

Where $K_{LE} = 0.5$ and $K_{TE} = 0$.

(h) Wing Box Weight Penalty - For the OTW/IBF configuration, the bleed air from the engine is assumed to be routed through the wing box to the trailing edge flap interior. This routing causes a weight penalty to the wing box which has been assessed by comparative analytical analysis of the wing box components. It is assumed that spar loads are transferred across the bleed air penetration width by a truss system with vertical members which are continuous from the front to the rear beam and serve as ribs; the diagonal truss members transfer the wing shear loads and are located on the front and rear beams; engine and nacelle attachment loads are carried through the nacelle structure to wing attachment ribs at each side of the bleed air penetration bay. The resultant wing box weight penalty over the bleed air penetration bay has been estimated as follows:

$$\Delta W_{SPARS} = 2\,(W_{SPAR})_i$$

$$\Delta W_{RIBS} = 1\,(W_{RIB})_i$$

where, $(W_{SPAR})_i$ and $(W_{RIB})_i$ are the spar and rib weights of the uncut wing box over the span of the bleed air penetration bay.

The foregoing weight considerations were incorporated into the weight estimation logic as follows:

- $\Delta W_{WEBS} = 3.62 \times 10^{-5}\,(N)\,(W/S)\,(S_W)\,(D_{NAC} \times N_E \times K_E)$
- $\Delta W_{CAPS} = 5.5 \times 10^{-5}\,(N)\,(W/S)\,(S_W)\,(D_{NAC} \times N_E \times K_E)\,(AR \quad TCE)$
- $\Delta W_{BOX} = \Delta W_{WEBS} + \Delta W_{CAPS} + \Delta W_{RIBS}$

where

D_{NAC} = nacelle maximum diameter (ft) which is assumed to be the width of the bleed air penetration bay

N_E = number of engines per aircraft

K_E = wing thickness factor influenced by the number of engines

if $N_E = 2$, $K_E = 1.35$

if $N_E = 4$, $K_E = 1.2$

W/S = wing loading = $W_G \div S_W$

(i) Estimated Wing Weight - The total estimated wing weight for the OTW/IBF configuration now results from combining the foregoing increments in the following manner:

$$W_W = W_{BOX_O} + \Delta W_{BOX} + W_{CS} + W_{SEC}$$

A baseline wing, generally similar to that used previously but having a taper ratio of three-tenths, was input to the Wing Weight Multi-Station Analysis computer program to obtain comparative data for chocking the parametric weight estimating logic. Table VI presents a comparative wing weight summary of the weights derived from the parametric wing weight logic and from the Wing Weight Multi-Station Analysis (WMSA); it demonstrates correlation within 3.5 percent. The major wing design parameters are also indicated in this table. For this wing, the input to the "WMSA" program included estimated torsional stiffness requirements (i.e., required torsional stiffness equal to 90 percent of strength designed bending stiffness); major external load parameters including 2g taxi, 2.5g maneuver, 2g takeoff and landing, and 50 fps gust at cruise speed; 7075-T73 material for wing structural members with a gross section fatigue stress cut-off of approximately 40 KSI; and various aerodynamic and geometry constants. The "WMSA" program computes balanced external loads, material required for strength and stiffness, geometry data, and estimates for secondary structure and control surfaces. (Sample output information from the "WMSA" program is given in Section 6.7 for the mechanical flap configuration.)

TABLE VI - COMPARATIVE WING WEIGHT DATA
- PARAMETRIC AND "WMSA" METHODS

	PARAMETRIC EQUATIONS Kg (LB)			
BASIC WING WEIGHT (W_{WO})	5704	(12,575)		
SUBTRACT:	-2636	(-5,811)		
BASIC SECONDARY STRUCTURE	-927	(-2,044)		
BASIC T.E. FLAPS	-1461	(-3,221)		
BASIC AILERONS	-248	(- 546)		
BASIC WING BOX WEIGHT	3068	(6,764)	3310	(7,298)
OTW/IBF CONTROL SURFACES	3544	(7,812)	3402	(7,499)
TRAILING EDGE FLAPS	2331	(5,138)	2263	(4,990)
AILERONS	498	(1,098)	498	(1,098)
LEADING EDGE FLAPS	715	(1,576)	640	(1,411)
SECONDARY STRUCTURE	625	(1,378)	795	(1,753)
WING BOX WEIGHT PENALTY	430	(949)	430	(949)
TOTAL WING WEIGHT	7667	(16,903)	7938	(17,499)
(PERCENT DIFFERENCE)				(3.53)

WING DESIGN PARAMETERS:

S_W = 156.6 m^2 (1567 SQ.FT.), AR = 7.73, TR = 0.3, N = 3.75,

W_G = 64,400 Kg (141,976 LB), MISSION FUEL = 7792 Kg (17,179 LB),

TCR = 14.26%, TCT = 10.9%, TS = 27.6 KN/cm^2 (40,000 PSI),

NACELLE WEIGHT PLUS ENGINES AND SYSTEMS = 8444 Kg (18,616 LB),

WR = 7792 Kg (17,179 LB) + 8444 Kg (18,616 LB) = 16,237 Kg (35,795 LB), NE = 2,

D_{NAC} = 2.59 m (8.5 FT) (ENGINE THRUST = 161.8 KN (36,368 LB) PER ENG.,

FPR - 1.35, WING SWEEP (1/4C) = 20 DEG.,

CRUISE MACH = 0.8, ϵ_F = ϵ_{AIL} = 0.4, ϵ_{LED} = 0.18,

HIGH-WING CONFIG. WITH FUSELAGE MOUNTED MLG (CWI = 0.95),

η_{FO} = 0.7, η_{FI} = 0.11 (FUSELAGE WIDTH = 3.69 m (12.1 FT.)

4.8.2 Bleed Air Component Weight

For the OTW/IBF configuration, engine fan bleed air is collected inside the nacelle and routed through the wing box into the trailing edge flap cavity. Once inside the flap, the bleed air is distributed spanwise for flap internal blowing and boundary layer control for the ailerons. The ducting is continuous from tip to tip and provides cross-ship distribution for engine-out operation. Boundary layer air to the aileron is controlled by a gate-type valve at the flap/aileron interface; the aileron can also operate as a flap.

The weight estimating logic for the bleed air components was derived from analytical analysis of a design baseline and reflecting the design parameters as functions of the known parameters within the vehicle-sizing computer program. The following reflects the derivation of the sizing parameters, the weight estimation logic, and the component weights for the baseline configuration identified in Table VI.

(a) Sizing Parameters - The bleed air component weights are primarily influenced by the amount of fan air bleed, width of the wing box, width of the fuselage, number of engines, engine thrust, engine fan pressure ratio, wing box depth, and nacelle width.

- Input Data:

  FPR = Engine Fan Pressure Ratio

  T = Thrust per engine (lbs.)

  N_E = Number of engines per aircraft

  D_{NAC} = Nacelle Diameter

  PCTBLC = Fan bleed air for IBF (%)

  S_W = Wing Area (sq-ft)

  AR = Wing Aspect Ratio

  TCE = Wing effective thickness to chord ratio (%) (defined on Figure 127)

  FW = Fuselage Width (ft)

- Fan Air Mass Flow:

FPR	1.325	1.35	1.4	1.5	1.574
$F_G/\dot{m}$ KN/Kg/sec (lb/lb/sec)	23.05 (23.5)	238.4 (24.3)	253.1 (25.8)	279.6 (28.5)	294.3 (30.0)
$\dot{m}/A$ Kg/sec/m^2 (lb/sec/ft^2)	122.6 (25.1)	124.5 (25.5)	128.9 (26.4)	136.2 (27.9)	141.1 (28.9)
F_G/A KN/m^2 (lb/sq. ft.)	28.25 (590)	29.26 (620)	32.56 (680)	38.06 (795)	41.51 (867)

$F_G/A \triangleq 1112 \times (FPR) - 880$ = Gross thrust per unit area for the fan air at M = 0.2 (lbs. per sq. ft.)

(b) Bleed Air Component Weight Estimation - From the above input data, the various component weights are estimated using the following logic:

- Determine $F_G/A = 1112 \times FPR - 880$
- Determine Ke = engine location factor to account for wing thickness distribution
  $K_E = 1.35$ for 2 engine configuration
  $K_E = 1.2$ for 4 engine configuration
- Determine $D_{MAX\ (1)}$ = maximum duct diameter based upon the average wing thickness at the front and rear beam (inches)
  $D_{MAX\ (1)} = 0.064 \times (KE) \times (TCE) \times (SW/AR)^{.5}$
- Determine ND = maximum number of ducts through the wing box based upon the wing thickness, minimum duct separation for each engine, and nacelle width
  $ND = 10.91 \times D_{NAC} \div D_{MAX\ (1)}$ (integerized by truncating to the integer value)
- Determine D_{MAX} = maximum duct diameter based upon nacelle width and wing depth (inches)
  $D_{MAX} = 10.91\ D_{NAC} \div ND$

- Determine A_{MAX} = maximum available area for fan air bleed flow through the wing box (sq. inches)

  $A_{MAX} = .7854 \text{ X NDX } (D_{MAX})^2$

- Determine FA = fan air cross-sectional area based upon mass flow (sq. inches)

  $FA = 144 \text{ X T} \div (F_G/A)$

- Determine MAXBLD = maximum percent bleed from the fan air based upon the geometry constraints

  $MAXBLD = 100 \text{ X } (A_{MAX}) \div (FA)$

- Compare the input desired PCTBLC with the MAXBLD and set the minimum value = PCTBLD

  That is

  $PCTBLC \geqq PCTBLD \leqq MAXBLD$

- Determine BFA = fan bleed air area (sq. inches)

  $BFA = (PCTBLD/100) \text{ X } (FA)$

- Determine DD = duct diameter (inches)

  $DD = 1.128 \, (BFA/ND)^{.5}$

- Determine LB = average wing box width (inches)

  $LB = 5.04 \, (K_E) \, (SW/AR)^{.5}$

- Determine LF = cross ship duct length (inches)

  $L_F = 12 \text{ X FW}$

- Determine the following duct weight variables:

  $V_1 = (ND) \, (N_E) \, (DD)^2$

  $V_2 = (LB) \, (ND) \, (N_E) \, (DD)$

  $V_3 = (LF) \, (DD) \, (ND \text{ X } N_E)^{.5}$

- Determine the following bleed air component weights:

  1. Fan Air Shutter (air collector in the nacelle)

     $W_1 = .0908\ V_1$

  2. Wing Box Ducts

     $W_2 = .019\ V_2 - .0138\ V_1$

  3. Aileron Air Gate Valves

     $W_3 = .0449\ V_1$

  4. Cross-Ship Ducting

     $W_4 = .0276\ V_3$

  5. Cross-Ship Isolation Valve

     $W_5 = .0243\ V_1$

  6. Valving Controls and Miscellaneous

     $W_6 = .15\ (\Sigma W_{1 \rightarrow 5})$

- Determine the total duct system weight (W_{DUCTS})

  $W_{DUCTS} = \Sigma (W_{1 \rightarrow 6})$

(c) Design Base Point Weights - For the baseline wing with a three-tenths taper ratio, the foregoing logic was followed to compute individual component weights. The resulting values were scrutinized in the light of potential design systems for such a configuration and deemed to be of reasonable proportions. The bleed air component weights computed for this configuration from the above logic are as follows:

- Computed Data -

  PCTBLD = 15.6%

  DD = 42.4 cm (16.7 inches)

  LB = 246.1 cm (96.9 inches)

  L_F = 368.8 cm (145.2 inches)

$N_D = 6$

$N_E = 2$

$V_1 = 6 \times 2 \times 16.7^2 = 3347$

$V_2 = 96.9 \times 6 \times 2 \times 16.7 = 19419$

$V_3 = 145.2 \times 16.7 (6 \times 2)^{.5} = 8400$

- Bleed Air Component Weight
  1. Fan Air Shutter = 137.9 Kg (304 lbs.)
  2. Wing Box Ducts = 146.5 Kg (323 lbs.)
  3. Aileron Air Gate Valves = 68.0 Kg (150 lbs.)
  4. Cross-Ship Ducting = 105.2 Kg (232 lbs.)
  5. Cross-Ship Isolation Valve = 36.7 Kg (81 lbs.)
  6. Valving Controls and Misc. = 73.9 Kg (163 lbs.)

  TOTAL WEIGHT = 568.4 Kg (1253 lbs.)

4.8.3 Nacelle Weight

The nacelle weight items were estimated from detailed analysis of baseline engine plus nacelle design data. Engine thrust, weight, geometry, and scaling factors were obtained from "QCSEE" studies using the various Detroit Diesel Allison engine configurations. Nacelle structure and thrust reverser weights were then related to the engine parameters to derive nacelle weights for the baseline engines. The nacelle structure includes the cowling, doors, acoustic treatment, fan and primary exhaust nozzles, and power plant package support structure. The supporting structure for the OTW/IBF configuration is integral with the nacelle. Design point stress analysis was used to establish a base point for supporting structure weight which was then scaled by engine weight ratio to obtain weight values for the various engine configurations. The other nacelle component weights were determined from detailed weight data derived for the "QUESTOL" research airplane proposal and for the "QPLT" (Quiet Propulsive Lift Technology) research airplane studies. These other nacelle component weights were found to be wetted area dependent. DDA (Detroit-Diesel-Allison) engine scaling relationships indicated that maximum engine diameter and length were each dependent upon the square root of the

rated thrust. Since the engine weight scaling factor is approximately a linear function of thrust, the wetted area (and nacelle weight) was then a linear function of engine weight for a given engine configuration family. Thrust reversers and variable fan nozzle component weights were also determined by a linear function of engine weight for a given engine configuration family. The nacelle and thrust reverser weight, therefore, was handled in the aircraft sizing computer program by an input engine family data which included the nacelle and thrust reverser weight ratios with respect to engine weight. Table VII gives the nacelle and thrust reverser weight and their weight ratios as determined for each engine family. The nacelle weights shown by this figure are determined for conventional material utilization. The sizing program contains a composite material factor for reflecting advanced composite material utilization. The factor used in 0.85 (as used in reference 2), which was determined from NASA Advanced Transport Technology (ATT) studies. This means that composites are assumed to result in a 15 percent weight reduction from conventional nacelle weights for similar size and loading condition. The absolute weight reduction is rather larger since it includes the cascaded benefits of a reduction in the size of vehicles.

4.8.4 Propulsion Weight

The propulsion weight items are composed of the engine weight, thrust reverser weight, engine systems, and the fuel system. The engine weight is derived from the engine configuration family data using the base engine weight and rated thrust. The engine weight equation is:

$$W_E = T \ (W_E/T)_B^{1.02}$$

where, T = the required engine thrust

$(W_E/T)_B$ = base engine weight to thrust ratio

The 1.02 exponent in the above equation was derived from the Detroit Diesel Allison scaling curves. The thrust reverser weight was identified in the preceding section on nacelle weight. The engine systems weight was derived from contemporary airplane data and includes the cooling, lubricating, starting, and engine control systems. Its equation in the sizing program is:

(BASELINE ENGINES CONVENTIONAL MATERIALS)

ITEM	(1)	(2)	(3)	(4)	(5)	(6)
BASELINE ENGINE	-	PD287-6	PD287-11	PD287-39		PD287-23
FAN BLADE CONFIG.	VP	VP	FP	FP	FP	FP
FAN PRESSURE RATIO	1.25	1.325	1.35	1.40	1.47	1.50
BASE ENGINE THRUST - KN	129.9	122.8	128.1	89.0	97.9	89.0
- (LB)	(29,200)	(27,600)	(28,800)	(20,000)	(22,000)	(20,000)
BASE ENGINE WEIGHT - Kg	1,996	1,841	1,905	1,329	1,746	1,404
- (LB)	(4,400)	(4,059)	(4,200)	(2,930)	(3,850)	(3,095)
THRUST REVERSER WEIGHT - Kg	255	192	194	115	106	102
- (LB)	(562)	(423)	(427)	(253)	(233)	(224)
NACELLE WEIGHT - Kg	1,589	1,364	1,427	929	982	948
- (LB)	(3,504)	(3,008)	(3,145)	(2,049)	(2,164)	(2,089)
INLET ASSEMBLY - Kg	263	211	208	146	137	133
- (LB)	(580)	(465)	(459)	(321)	(303)	(293)
UPPER FAN CASE COWL - Kg	60	42	50	30	23	25
- (LB)	(132)	(93)	(110)	(67)	(50)	(55)
FAN DUCT COORS - Kg	311	260	275	195	178	187
- (LB)	(685)	(574)	(607)	(430)	(392)	(413)
UPPER FAN DUCT-FIXED - Kg	92	86	92	69	65	75
- (LB)	(203)	(190)	(203)	(153)	(144)	(166)
CORE COWL - Kg	184	209	209	148	159	182
- (LB)	(406)	(461)	(461)	(327)	(351)	(401)
PRIMARY EXHAUST SYSTEM - Kg	184	158	164	85	103	91
- (LB)	(405)	(348)	(362)	(188)	(226)	(201)
FAN EXHAUST STRUCT. - Kg	230	161	174	88	91	73
- (LB)	(508)	(355)	(384)	(193)	(201)	(160)
ENGINE MOUNTS - Kg	41	38	39	27	36	29
- (LB)	(91)	(84)	(87)	(59)	(79)	(64)
FRAMES, LONGERONS, FITTINGS - Kg	224	199	214	141	190	152
- (LB)	(494)	(438)	(472)	(311)	(418)	(336)
W_{TR}/W_E	0.128	0.104	0.102	0.086	0.061	0.073
W_{NAC}/W_E	0.796	0.758	0.749	0.699	0.562	0.675

TABLE VII: OTW/IBF NACELLE WEIGHT SUMMARY

$$W_{SYS} = 2\,(N_E)\,(W_E)^{.5}$$

where, N_E = number of engines

W_E = derived engine weight for the required engine size

The fuel system weight remains the same as used in reference 2, namely:

$W_{FS} = 0.5\,(S_W)$, where S_W = wing area (sq. feet)

The engine build-up items (e.g., generators, hydraulic pumps, constant speed drives) are included in the electrical and hydraulic systems groups. The analysis of reference 2 had accounted for the engine build-up items twice, both in the nacelle and propulsion weight groups and also the electrical and hydraulic weight groups.

4.9 NOISE ANALYSES

Section 2.8.2 of reference 2 presented the methods used in noise prediction which have been continued through the current phase with some modification and are summarized below:

- Jet Noise - SAE Aerospace Information Report 876
- Fan Noise, Turbine Noise, Core Noise - Based on bare engine data supplied by engine manufacturer with acoustic attenuation effects calculated by Lockheed.
- Flap Interaction Noise - Based on published data from scale model test programs.
- Aerodynamic Self Noise - From calculations based on flyover power off noise measurements of several aircraft, corrected for gear extension and flap settings.
- Ground Attenuation - Based on SAE AIR923.
- Aircraft Shielding - Estimates based on geometry of individual aircraft.
- PNL to EPNL Conversion - Derived from sound pressure levels and directivity patterns representative of STOL configurations and applied as a factor which is a function of source-to-observer distance and aircraft velocity.

4.9.1 Engine Noise Characteristics

Aircraft were designed using engines described in Section 4.2.1. Noise analyses were conducted for all these cases. The data indicated that emphasis should be placed on the following engines:

- Variable pitch fan with pressure ratio 1.25
- Fixed pitch fan with pressure ratio 1.35
- Fixed pitch fan with pressure ratio 1.47

The data on fan tip speed and bare engine noise plotted in Figures 129 and 130 are considered significant in choosing these engines. Both the 1.25 and 1.35 FPR engines have fan tip speeds of 229 m/sec (750 fps) and lower noise levels than the other engines. The 1.47 engine has a high tip speed; its overall noise level is representative of current advanced engines with bypass ratios of 5 to 6.

Typical component noise levels for these three engines are presented in Table VIII. A significant observation from the table is the dominance of forward fan noise in each case because of the attenuation and shielding of aft noise sources in the over-the-wing nacelle. The data represent wall treatment only and show that further inlet treatment may be effective in the OTW installation. (This is not the case in an under-wing installation as discussed in Section 6.8.)

The following compares the levels of reference 2 in which the nacelles had splitters in the forward and aft fan ducts:

1.35 FPR engines 500-foot sideline noise in PNdB

	Reference 2	Table
Suppressed Fan Noise	92.2/Engine	95.9/Engine
Total Noise - 2 Engines	97.4	100.0

4.9.2 Aircraft Design and Noise Data

The characteristics of the aircraft which furnished the principal correlations of noise level, fuel consumption, and economics at different fuel price levels are summarized in Table IX. The results of contour analyses are summarized in Tables X and XI. Detailed printouts of the aircraft characteristics are presented in the appendices.

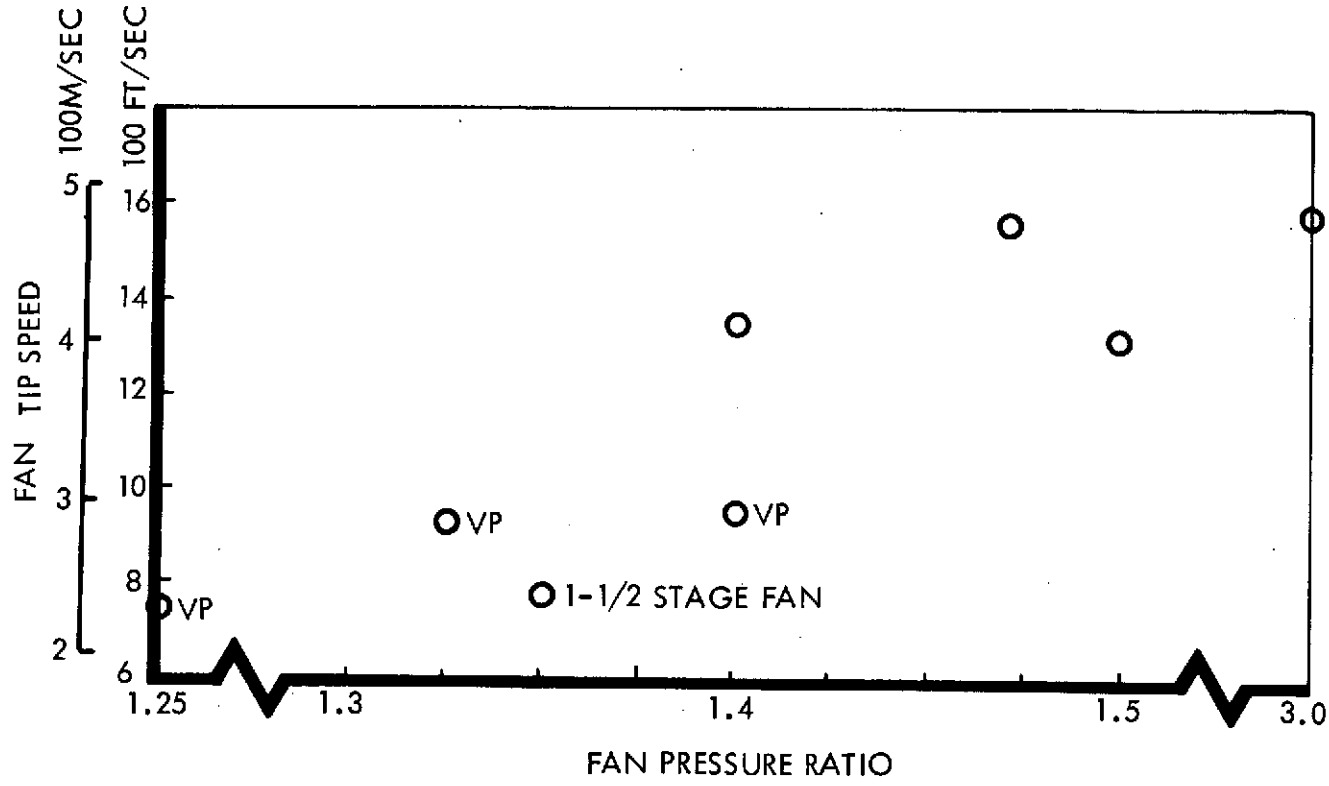

FIGURE 129: FAN TIP SPEED VS FAN PRESSURE RATIO

SINGLE ENGINE, BARE, 133 KN (30,000 LB.) RATED THRUST
152M (500 FT.) SIDELINE, 88M (290 FT.) ALTITUDE

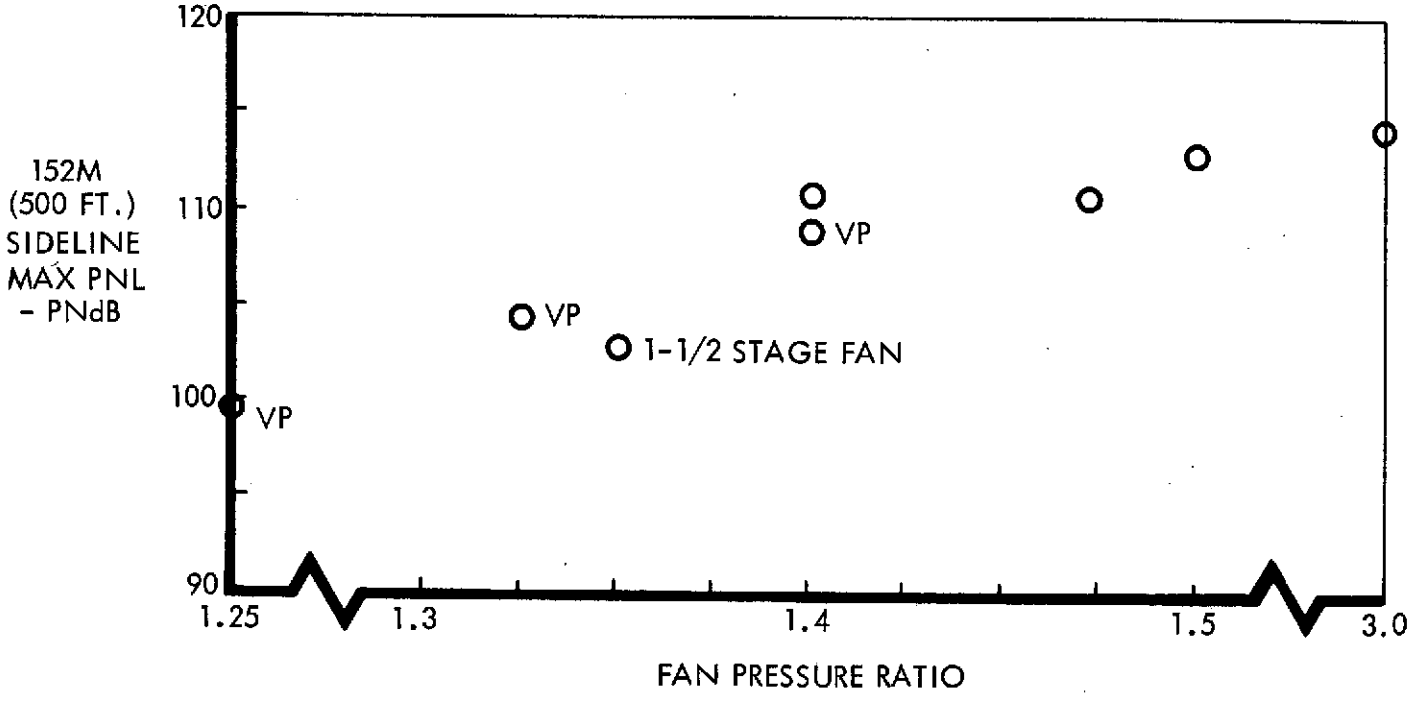

FIGURE 130: FAN NOISE VS FAN PRESSURE RATIO

SINGLE ENGINE, SHIELDING AND EGA NOT INCLUDED. WALL TREATMENT ONLY.

	NOISE LEVEL (PNdB)					
	1.25 FPR		1.35 FPR		1.47 FPR	
	FWD	AFT	FWD	AFT	FWD	AFT
FAN, UNSUPPRESSED	95.7	96.8	100.5	95.3	106.9	
FAN, SUPPRESSED	91.2	86.8	95.9	89.4	102.9	
FAN JET/FLAP	69.8	76.7	78.9	84.1	} 83.1	
PRI JET	56.5	63.2	58.8	63.9		
CORE	57.2	73.8	81.0	86.3	86.4	N/A
TURBINE	69.8	80.5	68.0	74.1	59.9	
AERO.	75.9	76.9	75.8	76.7	70.3	
SLOT JET	44.5	51.4	53.6	58.8	57.8	
TOTAL	95.1	93.5	100.0	97.2	109.6	
(NO. OF ENGINES)	2		2		4	
S.L.S. THRUST - LB.	39,800		36,377		12,195	
-KN	177		162		54	

TABLE VIII: OTW/IBF - COMPONENT NOISE SUMMARY (AT MAXIMUM 152 M (500 FT.) SIDELINE NOISE LOCATION)

TABLE IX : OTW/IBF AIRCRAFT FOR NOISE ANALYSIS

FIELD LENGTH 910 m. (3000 FT.)

ENGINE FPR	1.25	1.35	1.35	1.35* (S)	1.35	1.47	1.47* (S)
NO. OF ENGINES	4	2	4	4	4	4	4
AR	14.0	7.73	10.0	10.0	14.0	14.0	14.0
A/C OPTIMIZ BASIS	DOC-2	DOC-1	DOC-1/-2	DOC-2	DOC-4/-10	DOC-2	DOC-2
CR. ALTITUDE - m.	7620	9140	8230	8230	9140	9140	9140
(1000 FT.)	25	30	27	27	30	30	30
DES. CR. MACH NO.	0.70	0.80	0.75	0.75	0.70	0.75	0.75
RAMP GROSS WT.- 1000 Kg	56.7	68.1	56.0	56.5	54.2	59.1	59.1
(1000 LB)	124.9	150.2	123.5	124.5	119.4	130.3	130.3
RATED THRUST - KN	6.12	17.63	5.50	5.61	4.79	5.47	5.52
(1000 LB)	13.67	39.36	12.27	12.53	10.69	12.20	12.33
T.O. W/S - Kg/m^2	6813	449	583	583	530	542	542
psf	139.8	92.0	119.5	119.5	108.5	111.0	111.0
T/W INST.	0.391	0.480	0.363	0.363	0.327	0.343	0.343
T.O. FLAP - DEGREES	39.0	12.7	31.5	31.5	35.0	38.0	38.0
DIST. TO 10.7 m (35') : m	690.7	564.8	709.9	709.9	718.1	728.8	728.8
(FT.)	2266	1853	2329	2329	2356	2391	2391
VELOCITY - Kph	207	224	207	207	202	209	209
(KTS)	112	121	112	112	109	113	113
SEC. SEGM CLB. - DEG.	8.12	13.48	7.02	7.02	6.25	6.86	6.86
DIST OF CUTBACK - m.	2114	1810	2370	2370	2569	2417	2417
(FT.)	6935	5939	7777	7777	8430	7930	7930
CUTBACK POWER SETTING	0.76	0.81	0.83	0.83	0.79	0.74	0.74
CLB. ANGLE AFTER CB	3.87	9.49	4.10	4.10	3.19	2.87	2.87
APPROACH ANGLE - DEG.		5.2	5.2	5.2	4.2		
APP. POWER SETTING		0.38	0.67	0.67	0.71		
APP. VEL. - Kph	182.2	182.2	182.2	182.2	176.7		
(KTS)	98.4	98.4	98.4	98.4	95.4		

* SPLITTER INSTALLED IN INLET

TABLE X: SUMMARY OF OTW/IBF NOISE
FIELD LENGTH 910 m (3000 ft)

ENGINE FPR	1.25	1.35	1.35	1.35*(S)	1.35	1.47	1.47*(S)
NO. OF ENGINES	4	2	4	4	4	4	4
AR	14.0	7.73	10.0	10.0	14.0	14.0	14.0
SIDELINE NOISE							
EPNdB @ 152 m. (500 FT)	90.3	97.4	95.2	92.5	94.7	106.5	102.7
305 m. (1000 FT)	84.8	91.9	89.8	87.0	89.3	100.7	97.3
FAR 36 PT.	76.9	87.9	80.0	77.2	79.5	90.3	87.6
TAKEOFF FLYOVER							
EPNdB @ 1220 m. (4000 FT)	97.0	98.3	103.3	100.6	103.8	115.0	111.2
@ 1830 m. (6000 FT)	93.6	95.6	99.9	97.2	100.3	111.5	107.7
FAR 36 PT	79.9	78.1	85.3	82.1	86.2	98.2	94.9
TAKEOFF AREAS:							
KM^2 @ 95 EPNdB	0.205	0.533		0.326	0.567	6.570	3.286
90 EPNdB	0.531	1.202	1.518	0.824	1.448	16.298	9.800
85 EPNdB			4.454	2.328		38.350	
80 EPNdB	4.094	6.842	11.209	6.350	12.159	79.965	50.757
SQ. MI. @ 95 EPNdB	0.079	0.206		0.126	0.219	2.537	1.269
90 EPNdB	0.205	0.464	0.586	0.318	0.559	6.293	3.784
85 EPNdB			1.720	0.899		14.808	
80 EPNdB	1.581	2.642	4.328	2.452	4.695	30.877	19.599
TAKEOFF FOOTPRINT LENGTH:							
KM @ 95 EPNdB	1.386	1.601		1.685	2.303	9.312	6.440
90 EPNdB	2.090	2.176	3.672	2.295	3.652	15.270	11.628
80 EPNdB	6.442	5.605		8.070	12.582	34.878	27.517
FT @ 95 EPNdB	4,546	5,253		5,529	7.556	30,550	21,130
90 EPNdB	6,856	7,139	12,047	7,529	11,980	50,100	38,150
80 EPNdB	21,135	18,389		26,477	41,280	114,430	90,280
APPROACH NOISE:							
EPNdB @ 610 m. (2000 FT)	96.4	98.4				117.2	
@ 1850 m. (1 N. MI.)	88.1	90.3	92.6			109.3	
90 EPNdB AREA KM^2	0.243	0.477	0.844			17.007	
SQ. MI.	0.094	0.184	0.326			6.567	

TABLE XI: OTW-IBF APPROACH FOOTPRINTS

910 m. (3000 FT.) FOUR-ENGINE AIRCRAFT OPTIMIZED FOR DOC-2.

ENGINE FPR	1.25	1.35		1.47
NO. OF ENGINES	4	4	2	4
FLYOVER EPNdB				
610 m. (2000 FT.) FROM THRESHOLD	96.9		98.4	117.2
1.85 Km (1 N.M.) FROM THRESHOLD	88.7	92.6	90.3	109.3
AREAS: 90 EPNdB - SQ. Km	0.290	0.844	0.477	17.01
- (SQ. MILES)	0.112	0.326	0.184	6.567
80 EPNdB - SQ. Km	3.328	6.974	4.752	76.57
- (SQ. MILES)	1.285	2.693	1.835	29.567
LENGTHS: 90 EPNdB - m.	1.554			
- (FT.)	5,100			
80 EPNdB - m.			6,200	49,500
- (FT.)	17,800	25,500	20,600	105,500

Sideline and flyover noise levels are summarized in Figure 131. On the left graph EPNdB levels at 152 m (500 ft), 304 m (1000 ft) and 648 m (2125 ft - 0.35 N. Mi) are shown for aircraft with each of the three FPR engines. Optimum airplane designs for DOC-2 are represented; thus, the airplane with 1.25 FPR engines has a design cruise speed of M0.70 and those with 1.35 and 1.47 FPR engines are designed for M0.75. As noted earlier, four engine aircraft have better fuel consumption and lower DOC at fuel prices of double the 1972 price level. These are the basic cases plotted in Figure 131. Also shown for reference are the sideline noise levels for 2-engine aircraft optimized for DOC-1 with M0.8 cruise speed. Sideline noise levels of the latter are 2 to 3 dB higher at 150 to 300 meters. Flyover noise levels in the right hand graph are 1220 m (4000 ft), the Sperry box definition, at field length plus 610m (2000 ft), an alternate Sperry box interpretation, and at 6.5Km (3.5 N.Mi.).

It may be noted that sideline noise of FAR 36 minus 13 dB can be achieved by the aircraft with FPR 1.47 engines but that the flyover noise of this four-engine aircraft is just at the FAR 36 level. However, these data refer to the use of cutback to the performance minima allowed by FAR 36 in order to minimize the footprint at the high (close-in) noise levels which most greatly affect the community. An alternate, but equally acceptable, technique could be devised which would steepen the climb gradient and reduce the flyover point takeoff noise level per se. Two-engine aircraft with inherent better climb capability also show significantly lower levels at FAR 36 distances. Four-engine aircraft with 1.35 FPR engines are 24, 13, and 11.4 dB below FAR 36 for sideline, takeoff flyover, and approach noise. The corresponding two-engine aircraft are 16, 20, and 14 dB below FAR 36 levels.

Takeoff footprint areas and lengths are plotted in Figures 132 and 133 for different noise contours and engine fan pressure ratios. As would be expected from its climb gradient, the 2-engine aircraft has considerably shorter footprints and the area of the 80 EPNdB contour is considerably smaller than for 4-engine cases. Approach footprint areas and

OTW/IBF 4-ENGINE 910M (3000 FT.) F.L. 926 KM (500 N. MI.) DOC-2

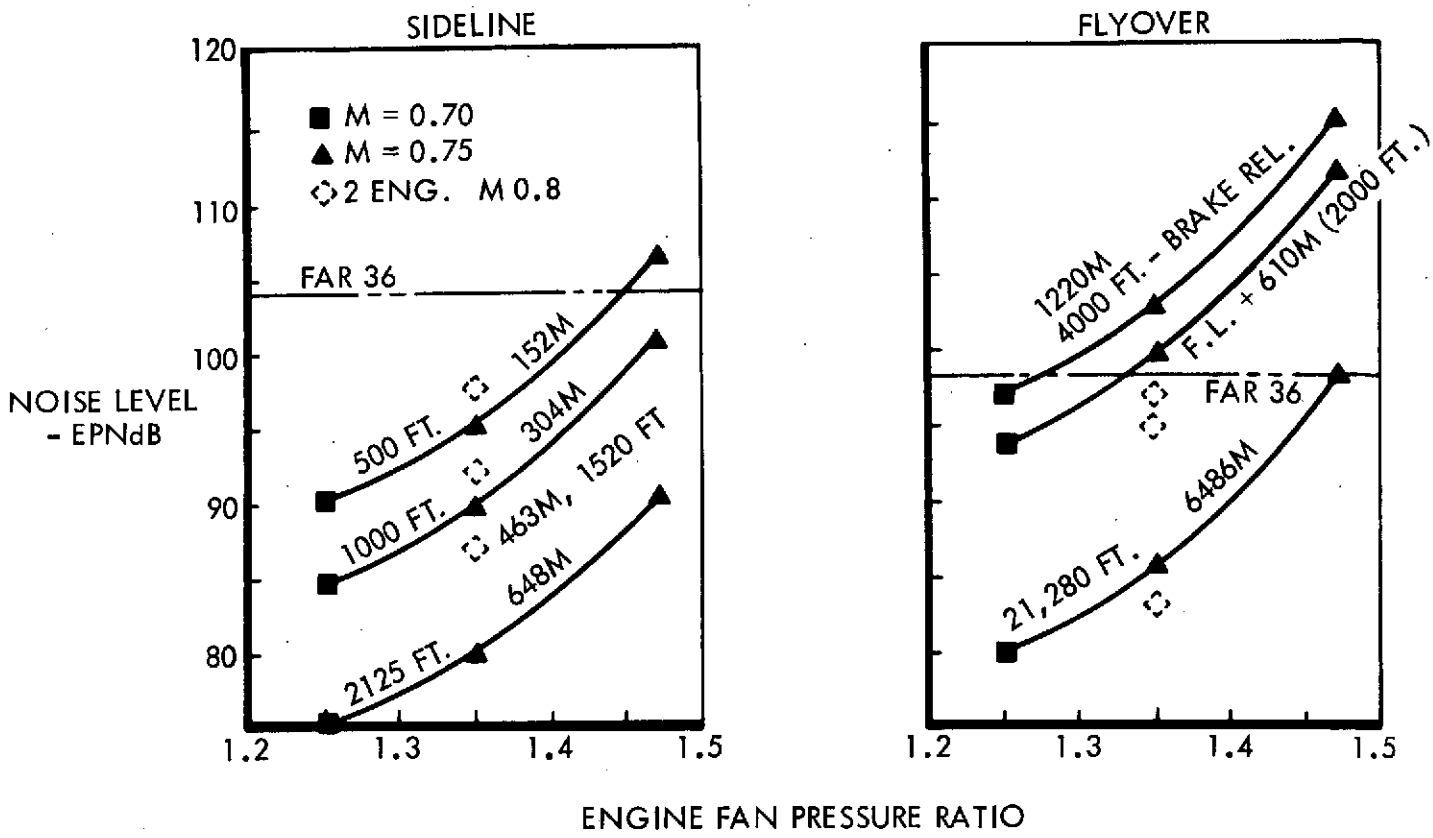

FIGURE 131: TAKEOFF NOISE LEVEL VS FAN PRESSURE RATIO

OTW/IBF 4-ENGINE 910M (3000 FT.) F.L. 926 KM (500 N. MI.) DOC-2

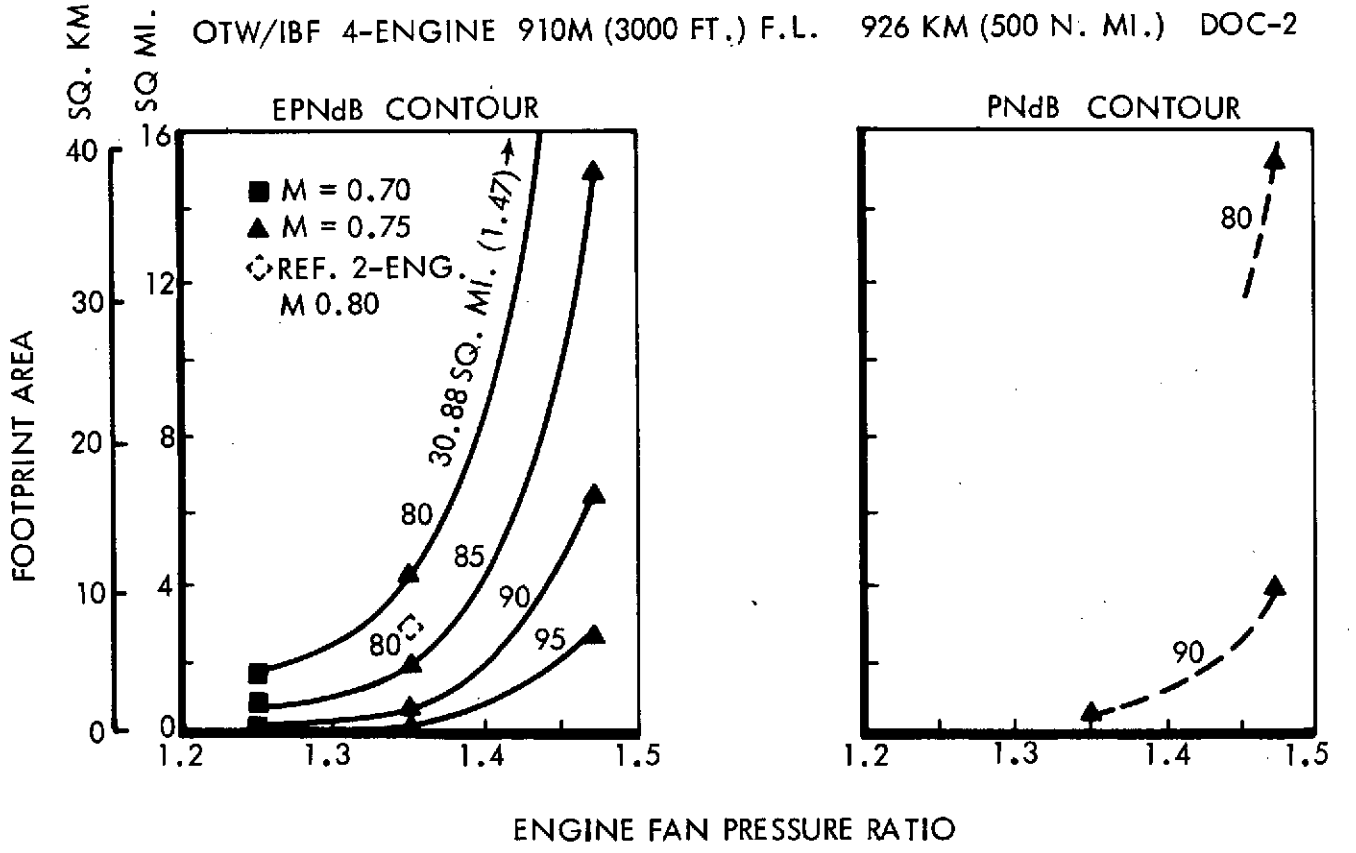

FIGURE 132: TAKEOFF FOOTPRINT AREA VS FAN PRESSURE RATIO

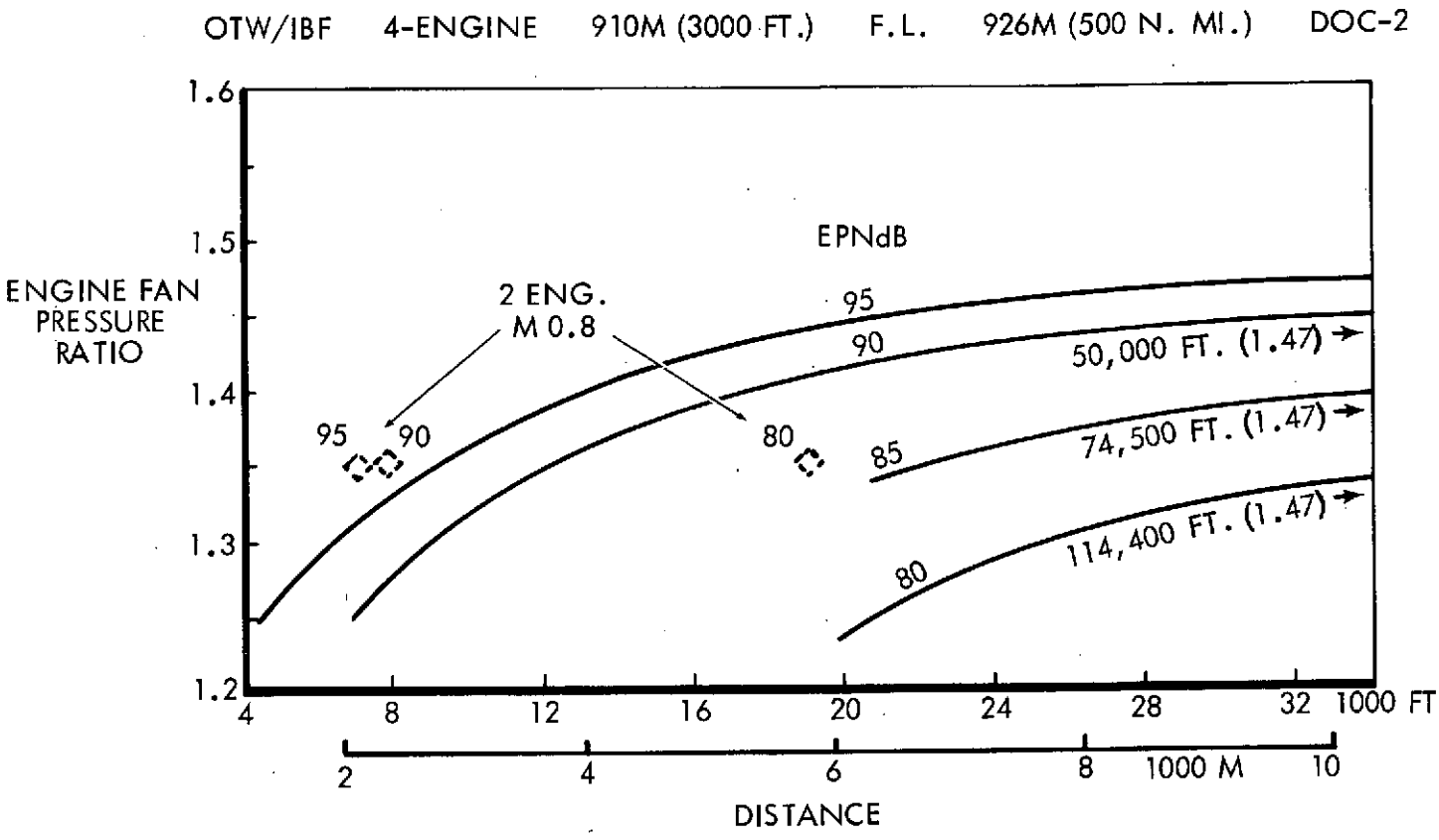

FIGURE 133: TAKEOFF FOOTPRINT LENGTH VS FAN PRESSURE RATIO

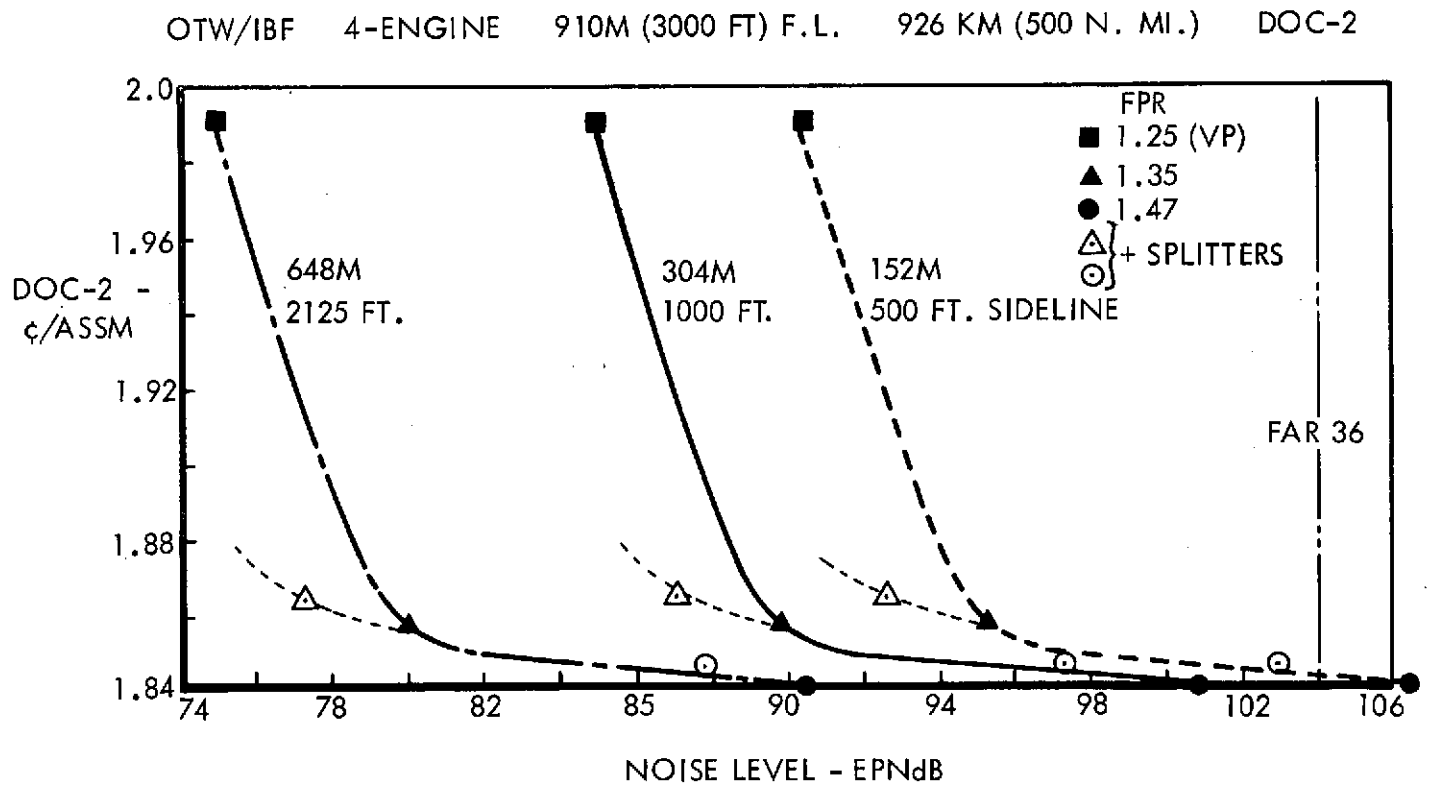

FIGURE 134: DOC VS SIDELINE NOISE LEVEL

lengths for the same design cases are shown in Table X.

The direct operating cost at twice 1972 fuel prices (DOC 2) is shown in Figure 134 as a function of sideline noise level. Figures 135 and 136 show DOC-2 as a function of flyover noise level and takeoff footprint area. It may be noted that DOC-2 increases slightly as the noise level decreases from that of the 1.47 FPR engines to that of the 1.35 FPR engine, then sharply increases for the quieter FPR 1.25 engine. Thus, the knee of the curve is represented by the aircraft with FPR 1.35 engines and the economics associated with the previously-quoted Part 36 minus 14 to 16 dB.

The effects of an inlet splitter on DOC-2 and on noise level of the 1.47 and 1.35 FPR engines are shown in Figures 134, 135, and 136. Reductions of 2 to 3 dB were achieved with approximately the same penalty in performance and costs which would be obtained by the same noise reduction achieved by lowering the engine fan pressure ratio. The curves show an indication of greater superiority than this in the inlet splitter approach when applied to the 1.35 FPR engine. However, this apparent indication is considered misleading since the fairing of the curve might well pass through the point represented by the splitter if the cost penalty for the variable pitch fan were eliminated from the 1.25 FPR case. This trend is shown with a dotted line in the figures.

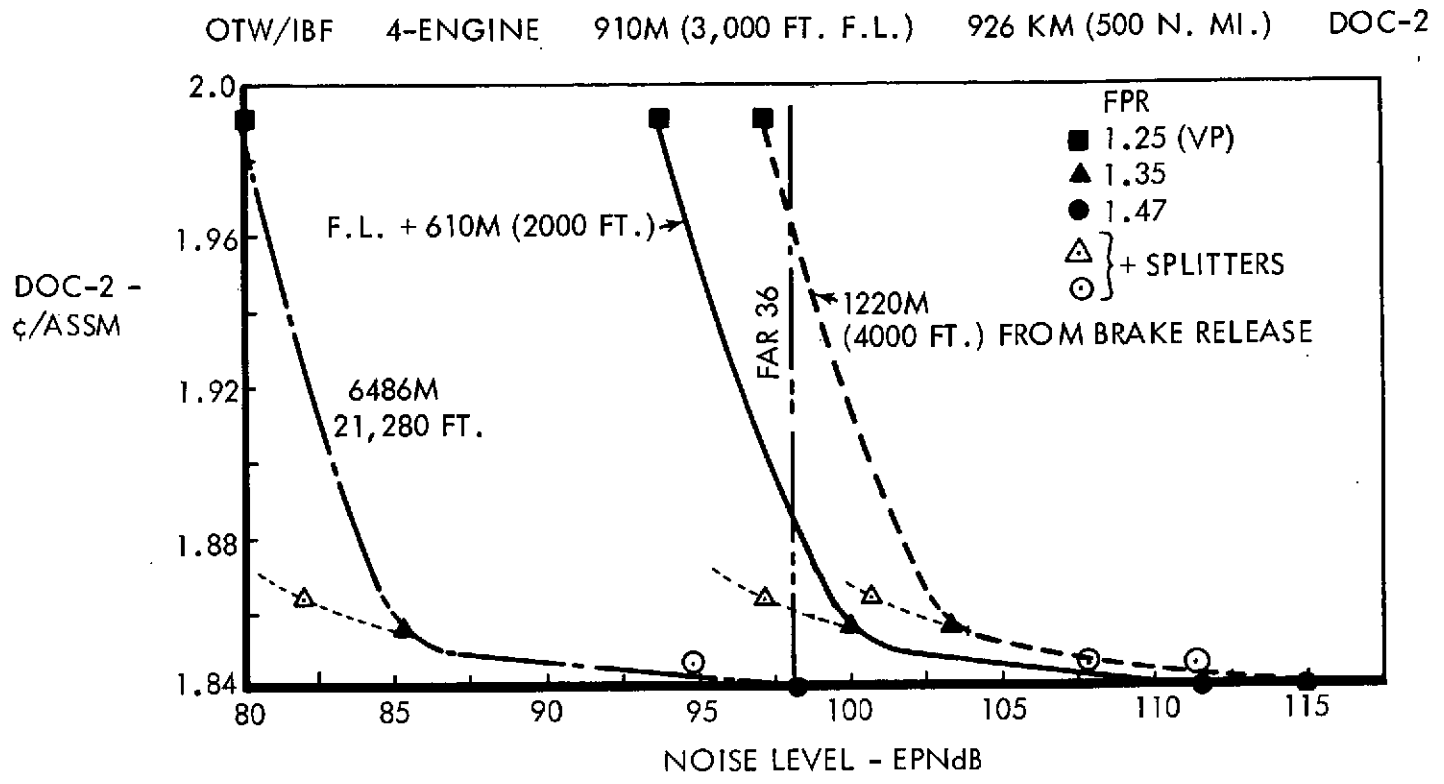

FIGURE 135: DOC VS FLYOVER NOISE LEVEL

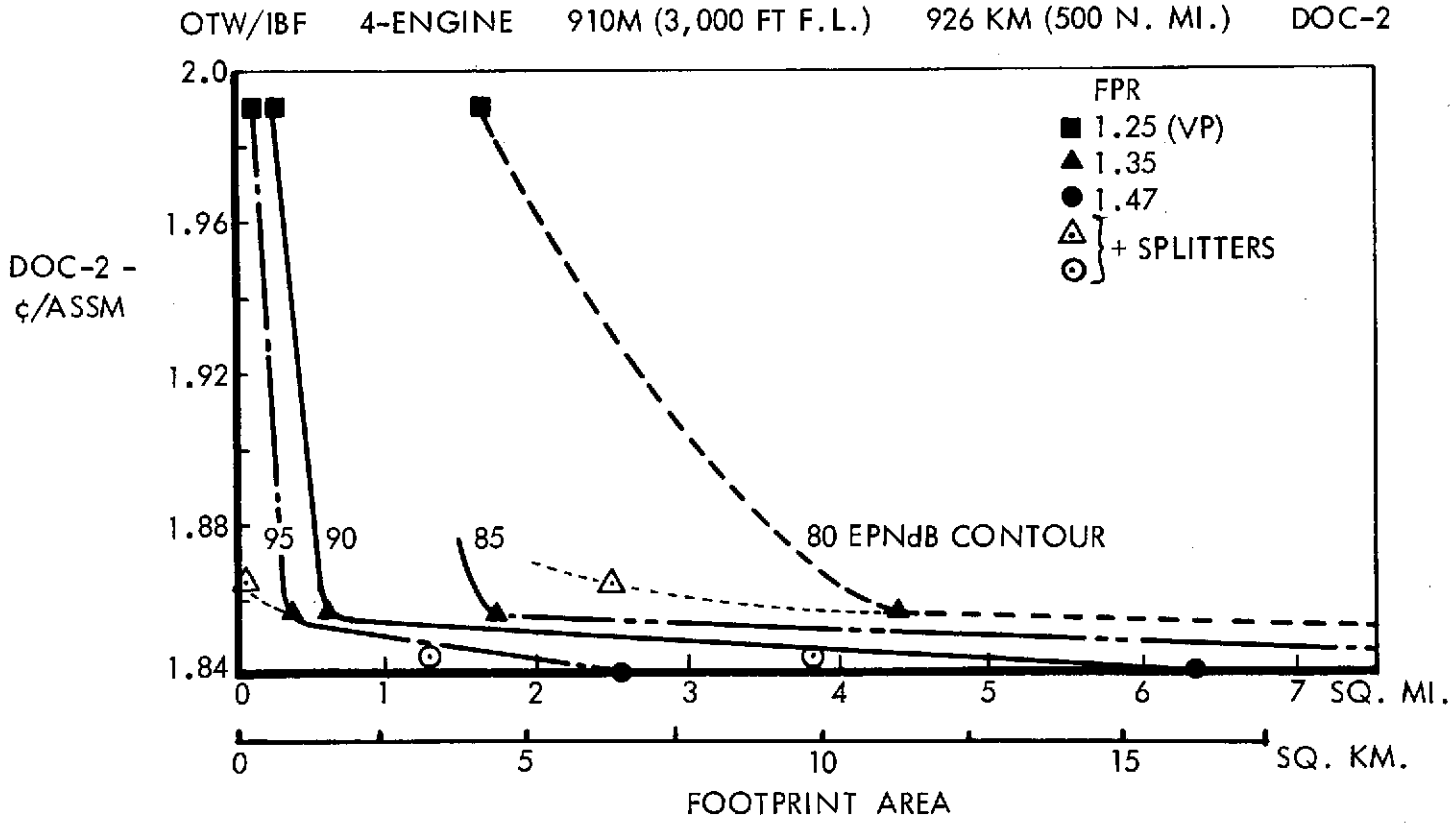

FIGURE 136: DOC VS TAKEOFF FOOTPRINT AREA

4.10 OTW/IBF DESIGN

4.10.1 OTW/IBF Aerodynamic Design

The detailed aerodynamic design of an efficient OTW/IBF configuration can only be accomplished through a judicious compromise of several criteria which are frequently in conflict. For example, a high aspect ratio OTW nozzle may be beneficial to low-speed flow turning and $C_{L\ MAX}$ performance, and yet produce undesirable effects in high speed flight, such as excessive scrubbing drag, internal duct losses, and interference drag. Initial NASA-Langley experiments in the late 1950's aimed primarily at the low-speed high lift side of the essentially dual design problem. Recent efforts, however, are recognizing the equal importance of the high speed aspects and over-all compromise with system design requirements. Recent sources of data include wind tunnel tests at NASA-Langley, NASA-Ames, Lockheed-Georgia testing on QPLT configurations, and the extensive MST testing conducted by Boeing on the YC-14 configuration. Although the current systems study contract does not fund wind tunnel testing of OTW/IBF models, tests conducted at Lockheed-Georgia under other funding has been significantly influenced by study results and recommendations.

Analysis of available test results and publications reveals some pertinent differences in aerodynamic design concepts between the baseline 910 m. (3000 ft.) OTW/IBF configuration derived in this study and the YC-14 configuration adopted by Boeing despite their related high lift systems. Accordingly, a discussion of aerodynamic concepts is presented here and related to these respective configurations. The baseline OTW/IBF concept has been depicted in Figure 60 and may be compared with the YC-14 configuration shown in Reference 25 . An immediate point of difference to be noted is the low sweep angle of the YC-14 wing and the consistency of its over-all appearance with a lower cruise Mach No. As discussed in Section 4.2, even the nominally low FPR engine generally has a supercritical nozzle pressure ratio at M = 0.8 and representative cruise altitudes, but the initial appearance of supercriticality as cruise speed is increased will occur at a higher Mach No. for the lower FPR engine. Thus, the

aerodynamic problems presented by the wing/nacelle interaction in either case are considered to be of similar magnitude and equally soluble with similar levels of detail design effort.

It should also be noted that the nacelles of the hybrid concept are both farther outboard on the wing, and are mounted more rearward on the chord than those of the YC-14. Reference 25 indicates that the most inboard location possible was found to be the most favorable high speed position for the YC-14. To quote, "Here, the flow fields of the nacelles tend to combine with the flow field of the fuselage making the three elements act as a single three-dimensional body, thereby reducing the interference drag and Mach number drag rise." However, the choice of this location now appears to have led to low speed problems as indicated by the subsequent canting of the nozzle exit outboard to prevent the exhaust jet from extending over on the body appreciably and degrading flow turning and $C_{L\ MAX}$. On the baseline hybrid an alternative to moving the nacelles quite so far inboard has been adopted. In this case, a leading edge fillet has been added to the wing to give actually a three-dimensional body continuity to the wing-body-nacelle junction. By allowing a slightly more outboard position of the nacelles, however, the need to cant the nozzle outboard for reasons of high lift efficiency has been avoided. The position of the nacelle exit relatively far forward on the wing chord (50%) for the YC-14 compared with approximately 60% for the hybrid is dictated by the relative severity of the landing requirements. To meet its landing requirements, the YC-14 must approach at 85 knots as noted in Reference 25. The hybrid can meet its landing distance requirement with an approach speed of approximately 98 knots at similar wing loading to the YC-14. The very slight degradation in maximum lift (noted in Figure 20) for the rearward nozzle exit appears justified in order to avoid excessive overhang of the nacelle over the leading edge and to minimize the area of the wing which will be scrubbed by engine jet efflux at cruise conditions.

Preliminary high speed tests with both unpowered and powered OTW nacelles indicate the need to consider the particulars of each OTW configuration before deciding whether to allow the small jet flap effect at cruise speed to increase wing inboard

loading or even to lessen inboard loading by a slightly negative flap movement. In the case of the configuration shown in Figure 40, for example, the wing initially had a high inboard loading before addition of the nacelles, and extensive wing filleting was required to avoid undesirable further loading up of the inboard wing due to the nacelles. A final OTW nacelle drag increment of the same magnitude as for a conventional under-the-wing pylon mounted type was achieved after this treatment as shown by Figure 44.

Recent tests have also been conducted in the Compressible Flow Facility at Lockheed-Georgia to substantiate the performance of the high technology airfoils used for the hybrid OTW/IBF wings as well as for the other types of high lift configurations. Figure 137 depicts the airfoil tested. Compared to a C-5 type section, the high technology section is approximately 4% thicker for a given design point as shown by the results in Figure 138 and the section is applicable to all system configurations once simple-sweep corrections have been considered in its use. For the inboard wing behind the OTW nacelle, however, aft camber would have to be decreased significantly to avoid high speed interference due to jet efflux from the engines.

4.10.2 OTW/IBF Powered Lift Installations

The DDA PD287-11 engine requires a separate primary nozzle exhaust. This requirement is not common to all prospective future engines but is also not unique to the PD287-11. Under a subcontract, DDA investigated the feasibility of mixing the fan and primary discharges of the -11 engine and found that it could be achieved with only moderate performance degradations. Inasmuch as definitive information was not available for the mixed configuration, the separate primary exhaust was retained. This requirement dictates a primary exhaust duct that will divert the hot primary exhaust flow off the wing and flap surface and provide for a blanket of cooler fan air between the primary exhaust and those surfaces. With the thinned fan flow, this can only be achieved by diverting the primary flow to the top of the nacelle. This configuration results in a bifurcation of the fan exhaust stream along the top of the nacelle with a splitter to divide the flow around the core engine and primary exhaust. This same splitter may conveniently serve to house the engine mounting and system connections.

- GELAC IS PRESENTLY INVESTIGATING A 16% THICK SUPERCRITICAL AIRFOIL FOR STOL APPLICATIONS

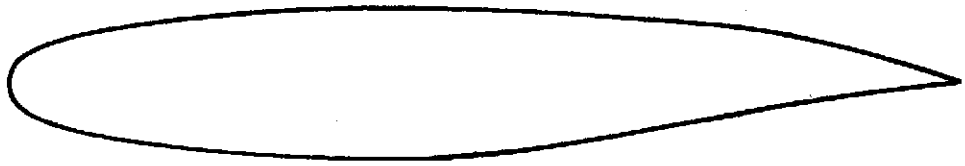

- DESIGN FEATURES
  - SUPERCRITICAL UPPER SURFACE PROVIDES WELL BEHAVED FLOW CHARACTERISTICS WITH SMALL SHOCK
  - REDUCED AFT LOADING AND CAMBER ALLOWS LARGE T/E ANGLE AND REAR BEAM DEPTH
  - LARGE L/E RADIUS GIVES HIGH CLEAN CONFIGURATION $C_{L\ MAX}$
- PRELIMINARY WIND TUNNEL TESTS INDICATE THAT RELATIVE TO NASA 65-213 AIRFOIL
  - $C_{L\ MAX}$ INCREASES FROM 1.2 TO 1.5 AT $R_N = 3.5 \times 10^6$
  - M_D INCREASES FROM 0.72 TO 0.75
  - T/C INCREASES FROM 13% TO 16%

FIGURE 137: AIRFOIL TECHNOLOGY SUBSTANTIATION

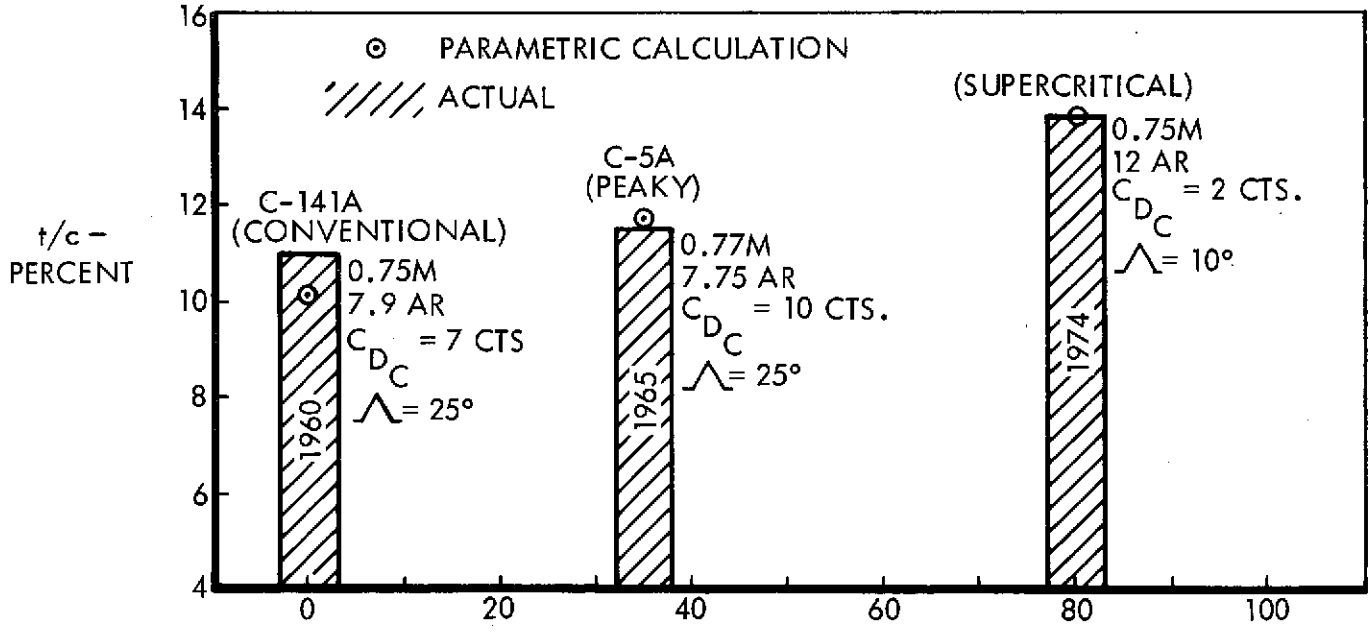

FIGURE 138: THICKNESS CHORD COMPARISON OF AIRCRAFT WITH VARIOUS AIRFOIL TECHNOLOGY LEVELS

The unique location of the engine poses structural mounting challenges but these do not impact the exhaust system other than to restrict the location of some of the functional, variable geometry features. These must not violate the structural integrity of the configuration.

The functional requirements of the nacelle are clearly defined while the manner in which they are achieved is flexible and, in some cases, not clearly defined by precedent or test data. The requirement for spreading and thinning the fan exhaust nozzle is perhaps most restricted by the h/r ratio dictated by the criteria for maintaining attached flow over the wing, Coanda turn and flap surface. This requirement is more specifically discussed in Section 4.2.6. From the criteria presented in that section, it is concluded that the limiting nozzle height to flap knee radius ratio h/r of 1.05 is required to maintain attached flow at a 1.35 fan pressure ratio with a flap deflection of 45° at a freestream q_∞ of 150 Kg /m^2 (30 psf_a) (equivalent to approximately 176 Km/hr. or 95 knots). In view of the observation in Section 4.2.6 that the zero q_∞ attachment criteria curve is slightly optimistic relative to the test cases, an h/r below 1.05 should be selected to provide some conservatism. A target h/r of 0.75 would provide sufficient conservatism for a variation in the ratio of flat (or near flat) chord surface, f, of theflap to the flap knee radius, r. For the practical airplane configuration, this flat surface chord is limited such that an f/r of approximately 1.5 to 2.0 is the maximum while the criteria curves in Section 4.3.5 were based on a f/r of 4. The criteria were derived from data in which the nozzle (slot) discharged at the knee of the Coanda surface which is consistent with the selected configuration.

The nozzle configuration of the baseline mission vehicle described in Section 4.4 reduces the nozzle height to a value which is consistent with the flap design for values of h/r and f/r meeting the criteria. This nozzle configuration is basically rectangular with an effective aspect ratio of approximately 5. The flat upper surface of the nacelle adopted to facilitate the dual purpose flaps that serve to trim the fan exit area and also to block this area when reversed thrust is required. The outboard sides of the fan exit passages have been cut back to allow further spreading of the fan flow predominantly

along the wing/flap surface. It is recognized that an ultimate production nozzle configuration would require extensive configuration oriented testing and might well differ from that shown in Section 4.4. However, it would retain a quasi-rectangular shape with the primary modifications probably associated with the outboard sides of each fan passage. it will be noted from the plan view of this configuration that there is significant flare to the nozzle. Efforts to restrict this resulted in a nozzle height that was too large for compatibility with the Coanda attachment criteria and flap design.

The requirement for a high capacity, high recovery fan bleed for the IBF system in the high lift mode poses particularly difficult problems. In the bleed mode, the system must provide approximately 15 percent of the total fan flow to the bleed system, must have good total pressure recovery, must not unduly compromise the nacelle configuration and must not mismatch the fan or produce adverse distortion to the fan discharge. The latter requirement is related to the fan stall and structural tolerance to discharge distortion. In the cruise mode, the closed bleed extraction port must not cause excessive duct flow Mach numbers or losses and must not produce distortions in the fan exit stream.

Under a separate contract, DDA was asked to investigate alternate means for extracting this bleed. The results of this study were reported in DDA EDR 8058, Vol. I, December, 1973 (reference 28). One basic system for bleeding fan air was postulated in this study and investigated with three types of bleed extraction ports. All included a manifold plenum collector (with numerous discrete scoops spread around the lower 270° of the fan discharge outer diameter) which ducted the bleed flow into the wing box. Figure 139 presents the duct loss data from this study converted into IBF nozzle thrust compared to bled thrust and both expressed as a percent of the total fan thrust. From this figure, it will be seen that both the rectangular slot inlet and the divergent ramp inlet result in a prohibitively large loss of thrust at the IBF nozzle exit. Neither of these systems were capable of achieving the level of thrust required in the flap system. The total head scoop was capable of achieving the required bleed flow but at thrust losses in excess of 30 percent of the bled fan thrust. This was still considered to be excessive and was largely the result of the plenum collector which could not provide adequate diffusion of the extracted stream

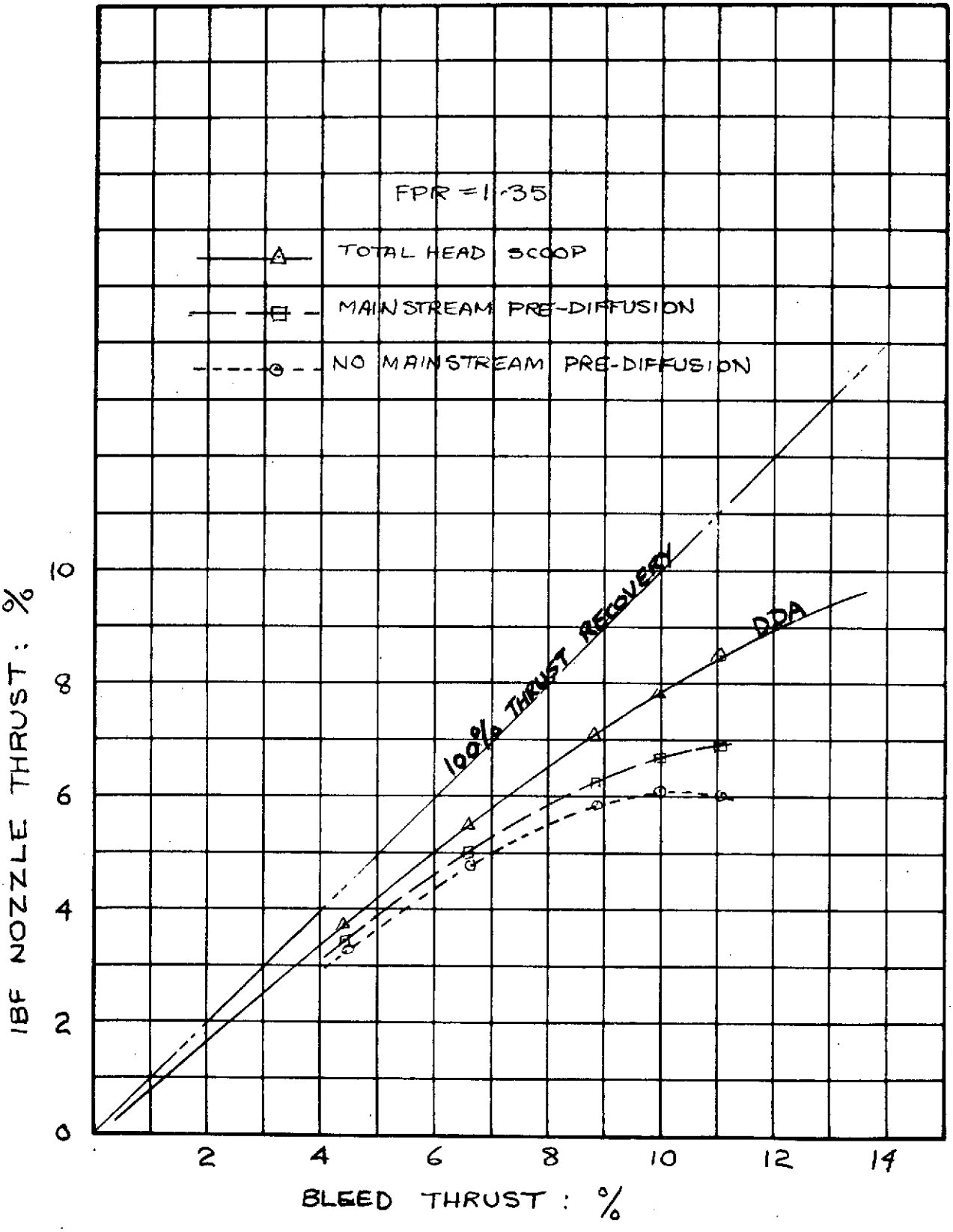

FIGURE 139: EFFECT OF ALTERNATE IBF BLEED CONFIGURATIONS

and required the air to follow a rather tortuous path to reach the wing box. In view of these considerations, a more straightforward approach has been taken to achieve the desired bleed characteristics. A large, single extraction point is provided in the bottom of the fan duct with the bled flow passing into and through the wing box with essentially no turns. The selected configuration presented in Figures 140 through 146 represents only one of a number of schemes to achieve this bleed. These figures illustrate a diverter door that is hinged at the aft end and raises into the stream when bleed is desired. Conceptually, this scheme allows for good match with the engine and ducting for variable bleed extraction. With this configuration, the maximum flow and consequently duct velocities would occur in the fan duct downstream of the extraction location when no bleed is being extracted. The fan duct is therefore designed for the no-bleed configuration in order to achieve good cruise performance. When bleed is to be extracted, the deflector is raised into the stream with diffusion of the bled air taking place under the deflector. The main stream of the fan air also diffuses as a consequence of the reduction in flow in the fixed portion of the fan duct. The configuration shown is not considered entirely satisfactory, however, since spillage of the air entrapped under the deflector can occur around the edges of the deflector. If the diffusion of the bled air and the main fan stream are equalized , this would not present a problem and could possibly be achieved by carefully developing the system. An alternative would be to block off any spillage around the edges by making the deflector door more rectangular and bounding the edges by streamlined fences. Experience with duct development would indicate that careful finning of this configuration could achieve the desired bleed without unduly distorting the flow at the fan discharge even though the leading edge of the deflector is close to the fan. The deflector door is powered closed in the event of an engine failure to prevent backflow into the engine in the manifolded IBF system.

An alternative to this system is to hinge the deflector door at the forward end. In this configuration, diffusion of the total fan stream takes place prior to the diversion of the bleed air into the wing. This configuration has the advantage of moving the point of extraction downstream thus providing some further relief from the fan distortion problem but this system would be designed for a narrow range of extraction rates. Again, the fan ducting is designed for the no-bleed case to achieve good cruise performance.

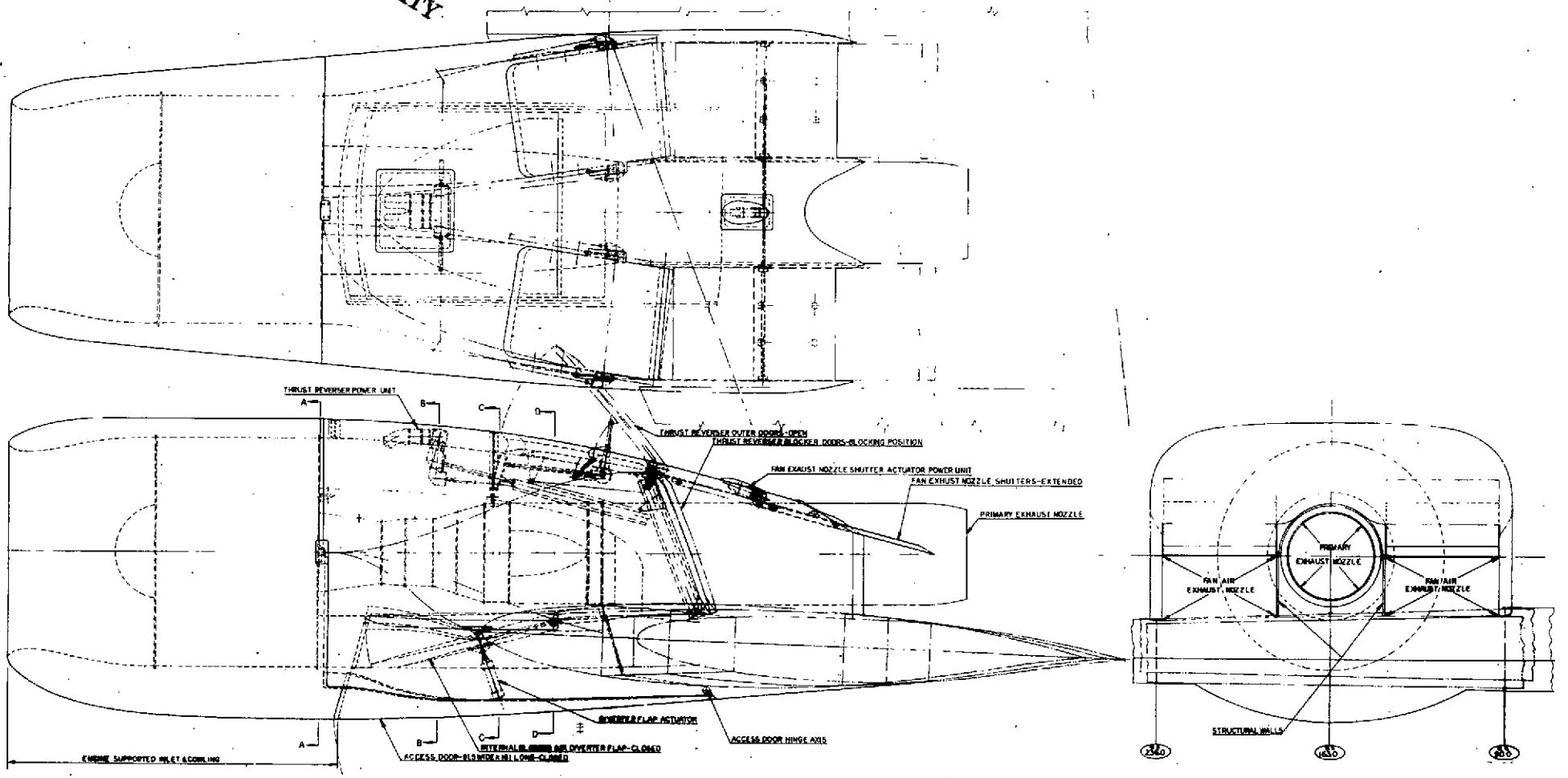

FIGURE 140: POWER PLANT INSTALLATION (1)

FIGURE 141: POWER PLANT INSTALLATION (2)

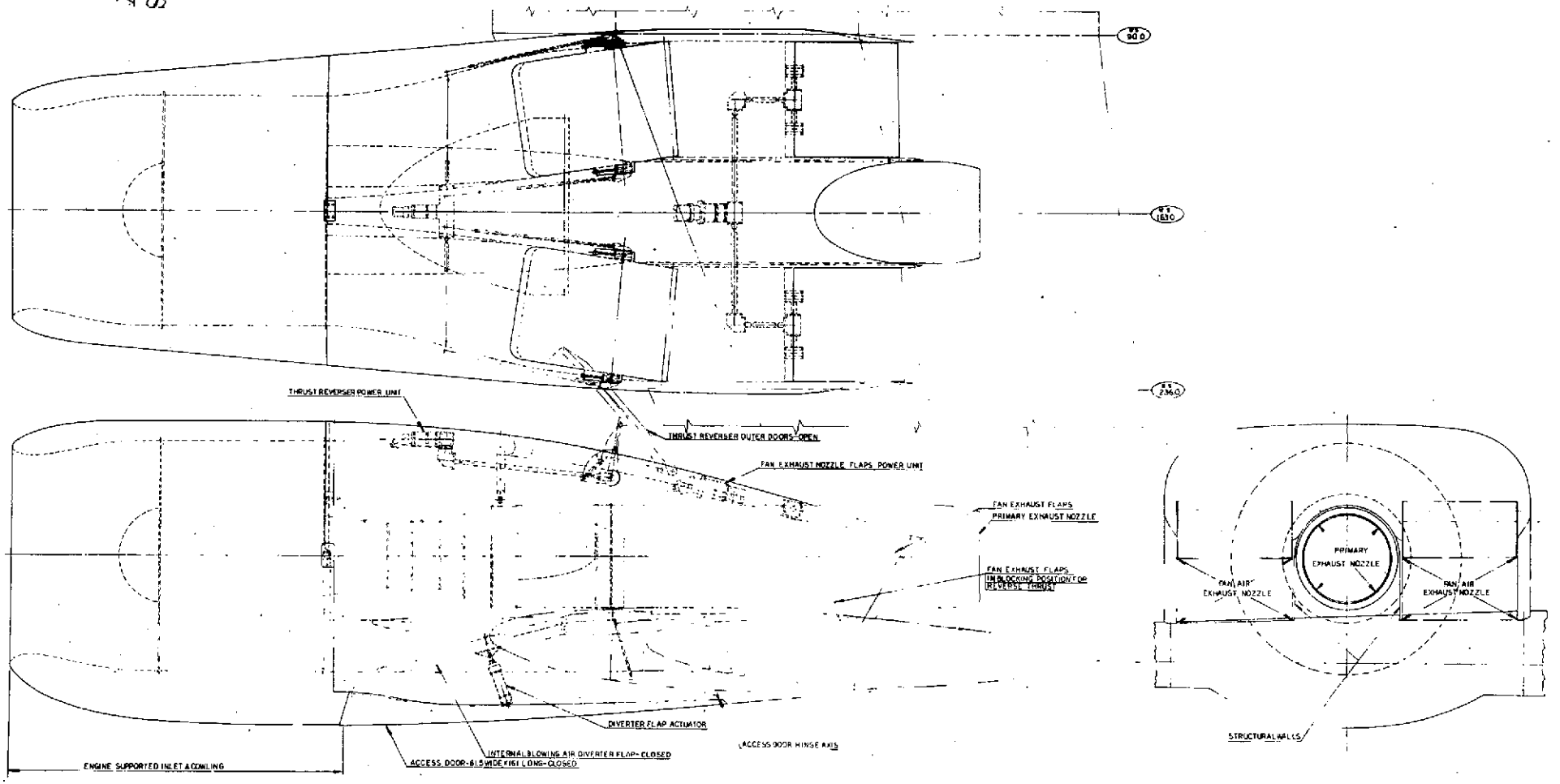

FIGURE 142: POWER PLANT INSTALLATION (3)

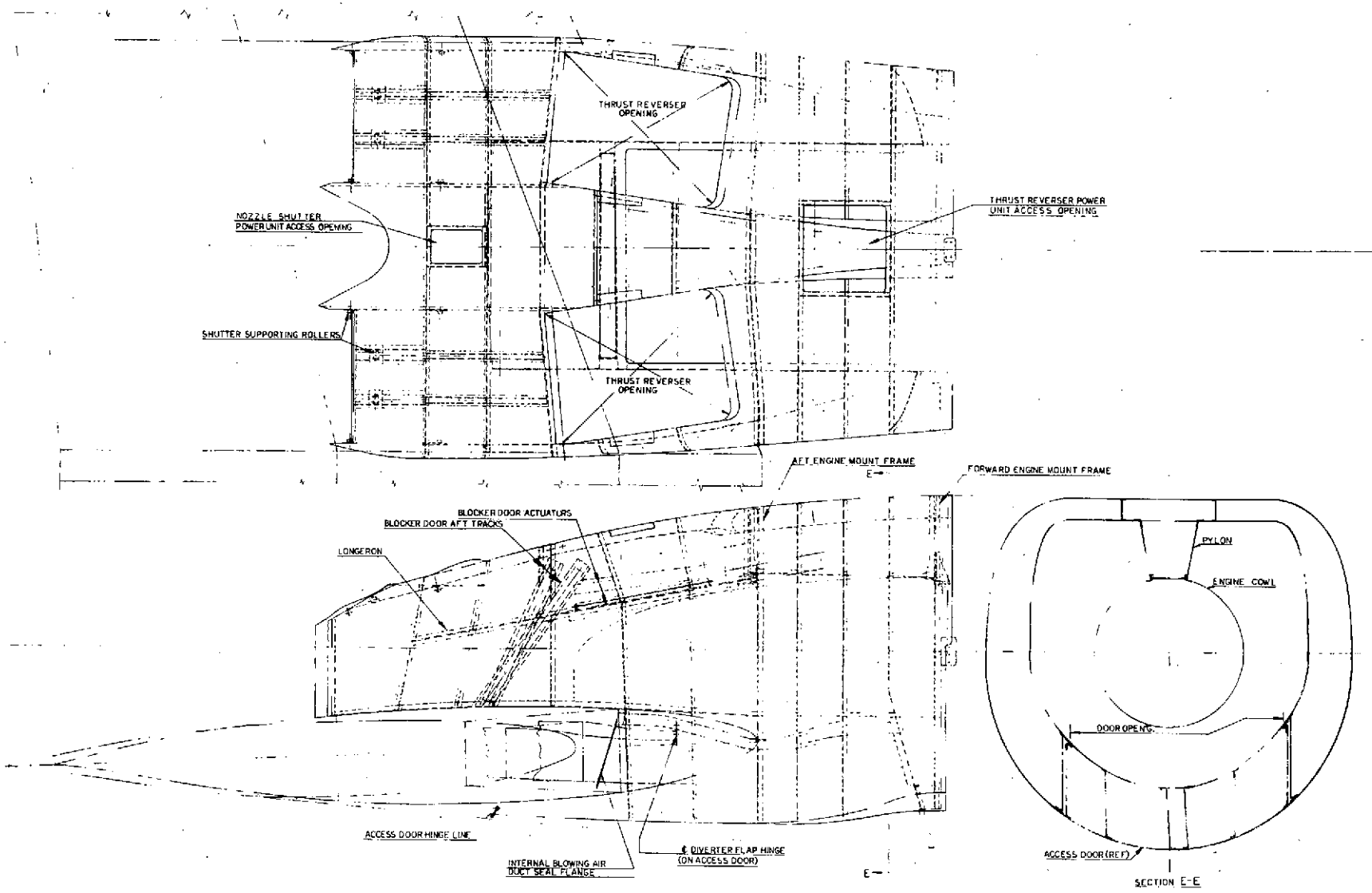

FIGURE 143: NACELLE FIXED STRUCTURE

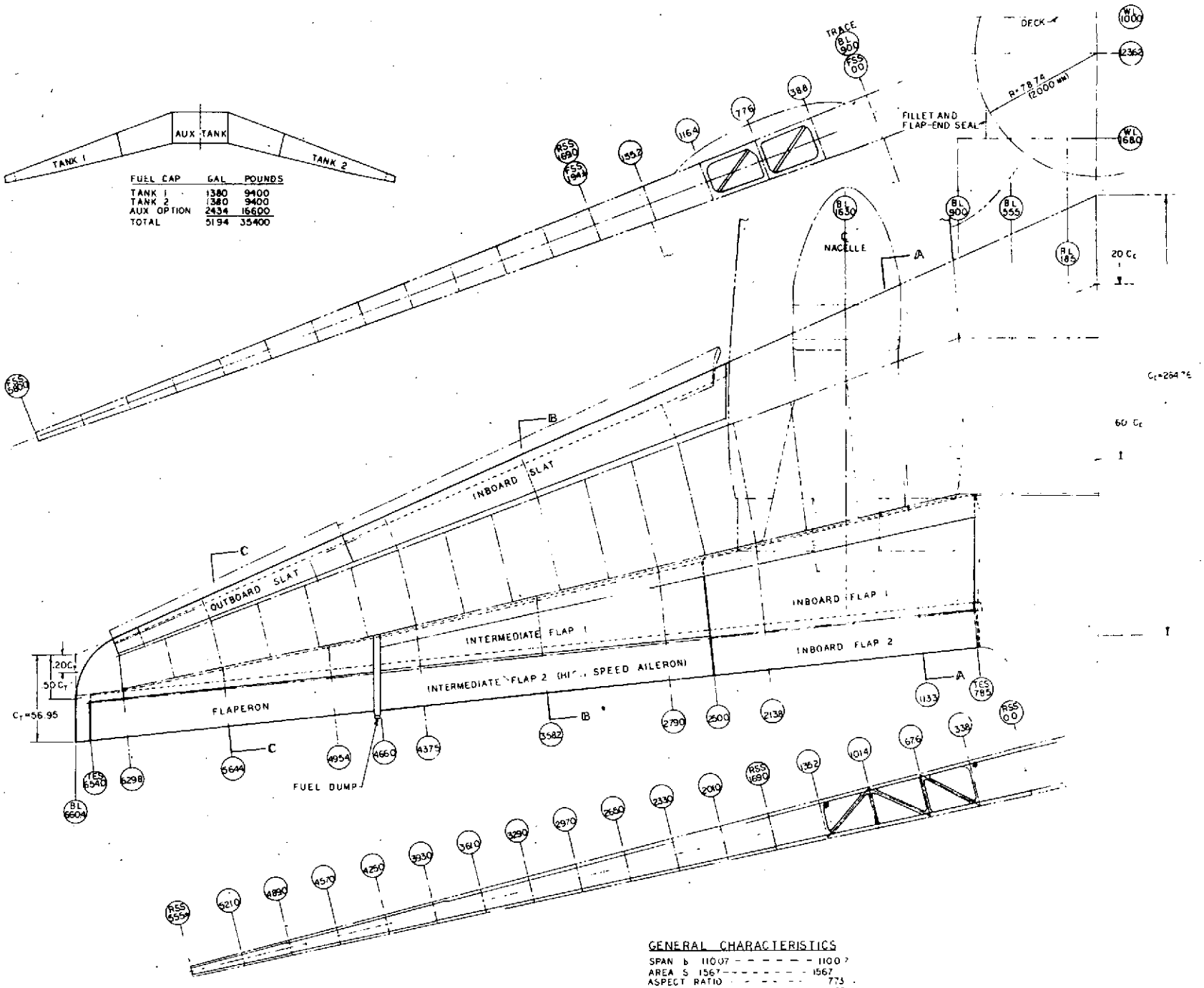

GENERAL CHARACTERISTICS

SPAN b	1100.7		1100.7
AREA S	1567		1567
ASPECT RATIO			7.73
TAPER RATIO			.20
MAC	196.17	C_t	284.76
$\bar{Y}$	256.8	C_T	56.95
SWEEP $\Lambda_{c/4}$			20°

FIGURE 144: WING STUDY (1)

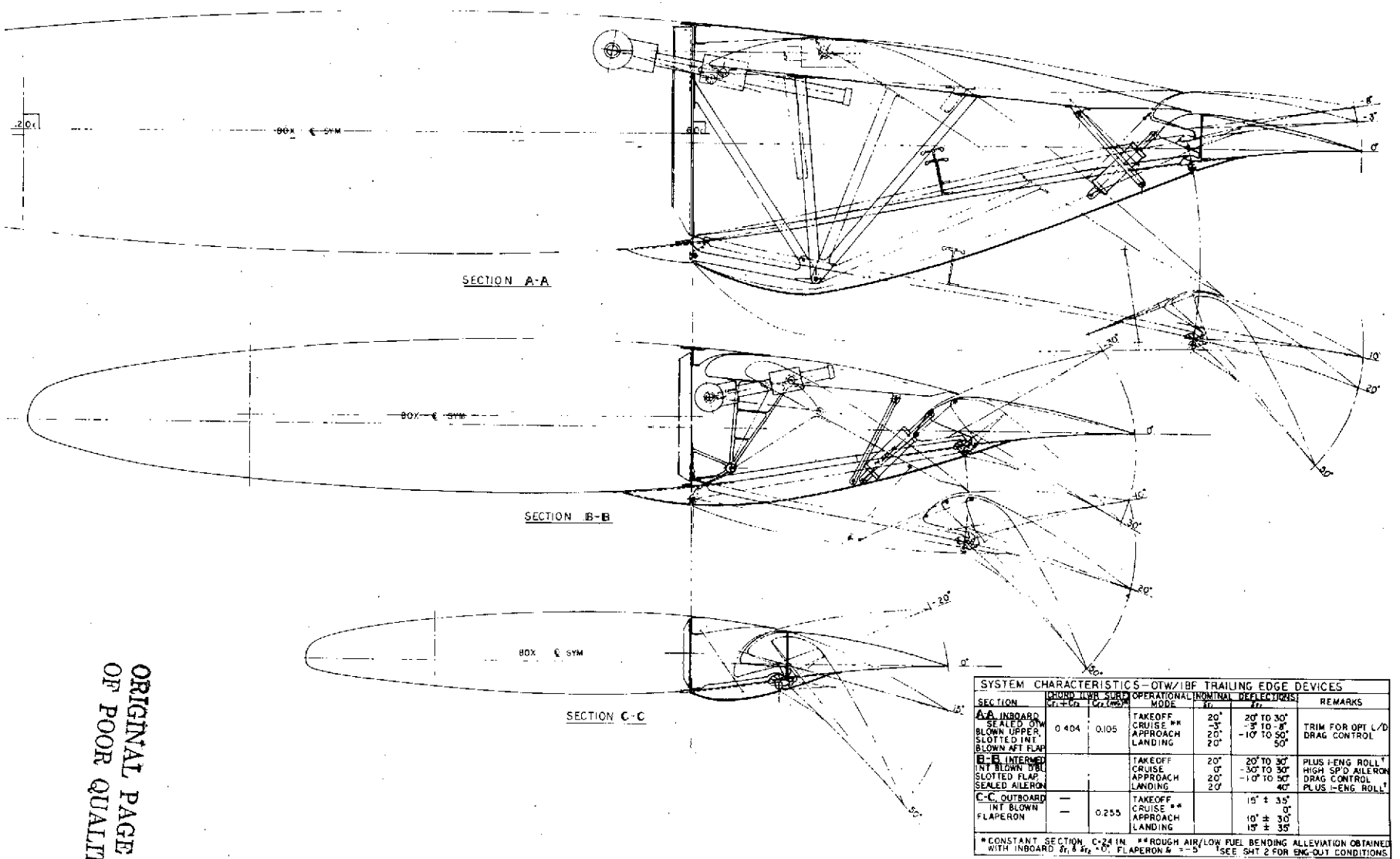

SYSTEM CHARACTERISTICS—OTW/IBF TRAILING EDGE DEVICES

SECTION	CHORD (LWR SURF) $C_{f_1}+C_{f_2}$	CHORD (LWR SURF) C_{f_1} (MIN)	OPERATIONAL MODE	NOMINAL DEFLECTIONS δ_{f_1}	NOMINAL DEFLECTIONS δ_{f_2}	REMARKS
A-A, INBOARD SEALED OTW BLOWN UPPER, SLOTTED INT BLOWN AFT FLAP	0.404	0.105	TAKEOFF CRUISE ** APPROACH LANDING	20° -5° 20° 20°	20° TO 30° -3° TO -8° -10° TO 50° 50°	TRIM FOR OPT L/D DRAG CONTROL
B-B, INTERMED INT BLOWN OTB SLOTTED FLAP, SEALED AILERON			TAKEOFF CRUISE APPROACH LANDING	20° 0° 20° 20°	20° TO 30° -30° TO 50° -10° TO 50° 40°	PLUS 1-ENG ROLL† HIGH SP'D AILERON DRAG CONTROL PLUS 1-ENG ROLL†
C-C, OUTBOARD INT BLOWN FLAPERON	—	0.255	TAKEOFF CRUISE ** APPROACH LANDING		15° ± 35° 10° ± 30° 15° ± 35°	

*CONSTANT SECTION, C=2.4 IN. **ROUGH AIR/LOW FUEL BENDING ALLEVIATION OBTAINED WITH INBOARD δ_{f_1} & δ_{f_2} = 0°, FLAPERON δ_a = -5° †SEE SHT 2 FOR ENG-OUT CONDITIONS

FIGURE 145: WING STUDY (2) (FLAP AND AILERON)

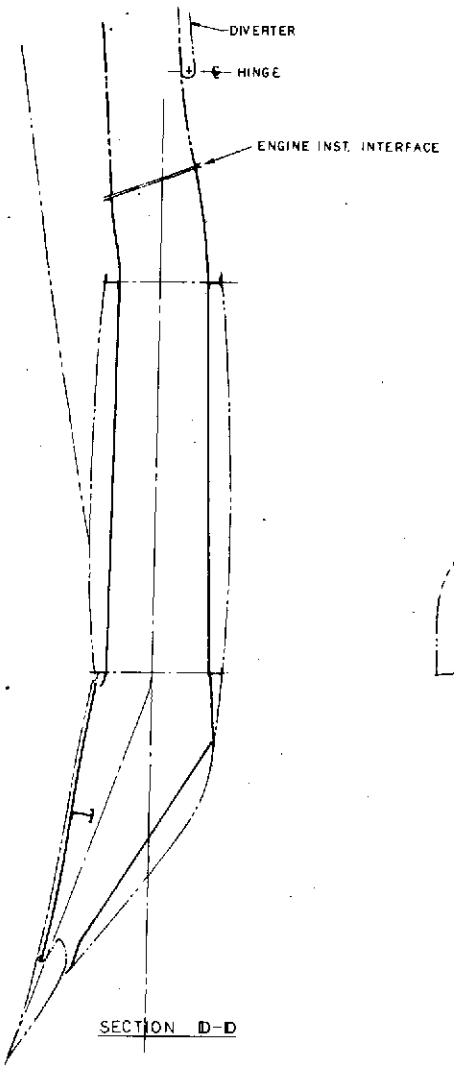

SECTION D-D

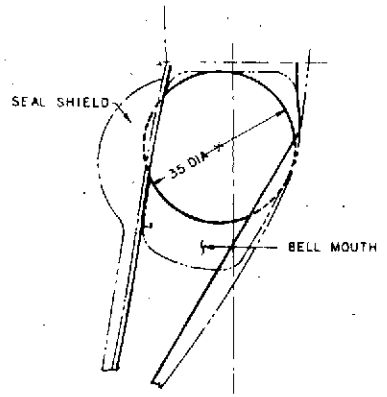

SECTION H-H

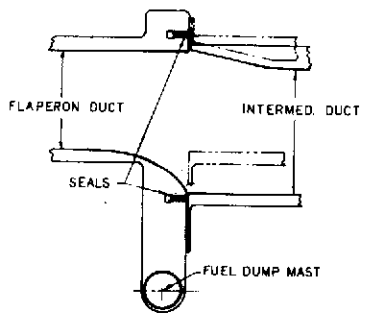

SECTION F-F

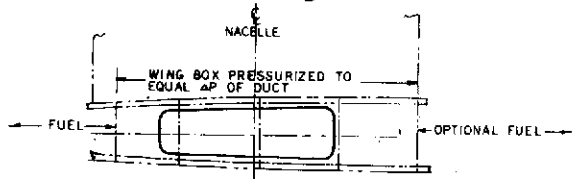

SECTION E-E

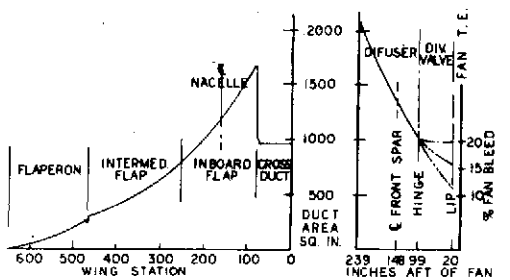

INTERNAL BLOWING DUCT AREAS – SPANWISE & AXIAL

SCHEDULE OF TYPICAL SURFACE DEFLECTIONS, SLOT GAPS AND AREAS

FLIGHT CONDITION		TAKEOFF 2-ENG	LAND 2-ENG	LAND 1-ENG	ROLL CONT. 2-ENG LAND	ROLL CONT. 1-ENG T. O.	ROLL CONT. 1-ENG LAND
INBOARD FLAP	δ_1	20°	20	20	20 20	20 20	20 20
	δ_2	30°	50	20	50 50	30 30	50 50
	GAP$_2$	.6 IN.	.8	.4	.8 .8	.6 .6	.8 .8
(A b=172)	AREA$_2$	103 IN^2	138	69	138 138	103 103	138 138
INTERMED. FLAP	δ_1	20	20	20	20 20	20 20	20 20
	δ_2	30	40	20	40 40	50* 10*	50* 10*
	GAP$_1$	.7	.7	.7	.7 .7	.7 .7	.7 .7
	GAP$_2$	.6	.7	.5	.7 .7	.8 .4	.8 .4
(A b=215)	AREA$_1$	150	150	150	150 150	150 150	150 150
	AREA$_2$	129	150	107	150 150	172 86	172 86
FLAPERON	δ	15	15	10	50 -20	50 -20	50 -20
	GAP	.5	.5	.4	1.2 .1	1.2 .1	1.2 .1
(A b=184)	AREA	92	92	74	221 18	221 18	221 18
SLOT AREA PER SIDE		474	530	400	659 456	646 357	681 392
TOTAL AREA		948	1060	800	1115	1003	1073
DIVERTER % BLEED		13 13	15 15	0 20	15 15	0** 20	0** 20
CROSSFLOW, % OF ONE ENGINE BLEED		0	0	50	9	64	63

*HARD OVER ROLL COMMAND IN FLAPS-DOWN TRIM ENGAGES INTERMEDIATE FLAP 2 FOR ADDITIONAL ROLL CONTROL AS REQ'D.
**ENGINE P_3-DROP SIGNAL CLOSES DIVERTER AND OPENS ONE ON OPPOSITE ENGINE TO MAX POSITION.

FIGURE 146: WING STUDY (3) (INTERNAL BLOWING SYSTEM)

The ultimate configuration of the basic concept of the large, single point extraction, diffusing straight into the wing box would require careful development but previous experience on duct development indicates that such a system is achievable.

The PD287-11 engine requires an increase in effective fan nozzle area in the low flight speed range relative to the cruise areas. This requirement appears to be typical of the advanced technology, high bypass, moderate FPR engines. The requirement is dictated by the stall margins and component efficiencies of the fan and core compressors that require a scheduled variation in the effective fan nozzle area across the flight Mach number range. Tolerances of the engine components is such that some deviation is permissible from the scheduled variation over the entire spectrum if some performance degradations are acceptable. The major variation is required at flight conditions between approximately 0.2 and 0.5 Mach. Early in the study, it was conceived that the IBF flow in the low Mach region could provide the effective fan exhaust area increase to meet the requirement and the cruise area would then be fixed. This concept appeared feasible at that time recognizing that some compromises in the IBF flow quantity and schedule would be required. In this continued study, DDA was contracted to make further investigation of this concept and their findings are reported in reference 28. DDA found that the step change that occurred when the IBF bleed was cut off was outside the tolerances of the engine components, regardless of the cut-off Mach number, and concluded that some relief from the step change was required. The alternatives were a separately adjustable nozzle flap, a variable pitch fan, and a variable bleed.

It was considered doubtful that the variable pitch feature of the fan could be justified on the basis of this requirement and would be useful only when the variable pitch fan had been selected for other reasons. The use of variable bleed would require the continuation of some IBF flow through the climb mode when the flaps have been stowed. This would entail further complication of the flap system, entail some performance loss and have limited flexibility. It was concluded that the fan nozzle exit blockers for reverse operation could be configured to provide the nozzle area trim requirements to be used in conjunction with the step change IBF bleed. This system appeared to be the most flexible and

entail the least penalties. This configuration is reflected on Figure 142.

Tests of the OTW and hybrid concepts performed by NASA, Lockheed, and others indicate some benefits relative to Coanda flaps by placing a deflector over the fan nozzle exit. The deflector has the effect of reducing the nozzle 'h' thereby creating a better h/r and also spreading the nozzle efflux over the flap, thereby increasing the super-circulation lift. An illustration of such a nozzle is shown on Figure 140. Unfortunately, this concept is basically contrary to the requirements for an increased effective fan nozzle area in the low speed regime since the effect of the deflector can only be in the direction of decreasing the effective nozzle area. In these study configurations, this problem is of course relieved to some extent by the large IBF bleed but it is questionable whether sufficient bleed could be achieved to make up for the effect of the deflector on the fan nozzle area. In addition, the capability for trimming the area would still be required which is somewhat incompatible with the deflector. The most attractive solution for this requirement appears to be the inclusion of variable flaps on the side of the nozzle similar to those employed earlier on the top nozzle surface. These would have the effect of allowing the fan flow to spread even further. The primary problem associated with these flaps would be their interference with the nacelle structure and the maintainance of reasonably good nozzle flow characteristics.

The reversed thrust capability is provided in the study nacelle by inclusion of large doors in the top of the nacelle, hinged at their aft ends. These doors open upward providing egress for the fan air and are used in conjunction with the previously discussed fan duct. This type of reverser provides a high effectivity with low reingestion and no ground impingement or FOD problems.